

Graptolitic mudrocks and their implications for the taphonomy of organic compression fossils

Alexander Alfred Page
Department of Geology, 2007



Thesis submitted for the degree of Doctor of Philosophy

UMI Number: U501059

All rights reserved

INFORMATION TO ALL USERS

The quality of this reproduction is dependent upon the quality of the copy submitted.

In the unlikely event that the author did not send a complete manuscript and there are missing pages, these will be noted. Also, if material had to be removed, a note will indicate the deletion.



UMI U501059

Published by ProQuest LLC 2013. Copyright in the Dissertation held by the Author.
Microform Edition © ProQuest LLC.

All rights reserved. This work is protected against
unauthorized copying under Title 17, United States Code.



ProQuest LLC
789 East Eisenhower Parkway
P.O. Box 1346
Ann Arbor, MI 48106-1346

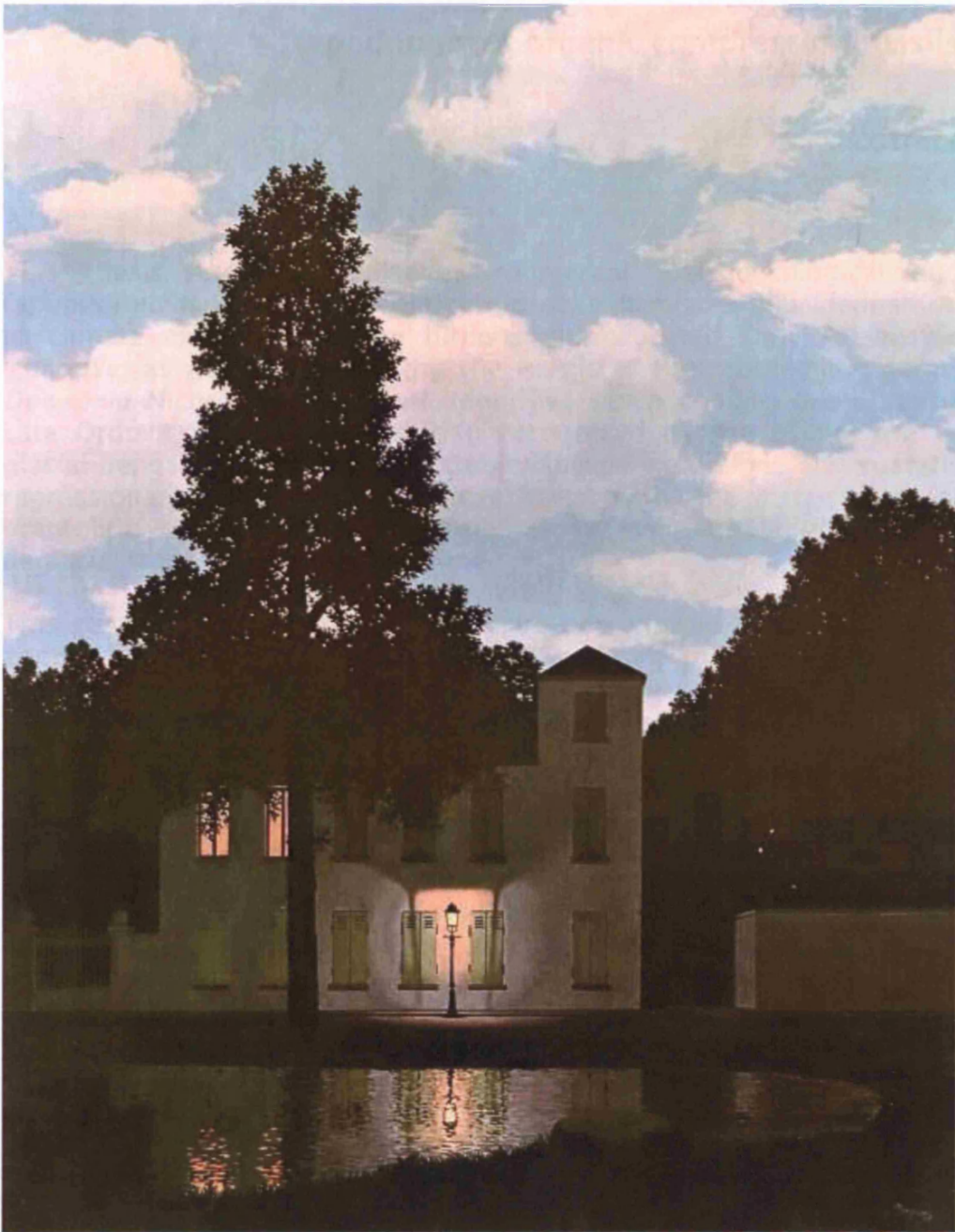
Declaration

This dissertation is the result of my own work and includes no work done in collaboration with others except where otherwise noted in the text.

Statement of length

Following consultation with my supervisors, approval has been obtained from the Graduate Office and Dean of Science for this thesis to exceed the suggested limit of 30,000 words. It therefore satisfies the requirements for examination as laid out in *Postgraduate Regulations* and *Notes for the guidance of candidates*.

AAP, Cambridge



"If the fool would persist in his folly he would become wise"
William Blake, The Marriage of Heaven and Hell (Proverbs of Hell)

Graptolitic mudrocks & their implications for the taphonomy of organic compression fossils

Abstract

This thesis addresses palaeoenvironmental, palaeoecological and taphonomic aspects of graptolitic mudrocks. It relates their deposition to climate modulation in an hitherto-unrecognised Early Palaeozoic Icehouse, as well as reassessing the fossils of the problematic genus *Dawsonia* Nicholson. This work identifies seven cooling events in the Late Ordovician and Early Silurian recognised by the occurrence of glacial deposits coincident with stable isotope excursions and eustatic regressions. Comparison of these data with the occurrence of graptolitic shales reveals that widespread anoxia occurred in deglacial transgressions at this time.

This study suggests that graptolites are best viewed as a mixed layer zooplankton and that their occurrence in anoxic mudrocks should be regarded as representing the conditions they were preserved in rather than those in which they lived. Meanwhile, the documentation of rare occurrences of graptolites in oxic facies and those from above the storm wave base shows that they could live in shallow well oxygenated waters.

Though anoxia alone is insufficient to explain the fossilisation of organic fossils, it is clear that fossilisation under such conditions does not render such fossils entirely inert or homogeneous. Analysis of multifaunal assemblages and others where graptolites co-occur with shelly fossils and pyrite shows that graptolites acted as the locus for phyllosilicate growth in very low-grade metamorphism. The expulsion of volatiles in maturation may have catalysed the formation of phyllosilicates on these fossils.

This phenomenon may also account for the formation of phyllosilicate films on Burgess Shale fossils. Here differences in the diagenesis of labile and recalcitrant anatomy resulted in the formation of distinct phyllosilicate assemblages on either anatomical type. It seems that these phyllosilicates formed too late to be responsible for decay retardation and for the exceptional preservation of Burgess Shale fossils.

Alex Page

Acknowledgements

I would like to thank my supervisors – Jan Zalasiewicz, Mark Williams (both Leicester), Phil Wilby (BGS), and Barrie Rickards (Cambridge) – whose faith, patience, wisdom and offers of lifts have helped me immeasurably throughout the course of my studies. Of these happy few, I would especially like to thank Jan, who listened intently to my latest harebrained thoughts and gently steered me towards productive outputs as well as diplomatically dealing with the *persculptus* incident and suggesting what music or literature I may profitably consume.

In addition, I would like to thank Sarah Gabbott (Leicester), David Harper (Copenhagen), Mike Howe, Stewart Molyneux (both BGS), Adrain Rushton (NHM), Sarah Sherlock (OU) and an anonymous reviewer who provided constructive criticisms of earlier versions of chapters 2-5. Dave Gladwell (Leicester), Phil Wilby, Dick Merriman & Rob Barnes (BGS) gave me access to their data for Figs. 1.2 & 3.5 and Tables 4.4 & 5.1 respectively. Phil Wilby & Sarah Gabbott provided assistance with SEM techniques for Chapters 3 & 5 and, along with Mark Williams, assisted me in compiling some of the figures in Chapters 2, 3 & 5.

I gained valuable Technical support from Rob Wilson, Rob Kelly, Nick Marsh, Sarah Lee & Colin Cunningham (Leicester), Phil Crabb (NHM) and Ian Marshall & Dudley Simons (Cambridge). Jim Floyd (BGS), Eddie Blackett, Claire Cordon, Bob Ganis, & Andrea Snelling (all Leicester), Jakob Vinther (Copenhagen) & Leo Peskett (independent rice consultant) provided me with assistance in the field, as did my supervisors. I'd also like to thank Paul Shepherd, Louise Neap, & Pauline Taylor (BGS), Matt Lowe, Dan Pemberton, Mike Dorling & Uncle Rod (Sedgwick Museum), Claire Mellish (NHM) & Ed Landing, Linda Hernick & Frank Mannolini (NYSM) for diligently searching out long-forgotten specimens and arranging loans and visits.

My studies were supported by the Leicester Geology Alumni society, and living in my final year was made somewhat more salubrious by a

Project Assistantship at Cambridge funded by the Leverhulme Trust. I would also like to acknowledge financial support from the John Whitaker Prize, The Sylvester Bradley Awards of both Leicester & PalAss, two PalAss conference grants and conference grants from CHRONOS & the Antarctic Cryosphere Fund (BAS). Meanwhile, the Heads of Department at both Leicester & Cambridge allowed me full use of their facilities as did Professor Kavanagh (St Radegund's College).

And to the lengthy roll call given above, I wish to add those with whom I've exchanged (generally) productive and useful conversations, emails, discussions, and/or received hospitality, namely and in no particular order: Big G; Paddy Orr & Maria McNamara (UCD); Nick Butterfield, Uwe Balthasar, Tom Harvey & Lucy Wilson (Cambridge); Joe Botting & Lucy Muir (NHM); Rob Barnes, Dick Merriman & Chris Vane (BGS); Chuck Mitchell, Jorge Maletz & Jay Zambino (SUNY Buffalo); Dan Goldman (Dayton); Sue Rigby (Edinburgh); Denis Bates (Aberystwyth); Peter Allison (Imperial) and Andy Gale (often over an agreeable Burgundy); whilst, at Leicester, I'd also like to thank all of the members of the Palaeobiology Research Group; as well as Steve Temperley, Mike Branney, Richard England & Mike Norry (with the latter extending my knowledge of Anglo-Saxon terms), plus Graham Andrews, Natalie Thomas, Ma Xiaoya, Pablo, James Howard, Rachel Backus, Dan, Chris Smith-Duque, Rippers, Douwe (not least for bequeathing me his collection of posing pouches), The Jow (though I don't know why), Hutch, Prak, Superfan and, of course, Stickleback Dave; the Marquis of Wellington did little to assist my studies.

As my Scoutmaster said "spread the blame".

Contents

1.	The introduction to the work	9
2.	Graptolitic mudrocks as transgressive black shales in the Early Palaeozoic Icehouse	19
2.1	Introduction	
2.2	Palaeoclimatic context for understanding graptolitic mudrocks	
2.3	The Early Palaeozoic Icehouse	
2.4	Oxic-anoxic stratigraphy and sea-level in the EPI	
2.5	A simple model for carbon burial and glacioeustasy in the EPI	
2.6	Discussion	
2.7	Conclusions	
3.	<i>Dawsonia</i> Nicholson: revealing the diversity of the fauna preserved in graptolitic mudrocks	86
3.1	Introduction	
3.2	History of research	
3.3	Material and methods used in this study	
3.4	The nature of <i>Dawsonia</i> Nicholson	
3.5	Discussion	
3.6	Conclusions	
3.7	Systematic palaeontology	
4.	Maturation of graptolites catalyses phyllosilicate formation in very-low grade metamorphism	121
4.1	Introduction	
4.2	Material and methods	
4.3	Results and their implications for phyllosilicate authigenesis	
4.4	A simple model for phyllosilicate formation on graptolites	
4.5	Discussion	
4.6	Conclusions	
4.7	Repository, specimen and white mica crystallinity data	
5.	A reassessment of the taphonomy of the Burgess Shale by comparison with graptolitic mudrocks	154
5.1	Introduction	
5.2	Material and methods	
5.3	Results	
5.4	Model to account for kerogen-specific phyllosilicates	
5.5	Comparison with the Burgess Shale and BST preservation	
5.6	Conclusions	
6.	In which the work is concluded	170

Tables & Figures

List of tables

- 2.1 Glacial maxima in the EPI
- 2.2 Evidence for ice-formation during the EPI
- 2.3 Faunal distribution data for (a) reef builders, (b) benthos & (c) plankton
- 2.4 Compilation of stable carbon and oxygen isotope data
- 4.1 Authigenic minerals associated with different bodies
- 4.2 Threshold KI values for phyllosilicate formation on graptolites
- 4.3 Specimens included in Table 4.1
- 4.4 Specimens and KI data included in Table 4.2
- 5.1 Late diagenetic phyllosilicates formed on different kerogens

List of figures

- 1.1 Models for graptolite palaeoecology and their preservation in anoxic mudrocks
- 1.2 Geochemical evidence for preservation of graptolites under oxic conditions
- 2.1 Changes in the nature of the carbon cycle through Phanerozoic time
- 2.2 Transgressive anoxia in the EPI
- 2.3 Oxic/anoxic stratigraphy for the EPI
- 2.4 The *persculptus* graptolite Zone anoxic event
- 2.5 The *sedgwickii* graptolite Zone glaciation
- 2.6 Model for deglacially transgressive black shales in the EPI
- 3.1 Photomicrographs of supposed graptolite reproductive organs
- 3.2 Nicholson's illustrations of supposed graptolite ovarian capsules
- 3.3 Linguliform brachiopods and a graptolite from the Lévis Shale, Canada
- 3.4 *Caryocaris acuminata* (Nicholson 1873) from the Lévis Shale, Canada
- 3.5 Morphometric analyses
- 3.6 Preservation of Nicholson's type material and a graptolite scopula
- 4.1 Photomicrographs illustrating graptolite preservation
- 4.2 Authigenic phyllosilicates associated with graptolites in hand specimen
- 4.3 Elemental maps of graptolites, shelly fossils and diagenetic pyrite
- 4.4 Thin sections showing authigenic minerals in graptolitic mudrocks
- 4.5 Petrography of phyllosilicate 'coronas' and quartz strain shadows
- 4.6 Phyllosilicate authigenesis facilitated by volume-loss in maturation
- 4.7 The diagenetic history of graptolitic mudrocks
- 4.8 Alternative models for growth of phyllosilicates on graptolites
- 5.1 Fossil preservation in the Burgess Shale and graptolitic mudrocks
- 5.2 Kerogen-specific elemental distribution
- 5.3 Kerogen-specific phyllosilicate assemblages
- 6.1 Comparison between graptolite diversity and anoxia

1. The introduction to the work

Understanding the fossil record and its relation to the Earth system is vital to our understanding of both biotic and climatic evolution. These processes themselves are, of course, interlinked (e.g. Darwin 1859; Lovelock 1972; Lovelock & Margulis 1974; Lovelock & Watson 1983; Staley 2004). Whilst through its fine detail an individual fossil may provide vital information on evolution, its context can also be used to interpret changes in climate and the environment. The latter, of course, provides a major cause of selection in evolution. For example, fossil graptolites cannot be understood outside of the environment in which they existed, whilst Early Palaeozoic climate and oceanography cannot be understood without its geological record. Many recent works relate the pattern of evolution in the Early Palaeozoic (Sepkoski 1981; Brenchley *et al.* 2003; Droser & Finnegan 2003; Harper 2006; Krug & Patzkowsky 2007) to large-scale environmental and ecological change (e.g. Vermeij 1987, 1995; Butterfield 1997, 2001; Jeppsson 1997, 1998; Botting 2001; Zhuravlev 2001; Orr 2001b; Brenchley *et al.* 2003; Chen *et al.* 2005). However, if the palaeontological record of both climate and evolution is to be read properly, one needs to appreciate the intrinsic bias in fossilisation through the study of taphonomy (cf. Efremov 1940; Shipman 1981; Allison & Briggs 1991; Cherns & Wright 2000; Butterfield 2005).

The preservation of organic compression fossils in marine mudrocks represents a notable constituent of the Early Palaeozoic fossil record (Sepkoski 1981). This interval witnessed the origin of complex metazoans and marine food-webs (Butterfield 1997), but preceded the origin of significant terrestrial ecosystems (Berner 1998; Gensel & Edwards 2001). Unlike modern oceans, the Early Palaeozoic oceans are characterised by extensive intervals of marine anoxia (Berner 2003), in which even shallow waters in the photic zone may have been devoid of free oxygen (Pancost *et al.* 1998). At these times the preservation of organic carbon in anoxic and dysoxic mudrocks may have had a significant role in regulating the concentrations of atmospheric oxygen and carbon dioxide, representing an alternative solution to the Earth's

carbon budget (e.g. Ridgwell 2005). The maturation of these kerogens during diagenesis and very-low grade metamorphism has given rise to some of the world's largest oil and gas reserves (Berner 2003), whilst the exceptional preservation of soft-bodied animals in siliclastic rocks – in so-called Burgess Shale-type preservation (Butterfield 1990, 2003) – underpins our knowledge of early animal evolution (cf. Conway Morris 2006).

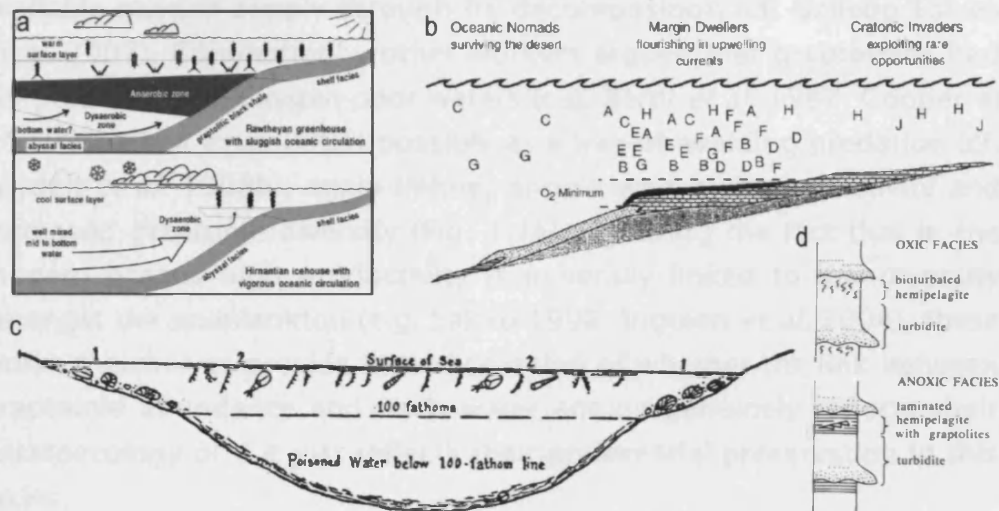


Fig. 1.1 Models for graptolite palaeoecology and their preservation in anoxic mudrocks: (a) graptolites as mid-water zooplankton that occupied the dysaerobic zone, with changing ocean circulation between the Rawtheyan greenhouse and Hirnantian Icehouse (see also Chapter 2) linked to a demise in the dyoxic midwater niche, a putative mechanism for their decline in the end-Ordovician mass extinction (after Chen *et al.* 2005; cf. Finney *et al.* 2007); (b) graptolites as margin dwelling zooplankton that thrived in areas of high productivity driven upwelling which also induced anoxia due to increase export production (after Finney & Berry 1997); (c) graptolites as mixed-layer zooplankton, with their ecology independent of the anoxic deep waters in which they were preserved (after Marr 1926); (d) schematic logs showing the variation between typical oxic (non-graptolitic) and anoxic (graptolite preserving) deep water facies (from Zalasiewicz 2001, after Cave 1979).

Graptolitic mudrocks are a widespread and abundant facies that were deposited below the storm wave base in dysoxic or anoxic conditions (e.g. Zalasiewicz 2001) and organic compression fossils are commonly preserved in these rocks (e.g. Chapman 1991; Palmer 1991; Underwood 1992). This is by far the most common mode of

preservation of graptoloids (Chapman 1991; Palmer 1991; Underwood 1992), which previous workers have generally linked to their mode of life. For example, Finney & Berry (1997) argued that graptoloids flourished in areas of high productivity brought about by upwelling along the shelf margin, achieving their maximum diversity and abundance under such conditions (Fig 1.1b). They argued that this increased productivity led to an increased “faecal express” which brought an excess of organic matter into deep water, consuming the available oxygen supply through its decomposition (cf. Gallego-Torres *et al.* 2007). Contrastingly, other workers argued that graptoloids had adapted to live in oxygen-poor waters (e.g. Berry *et al.* 1987; Cooper *et al.* 1991; Chen *et al.* 2005) possibly as a way of avoiding predation (cf. Loydell *et al.* 1998b), again linking anoxia with high productivity and increased graptolite diversity (Fig. 1.1a). Ignoring the fact that in the modern oceans high productivity is generally linked to low diversity amongst the zooplankton (e.g. Sakko 1998; Irigoien *et al.* 2004), these works themselves provide little discussion of whether the link between graptoloid abundance and deep water anoxia genuinely reflects their palaeoecology or if it just reflects their preferential preservation in this facies.

In an insightful and often overlooked work, Marr (1925) provided an alternative view of graptoloid palaeoecology (Fig 1.1c). He argued that graptolites were restricted to the upper part of the water column above the pycnocline – the so-called mixed layer whose depth generally coincides with Marr’s “100 fathom line” (Monterey & Levitus 1997) – beneath which the water column was anoxic (hence “poisoned”) during the deposition of graptolitic mudrocks. These deep waters, of course, could be well-oxygenated at other times (see Fig. 1.1d). This work was based on a view that the deposition of graptolitic mudrocks occurred during intervals when the water column was highly stratified, such as in the present day Black Sea (e.g. Stewart *et al.* 2007), impeding the circulation of oxygen-rich waters reaching the deeper parts of the water column; a corollary being that the circulation of oxygen-rich deep waters occurred in the intervals between the deposition of graptolitic mudrocks. More recent studies have documented transitions between graptolitic and bioturbated facies in deep-water

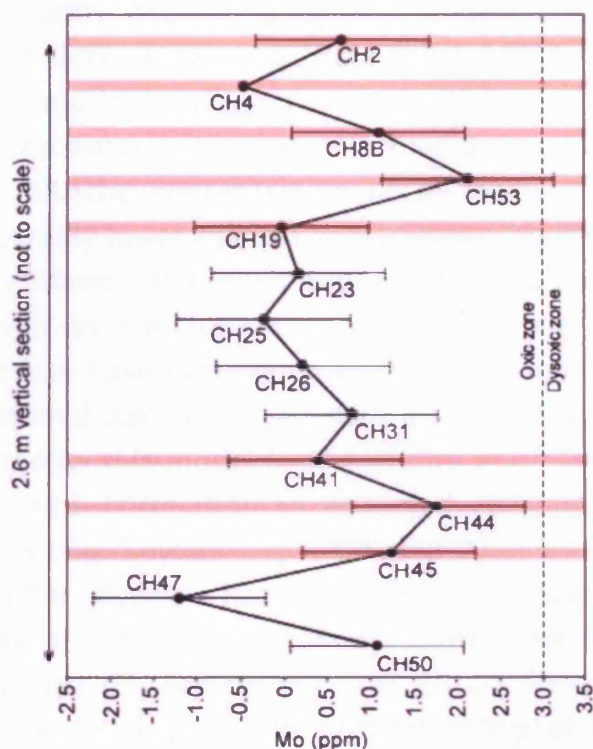


Fig. 1.2 Geochemical evidence for preservation of graptolites under oxic conditions. Mo concentration for a measured section from the Church Quarry in the Leintwardine area of the Welsh Borderland (see Siveter 2000, p. 357) where the graptolite *Saetograptus leintwardinensis* (Lapworth) is preserved alongside a fauna of well-preserved echinoderms and arthropods (Whitaker 1962). The Mo proxy gives the oxic-dysoxic transition at 3 ppm (after Piper & Perkins 2004) as marked with the dashed line, with the graptolite-bearing levels (pink lines) occurring entirely in oxic facies. Plotted from data courtesy of David Gladwell (unpublished PhD thesis, University of Leicester) with permission.

strata during the Early Palaeozoic (Figs 1.1a,d & 2.3), which related to deposition in anoxic and well-oxygenated intervals respectively (e.g. Cave 1979; Zalasiewicz 2001). Such transitions were noted by Jeppson (1990, 1997) who attributed changes in deep water redox conditions to changes in the site of deep water formation. At the present day thermohaline circulation in the oceans is largely driven by the sinking of dense waters from the ocean's surface, such deep-waters may be produced from the sinking of highly saline waters created in low latitude regions or from cool saline waters created by brine rejection in

ice formation at high latitudes; the rate and nature of ocean circulation can vary significantly depending on the relative contributions from either source of deep water (e.g. Rahmstorf 2002). Jeppson (1990, 1997) linked anoxia in deep-water environments to the circulation of warm, saline deep waters which were formed at low latitudes in warm intervals; after all, the concentration of dissolved oxygen in warm water is considerably lower than in cooler water. Meanwhile, he linked well-oxygenated deep-water environments to vigorous thermohaline circulation driven by the formation of cool, dense waters at high latitudes which may have been aided by ice formation (e.g. Figs 1.1a & 2.6). Though several authors have noted that the Silurian 'cycles' and 'events' predicted by this model (e.g. Aldridge *et al.* 1993; Jeppsson *et al.* 1995) bear little correlation to observed changes in deep water redox conditions (e.g. Loydell 1998; Chapter 2) or even climate (Kaljo *et al.* 2003), little attempt has been made to assess the relation between climate and deep water anoxia during the Early Palaeozoic using empirical data (cf. Armstrong *et al.* 2005). Such work may also have a significant bearing on our understanding of how graptoloid palaeoecology and preservation actually relate to marine anoxia.

Anoxia alone is an insufficient explanation for the preservation of graptolites as organic compression fossils (e.g. Foree & McCarty 1970; Allison 1988a, b). For example, the poorly preserved scopula illustrated in Fig. 3.1f has clearly undergone decay relative to the well-preserved examples shown in Fig. 3.1d. Both macrofossil graptoloids and graptolite fragments may be preserved in facies that were deposited in well-oxygenated conditions (e.g. Armstrong & Coe 1997; Floyd & Williams 2001; Fig. 1.2), which also indicates that they did not exclusively dwell in or above oxygen-poor waters (cf. Berry *et al.* 1987). In fact, if anoxia were necessary for graptolite preservation, it seems unlikely that dendroids would ever be found *in situ* (cf. LoDuca & Brett 1997). Though graptolite periderm was principally composed of collagen, which is a relatively recalcitrant biopolymer, this undergoes decay through peptide bond hydrolysis which can occur under oxygen-poor or anoxic conditions (Collins & Gernaey 2001). So, though anoxia may slow the decay of graptolites, another factor is needed to explain their organic preservation in the fossil record (cf.

Allison 1988b). Thus, occurrence of such fossils in graptolitic mudrocks may not accurately reflect the living community or its palaeoecology.

In a series of recent works on organic preservation, Gupta *et al.* (2006a-b, 2007a-b) have argued that carbonaceous fossils preserving recalcitrant, cuticular matter are a product of *in situ* polymerisation reactions resulting in the incorporation of lipids into an aliphatic macromolecule within the subfossil. They argue that this process served to convert a labile, decaying carcass into a more stable, homogenous kerogen (e.g. Gupta *et al. passim*). Though this presents a compelling and sophisticated argument as to how an organic-walled fossil may have avoided decay to enter the geological record, these works suffer from a significant problem in as far as they have not provided any evidence as to when or how this stabilisation actually occurred. Avoidance of decay prior to lithification is essential to the preservation of an organic walled fossil (Briggs 2003), but this might be achieved by various routes (Allison 1998a, b) which may or may not include *in situ* polymerisation in early diagenesis. Gupta *et al. (passim)* compared the composition of living tissue with the compositions of similar animals and plants from the fossil record, showing that the fossils are preserved as relatively stable kerogens rather than unaltered organic material. Now, though these kerogens are undoubtedly less decay prone than the original organic material, and though it is clear that the conversion from a labile biomolecule to a recalcitrant geomolecule has occurred, it is entirely unclear as to at what point in the fossil's taphonomic history this transition occurred. By selecting taxa from strata which have undergone a long and complicated burial history (e.g. Armstrong *et al.* 1992), it seems uncertain whether the organisms considered by Gupta *et al.* (2006b, 2007a-b) immediately underwent conversion from being a rotting carcass to being a stable, homogenous kerogenous fossil in its earliest diagenesis – a process that may have served to slow its decomposition such that it could survive the transition from the biosphere to the geosphere – or whether more decay-resistant compounds were selectively preserved (e.g. Baas *et al.* 1995) before undergoing a slow conversion into more stable, homogenous kerogens during the rock's

burial diagenesis (with the subfossil in this case having survived decay by some other means). After all, it is well documented that increases in temperature and pressure result in the conversion of kerogens to more stable, homogenous compositions during their maturation (Stankiewicz *et al.* 2000; Gupta *et al.* 2006a), which no doubt helps explain the higher fidelity of molecular preservation in fossils from younger strata compared to those from older strata (e.g. Stankiewicz *et al.* 1998) which will have generally undergone a more complex sequence of deep burial and exhumation. So, though this *in situ* polymerisation hypothesis provides one example of a process which may lead to the preservation of graptolites as organic compressions, it has yet to be demonstrated that this process occurred in the timescales and conditions associated with decay avoidance in the interval prior to fossilisation.

An alternative explanation for the preservation of organic fossils may come from clay-organic interactions in early diagenesis. Clay minerals are well known to have a strong affinity for organic matter (e.g. Caton 1954; Stotzky 1980; Lagaly 1984; Odom 1984; Curtis 1985; Petrovich 2001; Curry *et al.* 2007) and in various studies it has been noted that clay-organic interactions may be linked to the preservation of organic matter. For example, Tissot & Welte (1984, p. 54) noted a general correlation between high organic preservation and clay mineral content in marine sequences, whilst the adsorption of enzymes on to and within clay minerals may inhibit degradation (Alexander 1965, 1973; Theng 1979; Stotzky 1980). The latter mechanism has been invoked to explain organic preservation in marine mudrocks (e.g. Butterfield 1990, 1995). Likewise, Petrovich (2001) suggested that the adsorption of clays onto organic substrates may have inhibited degradation, and Curry *et al.* (2007) argued that such a process may result in enhanced preservation of organic matter, which may also be aided by the relatively low porosity of such fine-grained sediments (cf. Rothman & Forney 2007).

Clay-organic interactions may result in the tanning of organic molecules, increasing their recalcitrance during early diagenesis. Tanning is the polymerisation of organic compounds (such as collagen)

by the formation of cross-links between adjacent molecules. This process confers a notable resistance to breakdown in collagen (e.g. Lastowka *et al.* 2005; Aufderheide 2003). For example, scolecodonts, the jaws of polychaete worms, are composed of highly tanned collagen and are significantly more decay-resistant than the less tanned collagen of the worm's cuticle (Briggs & Kear 1993). This is no doubt reflected in the relatively abundance of scolecodonts and the scarcity of polychaete body fossils in the fossil record (Sutton *et al.* 2001). Such tanning of organic molecules may be achieved through clay-organic reactions (Solomon & Loft 1968; Solomon & Rosser 1965; Solomon & Swift 1967). As this process has been experimentally demonstrated, and is commonly applied in the chemical industry, it is clearly a process that can act on human rather than geological timescales (cf. discussion on *in situ* polymerisation above), and as such may perhaps account for some degree of decay avoidance in early diagenesis.

Like many graptolites, the exceptionally preserved fossils of the Burgess Shale are preserved as organic compressions coated by a thin film of phyllosilicates (e.g. Conway Morris 1977; Orr *et al.* 1998). Fossil-bearing horizons were deposited in the exaerobic zone, where the oxic-anoxic transition occurs at the sediment-water interface (Powell *et al.* 2003). As noted above, it has been argued that the preservation of its fossils may result from early diagenetic clay-organic interactions (e.g. Butterfield 1990, 1995; Petrovich 2001; Wilson 2004), with Orr *et al.* (1998) even suggesting that the phyllosilicate films may represent permineralisation in early diagenesis. Contrastingly, the authigenic phyllosilicate films that occur on graptolites have been viewed as 'strain shadows' that formed in their low-grade metamorphism (e.g. Underwood 1992). Both the formation of phyllosilicates and the maturation of organic carbon occur in very-low grade metamorphism, and both of these processes may have a significant effect on the porosity and permeability of mudrocks during the time of hydrocarbon generation and migration (Freed & Peacor 1989; Hunt 1996). These fossils can also form the site of formation of several other late-stage authigenic phases, including monazite (Wilby *et al.* 2007), showing that they do not remain inert after their initial decay avoidance and preservation as organic

compressions. Instead, it seems best to view fossil preservation as something more than just a picture of early diagenesis, but instead part of a long taphonomic history stretching from death and early diagenesis to burial and exhumation.

This thesis examines the taphonomy of graptolites and graptolitic mudrocks with its broader context. It develops a constrained taphonomic history for graptolites, which is used to reassess the late diagenetic history of fossils in the Burgess Shale. The fossils of the Burgess Shale are exceptionally preserved, displaying labile anatomy and organic residues which are not seen in graptolitic mudrocks, no doubt in part reflecting the differences in the earliest taphonomic histories of these two settings, with sedimentation in the fossil-bearing levels of the Burgess Shale dominated by catastrophic debris-flows (Allison & Brett 1995; Gabbott & Zalasiewicz 2007) or tempestites/turbidites (Piper 1972; Whittington 1980), and sedimentation in the fossil-bearing layers of graptolitic mudrocks dominated by hemipelagic setting with less frequent turbiditic input (e.g. Cave 1979). The early diagenesis of Burgess Shale fossils remains uncertain (Butterfield *et al.* 2007), no doubt due to its being a “one-off” deposit that lacks any low-grade lateral equivalent (Powell 2003). However, its early diagenesis may be inferred by comparing its taphonomic history with that of other organic compression fossils. In doing so one may establish which events in its history are normal geological processes, and which are unique to the Burgess Shale and as such plausibly responsible for the exceptional preservation of its fossils.

This thesis is written as a series of papers which are intended for publication. Manuscripts based on Chapters 2 & 3 have already been submitted, with the former currently in press, and Chapters 4 & 5 are to be edited with a view to their submission. The aim is that each of these Chapters serves as a unique contribution on a different aspect of organic preservation and graptolitic mudrocks. Chapters 2 & 3 deal with the depositional conditions and palaeoecology of graptolitic mudrocks, with Chapter 2 examining marine anoxia in a global environmental context and Chapter 3 examining the fauna preserved alongside graptolites by reassessing the genus *Dawsonia* Nicholson.

Chapters 4 & 5 analyse the taphonomy of multifaunal assemblages (such as those discussed in Chapter 3) to examine the very-low grade metamorphism of organic compression fossils, with Chapter 4 focussing on the link between maturation and phyllosilicate formation during conditions associated with economic hydrocarbon generation, and Chapter 5 using this knowledge to reassess fossil preservation in the Burgess Shale.

The evolution of both ecosystems and the global environment are intrinsically linked (e.g. Darwin 1869; Lovelock 1972; Lovelock & Margulis 1974; Lovelock & Watson 1983; Staley 2004), with the preservation of organic compression fossils central to our understanding of both processes during the Early Palaeozoic (e.g. Butterfield 1997; Chen *et al.* 2005; Conway Morris 2006). A long history of graptolite research (see Elles & Wood 1901-1918; Rushton *et al.* 1991; Rickards 1999) has given rise to a well-constrained stratigraphic succession, suitable for assessing how environmental change between shallow and deep waters and high and low latitudes may relate to climatic forcing. This provides a simplified Earth system framework against which the evolutionary patterns of diversification and extinction may later be assessed on the largest scale. Abundant, well-documented collections of fossil graptolites may be used to assess the detail of fossil anatomy and preservation, with careful microscopic study allowing a better understanding of either their morphology or taphonomy. Taphonomic histories can be used to investigate the processes involved with oil formation, rock deformation and fossil preservation, all of which is part of the longer history of Earth's evolution. It is my firm belief that this combined approach, where information from the fossil record is considered in both its intricate detail and larger context, is a useful way to gain some understanding of the biotic and geological evolution of our planet.

2. Graptolitic mudrocks as transgressive black shales in the Early Palaeozoic Icehouse

Abstract: The Early Palaeozoic Icehouse (Late Ordovician-Early Silurian, *c.* 455-425 Ma) was a remarkable event in the Earth's climatic history, marked by extensive glaciations occurring at a time of elevated atmospheric CO₂. The oceanography of the Early Palaeozoic Icehouse was markedly different from that of modern oceans, with frequent episodes of oceanic anoxia and high concentrations of CO₂ which may have acidified the oceans and restricted carbonate burial. Thus, the marine organic carbon reservoir may have more strongly influenced long-term changes in atmospheric CO₂ than at present. Deposition of black shales, principally graptolitic mudrocks, may have represented a major sink for atmospheric carbon. Sequence stratigraphy reveals that the deposition of extensive graptolitic mudrocks occurred in transgressions, whereas regressions are characterised by deposition of bioturbated facies, allowing changes in lithofacies and deep water redox conditions to be related to the Early Palaeozoic carbon cycle. Assuming increased temperature is a function of increased atmospheric CO₂, and that glacioeustatic sea-level can serve as a proxy for temperature due to changing ice volume, I infer that the deposition of graptolitic mudrocks as transgressive black shales may have acted as a negative feedback mechanism, drawing down CO₂ and preventing the onset of runaway greenhouse conditions.

2.1 Introduction

Deep water sequences in Early Palaeozoic strata are typified by graptolitic mudrocks (e.g. Berner & Raiswell 1983; Berner 2003), which themselves interleave with bioturbated non-graptolitic mudrocks, representing transitions between anoxic and oxic depositional conditions (Zalasiewicz 2001). Graptolitic mudrocks are black shales that have been interpreted as either representing [a] deposition in

upwelling zones, with increased export production inducing anoxia (e.g. Finney & Berry 1997; Lüning *et al.* 2000, 2005), or [b] deposition in anoxic conditions when increased stratification of the water column resulted in deep water anoxia (e.g. Marr 1925; Armstrong *et al.* 2005). Many authors have argued that the preservation of graptoloids in anoxic sediments indicates that graptoloids either inhabited [1] upwelling zones (e.g. Finney & Berry 1997) or [2] dysoxic middle waters (Berry *et al.* 1997; Chen *et al.* 2005), a corollary being that graptoloids were less abundant in well-oxygenated waters and areas that did not favour upwelling. Meanwhile, changes in deep water circulation, theoretically resulting in changes between graptolitic and bioturbated facies, have linked transitions between warmer and cooler climate modes in the Ordovician and Silurian (e.g. Jeppsson 1990, 1997; Kaljo *et al.* 2003). Though anoxia on a local scale may undoubtedly be due to either [a] upwelling and increased export production or [b] changes in circulation due to eutrophication of restricted basins, this chapter takes a more holistic approach to graptolitic mudrocks, assessing the deposition of extensive graptolitic mudrocks with reference to changes in palaeoclimate and palaeoceanography. To make such a study, I have chosen the interval from of the late Caradoc to early Wenlock, in which repeated glacial and interglacials (see section 2.2) allow such a comparison to be made.

2.1.1 Current views on the Early Palaeozoic environment

The Early Palaeozoic represents an important interval in Earth biosphere evolution. It post-dated the origin of large metazoans and complex, tiered marine food webs (Butterfield 1997), and is succeeded by the radiation of land-plants (Berner 1998; Gensel & Edwards 2001). It therefore represents an intermediate state between the oxygen-poor Proterozoic palaeoenvironment and the well-oxygenated world of the Late Palaeozoic and the post-Palaeozoic (Berner 2003; Catling & Claire 2005). This interval marks a non-actualistic solution to the Earth's carbon budget. Though generally considered an interval of long-lived, stable greenhouse conditions (e.g. Gibbs *et al.* 2000; Montañez 2002; Church & Coe 2003, fig 5.4), major glaciations nonetheless occurred in the late Ordovician and early Silurian (Table 2.2). These glaciations occurred at elevated atmospheric CO₂ (Royer 2006) and transitions

between oxic and anoxic marine conditions were frequent (Figs 2.1d & 2.2). In a time before the evolution of a complex land biota, most of the organic carbon reservoir must have existed in oceans, where it was buried as black shale (Fig. 2.1). Despite recent advances in general circulation models (GCMs) and the application of climatically-sensitive stable isotopes to infer palaeoenvironmental change, Early Palaeozoic climate remains somewhat enigmatic, no doubt in part due to its lack of analogue in the modern world.

Instead, the Early Palaeozoic needs to be understood in its own terms. Much as Charles Lapworth, Adam Sedgwick and Roderick Murchison carefully unpicked the undifferentiated 'greywacke' successions mapped by William Smith and Charles Lyell in the nineteenth century, and established the stratigraphic divisions of the Lower Palaeozoic (Rudwick 1985; Secord 1986; Oldroyd 1990), the twenty-first century sees the need for Early Palaeozoic workers to return to its stratigraphy and establish how global lithostratigraphic patterns of continental weathering and carbonate and black shale burial relate to its palaeoclimate, thereby determining the large-scale controls on the carbon cycle at this time.

2.1.2 The Early Palaeozoic carbon cycle and climate

Understanding chemical oceanography and carbon cycling in the Early Palaeozoic is difficult. The precise magnitude of atmospheric CO₂ at this time is uncertain, and the relation between CO₂ regulation and Early Palaeozoic climate is not fully resolved (see discussions in Ridgwell 2005 and Royer 2006). However, available proxy data agree well with Berner & Kothavala's (2001) GEOCARB III model of atmospheric CO₂ levels over Phanerozoic time (Crowley & Berner 2001; Royer *et al.* 2004; Royer 2006), providing support for extremely elevated CO₂ levels in this interval (Fig. 2.1a). This provides support for key assumptions of the GEOCARB model and its descendents. Among these assumptions is that long-term drawdown of atmospheric CO₂ into the oceans was a consequence of [a] continental silicate weathering and burial in carbonates, and [b] photosynthesis and burial of organic carbon (Berner 1991, 1994, 2006; Berner & Kothavala 2001). CO₂ regulation must have been reflected in the specific pattern

of organic and inorganic carbon burial in the Early Palaeozoic (Fig. 2.1), which also differs notably from that of the Neoproterozoic (Rothman *et al.* 2003) and the rest of the Palaeozoic (Berner 2003).

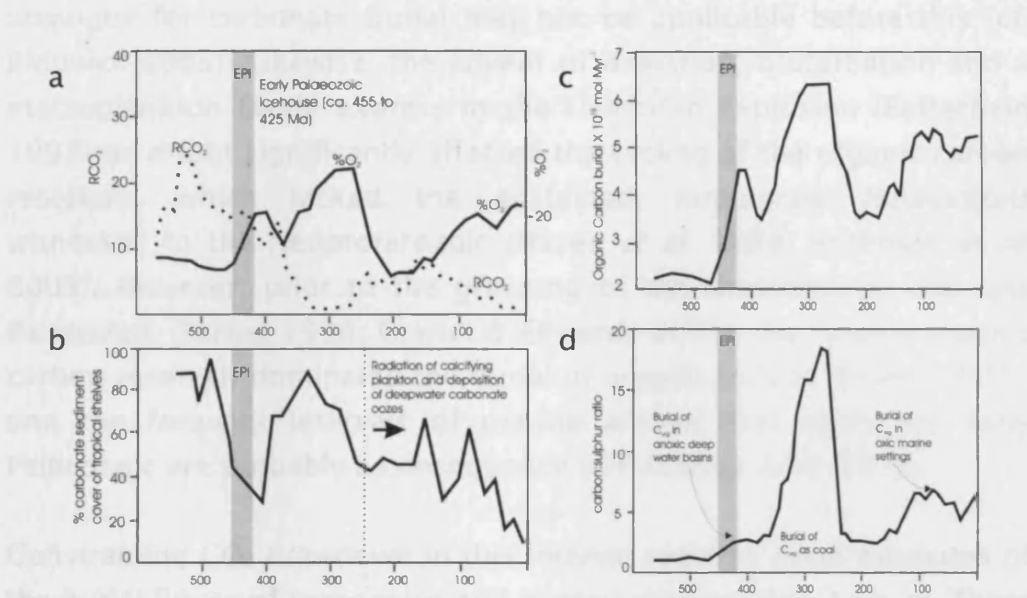


Fig. 2.1 Changes in the nature of the carbon cycle through Phanerozoic time: graphs showing that the Early Palaeozoic was dominated by organic-carbon burial in deep-marine anoxic waters under conditions of elevated atmospheric CO₂. (a) Temporal changes in atmospheric CO₂ relative to pre-industrial levels and partial pressure of atmospheric O₂ (after Berner 2001; Berner & Kothavala 2001). (b) Reduced carbonate deposition during the EPI as recorded in the relative proportion of low-latitude (<30° N/S) shelf-area occupied by carbonate sediments with time (data from Walker *et al.* 2002). (c) Temporal changes in organic carbon burial flux, showing a notable high in the EPI when organic carbon was predominately buried in black shales (after Berner 2003). (d) Ratio of the accumulation rate of organic carbon and pyrite-sulphur (C/S) in sediments versus time (after Berner 2003): low C/S-values reflect deposition of organic carbon in euxinic basins, high values correspond to burial in terrestrial fresh-water swamps, and intermediate values are found in normal marine sediments (Berner & Raiswell 1983). After Page *et al.* (2007).

In the Early Palaeozoic, carbonate burial was generally restricted to the continental shelves (Walker *et al.* 2002), whilst organic carbon was predominately buried in deep-water anoxic environments (Fig. 2.1d). The advent of biomineralisation in the Cambrian explosion facilitated carbonate burial relative to the Neoproterozoic (Rothman *et al.* 2003; Ridgwell 2005). However, the Early Palaeozoic may have lacked a well-developed marine carbonate buffer, which is highly sensitive to

increased atmospheric CO₂ (Barker *et al.* 2003). The radiation of the calcifying plankton in the Triassic profoundly affected the pattern of marine carbonate deposition (Martin 1995), and a modern ocean analogue for carbonate burial may not be applicable before this (cf. Ridgwell 2005). Likewise, the advent of digestion, bioturbation and a macroplankton faecal express in the Cambrian explosion (Butterfield 1997) no doubt significantly affected the cycling of the organic carbon reservoir, which lacked the sustained, large-scale fluctuations witnessed in the Neoproterozoic (Hayes *et al.* 1999; Rothman *et al.* 2003). However, prior to the greening of the continents in the Late Palaeozoic (Berner 1998; Gensel & Edwards 2001), the marine organic carbon reservoir dominated the burial of organic carbon (Berner 2003), and the frequent intervals of marine anoxia that typify the Early Palaeozoic are probably a consequence of this (Figs 2.1d & 2.3).

Constraining CO₂ drawdown in this interval requires good estimates of the burial fluxes of carbonates and organic carbon (Figs 2.1b, c). There are two ways of achieving such estimates. The first approach takes the known volume of carbon held in preserved strata and applies a correction to account for the progressive volume-loss due to erosion, subduction and metamorphism (e.g. Berner & Canfield 1989; Walker *et al.* 2002). The second approach applies GCMs and/or geochemically appropriate mass-balance models to proxy and/or mass flux curves (e.g. Berner 2003; Locklair & Lermann 2005; Ridgwell 2005). Neither of these methods is without problems: the former depending heavily on the dataset and the latter depending on the assumptions of the model. Though sophisticated approaches such as GCMs or multifactor box modelling allow palaeoclimatic hypotheses to be quantitatively established and/or tested, they may be extremely sensitive to certain parameters and differing algorithms can produce different results based on similar datasets (see Haywood *et al.*, 2005). Moreover, GCMs are highly dependent on changes in palaeogeography, ocean bathymetry, pCO₂, insolation and albedo. So, unless these factors are well constrained, their results should be considered conservatively before universally accepting their applicability in non-actualistic environments (cf. Ridgwell 2005).

The Early Palaeozoic climate includes the seemingly paradoxical occurrence of extensive glaciations (the Early Palaeozoic Icehouse or EPI as defined below) at elevated atmospheric CO₂ (Royer 2006). Given the long-recognised coupling of CO₂ and temperature (Arrhenius 1896; Chamberlin 1899) and more recent affirmations of the sensitivity of temperature to CO₂ (e.g. Shackleton 2000; Zachos *et al.* 2001; Kump 2002; Siegenthaler *et al.* 2005), a link between CO₂ and temperature in the Early Palaeozoic seems reasonable. Decreased cosmic ray flux may have also contributed to globally cooler temperatures during the EPI (Veizer *et al.* 2000; Shaviv 2002; Shaviv & Veizer 2003), but this was insufficient to induce glaciation alone (Royer 2006).

Most models suggest that atmospheric CO₂ was the key control on temperature and ice formation in the Ordovician and Silurian, predicting a pCO₂-ice threshold around 3000 ppm (Kump *et al.* 1999; Hermann *et al.* 2003, 2004a, b; Royer 2006). These values are significantly lower than the GEOCARB III or GEOCARBSULF estimate for Hirnantian CO₂ levels at *c.* 4000 ppm (Berner & Kothavala 2001; Berner 2006). The GEOCARB/GEOCARBSULF estimates are consistent with estimates from goethite (Yapp & Poths 1992) and significantly lower than the single palaeosol-based estimate of CO₂ for the Ashgill at *c.* 5600 ppm (Royer 2006). However, these models operate on longer timescales than the duration of the short-lived Hirnantian glacial maximum (cf. Sutcliffe *et al.* 2000), so the discrepancy between the estimated CO₂-ice threshold and estimates of atmospheric CO₂ may not be inconsistent (cf. Royer 2006). That is, glacial events could have been too rapid to be captured by either these models or the sparse proxy record. Individual glaciations in the EPI may have been short-lived events related to rapid CO₂ drawdown and cooling (e.g. Kump *et al.* 1999).

2.2 Palaeoclimatic context for understanding graptolitic mudrocks

Lithostratigraphic correlation may establish a link between deposition of CO₂ sinks and glaciations during the Early Palaeozoic. CO₂ may be drawn down from the atmosphere and sequestered in rocks by [a] photosynthesis and burial of organic carbon, or [b] continental silicate

weathering and carbonate deposition. The stratigraphic occurrence of carbonates and argillaceous sediments has been well documented in the identification of Primo/Secundo or Humid/Arid episodes (e.g. Jeppsson 1990, 1997; Aldridge *et al.* 1993; Jeppsson *et al.* 1995; Bickert *et al.* 1997; Cramer & Saltzman 2007; see also discussion). I adopt a complementary approach by comparing the stratigraphic distributions of black shales (such as graptolitic mudrocks) with sea-level curves, and isotopic data. In an icehouse world where high latitude glaciation mediates sea-level, glacioeustasy may act as a crude proxy for temperature (if more ice formed at lower temperatures, it should be reflected in lower sea-level). If atmospheric CO₂ was a function of temperature, relating organic carbon burial in black shales to changing sea-level may then provide a first order approximation of the relation between anoxia and the carbon cycle in the considered interval.

2.2.1 Criteria for recognising glaciations

The glacial maxima identified in the EPI (Table 2.1) are recognised using an argument similar to that employed by Brenchley *et al.* (1994). Namely, glacial maxima occur when rapid regressions are accompanied by synchronous oxygen and carbon evidence excursions consistent with glaciation, if there is contemporaneous evidence of cooling especially in glacial deposits. Ice formation may be recognised from either the deposition of diamictites containing glaciogenic clasts, ice rafted debris in distal marine settings, or from glacial erosive features (Eyles 1993). However, evidence of ice may not necessarily be evidence of glacial maxima. Even ignoring mountain ice, ice-sheets may persist through interglacials, and diamictites themselves in fact record the melting of ice rather than its formation (Eyles 1993). Also, extensive glaciations could conceivably cannibalise evidence of earlier glacial events through erosion especially if sea level is progressively lower. For example, the glaciotectonic unconformity of Caradoc-Hirnantian age that persists through much of Africa and Arabia (Legrand 1974; Destombes *et al.* 1985; Sutcliffe 2001; Ghienne *et al.* 2007) may obscure evidence of any potential pre-Hirnantian ice advances that may have occurred in this interval. With this in mind I have also incorporated faunal data into this study as these data may provide

evidence of cooling to augment those derived from the occurrence of glaciogenic sediments.

Correlation between high-latitude glacial deposits and equivalent low-latitude strata may be hindered by [a] the low abundance of graptolites in high-latitude environments and the presence of endemic faunas (e.g. Underwood *et al.* 1997; Lüning *et al.* 2000; Zalasiewicz 2001; Legrand 2003), and [b] the general absence of limestone-hosted shelly faunas in these settings (e.g. Walker *et al.* 2002, cf. Fortey & Cocks 2005). However, if the co-occurrence of ice formation with regressions and positive $\delta^{13}\text{C}$ and $\delta^{18}\text{O}$ excursions is not contradicted by biostratigraphic data, then it seems more parsimonious to consider them to be related to a glaciation rather than being caused by separate events.

This approach depends on the selection of high quality datasets with well-resolved stratigraphies, and accurate correlations. These are discussed below. I have been cautious in assigning evidence of ice formation to the glacial maxima, as discussed below. In addition the reader should note that from hereon in I generally use the more generic term 'black shale' rather than 'graptolitic mudrock'. This reflects more general usage in referring anoxic sediments rather than denoting a different facies, after all, all of the black shales referred to in this chapter are all graptolitic to a greater or lesser extent.

2.2.2 Choice/interpretation of datasets and correlations

Stratigraphic framework: my correlations follow those of Cooper & Sadler (2004) for the Ordovician, and Melchin *et al.* (2004) for the Silurian, although I correlate the Llandovery-Wenlock boundary to Ireviken datum 2 (see next paragraph). In addition, I refer to Nölvak *et al.* (2006) for correlation of the Ordovician timescale in Estonia to the global standard. I refer to other stratigraphic compilations in the text as necessary and assume that all major isotopic excursions are globally synchronous.

The International Commission on Stratigraphy website notes that the correlation of the Llandovery-Wenlock boundary GSSP is "imprecise"

(www.stratigraphy.org). To resolve this, the stratigraphy of the late Telychian-early Wenlock interval has received much attention of late (e.g. Jeppsson 1997; Loydell *et al.* 2003; Munnecke *et al.* 2003; Mullins & Aldridge 2004; Cramer & Saltzman 2005, 2007). The absence of taxonomically identifiable graptolites in the GSSP (Mullins & Aldridge 2004) makes correlation to graptolite zones uncertain (Melchin *et al.* 2004). However, the GSSP has a good conodont and microfossil stratigraphy, although the position of the golden spike does not correspond to the base of any particular biozone (Mabillard & Aldridge 1985; Mullins & Aldridge 2004). Instead, recent works have correlated this boundary at a slightly younger level, namely Ireviken datum 2 (e.g. Loydell *et al.* 2003; Calner *et al.* 2004). This represents the boundary between the lower and upper *Ps. bicornis* conodont zonal levels (Jeppsson 1997), which is close to the base of the *murchisoni* graptolite Zone (Loydell *et al.* 2003). This level has been suggested as a correlatable level for the boundary on the International Commission on Stratigraphy website (www.stratigraphy.org).

Most original works on Ordovician deposits (Table 2.2) correlate these strata to the British stages (cf. Fortey *et al.* 1995, 2000). As such, I refer to these stages throughout this chapter (the relations between the British stages and the international stages of Cooper & Sadler [2004] are shown in Fig. 2.2). However, I use the term Hirnantian *sensu* Cooper & Sadler (2004) as this stage is well-defined with good global correlation. I note that the definition and correlation of the British Ordovician stages is not unproblematic (Fortey *et al.* 1995, 2000; Cooper & Sadler 2004). The recent placement of the GSSPs for these stages reflects improved Ordovician biostratigraphy. The recently-named Sandbian and Katian stages of the Ordovician are defined on the well-correlated first appearances of the graptolites *Nemagraptus gracilis* and *Ensigraptus caudatus*, even though, the first appearance of these graptolites is locally diachronous (cf. Williams *et al.* 2003, 2004). Therefore, I feel that the historical correlation of glacial deposits to the British stages and my use of the UK oxic-anoxic stratigraphy justify my reference to these 'old-fashioned' terms and wish to highlight that use of old terms does not necessarily reflect the employment of outmoded correlations.

Sea-level curves: The sea-level curves illustrated in Figure 2.2 are based on sequence stratigraphic analyses of shallow-water facies. These may be 'calibrated' to the depths of such facies in modern environments (Ross & Ross 1996), though such estimates may also vary according to sediment flux or local topography (Orr 2001a). Nevertheless, other methods for estimating sea-level change possess inherent uncertainties. Faunally-derived sea-level curves may represent changes in palaeoenvironment rather than deepening *per se* (Orr 2001a). For example, 'quantitative' sea-level curves based on conodont assemblages do not produce consistent results in different environments (e.g. Zhang *et al.* 2006). Glacial maxima within the EPI may be associated with faunal turnover and changes in oceanic temperature and oxygenation. As such, faunally derived sea-level curves do not necessarily provide independent evidence of glacioeustasy in this interval. I only make passing reference to Loydell (1998), even though this offers well-defined evidence of Silurian sea-level change with good stratigraphic control. However, there is no curve defined using a comparable method for the Ordovician. And, as Loydell's (1998) sea-level curve uses deposition of graptolite shale as a criterion for establishing sea-level change, employing it would preclude an independent test of the relationship between sea-level and black shale distribution during the EPI.

Though I have used sea-level curves for the Ordovician and Silurian by different authors (Ross & Ross 1996 and Nielsen 2003a); both are compiled using the same method and correlate sequences in North America and Baltoscandia. As the Iapetus Ocean closed there may have been an increased local-tectonic component in the Laurentian record of sea-level change during the EPI (e.g. McKerrow *et al.* 2000). Nevertheless, correlation between two palaeocontinents reduces the chance of conflating relative tectonic changes with global changes in sea-level, and significant global events should register above local noise. The Nielsen (2003a) sea-level curve for the Ordovician shows a strong correlation with the equivalent sea-level curve by Ross & Ross (1995), but offers better stratigraphic resolution. Meanwhile, the Ross & Ross (1996) curve for the Silurian employs a method consistent with

that used by Nielsen (2003a) in the Ordovician. The original Ross & Ross (1996) sea-level curve has poor biostratigraphic control in the late Telychian (Loydell 1998), with the authors referring to an undifferentiated *crenulata* zone between the *griestoniensis* and *centrifugus* zones. This interval can be differentiated into four graptolite zones (e.g. Loydell *et al.* 1998a). As such, Figure 2.2 illustrates an amended version of the Ross & Ross (1996) curve based on the recorrelation of their original stratigraphy by Loydell (1998).

The sequence stratigraphic patterns observed by Ross & Ross (1996) may be consistent with 20-60 m changes in sea-level in less than 1-2 Ma. The rates and frequency of sea-level change during the EPI (Ross & Ross 1996; Nielsen 2003a, b) are consistent with third-order sequence stratigraphic cycles. They are therefore more likely glacially than tectonically forced (Church & Coe 2003).

Stable isotopes: The stable isotope data presented in Table 2.4 are based on compilations of $\delta^{13}\text{C}_{\text{PDB}}$ and $\delta^{18}\text{O}_{\text{PDB}}$ analyses from published data. Selected data are based on measurements from single specimens of brachiopods with some early diagenetic carbonate cement analyses included for the Late Ordovician as the brachiopod data was of poor resolution in this interval. Selected data were harvested from the following works Marshall & Middleton (1990), Middleton *et al.* (1991), Qing & Veizer (1994), Wadleigh & Veizer (1992), Azmy *et al.* (1998), Veizer *et al.* (1999) and Tobin *et al.* (2005), and recalibrated to the Ordovician and Silurian age models published in Cooper & Sadler (2004) and Melchin *et al.* (2004). These data are thought to represent unaltered sea water signatures for palaeolatitudes $< 30^\circ\text{N/S}$ on the basis of SEM microstructural and trace element analyses: though cathode luminescence may be a suitable for diagnosing diagenetic alteration of carbon isotope signals it is an unreliable indicator of alteration of oxygen isotope values (Marshall & Middleton 1990; Marshall *et al.* 1997), hence my adoption of the more rigorous trace element test of diagenetic alteration.

Stable isotope data from the secondary layer of brachiopod shells have been shown to be a reliable indicator of the original seawater isotopic

composition (e.g. Marshall *et al.* 1997; Azmy *et al.* 1998). Modern brachiopods secrete a low-Mg calcite shell at or near isotopic equilibrium with seawater (Lowenstam 1961; Carpenter & Lohmann 1995; James *et al.* 1997), which tends to resist diagenesis (Azmy *et al.* 1998; Marshall *et al.* 1997). The isotopic composition of their shells shows little deviation due to vital effects at the present day (Carpenter & Lohmann 1995). Analysis of multi-taxon assemblages in the Silurian suggests that vital effects may not have been significant in the Palaeozoic (Samtleben *et al.*, 2001). Hence, these fossil data have been regarded as representative of the isotopic composition of Early Palaeozoic sea-water (e.g. Veizer *et al.* 1997; Samtleben *et al.* 2001).

The veracity of the isotope data presented in Fig 2.2 and Table 2.4 can be determined by comparison with other isotope stratigraphies determined for this interval. The positive $\delta^{13}\text{C}$ excursions shown in Fig 2.2 can be seen in isotope stratigraphies for bulk rock carbonates based on analyses from North America (e.g. Patzkowsky *et al.* 1997; Saltzman 2005; Saltzman & Young 2005; Cramer & Saltzman 2006) and Baltica (e.g. Ainsaar *et al.* 1997; Kaljo *et al.* 2003, 2004). Whilst the $\delta^{13}\text{C}$ and $\delta^{18}\text{O}$ data presented are generally congruent with data obtained from brachiopod material not incorporated in my compilation, namely the low-resolution Ordovician curve published by Shields *et al.* (2003) and the Wenlock-Ludlow curves of Bickert *et al.* (1997) and Samtleben *et al.* 2001). These $\delta^{18}\text{O}$ data from brachiopods are also similar to $\delta^{18}\text{O}$ data obtained from phosphatic fossils such as conodonts (Veizer *et al.* 1999, 2005) suggesting they are a reliable indicator of the isotopic composition of sea water.

Positive $\delta^{18}\text{O}$ excursions can be achieved by decreases in temperature or increases in salinity (e.g. Hays & Grossman 1991). The latter can be achieved due to increased ice volume or decreased freshwater input, and both may occur along with decreased temperature in glaciations (e.g. Azmy *et al.* 1998; Tobin *et al.* 2005). Though changes in salinity alone have been argued to account for the positive isotope excursions observed in this interval (e.g. Samtleben *et al.* 1996; Bickert *et al.* 1997), such changes represent salinity change of up to 14‰, which is an implausibly large change that cannot be tolerated by brachiopods

(Azmy *et al.* 1998). As such, I interpret these positive excursions as representing decreases in temperature, which may be accompanied by smaller increases in salinity. Therefore, positive $\delta^{18}\text{O}$ excursions can be related to glaciations if consistent with other evidence (e.g. Brenchley *et al.* 1994; Azmy *et al.* 1998).

Kump & Arthur (1999) and Kump *et al.* (1999) show that positive $\delta^{13}\text{C}$ excursions can be achieved by [a] increasing productivity, [b] increasing the burial flux of organic carbon, or [c] by positive excursions in the $\delta^{13}\text{C}$ value of riverine input into the marine carbon reservoir due to increased terrestrial carbonate weathering. These alternatives can be distinguished by analysis of coupled patterns of organic and inorganic carbon isotopes (cf. Kump & Arthur 1999; Kump *et al.* 1999). For example, coupled organic and inorganic $\delta^{13}\text{C}$ data are available for the Hirnantian glaciation, and these positive $\delta^{13}\text{C}$ excursions have been interpreted as representing changes in weathering (Kump *et al.* 1999; Melchin & Holmden 2006). This excursion occurs during a major regression (e.g. Brenchley *et al.* 2004; Melchin & Holmden 2006), which exposed shallow marine carbonates to terrestrial weathering, resulting in a more positive $\delta^{13}\text{C}$ value of river waters (Kump *et al.* 1999). Given that all the positive $\delta^{13}\text{C}$ excursions of the EPI correspond to lowstands in cooler intervals with decreased organic carbon burial in deep water settings (Table 2.1; Fig. 2.2), all positive $\delta^{13}\text{C}$ excursions may reasonably be interpreted as being due to increased weathering of shallow carbonates exposed in regressions.

The positive $\delta^{13}\text{C}$ excursion isotope excursion associated with the Hirnantian glaciation is hard to reconcile with increased productivity or organic preservation (cf. Brenchley *et al.* 1994). This event is coincident with a mass extinction (e.g. Sutcliffe *et al.* 2000; Chen *et al.* 2005), when there is no evidence of increased organic burial in even the deepest water facies (e.g. Armstrong & Coe 1997). I therefore believe it is best to consider the positive carbon-isotope excursions of the EPI to represent cooler events if they are coincident with regression (e.g. Patzkowsky *et al.* 1997; Azmy *et al.* 1998; Kaljo *et al.* 2003; Tobin

et al. 2005; Johnson 2006), and that these excursions may be related to glaciations if consistent with other evidence.

Faunal distribution data: To critically assess cooling events in the pre-Hirnantian part of the Ordovician, I have incorporated faunal distribution data into this study (Table 2.3). These have been compiled from published reviews rather than original works, principally Webby *et al.* (2004a and refs therein) in which certain groups are covered more thoroughly in the interval considered in this period than others. These works are generally at a coarser stratigraphic resolution than the other data, and are correlated to the Ordovician timeslices of Webby *et al.* (2004a), which have the following durations TS 5a-b: *gracilis* Zone - mid *foliaceus* Zone (Katian - mid Sandbian); TS 5c: late *foliaceus* Zone - *clingani* Zone (late Sandbian - early Katian); TS 5d: *linearis* Zone (early Katian); TS 6a-b: *companulatus* Zone - *complexus* Zone (late Katian); TS 6c: *extraordinarius* Zone - *persculptus* Zone (Hirnantian). In compiling these data I have focussed on groups that have reasonably well resolved records that can be sensibly interpreted in a palaeoenvironmental context. I have generally avoided poorly-studied groups as well as groups with an incomplete record or poor stratigraphic control on their diversity, and groups whose taxonomic affinity or palaeoecology is poorly known.

In principle cooling may be inferred in from such data. Though of course the palaeoenvironmental signal in such diversity data is attenuated by a wide range of other factors not least the possibility that short-lived, rapid events may be swamped by other environmental influences if their duration was significantly shorter than the resolution of the diversity time slices. Besides which, any faunal signal that may be related to cooling or warming could be obscured by other environmental factors such as the fouling of reefs by increased erosion (e.g. Bickert *et al.* 1997), the emergence of cool water carbonate biotopes (Cherns & Wheeley 2007), the deepening of foreland basins during Orogeny (e.g. Paris *et al.* 2004) or changes in deep water redox conditions (e.g. Finney *et al.* 2007). There are also other influences on measured diversity patterns such as adaptive radiation through either [a] purely biotic processes, [b] facilitated by physical transitions among

major geographical regions (Miller & Mao 1995; Miller & Connolly 2001; Miller 2004), or [c] secular change in rock volume due to either changing sea-level or as a consequence of uplift, erosion and exposure (e.g. Smith & McGowan 2007), not to mention collection bias leading to some over sampled areas contributing anomalously to 'global' biodiversity (e.g. Paris *et al.* 2004). With this in mind a certain caution seems necessary in inferring palaeoclimatic data from faunal distributions, with a greater weighting given to events that are clearly expressed in well-studied groups.

Oxic-anoxic stratigraphy: Anoxic intervals are recognised from the occurrence of laminated hemipelagic mudrocks in deep-water settings (i.e. below storm wave base), which often contain graptolites. Graptolites are organic walled macrozooplankton and the majority of their fossil record comes from distal, anoxic mudrocks (Chapman 1991; Underwood 1992; Finney & Berry 1997). They may also be sporadically found in oxic facies, should they have undergone rapid burial (e.g. Fig 1.2). For example, *Stimulograptus sedgwickii* occurs in well-ventilated sandstones and siltstones in the Girvan area, UK (Floyd & Williams 2003), and in the shelf successions of the Llandovery area, Wales, UK (Cocks *et al.* 1984). Likewise, tiny graptolite fragments have been reported from rocks showing evidence of bioturbation (e.g. Armstrong & Coe 1997; Mullins & Aldridge 2004). Thus, the presence of graptolites in well-laminated, dark-grey or black mudrocks is evidence of anoxia rather than graptolite palaeoecology (cf. Berry *et al.* 1987). Similarly, the absence of macrofossil graptolites in poorly-laminated and/or burrowed paler grey shales is more typical of oxygenated bottom waters and sediments.

The oxic-anoxic stratigraphy for the EPI presented here (Fig. 2.3 and refs therein) is derived from correlating anoxic intervals in the deep-water record of UK successions. These successions are located in the Welsh Basin and Southern Uplands of Scotland, which occur on the lapetus margins of Avalonia and Laurentia respectively (Zalasiewicz 2001). They have a well-established, high resolution stratigraphy that allows such oxic-anoxic transitions to be recognised at a sub-graptolite zone resolution (e.g. Verniers & Vandenbroucke 2006). Thus, if anoxic

facies are deposited simultaneously in the Welsh Basin and the Southern Uplands, they represent at least an Iapetus-wide anoxic event (Fig. 2.2). Where intervals of anoxia in the Southern Uplands and Welsh Basin do not correlate, it may be that sediment redox conditions represent local rather than oceanic events. Leggett (1980) made a similar compilation for the Early Palaeozoic of the UK, employing stage level correlations. However, this higher resolution oxic-anoxic stratigraphy allows individual events to be correlated at a biozone level (e.g. Fig. 2.3).

The basis of the UK record as a reliable record of global marine anoxia requires consideration of the changing depositional settings of both the Welsh Basin and Southern Uplands. I select data from intervals where these strata were deposited in shelf and/or deep-basin environments. To establish the global extent, I also correlate this stratigraphy with redox changes recognised in the deep-water record of the Rheic and/or Palaeoethethys Oceans. As far as I am aware, the record of marine anoxia in the deep-water facies of the UK represents the only well-dated, continuous succession where the oxic-anoxic stratigraphy has been sufficiently documented to assemble a composite oxic-anoxic stratigraphy for the EPI.

The Welsh Basin was a restricted basin on the eastern margin of Avalonia. Its depositional setting and sedimentary history are reviewed by Woodcock (2000) and Zalasiewicz (2001). Local changes in freshwater run-off, nutrient input or upwelling may have induced localised anoxic events by altering productivity and stratification. Its sedimentary record stretches from the Cambrian to latest Silurian. Nevertheless, the widespread volcanism prior to the mid Caradoc significantly disrupted patterns of marine topography, subsidence and deposition (Woodcock 1990). This resulted in a more ambiguous and locally variable pattern of basin redox conditions at this time (cf. Leggett 1980). Once sediment input outpaced subsidence in the late Silurian (King 1994; Woodcock 2000), the basin became increasingly shallow and it rapidly filled with sediment. The oxic-anoxic stratigraphy of the Welsh Basin correlates extremely well with similar stratigraphies where available for the deep-water successions of the

Howgill Fells and Lake District, Northern England (cf. Rickards 1970; Hutt 1974; Rickards & Woodcock 2005). Thus, the Welsh Basin provides a well-resolved record of the oxic-anoxic stratigraphy of eastern Avalonia throughout the EPI.

In contrast, the Moffat Shale Group of the Southern Uplands is commonly thought to represent an ocean floor environment approaching a trench (Leggett *et al.* 1979; Leggett 1987). It may have been susceptible to changes in upwelling, which could have induced localised anoxia by increasing export production (e.g. Finney & Berry 1997). The Southern Uplands record of the EPI is contained within an accretionary prism formed from Iapetus thrust-slices during the Caledonian Orogeny (Leggett *et al.* 1979; Leggett 1987; Strachan 2000). The succession has an early Caradoc to late Llandovery age (Leggett 1980, 1987; Strachan 2000). Subsequently, the Moffat Shale Group was overlain by the massive flysch deposits of the Gala and Hawick groups of late Llandovery to Wenlock age (White *et al.* 1991). At a larger scale, the mudstones of the Moffat Shale Group comprise a generally distal, condensed succession of Ordovician and early Llandovery age, with slightly more expanded and proximal facies in the mid and late Llandovery. So, rather than being a restricted basin, the Southern Uplands provide a well-resolved record of open marine conditions throughout all but the terminal part of the EPI.

The major anoxic events of the Welsh Basin correlate well with those from the Southern Uplands where data are available (Fig. 2.3). Hence, there is no reason to believe that the late Llandovery-Wenlock of the Welsh Basin is unrepresentative of the Iapetus Ocean redox conditions, especially as synchronous changes are seen in northern England (cf. Rickards 1970; Rickards & Woodcock 2005). Thus, the oxic-anoxic stratigraphies of the UK basins (Fig. 2.3), from which I compiled the summary oxic-anoxic stratigraphy (Fig. 2.2), probably represent the best record available of oxic-anoxic transitions in low-latitude deep-waters during the EPI.

2.3 The Early Palaeozoic Icehouse

The Early Palaeozoic Icehouse (EPI) was an approximately 30 million year interval comprising seven currently recognised major cooling events (Table 2.1; Fig. 2.2). I propose that the EPI began with the Guttenberg Limestone carbon isotope excursion (GICE) in the Caradoc (Ordovician), and ended with Ireviken event deglacial transgression of the earliest Wenlock (Silurian). The EPI reached its greatest extent in the short-lived Hirnantian event identified by Brenchley *et al.* (1994), but there is good evidence for extensive ice formation and significant glacioeustatic change during the EPI (Tables 2.1 & 2.2; Fig. 2.2). Several other authors have argued for an extended period of glaciation (e.g. Frakes *et al.* 1992; Eyles 1993; Kaljo *et al.* 2003; Evans 2003; Ghiene 2003; Nielsen 2003a; Saltzman & Young 2005). The GICE event marks a sea-change in the carbon cycle, marking the onset on an interval characterised by rapid positive carbon isotope excursions (Saltzman 2005). This was accompanied by a change in the thermohaline behaviour of marine water apparent in the oxygen isotope record (Fig. 2.2), which coincided with onset of large-scale, rapid, third-to-fourth order variation in sea-level redolent of glacioeustasy (Nielsen 2003a, b). There are rare occurrences of glaciogenic drop stones and tillites at this time on Gondwana and in the Canadian Iapetan terranes (Table 2.2), though these are far less extensive than those associated with later glacial maxima. In his recent work on the onset of the Ordovician glaciation, Armstrong (2007) interpreted as a cooling event that marked the prelude to the Ordovician glacial maximum in the Hirnantian.

Most recent work on Early Palaeozoic glaciations has focussed on the Hirnantian (e.g. Sutcliffe *et al.* 2001; Hermann *et al.* 2004a, b; Armstrong *et al.* 2005; Le Heron *et al.* 2005) since Brenchley *et al.* (1994) argued for a short-lived Late Ordovician glaciation. This may partly reflect its coincidence with a mass extinction at a major stratigraphic division (e.g. Chen *et al.* 2000, 2005), as well as the deposition of major hydrocarbon source rocks in overlying strata (Lüning *et al.* 2000; Berner 2003). However, I have used the criteria similar to Brenchley *et al.* (1994) to recognise six further cooling

events in the EPI (see below). Namely, that sequence stratigraphic evidence for large, global low stands, coincident with positive $\delta^{13}\text{C}$ and $\delta^{18}\text{O}$ excursions suggests glacioeustasy and if there is contemporaneous evidence of ice formation or significant cooling, it seems likely that this was a glacial maximum (Table 2.1; Fig. 2.2).

2.3.1 Evidence for cooling in the EPI

Evidence of ice formation: The sedimentary record of glaciations in the EPI is predominantly held on Gondwana, with Ordovician deposits generally found in Africa, and Silurian deposits predominately in South America (Table 2.2; Eyles 1993; Díaz-Martínez & Grahn 2007). This continent-scale diachronism may reflect the movement of Gondwana across the South Pole (cf. Fortey & Cocks 2003).

Prior to the Hirnantian though the record of glacial deposits in Arabia and Saharan Africa is somewhat ambiguous. There is clear evidence of polyphase ice advance and glaciogenic sequences may contain many internal erosive unconformities (e.g. Ghienne *et al.* 2007). The general approach has been to treat these sequences as single units representing an interval of ice formation that extended from some time during the Caradoc or Ashgill and probably terminated in the *persculptus* Zone though may have extended until the Wenlock (Table 2.2; Beuf *et al.* 1971; Biju-Dival *et al.* 1981). The uncertainty in the age of these Ordovician deposits is summarised neatly by Legrand (2003, p. 19): “Many problems have been encountered with the uppermost Ordovician of the Algerian Sahara and adjacent regions... [a subsystem which includes all the ‘glacial’ formations disconformably laid down on the Saharan platform before the beginning of the Silurian]: (a) epeirogenic movements and erosion; (b) the nature of the glacial, periglacial, deltaic and fluvial sediments; (c) one glaciation, multiple glaciations or only a polyphase glaciation; (d) the varying importance of unconformities; (e) the age of the uppermost Ordovician formations, i.e. whether they are uppermost Ashgillian or upper Caradocian–upper Ashgillian and the precise age of the last *Hirnantia* fauna.”

Glaciogenic deposits have been reported from the late Caradoc of Bolivia, Peru and Argentina (Crowell *et al.* 1980), Morocco (Hamoumi

1999) and the Sahara (Beuf *et al.* 1977; Biju-Duval *et al.* 1981; Legrand 1988, 1993, 1995) though some of these earlier records have been redated as Ashgill in age (Paris *et al.* 1995; Ghienne *et al.* 2007), whilst a glaciogenic origin for the Moroccan deposits reported by Hamoumi (1999) has subsequently been challenged (Sutcliffe *et al.* 2001). In the Argentine Precordillera, there are at least three separate glacial advances that pre-date the *Hirnantia* Fauna and the coeval isotope excursion (Astini 1999; Peralta & Carter 1999; Sheehan 2001) though the absolute age of these deposits is unclear and the uncertain position of this terrane at this time hinders correlation with lateral equivalents. Likewise, in the Canadian Iapetan terranes exposed on Newfoundland, there are glaciogenic dropstones and tillites of Caradoc age, although no lateral equivalents have been reported on Avalonia or Laurentia, suggesting that this may represent localised (?mountain) ice formation; however, Caradoc-aged glaciogenic dropstones are also known from Libya (Massa *et al.* 1977; McDougall & Martin 2000; Table 2.2). So, though some diamictites that unconformably overly Caradoc or Ashgill age rocks in Gondwana are of probable Hirnantian age (Sutcliffe *et al.* 2001; Ghienne *et al.* 2007), there are also sporadic occurrences of pre-Hirnantian and probably Caradoc aged glaciogenic deposits on Gondwana and its peripheral terranes. Though the precise age of these deposits is currently poorly constrained, further study may yield important information concerning the extent and timing of pre-Hirnantian glacial advances.

Three periods of continent-wide diamictite deposition are recognised in the early Silurian of South America (Caputo 1998; Díaz-Martínez 2007). After the latest Llandovery, the South American record of glaciation becomes ambiguous. Glaciogenic diamictites in the San Gabán-Cancañiri-Zapla and Nhamundá Fms (Table 2.2) are overlain by strata yielding early Wenlock conodonts and late Telychian-early Wenlock chitinozoans respectively (Díaz-Martínez 2007; Grahn *in* Cramer & Saltzman 2007). The most recent works on these glacial deposits consider them as having an entirely Llandovery age (Díaz-Martínez 2007; Díaz-Martínez & Grahn 2007). Though the Kirusillas Fm of Bolivia contains diamictites of early Wenlock age (Merino 1991; Díaz-Martínez 2007), these lack glacially-abraded clasts

and are considered to be sediment gravity flows (Díaz-Martínez 2007; Díaz-Martínez & Grahn 2007).

It seems (not least from the isotopic and eustatic data) that land ice may have persisted throughout the EPI and that its formation may have influenced sea-level change. There is clear evidence for four episodes of widespread sea-ice formation during the Hirnantian and Llandovery, however, the extent and timing of ice advances remains ambiguous.

Faunal evidence of pre-Hirnantian cooling: The onset of the EPI corresponds to a notable faunal turnover, with many groups undergoing a decline in diversity, contrasting strongly with the rest of the pre-EPI Ordovician (Fig 2.2c; cf. Webby *et al.* 2004a). Armstrong (2007) showed that conodonts, ostracodes, and graptolites underwent a significant decline in normalised diversity at family and generic levels, interpreted as a consequence of cooling in the GICE event (Figs 2.2 & 6.1). It is certainly worth noting that these ecologically diverse clades are generally thought to achieve greater diversities at lower latitudes or warmer temperatures (Zalasiewicz 2001; Armstrong & Owen 2002; Cooper *et al.* 2004; Armstrong & Brasier 2005). This time also corresponds to a decrease in the relative extent of tropical carbonate platforms, which could reflect cooling (Fig 2.1b; Walker *et al.* 2002), and a faunal turnover amongst echinoderm clades (Sprinkle & Guensberg 2004).

Contrastingly, there appears to have been a warming episode in the mid Ashgill (*companulatus* and *anceps* zones), the so-called Boda event of Fortey & Cocks (2005). This was characterised by the poleward migration of a warm water fauna and the presence of carbonates at high latitudes. Though Cherns & Wheeley (2007) have since highlighted that these carbonates are of typical of a cooler water carbonate facies, the presence of even cool water carbonates at 60°N seems inconsistent with extreme glacial conditions in the mid Ashgill. A corollary of this short-lived relative warming event is that the preceding interval was relatively cold. In fact, Boucot *et al.* (2003) showed that prior to this warming event that a distinctive cool water fauna extended across Gondwana and its periphery and may have even

penetrated mid latitudes (Fig 2.2); they argued that this may have witnessed “extensive winter freezing conditions if not actual glaciation”.

Faunal distribution and diversity data may be used to test the possibility of cooling prior to the Hirnantian as discussed in Section 2.2.2. The GICE event and the Early Rakvere and Early Ashgill regressions occurred in an interval equivalent to time slices TS 5c-d of Webby *et al.* (2004a). So, if this interval was cooler than TS 5a-b (pre-EPI) and TS 6a-b (corresponding to the Boda event discussed above), this should be reflected in [1] decreased diversity of tropical reef building taxa; [2] migration of cool water taxa to lower latitudes; [3] decreased diversity at high latitudes especially in shallow-dwelling benthic taxa; and [4] decrease in the diversity of temperature-sensitive planktonic taxa, particularly in the range and relative abundance of pandemic taxa. Table 2.3 shows the following: [1] decreased diversity of stromatoporoids and tetradiid corals during TS 5c-d and minor extinction events in bryozoans and Baltoscandian rugose corals from TS 5c-d though Australasian rugose corals continue to increase in diversity in this interval; [2] beyond the palaeobiogeographic data discussed above, there is little other detailed information on faunal migrations at this time, although a cool water trilobite fauna migrated across Gondwana and the Argentine Precordillera during TS 5c-d; [3] nuculoid and solemyoid bivalves decrease in diversity at high latitudes during TS 5c-d and do not recover though there is little change in the diversity of gastropods or other bivalves which are common at low latitudes, there are also marked diversity minima in ostracodes in Gondwana and Estonia, from TS 5c-d brachiopods underwent a minor extinction event though trilobites were not similarly affected; [4] there was a major decrease in graptoloid diversity during TS 5c-d and the collapse of a cosmopolitan fauna, with a cool water endemic fauna emerging on Gondwana, whilst chitinozoans underwent a global decline in diversity from TS 5c-6c (if the anomalous Laurentia TS 5c-d bloom due to Taconic deepening is filtered out of the record). Though these faunal data present a more ambiguous signature of climatic variation than other evidence such as isotopic data or glaciogenic

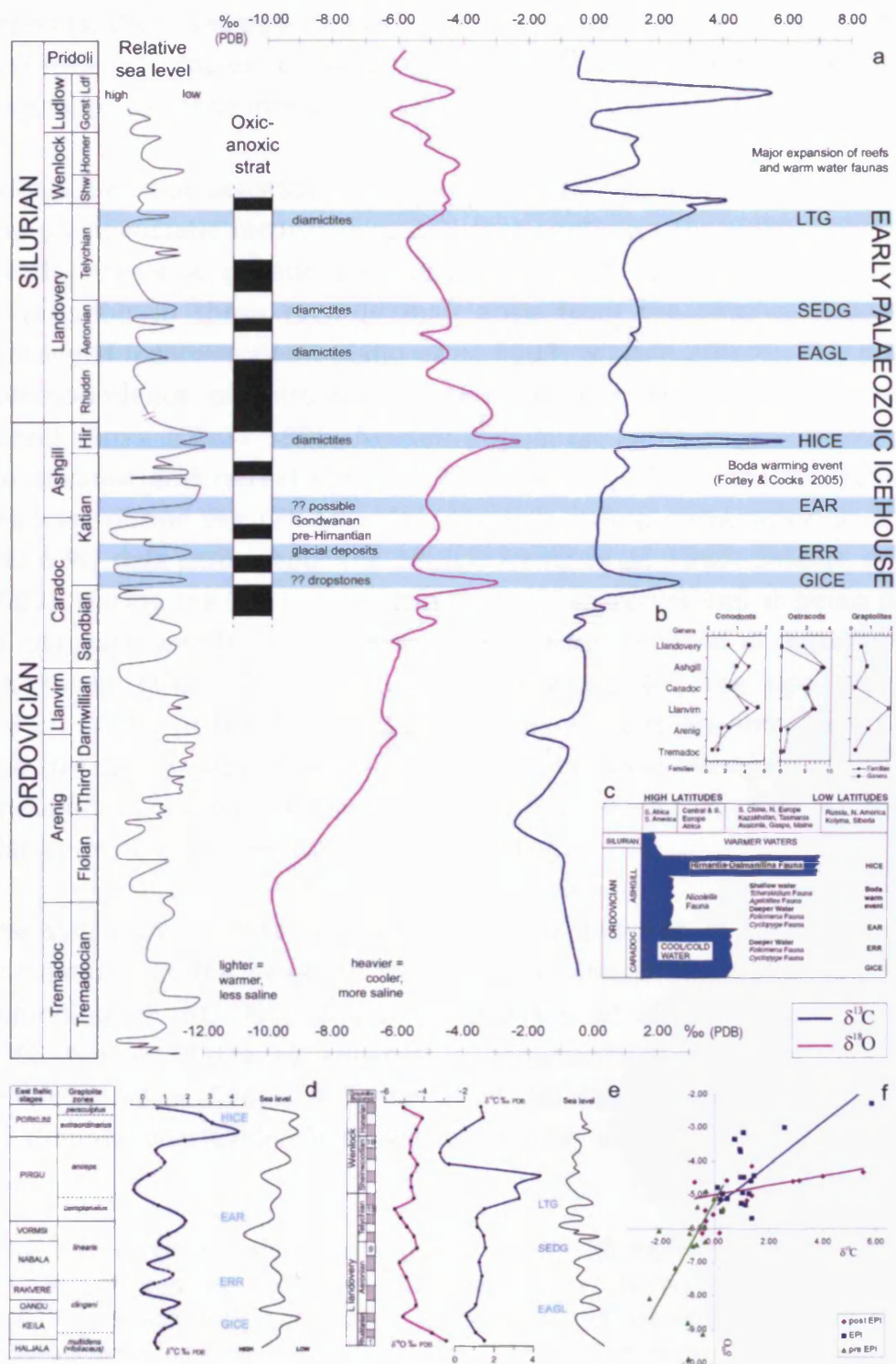


Fig. 2.2 Transgressive anoxia in the Early Palaeozoic Icehouse: (a) correlation of oxico-anoxic stratigraphy with glacioeustatic curves (after Nielsen 2004a [Ordovician] and Ross & Ross 1996 [Silurian]) and stable isotope curves (data in Table 2.4; (b) normalised diversity plots (after Armstrong 2007); (c) changing latitudinal distribution of brachiopod faunas in the Late Ordovician – early Silurian

deposits, there seems little evidence from faunal data to contradict the presence of cooler climatic episodes in the *clingani* – earliest *companulatus* zone interval.

Evidence of glacioeustasy: The coupled, rapid variation in the isotopic and glacioeustatic records (Fig. 2.2) that continues throughout the EPI clearly marks a genetic change in the Earth system. The strong co-variation in these records may arise from the interval being a prolonged icehouse event (Kaljo *et al.* 2003; Nielsen 2003b). The good correspondence of third/fourth-order variation in eustatic sea-level curves (Ross & Ross 1996; Nielsen 2003a, b), along with evidence of ice advance and retreat (Table 2.2) argues for ice-volume controlling sea-level during the EPI. Likewise, there is strong co-variation in $\delta^{13}\text{C}$ and $\delta^{18}\text{O}$ data throughout the EPI (cf. Azmy *et al.* 1998; Shields *et al.* 2003). During the EPI, I interpret positive $\delta^{13}\text{C}$ excursions as being due to increased weathering of shallow carbonates exposed in regressions (cf. Kump *et al.* 1999; Melchin & Holmden 2006; see also section 2.2.2). Whilst in the EPI, positive $\delta^{18}\text{O}$ excursions are interpreted as due to cooling rather than increased salinity alone (Azmy *et al.* 1998). Therefore, coupled, positive $\delta^{13}\text{C}$ & $\delta^{18}\text{O}$ excursions may indicate glaciations if consistent with other evidence.

The synchronous onset of significant, coupled isotopic and eustatic fluctuations at the onset of the Katian in the Ordovician, mark the beginning of the EPI (Fig. 2.2; Patzkowsky *et al.* 1997; Kaljo *et al.* 2003; Nielsen 2003a, b). This corresponds to the mid Caradoc *clingani* graptolite Zone (Cooper & Sadler 2004; Goldman *et al.* 2005). There is, though, also evidence of glacial erosion and a regression in the

Fig. 2.2 (*continued*) after Boucot *et al.* (2003); (d) high resolution isotope stratigraphy and sea-level curves for Ordovician of Estonia from Kaljo *et al.* (2003); (e) high resolution isotope stratigraphy and sea-level curves for the Silurian based on Azmy *et al.* (1998) and Loydell (1998) respectively; (f) scatter plot of Ordovician and Silurian stable isotope data from Table 2.4 with least-squared regression lines showing that coupled positive isotope excursions were unique to the EPI.

earliest Caradoc (Hamoumi 1999; Nielsen 2003a, b). The termination of the EPI is marked by the decoupling of isotopic and glacioeustatic variation in the earliest Wenlock (Fig. 2.2). In the latest Telychian, there is good evidence of ice (Table 2.2). Prior to the early Wenlock Ireviken excursion *sensu* Cramer & Saltzman (2005, 2007), there are coupled, positive excursions in $\delta^{13}\text{C}$ and $\delta^{18}\text{O}$ (Bickert *et al.* 1997; Azmy *et al.* 1998) during a regression (cf. Loydell 1998). The Ireviken excursion itself occurred at a time of climatic amelioration (Cramer & Saltzman 2005, 2007). It witnessed a positive $\delta^{13}\text{C}$ excursion at globally high sea-level (Cramer & Saltzman 2005, 2007). This positive $\delta^{13}\text{C}$ excursion was accompanied by a slight negative $\delta^{18}\text{O}$ excursion, which may indicate warming (Bickert *et al.* 1997; Azmy *et al.* 1998). The decoupling of isotopic and glacioeustatic co-variation in the early Wenlock (Fig. 2.2) marks a genetic change in the Earth system. It is unlike any interval in the EPI itself, and accompanied climatic amelioration witnessed in the development of extensive limestone reefs (e.g. Copper 1994; Brunton *et al.* 1998).

2.3.2 Climatic variation in the EPI

Within the EPI, individual glacial maxima were separated by warmer intervals (e.g. Fortey & Cocks 2005; Came *et al.* 2007), and recent research has highlighted clear variability in the Silurian palaeoenvironment (e.g. Jeppsson 1990; Aldridge *et al.* 1993; Bickert *et al.* 1997; Johnson 2006; Calner & Erikson 2006). Likewise, the Cenozoic Icehouse contains several notably warmer intervals in which ice may have been less extensive such as the Miocene and Pliocene (cf. Zachos *et al.* 2001). These warmer intervals along with the frequent evidence of ice formation and rapid, third/fourth-order variation in eustatic sea-level (e.g. Azmy *et al.* 1998; Caputo 1998; Loydell 1998; Hamoumi 1999; Ghiene 2003; Nielsen 2003a, b; Johnson 2006), suggests that ice sheets may have dynamically expanded and retreated during the EPI.

2.3.3 Major cooling events in the EPI

Seven cooling events in the EPI have been either assigned to existing named events or given stratigraphically descriptive names based on their nature. Some are referred to as regressions and others are called

glaciations depending on the weight of evidence. It seems that the pre-Hirnantian regressive events may have been influenced by the formation of land ice, with the Hirnantian and Llandovery glaciations characterised by relatively extensive advances of marine ice. I deal with each glacial maximum in turn below.

The Guttenberg regression (GICE) as defined in Table 2.1 and Figure 2.2 is named after the Guttenberg Limestone Member of the Decorah Fm in the Upper Mississippi Valley, USA, where the positive $\delta^{13}\text{C}$ excursion was first recognised (Hatch *et al.*, 1987). This carbon isotope excursion has subsequently been recognised elsewhere and is considered to represent a global event (e.g. Patzkowsky *et al.* 1997; Ainsaar *et al.* 1999; Kaljo *et al.* 2004). It was accompanied by a synchronous positive $\delta^{18}\text{O}$ excursion of earliest *clingani* graptolite Zone age (Shields *et al.* 2003; Tobin *et al.* 2005). The high-resolution chemostratigraphy of Ludvigson *et al.* (2004) shows that the GICE occurred after three other smaller positive $\delta^{13}\text{C}$ excursions, and that it took place in the *P. tenuis* conodont Zone and *americanus* graptolite Zone (equivalent to the earliest *clingani* Zone). In the Katian GSSP (Black Knob Ridge, Oklahoma, USA) there is a seemingly synchronous $\delta^{13}\text{C}$ excursion just above the Sandbian-Katian boundary (Goldman *et al.* 2005). This is coincident with the late Keila age regression noted by Kaljo *et al.* (2003) and Nielsen (2003a); and Ludvigson *et al.* (2004) also noted that the GICE occurred in a time of stratigraphical downlap. Due to the lack of well-dated glacial deposits in this interval (Table 2.2), there is no unambiguous link with ice formation, but it may represent a period of cooling as continental ice sheets were beginning to expand (cf. Patzkowsky *et al.* 1997).

The early Rakvere regression (ERR) is named after the stage in Estonia, where it is recognised in the carbon isotope and sequence stratigraphic records (Table 2.1; Fig 2.2). This regression took place within the latest *clingani* graptolite Zone (Nielsen 2003a), equivalent to the *A. superbus* conodont Zone (Nölvak *et al.* 2006). Though there is evidence for glacial erosion at this time (Table 2.2), there is no evidence for extensive tillite formation. This, along with its expression

Table 2.1 Glacial maxima in the EPI (*caption overleaf*).

Glacial maxima	Evidence for ice	$\Delta\delta^{13}\text{C}_{\text{PDB}}$	$\delta^{13}\text{C}_{\text{PDB}}$	$\Delta\delta^{18}\text{O}_{\text{PDB}}$	$\delta^{18}\text{O}_{\text{PDB}}$	extent of regression	Timing
Guttenberg regression	Poorly-dated glacial-erosive features in North Africa	$\sim+1.0\text{‰}$	$+1.7\text{‰}$	$\sim+2.3\text{‰}$	-2.7‰	Medium	early <i>caudatus</i> graptolite Zone
Early Rakvere regression	Poorly-dated glacial-erosive features in North Africa	$\sim+0.8\text{‰}$	$+1.8\text{‰}$	-	-	Medium	late <i>clingani</i> graptolite Zone
Early Ashgill regression	Poorly-dated Ashgill tillites and glacial erosive features in North Africa	$\sim+1.2\text{‰}$	$+2.0\text{‰}$	-	-	Large	end <i>linearis</i> graptolite Zone
Hirnantian glaciation	Pan-Gondwanan tillites & diamictites containing Hirnantia fauna	$\sim+4.0\text{‰}$	$+4.3\text{‰}$	$\sim+4.2\text{‰}$	0‰	Large	<i>extraordinarius</i> -early <i>persculptus</i> graptolite zones
Early Aeronian glaciation	<i>gregarius</i> Zone diamictite in South America	$\sim+2.0\text{‰}$	$+3.0\text{‰}$	$\sim+0.6\text{‰}$	-4.5‰	Small	<i>gregarius</i> (? <i>magnus</i>) graptolite Zone
<i>sedgwickii</i> s.l. glaciation	Well-dated diamictites in South America	$\sim+0.5\text{‰}$	$+2.0\text{‰}$	$\sim+0.7\text{‰}$	-4.4‰	Medium	<i>sedgwickii</i> graptolite Zone
late Telychian glaciation	Well-dated diamictites in South America	$\sim+1.5\text{‰}^*$	$+2\text{‰}^*$	$\sim+1.0\text{‰}^*$	-4.6‰^*	Large	? <i>insectus-lapworthi</i> graptolite zones

* these excursions occur in the late Telychian significantly preceding the Ireviken excursion *sensu* Cramer & Saltzman (2005, 2007).

in the sea-level and isotopic record, may indicate that it was a relatively small, short-lived event.

The early Ashgill regression (EAR) appears to be a more significant event based on both its sea-level and isotopic record (Table 2.1; Fig. 2.2). Nielsen (2003a) noted significant regression in the early Ashgill *complanatus* graptolite Zone. This is synchronous with regression and a positive $\delta^{13}\text{C}$ excursion noted by Kaljo *et al.* (2004) at the basal Pirgu stage in Estonia (Nölvak *et al.* 2006). There is good evidence for glacial sediments being deposited in the Ashgill of North Africa (which was close to the palaeomagnetic south pole). But this regression cannot be tied to any one particular high-latitude event, due to imprecision in the biostratigraphy of these successions (Table 2.2).

The Hirnantian glaciation (HICE) occurs as two pulses of glaciation within the *extraordinarius-persculptus* graptolite Zones (Sutcliffe *et al.* 2000). It represents the glacial maximum of the EPI and has received extensive study. It is well constrained and clearly globally extensive. The extent of the eustatic and isotopic variations associated with this are shown in Table 2.1 and Figure 2.2, with more detailed treatment of this event being found in Brenchley *et al.* (1994, 2003), Marshall *et al.* (1997) and Sutcliffe *et al.* (2001).

The early Aeronian glaciation (EAGL) has a significant expression in marine carbon isotope values, but this may also represent an increased effect of carbonate weathering relative to the Ordovician glaciations. There is clear evidence for ice-formation during the *gregarius*

Table 2.1 (*overleaf*) Name, age and evidence for each of the seven glacial maxima in the EPI; $\delta^{13}\text{C}_{\text{PDB}}$ = most positive value in positive carbon isotope excursion based on regional isotopic compilations; $\Delta\delta^{13}\text{C}_{\text{PDB}}$ = total change in carbon isotope values during positive isotope excursions based on regional isotopic compilations; $\delta^{18}\text{O}_{\text{PDB}}$ = most positive value in positive oxygen isotope excursion recorded in brachiopod shells; $\Delta\delta^{18}\text{O}_{\text{PDB}}$ = total change in oxygen isotope values during positive isotope excursions recorded in brachiopod shells; oxygen isotope data taken from Tobin *et al.* (2005) for the Guttenberg regression, from Brenchley *et al.* (1994) for the Hirnantian Glaciation in the Baltic region, and from Azmy *et al.* (1998) for all Silurian events; all other data compiled from Table 2.2, Fig. 2.2, Kalio *et al.* (2007). and references therein.

graptolite Zone (Tables 2.1 & 2.2), but this is a long interval, which can be subdivided into the *triangulatus*, *magnus* and *argenteus* zones (see Hutt 1974). Precisely how ice formation in this event correlates with sea-level is unclear: the Rhuddanian-Aeronian boundary regression seen in the Ross & Ross (1996) sea-level curve is not recognised in other records, which show marked regressions at or around the *magnus-argenteus* graptolite Zone boundary (Johnson *et al.* 1991; Loydell 1998; Johnson 2006). Azmy *et al.* (1998) show the onset of a positive $\delta^{13}\text{C}$ & $\delta^{18}\text{O}$ excursion in the *triangulatus* Zone, but do not present data for the *magnus* and *argenteus* zones. Kaljo *et al.* (2003) illustrate a longer $\delta^{13}\text{C}$ excursion, which both they and Johnson (2006) correlate to an early Aeronian glaciation.

The *sedgwickii* graptolite Zone glaciation (SZG) is discussed at length below. Loydell (1998) and Johnson (2006) both show major regressions at this time. Azmy *et al.* (1998) and Johnson (2006) argued for glaciations based on isotopic data, which I note correspond to well-dated diamictites (Table 2.2).

The late Telychian glaciation (LTG) is the final glacial maximum of the EPI. As noted above, the final pulse of diamictite deposition in South America can be assigned to the late Telychian, though cannot be constrained to any particular zone (Table 2.2). The late Telychian is coincident with regressions: Figure 2.2 illustrates a rapid sea-level fall in the late *insectus* graptolite Zone (see also the Appendix), while Loydell (1998) shows a rapid regression in the *lapworthi* graptolite Zone with a low stand throughout the *lapworthi-insectus* interval, also recognised in southwest Siberia by Yolkin *et al.* (1997). During this interval, Azmy *et al.* (1998) show a positive $\delta^{13}\text{C}$ and $\delta^{18}\text{O}$ excursion, beginning in the *crenulata* graptolite Zone and reaching a maximum in the *centrifugus* graptolite Zone. Likewise, Kaljo *et al.* (1998, 2003) show that the onset of this positive $\delta^{13}\text{C}$ transition occurred in the late Llandovery, with subsequent studies placing this in the *Pt. amorphognathoides* conodont Zone in Estonia (Kaljo & Martma 2006) and possibly towards its base (see Cramer & Saltzman 2005). As such, I suggest this glaciation occurred within the *lapworthi-insectus* graptolite Zone interval.

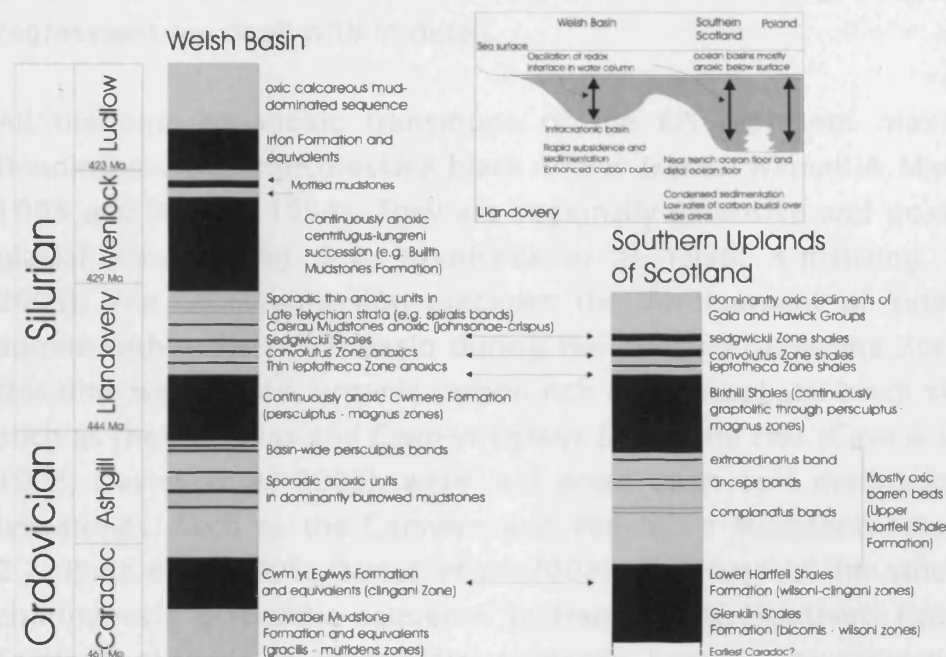


Fig. 2.3 UK oxidic/anoxic stratigraphy for the EPI. Correlation of marine anoxia between UK depositional basins based on the widespread occurrence of graptolitic mudrocks, with inset schematic showing the differing depositional environments associated with this facies. Stratigraphies and inset compiled from original work of Toghil (1968); Cave (1979); Baker (1981); White *et al.* 1991. Davies *et al.* (1997, 2003); Pratt *et al.* 1995; Zalasiewicz *et al.* (1995); Porębska & Sawłowicz (1997); Schofield *et al.* (2004); Verniers & Vandenbroucke (2006). Note that the Hirnantian and Llandovery oxidic-anoxic stratigraphy of the Welsh Basin bears close resemblance to the Lake District and Howgill Fells succession of Northern England (Rickards 1970; Hutt 1974; Rickards & Woodcock 2005). After Page *et al.* (2007).

2.4 Oxidic-anoxic stratigraphy and sea-level in the EPI

Correlating the UK oxidic-anoxic stratigraphy against glacioeustatic sea-level curves reveals a repeated relation between black shale deposition and deglacial transgressions throughout the EPI (Figs 2.2 & 2.3). Conversely, glaciations themselves correspond to well-oxygenated deep waters. Comparison with deep-water successions influenced by the Rheic and Palaeotethys oceans suggests these oxidic-anoxic transitions may have had global extent. The glacioeustatic

sea level and oxic-anoxic stratigraphy is discussed briefly below, before the post-Hirnantian transgression and *sedgwickii* Zone regressions are dealt with in detail.

All the oxic to anoxic transitions of the EPI represent maximum flooding surface transgressive black shales (*sensu* Wignall & Maynard 1993 and Wignall 1994). They are regionally extensive and post-date glacial maxima (Fig. 2.2; Woodcock *et al.* 1996; Armstrong *et al.* 2005). The GICE regression precedes the development of extensive anoxia within the Welsh Basin during the *clingani* graptolite Zone. At this time widespread, organic carbon-rich and phosphatic black shales, such as the Nod Glas and Cwm-yr-Eglwys Mudstone Fms (Cave & Dixon 1993; Davies *et al.* 2003), were laid down upon oxic mudrocks and limestones, such as the Carswyn and Penyraber Mudstone Fms (Fig. 2.2; Pratt *et al.* 1995; Davies *et al.* 2003). And even in the otherwise continuously graptolitic sequence in Hartfell Spa (Southern Uplands, Scotland) there is an afossiliferous interval between the *wilsoni* and *clingani* zones that could reflect a break in anoxia (cf. Zalasiewicz *et al.* 2005). In the Platteville-Decorah formations of eastern Iowa (USA) the Guttenberg Member is brown shale (Ludvigson *et al.* 2004). This occurs above a well-laminated shale and widespread phosphatic bed of the Spects Ferry Member and below the well-laminated shales and blackened/phosphatic hardgrounds of the Ion Member (Ludvigson *et al.* 2004). Likewise, pyritic graptolite shales of *clingani* Zone age Nakkholmen Fm. in the Oslo area (Norway) overlie limestones, as do coeval graptolite shales in the lower Mossen Fm. of Västergötland (Nielsen 2003a). This represents an oxic-anoxic transition that reflects a profound drowning event (Nielsen 2003a, b).

The early Ashgill regression preceded the *anceps* graptolite Zone transgression, with the UK record witnessing simultaneous intervals of black shale deposition in an otherwise oxic succession (Fig. 2.3). For example, the 'Red Vein' in Wales, a thin unit of anoxic mudstones bearing graptolites of probable *anceps* graptolite Zone age (e.g. Schofield *et al.* 2004), appears synchronous with the *anceps* bands in Scotland (Williams 1982). The Hirnantian glaciation, with an acme in the *extraordinarius* graptolite Zone (Sutcliffe *et al.* 2000), preceded the

deposition of globally extensive transgressive black shales in the *persculptus-acuminatus* graptolite zones (Fig. 2.4 & text below). Likewise the *sedgwickii* graptolite Zone glacial event is characterised by the deposition of oxic facies during a lowstand, which is sandwiched between transgressive black shales (Fig. 2.5 & text below). The *convolutus* graptolite Zone represents a major transgression and global highstand following the early Aeronian glaciation, with widespread black shale deposition noted in Loydell (1998), synchronous with the UK *convolutus* bands of graptolitic shale (Fig. 2.3). Similarly, the deglacial transgression in the latest Telychian is characterised by the onset of anoxia and the deposition of marine black shales in the *centrifugus* Zone in the UK. These include the BUILT Mudstones in the Welsh Basin (Woodcock *et al.* 1996; Zalasiewicz & Williams 1999) and the Brathay Mudstones in northern England (Rickards 1970; Rickards & Woodcock 2005). These were both deposited on essentially oxic, late Llandovery successions (Davies *et al.* 1997; Rickards & Woodcock 2005). In Baltoscandia, this event also sees the deposition of graptolitic shales on greenish grey marlstones in the Ohesaare core from Estonia (Loydell *et al.* 1998a) and on oolitic limestone/grey-green shale interbeds in Bornholm (Bjerreskov 1975; AAP unpublished observations April 2006). Similarly, Lüning *et al.* (2005) noted the deposition of “hot shales” on the north African/Arabian margin during the *centrifugus* to *firmus* graptolite zones. The relation between deglaciation, transgression and anoxia in the late Telychian-early Wenlock has been reviewed in depth by Cramer & Saltzman (2007). Further examples of transgressive black shales deposited after the Llandovery glaciations may be found in Loydell (1998).

During the EPI, the deposition of bioturbated facies, representing conditions of deep-marine oxygenation, occurred during regressions and glacial maxima (Brenchley 1988; Loydell 1998; Fig. 2.2). The Hirnantian and *sedgwickii* Zone glacial maxima correspond to intervals of grey shale and deposition of mottled (i.e. bioturbated) mudstones (Figs 2.4 & 2.5). Likewise, the positive carbon isotope excursion in the mid-*gregarius* graptolite Zone that marks the early Aeronian glaciation may correspond to the onset of oxic deposition in the mid-*magnus*

graptolite Zone of the Welsh Basin (Fig. 2.3). In Black Knob Ridge, Oklahoma, the maximum $\delta^{13}\text{C}$ excursion corresponding to GICE occurs in an interval with extremely diminished C_{org} content in an otherwise organic-rich sequence (Goldman *et al.* 2005). This perhaps represents an interval of increased deep-water ventilation (cf. Ludvigson *et al.* 2004). The early Rakvere regression (latest *clingani* graptolite Zone) may possibly correlate with the transition from black shales to limestone at Whitland, south Wales. Also, the Fjäckå Shales of Sweden are deposited on the well-oxygenated facies of the Slandrom Limestone of Sweden and Bestorp Limestone of Västergötland, representing transgressive black shales deposited after the early Rakvere event (Männil & Meidla 1994).

2.4.1 Transgressive anoxia: post-Hirnantian glaciation anoxic event

The late *persculptus* and *acuminatus* graptolite Zones are characterised by deposition of globally-extensive transgressive black shales (Fig. 2.4) immediately following the *extraordinarius*-early *persculptus* graptolite Zone acme of the Hirnantian glaciation (Sutcliffe *et al.* 2000, 2001), suggesting a fundamentally deglacial origin for the onset of global marine anoxia. This followed the enhanced deep ocean circulation and oxygenation that characterised the Hirnantian glaciation (Brenchley 1988; Brenchley *et al.* 1994; Armstrong & Coe 1997). High-palaeolatitude sedimentary successions typically consist of Hirnantian glacial deposits immediately overlain by black shales (e.g. Sutcliffe *et al.* 2001; Armstrong *et al.* 2005, 2006). Low-palaeolatitude settings see unambiguously oxic facies such as deep-water bioturbated mudstones overlain by deglacial black shales (e.g. Mu 1988; Armstrong & Coe 1997; Davies *et al.* 1997; Chen *et al.* 2000, 2005; Verniers & Vandenbroucke 2006). Shallow-water shelly faunas in low- to mid-palaeolatitudes may also be buried below *persculptus* graptolite Zone black shales (e.g. Bjerreskov 1975; Mu 1988; Davies *et al.* 1997; Chen *et al.* 2000, 2005), though some shallow successions in the palaeotropics may see limestone deposition going on uninterrupted (e.g. Barnes & Bolton 1988). These deglacial black shales are widely palaeogeographically distributed and represent a global event (Fig. 2.4) perhaps comparable to the Mesozoic oceanic anoxic events (cf. Cohen *et al.* 2004).

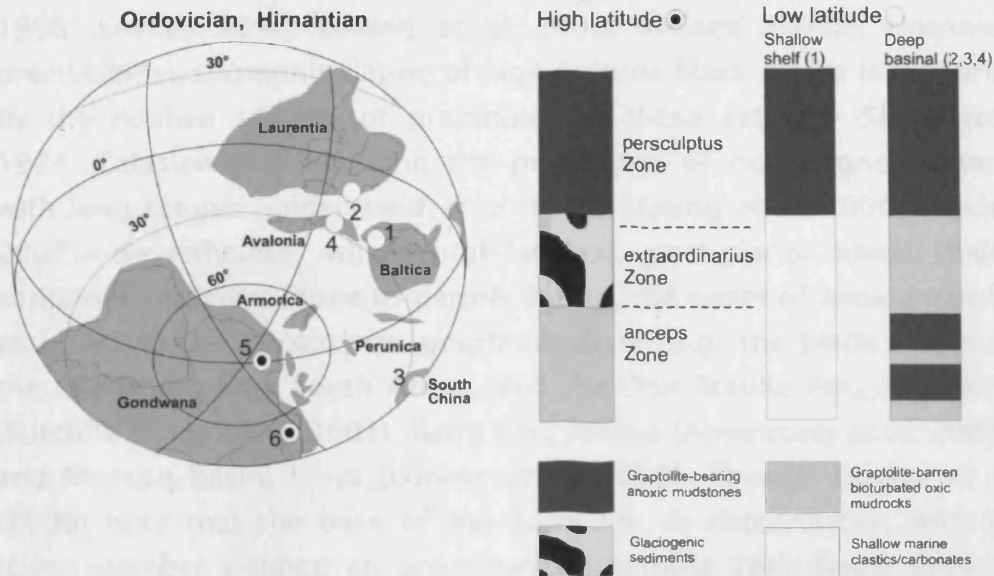


Fig. 2.4 The *persculptus* graptolite Zone anoxic event: schematic lithographic logs showing the onset of transgressive anoxia in different settings. Palaeogeographical reconstruction showing the position of continents and associated terranes in the Hirnantian, annotated with localities where black shale is deposited on a maximum flooding surface: 1. Bavnegård Well, Bornholm, Denmark (Bjerreskov 1975); 2. Dob's Linn, Scotland UK (Toghill 1968; Armstrong & Coe 1997; Verniers & Vandenbroucke 2006); 3. Fenxiang, Yingang, Yangtze region, southern China (Mu 1988; Chen *et al.* 2000, 2005); 4. Cwmere Fm., central Welsh Basin, UK, (Woodcock *et al.* 1996; Davies *et al.* 1997); 5. Murzuq Basin, Libya (Lüning *et al.* 2000); 6. Batra Fm., Jordan (Armstrong *et al.* 2005). Palaeogeographic reconstructions mainly after Torsvik *et al.* (1998). The relative position of Gondwana, Armorica, Baltica, Avalonia, Laurentia and Siberia are largely unmodified. The reversed position of the North China plate in equatorial northern latitudes and the southern low-latitude position of Tarim plate is after Zhao *et al.* (1996); the South China plate had drifted from temperate to low-southern latitudes and approached the North China Plate by the Late Ordovician. In the Ordovician Kazakhstan was not a single plate but an assemblage of island arcs and microplates (Apollonov 2000; Webby *et al.* 2000). In particular, palaeomagnetic data presented recently by Baženov *et al.* (2003) suggest that during the Late Ordovician North Tien Shan maintained a subequatorial southern position without any significant latitudinal displacement. After Page *et al.* (2007).

Deposition of regionally-extensive black shales on maximum flooding surfaces (*sensu* Wignall & Maynard 1993 and Wignall 1994) in the *persculptus* graptolite Zone provides strong evidence for their onset in

the end Ordovician-early Silurian transgression (Ross & Ross 1995, 1996; Loydell 1998; Lüning *et al.* 2000; Nielsen 2003a). However, precise biostratigraphic dating of high-latitude black shales is hindered by the relative scarcity of graptolites in these settings (Skevington 1974; Zalasiewicz 2001) and the prevalence of non-diagnostic taxa with long ranges (underwood *et al.* 1997; Lüning *et al.* 2000; Loydell 2007). Nevertheless, where high-latitude, post-glacial black shales contain a sufficient fauna to permit dating, the onset of anoxia can be assigned to the *persculptus* graptolite Zone: e.g. the black shales of the Cedarberg Fm., South Africa, and the Don Braulio Fm., Argentina (Sutcliffe *et al.* 2000, 2001); Batra Fm., Jordan (Armstrong *et al.* 2005); and Murzuq basin, Libya (Lüning *et al.* 2000). Though Lüning *et al.* (2006) note that the base of the Batra Fm. is diachronous, with its lower member yielding an *acuminatus* graptolite Zone fauna towards the (present day) North (Armstrong *et al.* 2005, 2006), this is neither inconsistent with the onset of anoxia occurring in the *persculptus* graptolite Zone, nor is it inconsistent with deposition of the Batra Fm. as a maximum flooding surface black shale. As the transgression continued into the early Silurian, the oxygen minimum zone would have shoaled further up the shelf (Armstrong *et al.* 2006). The formation of early Silurian black shales, such as at the base of the Qusaiba Shale, Saudi Arabia (Aoudeh & Al-Hajri 1995), is evidence that oceanic anoxia and deposition of maximum flooding surface black shales continued as the transgression continued.

The influx of deglacial melt-water in the oceans of the *persculptus* graptolite Zone may have been critical to the onset of transgressive anoxia: it may have increased marine stratification through the formation of low-salinity surface waters and, by providing a source of nutrients via continental weathering, stimulated marine productivity. This may be analogous to the formation of sapropels in the Neogene Mediterranean basin (Rohling & Gieskes 1989; Rohling 1994; Scrivner *et al.* 2004). Buoyant, low-salinity surface waters, strengthening the pycnocline in the deglacial Hirnantian ocean may have precluded deep-water thermohaline circulation to sufficiently maintain a well-oxygenated seafloor. Periglacial outwash may have carried sufficient nutrients to fuel the deposition of the 'hot shales' of North

Africa and Arabia (cf. Meybeck 1982), which are characterised by a total organic-carbon content of up to 17% (Lüning *et al.* 2000), well above that found in normal black shales.

Some authors have declared that “hot shale” deposition may be a result of upwelling (Lüning *et al.* 2000, 2005, 2006), but this is in disaccord with both their widespread, synchronous deposition, and with GCMs of Hirnantian circulation (Hermann *et al.* 2003, 2004a, b). Upwelling is a regionally-localised phenomenon and the oxygen minimum zone associated with upwelling zones is only stable on decadal time scales (Wignall 1994). Moreover, meridional and monsoonal coastal-upwelling is restricted to low- to mid-latitudes (Parrish 1982), so are unlikely to apply to the ‘hot shales’, which occur at high palaeolatitudes. Meanwhile, end-Ordovician continental configuration is inconsistent with widespread zonal coastal upwelling (Armstrong *et al.* 2006). Zonal upwelling occurs when north or south continental margins lie adjacent to the major zonal wind systems (Parrish 1982). Comparing modern palaeogeographical reconstructions (Scotese & McKerrow 1991; Cocks & Torsvik 2002) with the high-latitude zonal wind predicted in the late Ordovician atmospheric simulations of Parrish (1982) shows that major winds were primarily orthogonal to the Gondwanan margin, making widespread zonal upwelling untenable. This is borne out by recent, more sophisticated GCMs for the late Ordovician, that show predominately onshore ocean currents around the North African and Arabian margins of Gondwana (Hermann *et al.* 2003, 2004 a, b). As such, upwelling alone can neither account for the simultaneous onset of globally widespread anoxia in the *persculptus* graptolite Zone nor for the widespread high-latitude occurrence of the most organic-rich shales.

Furthermore, deglacial melting would most likely be to the detriment of the increased thermohaline circulation needed to sustain upwelling. In the Quaternary of the North Atlantic, intervals of meltwater outwash are associated with increased ocean stratification and more sluggish deep-water circulation (Rahmstorf 2002). Instead, an alternative nutrient source may lie in increased continental weathering during deglaciation, providing a major source of both major and trace

nutrients (Broecker 1982; Meybeck 1982) and stimulating productivity (as modelled by Kump & Arthur 1999). Given that the locus of glacial-melting is focussed on the Gondwana palaeocontinent, this nutrient source could explain the relatively increased organic content of high-palaeolatitude black shales compared to those in low-palaeolatitude black shales. This would leave anoxia at low-palaeolatitudes as a consequence of increased ocean stratification and decreased thermohaline circulation due to high-palaeolatitude ice melting. This, coupled with sediment starvation (cf. Wignall 1991), would lead to an expanded oxygen-minimum zone. Hence, periglacial run-off provides a mechanism for anoxia that would have simultaneously increased global sea-water stratification as well as stimulating productivity and export production (see schematic in Fig. 2.6). This highlights the fundamentally deglacial nature of transgressive black shales in the EPI.

2.4.2 Regressive oxygenation: the *sedgwickii* graptolite Zone event

The *sedgwickii* graptolite Zone is marked by global regression of plausibly glacial origin during which sediments were deposited in well-oxygenated deep water overlying earlier black shales (Table 2.1; Figs 2.2 & 2.5). Graptolites are rarely preserved in extensively bioturbated facies, though graptolites could clearly exist in well-oxygenated waters (Armstrong & Coe 1997; Floyd & Williams 2003). Therefore, bioturbated graptolite-free intervals in otherwise continually graptolitic successions may be taken as evidence of increased sedimentary ventilation, seen in both high and low-latitude successions in the Iapetus, Rheic and Palaeotethys oceans (Fig. 2.5 & references therein). It is clear that the boundary between the preceding *convolutus* graptolite Zone and the *sedgwickii* graptolite Zone is characterised by the development of oxic strata, and that widespread anoxia is again developed by the onset of the *guerichi* graptolite Zone (Loydell 1998).

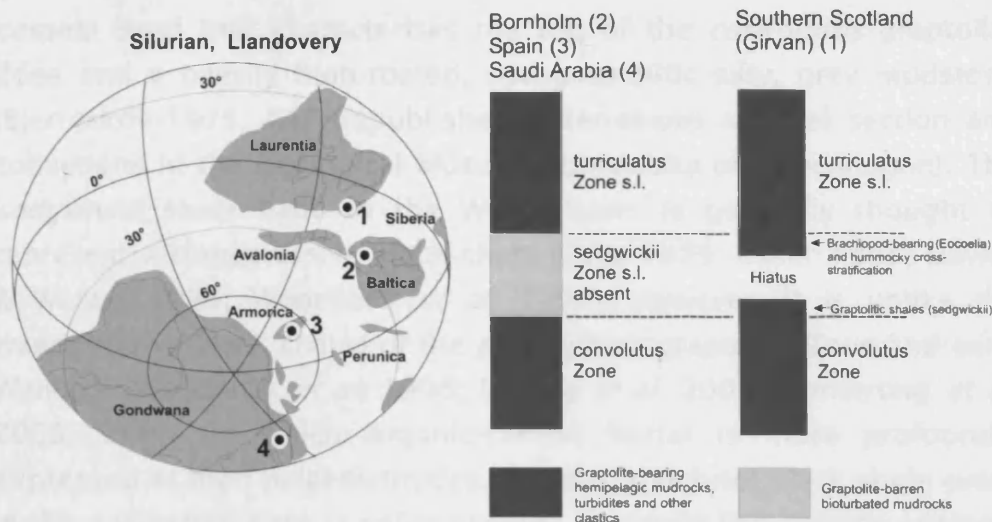


Fig. 2.5 The *sedgwickii* graptolite Zone glaciation: schematic lithographic logs showing evidence of regressive oxygenation. Palaeogeographical reconstruction showing the position of continents and associated terranes in the mid Llandovery, showing global event of deep-water oxygenation: 1. Girvan Group, southwest Scotland, UK (Floyd & Williams 2003); 2. Øleå, Bornholm, Denmark (Bjerreskov 1975); 3. Western Iberian Cordillera, northeast Spain (Gutiérrez-Marco & Štorch 1998); 4. Qusaiba Shale, Qalibah Fm., Saudi Arabia (Miller & Melvin 2005; AAP/JAZ/MW unpublished observations). Palaeogeographic reconstructions again mainly after Torsvik *et al.* (1998), with amendments as noted in Fig 4. Also, by the beginning of the Silurian, the amalgamation of some Kazakh crustal terranes probably led to the formation of a substantial land mass north of Tarim and South China (Koren *et al.* 2003). The position of Annamia close to South China and the Karakum-Tajik plate is mainly based on the strong affinities of the late Silurian (Ludlow-Pridoli) brachiopod faunas (Rong *et al.* 1995; Thong-Dzuy *et al.* 2001). After Page *et al.* (2007).

However, the *sedgwickii* graptolite Zone also contains a distinctive interval of black shale, which is only seen in certain successions from the Iapetus and Rheic oceans. In UK successions in Wales and Dob's Linn, this thin black shale is sandwiched between a sequence of grey shales and mottled mudstones (e.g. Toghill 1968; Cave 1979). The *sedgwickii* Zone of the Kullatorp core (Västergötland, Sweden) comprises greyish green mudstones in a succession of otherwise graptolitic black shales. However, the Silvberg and Gulleråsen-Sanden sections of Dalarna contain a finely-laminated shale yielding *St. sedgwickii* (Loydell 1998). In Bornholm, Denmark, however, there is an abrupt transition between the highly-graptolitic black shale of the

cometa Band that characterises the top of the *convolutus* graptolite Zone and a heavily bioturbated, non-graptolitic silty, grey mudstone (Bjerreskov 1975; AAP unpublished observations on Øleå section and collections in the Geological Museum, University of Copenhagen). The *sedgwickii* shale band in the Welsh Basin is generally thought to represent a transgressive black shale (Cave 1979; Baker 1981; Davies & Waters 1995; Woodcock *et al.* 1996). However, it is unlike the transgressive black shales of the *persculptus* graptolite Zone and early Wenlock (Woodcock *et al.* 1996; Lüning *et al.* 2005; Armstrong *et al.* 2005, 2006) in which organic-carbon burial is more profoundly expressed at high palaeolatitudes. Instead, this brief black shale event in the *sedgwickii* Zone is only observed at certain low-latitude settings. There is no major graptolitic shale burial associated with the *sedgwickii* Zone age strata in the Qusaiba Shale, Saudi Arabia (Zalasiewicz *et al.* 2007). This may reflect increased isolation of semi-enclosed basins at low sea-level, suggesting local rather than global significance (e.g. Loydell 1994).

There is good evidence of a regression within the lithofacies deposited during the *sedgwickii* graptolite Zone, and no graptolites have been recovered from the low-latitude successions of the Western Iberian Cordillera, Spain (Gutiérrez-Marco & Štorch 1998), the Prague Basin, Czech Republic (Štorch 1986, 1994), and the Canadian Arctic (Melchin 1989). In Girvan, southern Scotland, UK, the late *sedgwickii* Zone contains shallow-water brachiopods and deposits with hummocky cross-stratification in the Lower Camregan Grits Fm. overlying the black shales of the Pencleuch Shale Fm. (Floyd & Williams 2003), and in Spengill, Howgill Fells, UK, the *sedgwickii* graptolite Zone contains the only occurrence of limestones and grits in its Llandovery succession (Rickards 1970). The evidence for a regression in UK deep-water strata may correlate with the regressions recognised in the *sedgwickii* s.l. graptolite Zone in sequence stratigraphic analyses of shallow-water facies in Baltoscandia, North America, and Siberia (Ross & Ross 1996; Johnson 1996; Yolkin *et al.* 1997), and coincides with the formation of diamictite in Gondwana (Caputo 1998); whilst the overlying *guerichi* graptolite Zone itself appears to mark the onset of extensive marine

anoxia (Loydell 1998), which may be linked to a transgression (Fig. 2.2).

Increased oxygenation of the marine realm in the *sedgwickii* graptolite Zone may be a consequence of high-latitude ice formation stimulating more rapid thermohaline circulation, as is seen in the modern day Atlantic (Rahmstorf 2002). The *sedgwickii* Zone regression is coincident with diamictite deposition in South America (Caputo 1998; Table 2.1; Fig. 2.2), suggesting glacioeustatic control. The formation of marine ice would have resulted in brine rejection, creating cold, dense waters at high latitudes. On sinking, these may have driven a more vigorous deep-water circulation, providing a greater flux of oxygen to the deep oceans (see Fig. 2.6), consistent with the well-ventilated deep-water facies seen in glacial maxima during the EPI (Fig. 2.2; Brenchley 1988). The global cessation of anoxic facies at the end of the *convolutus* graptolite Zone and their return in the *guerichi* graptolite Zone reflects a third-order change in depositional style, consistent with a glacioeustatic control on oceanic redox state (Church & Coe 2003).

2.5 A simple model for carbon burial and glacioeustasy in the EPI

During the EPI there was a fundamental link between glacioeustatic sea-level change and the burial of organic carbon in deglacially transgressive black shales, which may have represented a negative feedback mechanism that served to stabilise climate (Fig. 2.6), and prevented the onset of runaway greenhouse conditions. Given that sea-level may represent a proxy for atmospheric temperature, which itself is a function of pCO₂, the deposition of globally extensive black shales on maximum flooding surfaces may have served to slow the initial warming after the glacial maxima by drawing down CO₂ from the ocean-atmosphere system. This would sustain the EPI and prevent the onset of greenhouse conditions that characterised most of the Early Palaeozoic (Frakes *et al.* 1992; Gibbs *et al.* 2000; Montañez 2002; Church & Coe 2003).

This model for deposition of black shales due to periglacial meltwater increasing both productivity and ocean stratification predicates that oceanic anoxia was intimately linked to glacioeustasy. Black shale deposition in transgressions may have been significant to influence cooling, and therefore a regression, by drawing down atmospheric carbon (see the schematic graph in Fig. 2.6). Likewise, the onset of well-oxygenated oceans due to brine rejection driving deep water circulation may have served to prevent organic carbon burial to sustain fully glacial conditions, which might have led to another transgression. With global marine oxygenation linked to ice formation and melting, I infer a strong link between organic carbon burial in black shales, sea level and atmospheric CO₂ during the EPI. This model now needs to be rigorously tested against both the sedimentary record of the EPI and by developing theoretical models of the carbon budget.

2.5.1 Black shale deposition and the EPI carbon cycle

Though I have clearly shown a strong link between black shale deposition and deglacial transgressions, relating anoxia and carbon-burial flux is not straightforward. Models of the carbon cycle show a significant increase in carbon burial as black shales close to the Ordovician-Silurian boundary (Fig. 2.1c). Meanwhile, Ronov *et al.* (1980) estimated that the amount of organic carbon buried in Ordovician and Silurian black shales is comparable to that in Permo-Carboniferous strata, a time when the organic reservoir may have exerted a significant influence on atmospheric CO₂ (e.g. Bruckschen *et al.* 1999). As the EPI corresponds to a major low in shelf-carbonate deposition, organic carbon burial in black shales may have been critical to regulating the carbon cycle (Fig. 2.1; Patzkowsky *et al.* 1997). The increase in atmospheric O₂ during this interval is consistent with increased organic-carbon burial (Fig. 2.1a, c; cf. Berner 2003; Catling & Clare 2005), empirically linking black shale deposition and atmospheric change. Though I have shown that widespread black shale burial occurs in transgressions, the lateral extent of black shale is unclear, making it hard to estimate the carbon burial flux from rock volume.

Oxic-anoxic transitions occur in open-ocean settings, demonstrating that this is not a phenomenon exclusive to restricted basins or epicontinental seas (cf. Porębska & Sawłowicz 1997). Similarly, anoxia may be developed in shelf settings relatively close to the storm wave-base, such as in the Qusaiba Shale of Saudi Arabia, where anoxic or dysoxic facies alternate with bioturbated mudstones and facies yielding benthic faunas (Miller & Melvin 2005). Precisely how shallow anoxic conditions may extend in the EPI is unclear (cf. Pancost *et al.* 1998). Whether these transgressive anoxic events represent shoaling of an expanded oxygen minimum zone onto the shelf or whether there was widespread whole oceanic anoxia in the EPI remains uncertain.

The oxygenation-depth profile of EPI oceans is largely unknown. I concur with Cramer & Saltzman (2005; 2007) that the deposition of organic carbon in epicontinental black shales cannot account for positive $\delta^{13}\text{C}$ excursions in the Silurian. As they noted, widespread deposition of black shales in epicontinental seas does not coincide with these excursions. Neither do these data show evidence for increased carbon burial in deep-water settings with strong oceanic influence during any of the positive $\delta^{13}\text{C}$ excursions (Table 2.1; Fig. 2.2). I also contest the suggestion of upwelling and increased carbon burial as an explanation for positive $\delta^{13}\text{C}$ excursions in the EPI (e.g. Young *et al.* 2005). All positive $\delta^{13}\text{C}$ excursions in the EPI are best explained by increased weathering of shallow marine carbonates in regressions (e.g. Kump *et al.* 1999; Melchin & Holmden 2006) as noted in the Section 2.7. Young *et al.* (2005) argued that the Guttenberg regression was synchronous with biomarker evidence for photic-zone anoxia based on the data of Pancost *et al.* (1998). This however represents a miscorrelation. The high-resolution stratigraphy of Ludvigson *et al.* (2004) demonstrates that the interval of photic zone anoxia identified by Pancost *et al.* (1998) corresponds to the Specks Ferry Member of the Platteville Fm. The Specks Ferry Member underlies the Guttenberg Limestone, preceding the EPI, whilst the Guttenberg regression corresponds to lithological evidence of a more oxic interval (cf. Ludvigson *et al.* 2004). As noted above, there is no direct evidence for increased organic carbon preservation or productivity during the positive $\delta^{13}\text{C}$ excursions of the EPI (cf. Chen *et al.* 2005). Because of

this, and the inability of upwelling to explain the synchronous onset of global anoxia, I attribute anoxia to increased deglacial outwash causing oceanic stratification (Fig. 2.6).

anoxia due to increased freshwater runoff from the continent, which augments this, amplifying drawdown of CO_2 in the oceans as

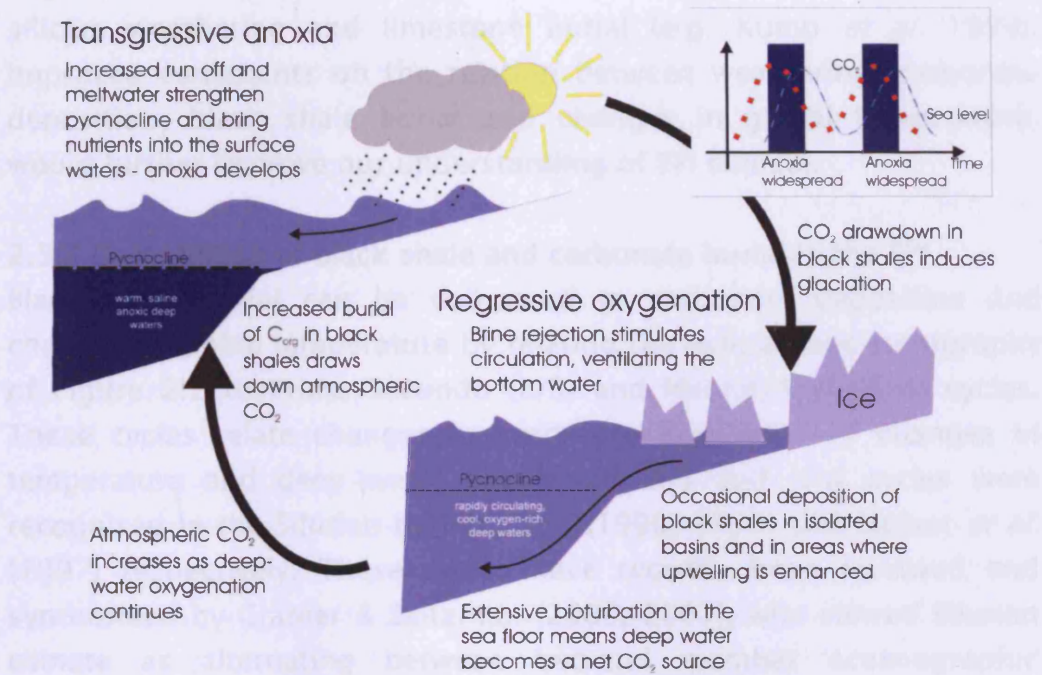


Fig. 2.6 Model for deglacially transgressive black shales in the EPI. Summary cartoon showing end-member transgressive and regressive oceans in the EPI, outlining a model in which transgressive black shale deposition may serve as a negative-feedback mechanism modulating glacioeustasy. Inset: schematic graphs showing the postulated relationship between CO_2 temperature and sea-level, given that intervals of transgressive black shale deposition may draw-down significant atmospheric CO_2 . After Page *et al.* (2007).

It is still unclear how black shale burial varies with regard to the burial of other facies associated with atmospheric CO_2 drawdown. On timescales greater than 1000 years carbonate burial provides a sink for CO_2 (Elderfield 2002). Continental silicate weathering draws down CO_2 over geological time scales and may have been the key driver of changes in atmospheric CO_2 over geologically long timescales (Holland 1978; Berner 1991; Raymo 1991; Kump *et al.* 1999; Cohen *et al.* 2004). As continental weathering is thought to increase with greater temperatures (Berner *et al.* 1983; Velbel 1993; Hovius 1998), and the rate of erosion appears to be greater in unstable (transitional) climates

than in stable greenhouse or ice-house climates (e.g. Shuster *et al.* 2005) one would expect a greater CO₂ drawdown due to weathering in transgressions. This model for drawdown of CO₂ in transgressive anoxia due to increased freshwater runoff from the continents would augment this, complementing drawdown of CO₂ to the oceans by silicate weathering and limestone burial (e.g. Kump *et al.* 1999). Improved constraints on the relation between weathering, carbonate deposition, black shale burial and changes in global temperature, would further improve our understanding of EPI climate.

2.5.2 Comparison of black shale and carbonate burial in the EPI

Black shale burial can be compared to carbonate deposition and changes in global temperature by relating the oxic/anoxic stratigraphy of Figure 2.2 to Primo/Secundo (P/S) and Humid/Arid (H/A) cycles. These cycles relate changes in carbonate deposition to changes in temperature and deep water circulation. P/S and H/A cycles were recognised in the Silurian by Jeppsson (1990, 1997) and Bickert *et al.* (1997) respectively. These cycles have recently been reviewed and synthesized by Cramer & Saltzman (2005; 2007), who viewed Silurian climate as alternating between two-end member oceanographic regimes. The first regime is characterised by cooler (P), wetter (H) climates with high sea-levels; argillaceous limestone deposition took place in shallower successions and black shales were deposited on the continental shelf, with oxic deep waters. The other regime is characterised by warmer (S), more arid (A) climates with lower sea-level; reefs formed in shallow successions and limestones were deposited on the shelf with black shales deposited in anoxic open oceans. It should, however, be noted that Jeppsson (1990, 1997) and Bickert (1997) differ in their views on where and when anoxia occur. Bickert *et al.* (1997) suggested the open oceans were anoxic throughout both H and A episodes with anoxia shoaling onto the shelf in H episodes. Jeppsson (1990, 1997) proposed oxic deep-waters occurred in P episodes with anoxia occurring on the shelf due to high productivity in these episodes; conversely, he proposed that S episodes were characterised by well-oxygenated shelf conditions and anoxia in the open oceans.

There is no simple relationship between the oxic-anoxic stratigraphy of the British Isles and either P/S or H/A cycles. In the Ordovician, Kaljo *et al.* (1999; 2004) recognised humid and arid episodes in both the mid-late Caradoc, which was predominately anoxic, and the Ashgill, which was predominately oxic (Fig. 2.3). Likewise, observations of glacial maxima and anoxia do not accord well with the P/S model. For example, the Spirodden Secundo episode lasts from the *persculptus* graptolite Zone until the *argenteus* graptolite Zone (Aldridge *et al.* 1993), a time I recognise as being a warmer deglacial interval. This episode has a similar duration to the anoxic conditions in the UK (*persculptus-magnus* graptolite zones interval) as shown in Figure 2.2. In contrast, the Malmøykalven Secundo episode (Aldridge *et al.* 1993) corresponds to the *sedgwickii* graptolite Zone, a period of globally-extensive oxic conditions and glaciation as discussed above. Moreover, the P/S episodes recognised in the Llandovery (Aldridge *et al.* 1993) do not correspond well with glacioeustatic sea-level changes or episodes of organic carbon burial in black shales (Fig. 2.2; Loydell 1998). There was a relatively low rate of limestone burial during the EPI (Fig. 2.1b), and glacial maxima show a clearer link between changes in oceanic redox state than they do with either P/S or H/A cycles. So, I suggest that ocean anoxia seems to reflect changes in atmospheric CO₂ and temperature, more clearly than carbonate deposition does.

2.6 Discussion

There are clearly deglacial anoxic events in the EPI, especially those in the *clingani*, *persculptus*, and *centrifugus* graptolite zones (Fig. 2.2) which conform well with the model of section 2.5. Likewise, there is clear evidence for increased deep-water ventilation and the deposition of well-oxygenated mudstones in glaciations themselves (Figs 2.2 & 2.5). However, it only addresses how black shale deposition may serve as a negative feedback to stabilise EPI climate rather than providing a mechanism for the onset and termination of ice formation in the EPI. Recognising repeated glacial maxima within the EPI, rather than just focussing on the Hirnantian event, significantly furthers our understanding of Early Palaeozoic climate. Characterising the

lithostratigraphic patterns associated with each glacial maximum has established a consistent set of events associated with ice-sheet formation and retreat. The factors associated with ice formation within individual EPI glacial maxima can be potentially inferred from these 'event stratigraphies'. The differences in scale between each of the glacial maxima may be used to infer which factors were most important for ice formation in the EPI. That is, the most important factors controlling ice formation are likely to be most strongly expressed in large events such as the Hirnantian glacial maximum, but only weakly expressed in smaller events. Once the factors which control ice formation in glacial maxima have been established it may be possible to infer what was responsible for the onset and termination of the EPI.

The widespread transgressive black shales in the EPI can be differentiated from those localised black shales that occur during this interval and even the transgressive black shales that occur in the Early Ordovician. Localised black shales such as the *sedgwickii* shales of Wales may represent the product of short-lived regional upwelling or increased stratification due to restricted circulation in an isolated basin. Whilst locally-extensive transgressive black shales that cannot be widely correlated could form in a similar manner to those described for locally-extensive transgressive black shales in the Jurassic such as the Oxford Clay (Wignall 1991, 1994). Though the 'Dictyonema Shales' are a transgressive black shale with seemingly global extent during the Tremadocian (Erdtmann 1982) they differ from those in the EPI as there is no evidence to support a switch between oxic and anoxic deep ocean waters accompanying the onset of their deposition. That is, the deposition of the 'Dictyonema Shales' on top of well-oxygenated facies in shelf environments represents a transgression of the pycnocline and chemocline rather than the onset of anoxia due to a transgression. Instead there is a continuous record of anoxia in the deepest water settings through the Late Cambrian and Early Ordovician seen in North Wales (Leggett 1980; Rushton 1982), the Oslo region of Norway (Bruton *et al.* 1982), in Siberia (Obut & Sobolevskaja 1962), in Ghuizhou, SW China (Lee & Chen 1962), on Newfoundland (Jenness 1963; Fortey & Skevington 1980) and in Nova Scotia (Hutchinson 1952)

and New Brunswick (Henningsmoen 1969; Landing *et al.* 1978), Canada. So while this transgressive black shale may overlie oxic shelf facies such as green shales and limestones in the Cow Head Group of Canada (Fortey & Skevington 1980; Fortey *et al.* 1982) its deeper water lateral equivalents in the same group show no break in anoxic deposition (Jenness 1963; Fortey & Skevington 1980). The same is true in Baltoscandia: on the shelf sequence exposed in Bornholm, Denmark, 'Dictyonema shales' conformably overlie shallow water Upper Cambrian sandstones with current ripples (Poulsen 1922; AAP unpublished observations on the Läså section), whereas in deeper water sections of the Oslo region the 'Dictyonema Shales' overlie the Upper Cambrian Alum Shales with no break in anoxia (Bruton *et al.* 1982). Thus, the widespread transgressive black shales of the EPI seem unique compared to this Early Ordovician transgressive black shale and other localised black shales. During the EPI, glacial-interglacial changes in thermohaline circulation profoundly affected deep water redox conditions.

I have employed stratigraphic correlation of sub-graptolite zone resolution to recognise individual glacial maxima within the EPI and their associated lithostratigraphic changes. By combining isotopic data with glacioeustatic curves and lithostratigraphic patterns there is considerable potential for developing a highly resolved Ordovician-Silurian global event stratigraphy. By comparison, biostratigraphy alone offers comparatively poor resolution and global coverage. The first appearances of many graptolites are diachronous (cf. Williams *et al.* 2003, 2004; Cooper & Sadler 2004). Likewise, the relative scarcity of graptolites in cool waters and in shallow environments (Skevington 1974; Finney & Berry 1997; Loydell 1998; Zalasiewicz 2001) may preclude accurate correlation between high and low latitudes (e.g. Lüning *et al.* 2000), and also between graptolite and conodont or shelly-fossil biostratigraphies (e.g. Mullins & Aldridge 2004). Contrastingly, carbon isotope stratigraphies appear to show good correlations between differing facies and palaeogeographical settings, allowing global correlation (e.g. Underwood *et al.* 1997; Melchin & Holmden 2006; Kaljo *et al.* in press). Moreover, the strong coupling of both positive carbon isotope excursions with changes in

deep-water redox conditions and glacioeustasy (Figs 2.2 & 2.6) represents a method of correlating third-order sequence stratigraphic changes, potentially providing a new tool for Early Palaeozoic stratigraphy. Likewise, this model for formation of transgressive black shales and their role in carbon burial (Fig. 2.6) may extend to other intervals. For example, the Toarcian oceanic anoxic event in the Jurassic saw continental run-off corresponding to the onset of anoxia, which induced CO₂ drawdown and subsequent cooling (Cohen *et al.* 2004)

In the EPI, neither the occurrence of glacial maxima nor oxic-anoxic transitions are regularly spaced (Fig. 2.2) and these events may therefore have been externally forced. The lack of observed cyclicity in the occurrence of glacial maxima suggests that the negative feedback due to CO₂ drawdown in transgressive black shale deposition was insufficient to create regular, self-sustaining glacial-interglacial cycles. The long intervals of anoxic marine conditions (e.g. late Caradoc, early Silurian and late Telychian-early Wenlock) and predominately oxic marine conditions (e.g. Ashgill, Telychian), may suggest that there was a second-order, possibly tectonic control on ocean redox conditions (see also Leggett 1980; Leggett *et al.* 1981). Likewise, the distribution of the currently recognised glacial maxima may be of second-order rather than third-order periodicity. Such second-order forcing, possibly by the opening and closing of oceanic gateways (e.g. Smith & Pickering 2003), or draw-down of CO₂ due to increased silicate weathering in orogenies (Kump *et al.* 1999), may ultimately be responsible for the conditions that facilitated ice-formation in the EPI.

2.7 Conclusions

This chapter highlights that extensive graptolitic mudrocks are best considered to be transgressive black shales, the deposition of which was controlled by climatically-induced changes in deep water circulation. The stratigraphic changes in the deposition of graptolitic mudrocks documented here differ significantly from those predicted by the so-called P/S and H/A cycles. This suggests that these models

do not fully account for changes in climate and oceanography during the EPI, although they do concur with this chapter in the notion that changes between oxic and anoxic deep waters are a consequence of changes in high latitude temperature. Though of course, on a local scale, other factors such as upwelling may be responsible for the deposition of graptolitic mudrocks, the widespread globally-simultaneous deposition of this facies rules out upwelling as its only governing factor. Likewise, the occurrence of graptoloids in oxic sediments (see section 2.7) indicates that they did not exclusively dwell in oxygen-poor waters. As such it seems wise to view graptoloids as a zooplankton whose palaeoecology was, at a first approximation, decoupled from deep water redox conditions. Though graptolite palaeoecology itself remains somewhat intangible, this work has significantly revised our understanding of palaeoceanography during this interval with the deposition of graptolitic mudrocks fundamentally linked to deglacial transgressions.

Meanwhile, recognising the EPI as a long-lived interval revises our understanding of Early Palaeozoic climate, showing a long-lived icehouse in an interval previously thought to be dominated by greenhouse conditions (cf. Brenchley *et al.* 1994; Gibbs *et al.* 2000; Montañez 2002; Church & Coe 2003; Royer 2006). Its *c.* 30 million year duration makes it comparable to other long-lived ice-houses such as those in the Cenozoic, Permo-Carboniferous and even the Neoproterozoic. All of these events are characterised by waxing and waning of ice-sheets on different time-scales with potentially different forcing and feedback mechanisms dependent on timescale. Moreover, each of these icehouses represents a markedly different solution to the Earth's carbon budget, and the locus and importance of organic burial varies considerably between them (cf. Fig. 2.1). Though atmospheric CO₂ levels appear to have controlled global temperature over geological time (Royer 2006), each of these ice-houses is characterised by a markedly different carbon-cycle, which needs to be understood in its own terms.

Though there are many uncertainties shrouding our understanding of glaciation in this interval, the EPI is notably different from those of the

modern oceans: it may have represented a time when the deposition of black shales in conditions of marine anoxia may have played a significant role in mediating the carbon cycle and climate.

TABLE 2.2 Evidence for ice-formation during the EPI

Stage	Age	Location	Palaeolat.	Evidence of ice	Evidence for age
CARADOC <i>sensu</i> Fortey <i>et al.</i> (1995, 2000) (TS 5)	"Llandeilo-Caradoc boundary" (Hamoumi 1999)	Lower Ktaoua Fm., Zagora, Morocco	80°S	Glacial pavement with polished surface displaying <i>roche moutonnée</i> -like forms, undulating surfaces, graze, score & nail-shaped groove joints (Beuf <i>et al.</i> 1971; Hamoumi 1999). This interpretation has been challenged by Sutcliffe <i>et al.</i> (2001) who propose a non-glacial origin for these features.	Surface forms base of L. Ktaoua Fm, which has <i>?gracilis-clingani</i> graptolite Zone age (Destombes <i>et al.</i> 1985) based on comparison of trilobite & brachiopod fauna with UK and Bohemia. Overlies 1 st Bani Formation of 'Llandeilo' age (Destombes <i>et al.</i> 1985) with erosive contact.
	"Lower Caradoc" (Hamoumi 1999)	Lower Ktaoua Fm., Zagora, central Anti-Atlas, Morocco	80°S	Surface remnants at corrie heads displaying battered & scoured surfaces, nivation hollows and thermokarst, on top of glaciotectionised and jointed glacio-marine deposits (Beuf <i>et al.</i> 1971; Hamoumi 1999). This interpretation has been challenged by Sutcliffe <i>et al.</i> (2001) who propose a non-glacial origin for these features.	Within L. Ktaoua Fm, which has <i>?gracilis-clingani</i> graptolite Zone age (Destombes <i>et al.</i> 1985), based on comparison of trilobite & brachiopod fauna with UK and Bohemia.
	Caradoc (Pickerill <i>et al.</i> 1979)	Gander Bay Tillites, Davidsville Group, Newfoundland, Canada.	65°S†	Diamictites and locally abundant dropstones (Pickerill <i>et al.</i> 1979)	The oldest strata in the Davidsville Group contain conodonts of Llanvirn-Llandeilo age; diamictites immediately underlie graptolitic slate of Caradoc age (Pickerill <i>et al.</i> 1979)
	Caradoc (Schenck & Lane 1981)	White Rock Fm., Nova Scotia, Canada	65°S†	Marine rafted tillite with clasts in small lenses and dropstone fabrics in varvites (Schenck & Lane 1981) quartz meta-arenites showing polished striations and grooves on facets (Schenck 1972)	Tillite overlain by "poorly preserved, limited [graptolite] fauna of Caradoc or younger age" (Schenck 1972; Schenck & Lane 1981)
	Caradoc (Massa <i>et al.</i> 1977)	Rhadames Basin, Libya	80°S	Glaciogenic dropstones (Massa <i>et al.</i> 1977)	Massa <i>et al.</i> 's (1977) stratigraphy based on Havlíček (1971).
	Caradoc (McDougall & Martin 2000)	Murzuk Basin, Libya	80°S	Dropstone textures with ice striations in Melaz Shuqran and Memouniat (McDougall & Martin 2000)	McDougall & Martin (2000) correlate with regional stratigraphies of Havlíček (1971) Legrand (1974) & Destombes <i>et al.</i> (1985).

CARADOC or ASHGILL	"middle Caradoc-Ashgill boundary" (Hamoumi 1999).	Touririne Fm, Eastern Anti Atlas, Morocco	75°S	"Frost dominated cold tidal [surface]... display (<i>sic.</i>) ice wedges, desiccation polygons and karstification" Hamoumi (1999). This interpretation has been challenged by Sutcliffe <i>et al.</i> (2001) who propose a non-glacial origin or these features.	Lower Touririne Sandstone member contains trilobite fauna comparable to " <i>peltifer</i> graptolite Zone" fauna of Letná Fm, Bohemia; Upper Touririne Sandstone member coeval with strata of <i>clingani</i> ? <i>complanatus</i> graptolite Zone age. Touririne Fm unconformably overlain by Hirnantian tillites. Stratigraphy in Destombes <i>et al.</i> (1985).
	pre-Hirnantian (Sheehan 2001)	Don Braulio Fm., Argentina	45°S †	Glaciogenic tillite evidence of three stages of terrestrial ice advance (Astini 1999; Peralta & Carter 1999).	Overlain by <i>Hirnantia</i> fauna, Hirnantian diamictites and $\delta^{13}C$ excursion, though the age of the individual advances themselves is poorly constrained (Astini 1999; Peralta & Carter 1999; Sheehan 2001).
ASHGILL (excluding Hirnantian <i>sensu</i> Cooper & Sadler 2004) (TS 6a-b)	"Upper Ordovician" (Legrand 1985)	Tamadjezt Fm*, Western Hoggar, Algeria	60°S	Buried landscapes shows glacial landforms, with striations, drumlins, vestiges of moraines, traces of solifluction, ?pingos; terrestrial and marine tillite deposits (Beuf <i>et al.</i> 1971; Biju-Duval <i>et al.</i> 1981; Legrand 1985).	Unconformably overlies strata of Caradoc age (Biju-Duval <i>et al.</i> 1981); marine facies may contain late Caradoc trilobites, brachiopods and graptolites (Gatinskiy <i>et al.</i> 1966); upper part of the formation contains middle-late Llandovery graptolites (Legrand 1970).
	"Upper Ordovician" (Tucker & Reid 1973)	Sierra Leone	50°S	Ice-drop tillites with carbonate boulders (Tucker & Reid 1973).	Lithological similarity to and correlation with similar deposits in Guinea which are overlain by Llandovery graptolite shales (Tucker & Reid 1973).
	Ashgill (Doré 1981)	Tillite de Feuguerolles, Normandy, France	40°S	Ice-drop tillites and diamictites with glacially striated clasts (Doré & Le Gall 1973; Doré 1981).	Conformably underlain by strata containing Caradoc age trilobites and other fossils (Robardet <i>et al.</i> 1972; Doré & Le Gall 1973; Doré 1981); conformably overlain by strata yielding latest Ordovician-earliest Silurian graptolite fauna (Phillipot & Robardet 1971; Doré 1981).
	"Late Ordovician" (Deynoux &	Taoudeni Basin, West Africa	70°S	Terrestrial and marine tillites in the area near the Hodh with striated boulders; glacially reworked deposits with outwash	Glacial deposits have erosive disconformity at their base (Deynoux & Trompette 1981; Deynoux, Sougy & Trompette, 1985) overlying the upper

	Trompette 1981)			fans "similar to the Icelandic sandur" (Deynoux & Trompette 1981); 'micro-cordons' that probably represent subglacial eskers in englacial tunnels; structures similar to fentes minces (Deynoux & Trompette 1981); glacial pavements and roches moutonnées with striations, furrows and crescentic fractures in the Hodh; glaciotectionic features including ice-push ridges and fractures en gradin (Biju-Dival <i>et al.</i> 1974).	part of Supergroup 2, which has an age near the Cambro-Ordovician boundary based on inarticulate brachiopods and trace fossils (Legrand 1969). Base comparable with Caradoc-Ashgill unconformity in the Hoggar, Tassilis & Anti-Atlas (Deynoux & Trompette 1981). Glacial deposits conformably but ?diachronously overlain by graptolite faunas of Upper Ashgill-middle Llandovery age (Underwood <i>et al.</i> 1998).
HIRNANTIAN <i>sensu</i> Cooper & Sadler 2004 (TS 6c)	<i>extraordinarius</i> graptolite Zone acme (Sutcliffe <i>et al.</i> 2000, 2001)	Northern Africa: Upper 2nd Bani Fm, Anti-Atlas Mts, Morocco; Djebel Serraf Fm, Ougarta Mts, Algeria	75°S	Synchronous, large-scale tillite and diamictite deposition; two phases of regionally-extensive glaciomarine shelf sequences and subglacial erosive surfaces; ice-contact fans, ice-rafted debris (Sutcliffe <i>et al.</i> 2000, 2001; see also Hamoumi 1999).	Hirnantia fauna within glaciogenic deposits, and in underlying formations (erosive contacts). Disconformably overlain by strata containing Rhuddanian graptolites (Destombes <i>et al.</i> 1985; Sutcliffe <i>et al.</i> 2000, 2001).
	<i>extraordinarius</i> graptolite Zone acme (Sutcliffe <i>et al.</i> 2000, 2001)	Melez Chograne & Memouniat Fms, Libya.	75°S	Glaciomarine shelf deposits, ice-rafted debris and erosive surfaces covered by ice-contact deposits (Havlíček & Massa 1973; Sutcliffe <i>et al.</i> 2001).	Hirnantia fauna throughout succession, overlain by Llandovery graptolites (Havlíček & Massa 1973; Sutcliffe <i>et al.</i> 2001).
	<i>extraordinarius</i> graptolite Zone acme (Sutcliffe <i>et al.</i> 2000, 2001)	Tichit glacial group, the Hodh, Mauritania	70°S	Glacially striated dropstones, diamictites (Deynoux & Trompette 1981; Ghienne 2003).	Dropstones coexist with graptolites of Upper Ashgill age (Underwood <i>et al.</i> 1998).
	<i>extraordinarius</i> graptolite Zone acme (Sutcliffe <i>et al.</i> 2000, 2001)	Pakhuis Fm., South Africa.	15°S	Tillites & diamictites, two subglacial erosive surfaces with striated pavements and boulders, ice-rafted debris. (Rust 1981; Sutcliffe <i>et al.</i> 2000, 2001)	Hirnantia fauna in conformably overlying Cedarberg Fm (Sutcliffe <i>et al.</i> 2001)
	?Hirnantian	Tabuk Fm., Arabian	50°S	Diamictites & tillites with some striated,	Tillite interfingers with late Caradoc age graptolite

		peninsula.		faceted and polished clasts; boulder pavements with striations. (McClure 1978).	shale also containing trilobites of late Caradoc or early Ashgill age (Young 1981); overlying Qusaiba Shale which contains a Rhuddanian graptolite fauna (Lüning <i>et al.</i> 2000)
	Hirnantian (Armstrong <i>et al.</i> 2005)	Ammar Fm., southern Jordan.	50°S	Tillite; glacial unconformity at base and two episodes of glacial incision; conglomerates with glacially faceted and striated clasts (Abed <i>et al.</i> 1993)	Conformably overlain by persculptus graptolite Zone fauna (Armstrong <i>et al.</i> 2005)
	Hirnantian (Caputo 1998)	Don Braulio Fm., Argentina	15°S†	Diamictite some striated, faceted and polished clasts (Büggish & Astini 1993)	Overlain by <i>Hirnantia</i> fauna (Sutcliffe <i>et al.</i> 2001)
	?Hirnantian (Caputo 1998)	Iapó Fm., Paraná Basin, Brazil.	25°S	Diamictites with faceted and striated clasts (Maack 1957; Rocha-Campos 1981)	Lithological comparison with South African and Argentinean tillites (Caputo 1998); Iapó Fm. discordantly overlies rhyolites of the Castro Group dated at 450±25 Ma (Bigarella 1970); correlation with interfingering Vila Maria Fm. suggests diamictite overlain by early Llandovery palynomorph and shelly fauna (Caputo & Crowell, 1985).
	Hirnantian	Prague Basin, Czech Republic	55°S	Two intervals of diamictite deposition (Brenchley & Storch 1989)	Conformably underlain by <i>Mucronaspis</i> fauna and <i>anceps</i> Zone graptolites; conformably overlain by Hirnantian fauna (Štorch & Mergl 1989)
LLANDOVERY (Rhuddanian)	?Rhuddanian	San Gabán-Cancañiri-Zapla Fms, Bolivia, Argentina & Peru	55°S	Widely extensive diamictites with striated and faceted clasts (Crowell <i>et al.</i> 1981; Caputo & Crowell 1985; Díaz-Martínez & Grahn 2007).	Oldest diamictite horizon overlain by Aeronian chitinozoan fauna and underlain by Rhuddanian chitinozoan (Díaz-Martínez & Grahn 2007). These formations unconformably overlie Caradoc strata showing evidence of Ashgillian deformation (Crowell <i>et al.</i> 1981);
	"Upper Ordovician or Lower Silurian" (Kennedy)	Stoneville & Beaver Cove Fms, Newfoundland, Canada.	60°S†	Diamictite beds; dropstones probably derived by iceberg rafting (Kennedy 1981)	Stoneville & Beaver Cove Fms are coeval (Kennedy 1981); former underlain by poorly preserved corals of Upper Ordovician or Lower Silurian age (McCann & Kennedy 1974) and lithological

	1981)				correlatives of its upper part have yielded Llandovery age fossils (Eastler 1969; Kennedy 1981).
LLANDOVERY (Aeronian)	<i>Gregarius</i> graptolite Zone (Caputo 1998)	Nhamundá Fm., Amazonas Basin Brazil	60°S	Diamictite; ice-push & ice-shear deformation structures (Carozzi <i>et al.</i> 1973; Caputo 1998)	Diamictite immediately overlain by <i>gregarius</i> Zone graptolite fauna and chitinozoan fauna (Grahn & Paris 1992; Caputo 1998)
	"late Aeronian-early Telychian" (Caputo 1998)	Nhamundá Fm., Amazonas Basin, Brazil	60°S	Diamictite; ice-push & ice-shear deformation structures (Carozzi <i>et al.</i> 1973; Caputo 1998)	Overlies <i>gregarius</i> Zone fauna; shales lateral to tillites yield an early Telychian chitinozoan fauna (Caputo 1998)
	?Aeronian	San Gabán-Cancañiri-Zapla Fms, Bolivia, Argentina & Peru	60°S	Widely extensive diamictites with striated and faceted clasts (Crowell <i>et al.</i> 1981; Caputo & Crowell 1985; Díaz-Martínez & Grahn 2007).	Overlies shales yielding Aeronian chitinozoans (Díaz-Martínez & Grahn 2007), overlain by shales and a younger diamictite horizon.
	Llandovery (Caputo 1998)	Ipu Fm., Parnaíba Basin & Cariri Valley, Brazil	70°S	Three diamictite layers (Caputo & Crowell 1985; Grahn & Caputo 1992); faceted pebbles (Kegel 1953).	Interfingers with Tianguá Fm, which contains Early Silurian chitinozoans and acritarchs (Caputo & Lima 1984); individual diamictites may correlate with the better dated diamictites in the Nhamundá Fm. (Grahn & Caputo 1992).
LLANDOVERY (Telychian, including <i>centrifugus</i> Zone)	late Telychian (Grahn in Cramer & Saltzman 2007)	Nhamundá Fm., Amazonas Basin, Brazil	70°S	Diamictites and tillites; ice-push & ice-shear deformation structures (Carozzi <i>et al.</i> 1973; Caputo 1998)	Late Telychian-early Wenlock Chitinozoan fauna in interfingering shales (Caputo 1998); first appearance of chitinozoa <i>M. margaritana</i> above the youngest tillite (Grahn in Cramer & Saltzman 2007).
	Late Telychian (Díaz-Martínez 2007)	San Gabán-Cancañiri-Zapla Fms, Bolivia, Argentina & Peru	65 °S	Widely extensive diamictites with striated and faceted clasts (Crowell <i>et al.</i> 1981; Caputo & Crowell 1985; Díaz-Martínez & Grahn 2007).	Youngest diamictite comformably overlain by Sacla limestone, which has early Wenlock age based on the occurrence of the conodont <i>O. sagitta rhenana</i> (Díaz-Martínez 2007). However, acritarchs and chitinozoans in intercalated shale horizons suggest a Llandovery-Wenlock boundary age (Suárez-Soruco 1995).

* Synonym of Felar Felar Fm. † Position Nova Scotian Iapetan terranes poorly constrained this interval; Kennedy (1981) thought it to have been on the margin of West Africa at this time. ‡ Position of the Argentine Precordillera poorly constrained at this interval.

TABLE 2.3a Diversity & distribution of reef builders, carbonate-hosted faunas and groups with a predominately tropic biotope. Time Slices after Webby *et al.* (2004a).

Time Slices	Fauna	Habitat and/or controls on distribution	Change in diversity and/or distribution
TS 5a-b	Stromatoporoid sponges	Shallow, warm-water (non-turbid) reef to bank carbonate habitats (Webby 2002), with marked temperature sensitivity (Nestor & Stock 2001) and general restriction to < 30° N/S (Webby 1992).	Continuation of Darriwillian radiation across low palaeolatitudes at both generic and species level (Webby 2004)
TS 5c			Increased rate of extinction at both generic and species level, rate of origination slows at a species level and decreases at a generic level (Webby 2004). Fauna restricted to low latitudes. Nestor & Stock (2001) report gradual extinction in the late Caradoc genera which they attributed to global cooling.
TS 5d			Minima in species and generic diversity, elevated rate of extinction at both species and generic levels compared to the Katian (Webby 2004) Nestor & Stock (2001) report gradual extinction in the late Caradoc genera which they attributed to global cooling.
TS 6a-b			Maximum diversity achieved at both generic and species levels, the latter especially may reflect the radiation of Aureliticidae in deeper water ramp environments including those at high latitudes (Webby 2004; Fortey & Cocks 2005; Cherns & Wheeley 2007)
TS 6c			Major decrease in diversity in the Hirnantian mass extinction; reef growth continued at tropical latitudes with significantly lowered diversity (Webby 2004)
TS 5a-b	Tetradiid corals	Tropical shallow marine carbonate platform and shelf settings forming reefs (Webby 2002) and microatolls (Webb 1997); decline of this group may reflect cooling either directly or indirectly (Webby <i>et al.</i> 2004b)	Major radiation across low latitude carbonate platforms, shelf margins and island arcs (Webby <i>et al.</i> 2004)
TS 5c			Diversity high, but rate of species disappearances outstrips appearances at onset of TS 5c-d decline (Webby <i>et al.</i> 2004)
TS 5d			Fall in species diversity (Webby <i>et al.</i> 2004)
TS 6a-b			Diversification event with the group once more achieving a similar distribution across low latitudes to that of TS 5a-b (Webby <i>et al.</i>

			2004)
TS 6c			Major decline in diversity and extinction.
TS 5a-b	Baltoscandian rugose corals	Shallow shelf dwellers favouring soft substrates with solitary forms probably favouring cooler waters and colonial forms probably favouring warmer waters (Webby <i>et al.</i> 2004b). Changes in the relative abundance of these taxa may reflect changes in water temperature due to the migration of Baltica towards the equator at this time (Webby <i>et al.</i> 2004b)	Origination of simple solitary morphotypes (Webby <i>et al.</i> 2004b)
5c			Diverse fauna at both species and generic levels including a few species of colonial genera ((Webby <i>et al.</i> 2004b)
5d			Minor extinction at both species and generic levels with decreased rate of species origination, though diversity still higher than TS 5b (Webby <i>et al.</i> 2004b)
6a-b			Decline in both generic and species diversity (TS 5d-6a) followed by diversification (TS 6a-b) with colonial genera more prevalent (Webby <i>et al.</i> 2004b)
6c			Increased level of species extinction matched by high rate of origination and continued diversification at both species and generic levels, with 75% of all genera surviving the Hirnantian mass extinction (Webby <i>et al.</i> 2004b).
TS 5a-b	Australian corals	Shallow marine, warm-water assemblages dominated by compound rugosans (Webby <i>et al.</i> 2004b)	Low-diversity fauna (Webby <i>et al.</i> 2004b).
TS 5c			Moderately diverse fauna (12 genera) following TS 5a-5b radiation (Webby <i>et al.</i> 2004b).
TS 5d			Peak normalised diversity with (14 genera).
TS 6a-b			Rapid decline in the fauna with local extinction in TS 5d which may have been related to tectonic processes such as the Benambran Orogeny, magmatic events, epirogeny and the formation of evaporitic basins that destroyed shallow carbonate habitats (Webby <i>et al.</i> 2004b)
TS 6c			No known fauna.
TS 5a-b	Bryozoans	Generally shallow water or reefal bioherms with limited wave action (Clarkson 1998); individual species may be temperature and salinity	Rapid diversification (Taylor & Ernst 2004)

		specific, though the group as a whole may be found in both warm water and cool water environments (cf. Cherns & Wheeley 2007). Ross (1985) suggested their diversity may track temperature.	
TS 5c			Peak diversity for Ordovician accompanied by onset of TS 5c-5d extinction (Taylor & Ernst 2004).
TS 5d			Diversity minima though extinction rate outstrips origination rate (Taylor & Ernst 2004).
TS 6a-b			Re-radiation with increased diversity prior to TS 6b extinction (Taylor & Ernst 2004) which may be linked to cooling (cf. Ross 1985; Sheehan 2001). Bryozoan mounds in cool water ramp carbonates at high and low latitudes (Cherns & Wheeley 2007).
TS 6c			Poorly diverse fauna and continued extinction event (Taylor & Ernst 2004).

TABLE 2.3b Diversity & distribution of predominantly benthic shelly fossils present in high, mid and low latitudes. Time slices as Table 2.3a.

Time slices	Fauna	Habitat and/or controls on distribution	Change in diversity and/or distribution
TS 5a-b	Gastropods (excluding pteropods)	Vagrant, benthic, marine (in the Ordovician at least) with extant forms occupying a broad range of environments (Barnes & Barnes 1998).	Major radiation with high origination rate at the generic level (Frýda & Rohr 2004)
TS 5c			Highly diverse fauna but with decreased origination rates and increased extinction rates (Frýda & Rohr 2004).
TS 5d			Slightly decreased diversity with rate of origination outstripped by extinction (Frýda & Rohr 2004)
TS 6a-b			Slight increase in diversity accompanied by marked increases in the rates of both origination and extinction in TS 6a with origination low and extinction high in TS 6b (Frýda & Rohr 2004).
TS 6c			Decreased greater diversity (though still more diverse than during TS 5a) with peak extinction rate for the Ordovician and little origination (Frýda & Rohr 2004).
TS 5a-b	Nuculoid & Solemyoid bivalves	Epifaunal with broad latitudinal distribution; Upper Ordovician witnessed radiation in lower latitudes and relatively decreased diversity at high latitudes (Cope 2002).	Stable generic diversity (Cope 2004)
TS 5c			Slightly decreased generic diversity (Cope 2004)
TS 5d			Generic diversity greater than TS 5c but lower than TS 5a (Cope 2004).
TS 6a-b			Gradual decrease in diversity, increase in percent extinction and extinction rate (Cope 2004).
TS 6c			Low diversity fauna restricted to low latitudes (Cope 2004).
TS 5a-b	Pteriomorphan & Anomalodesmatan bivalves	Byssate (Pteriomorphia) or burrowing (Anomalodesmata) bivalves generally restricted to low latitudes and carbonate platforms (Cope 2002)	Rapid diversification across low latitude platform carbonates (Cope 2004).
TS 5c			Stable high generic diversity (2004).
TS 5d			Stable high generic diversity (Cope 2004).

TS 6a-b			Further diversification resulting in Ordovician diversity maximum (Cope 2004)
TS 6c			Low diversity fauna only found in low latitude carbonates (Cope 2002, 2004)
TS 5a-b	Linguliform brachiopods	Dominantly benthic with long-lived planktotrophic larval phase with a widespread and even biogeographic distribution largely controlled by climatic factors (Harper <i>et al.</i> 2004).	High, stable generic diversity with all major linguliform ecologies already evolved (Harper <i>et al.</i> 2004).
TS 5c			Similar generic diversity to TS 5b although this interval witnessed a major increase in extinction rate (Harper <i>et al.</i> 2004).
TS 5d			Late Ordovician diversity minima and continued increase in extinction rate, off set in part by a slight increase in origination rate (Harper <i>et al.</i> 2004).
TS 6a-b			Re-radiation event accompanied by peak generic diversity for the Ordovician, although extinction rate was still increasing (Harper <i>et al.</i> 2004).
TS 6c			Major decrease in generic diversity across the whole clade in the end Ordovician mass extinction (Harper <i>et al.</i> 2004).
TS 5a-b	"articulate" brachiopods	Benthic with broad depth and latitudinal tolerance; notable variation in taxonomic composition in relation to different depth, substrate and climatic regimes (Harper <i>et al.</i> 2004).	Highly diverse fauna at the generic guild with all groups achieving their broadest geographic and ecological range for the Ordovician (Bottjer <i>et al.</i> 2001; Harper <i>et al.</i> 2004). Endemic faunas in high latitude Gondwana (Fortey & Cocks 2003, 2005).
TS 5c-d			Minor extinction event characterised by c. 20% decrease in generic diversity across most groups (although this event is less marked in the Pentamerids which were poorly diverse throughout TS 5a-d) though the nature of this event received little attention in the review by Harper <i>et al.</i> (2004). Cool water fauna in high latitudes Gondwana (S. America, S. Africa & the Mediterranean region), with <i>Foliomena</i> fauna in deeper waters at mid to low latitudes and warm, shallow water <i>Holorhynchus</i> fauna at low latitudes (Boucot <i>et al.</i> 2003)

TS 6a-b			Increased in standing diversity at generic level in most groups (however this may be not the case in corrected measures of diversity where this has been calculated [for Orthids and Strophomenids] suggesting this may be an artefact of sampling) accompanied by high rate of faunal turnover, with peak standing generic diversity achieved for the Rhynchonelliformea (Harper <i>et al.</i> 2004). Cool water fauna restricted within high latitude Gondwana, only occurring in S. America and S. Africa, with poleward migration of <i>Nicolella</i> fauna into the Mediterranean; warm, shallow water <i>Holorhynchus</i> fauna present in mid to low latitudes along with deep water <i>Foliomena</i> fauna (Boucot <i>et al.</i> 2003).
TS 6c			Major decrease in diversity in the end Ordovician mass extinction (Harper <i>et al.</i> 2004) with cool water <i>Hirnantia</i> fauna present at all but the most lowest palaeolatitudes and extinction of the deep water <i>Foliomena</i> fauna (Boucot <i>et al.</i> 2003).
TS 5a-b	Ostracodes	Benthic or nektobenthic – only one documented occurrence of an epiplanktic fauna in the Ordovician – with well-studied faunas from Laurentia, Baltica, Siberia and western Europe and a low diversity fauna on Gondwana throughout the Ordovician (Schallreuter 2004; Armstrong & Brasier 2005). Modern marine taxa known from a broad range of depth and latitudes with greater diversity at low latitudes (Armstrong & Brasier 2005).	Stable moderately diverse fauna at species level in Baltica, which at this time was at mid latitudes (Schallreuter 2004); in Perunica (high latitudes) there was a low diversity fauna in TS 5a, increasing in diversity during TS 5b (Schallreuter 2004).
TS 5c			Extinction events in both Baltica (mid latitude) and Perunica (high latitude); species diversity minima in Baltica in Keila stage with minor recovery during the Oandu and Rakvere stages (Schallreuter 2004).
TS 5d			Decreased species diversity in Baltica (mid latitudes), increased species diversity in Perunica (peak for Ordovician) which by this time had detached from Gondwana and was migrating south (Cocks & Torsvik 2002; Schallreuter 2004).
TS 6a-b			Increased species diversity in Baltica (peak for Ordovician), now at mid-low latitude, decreased species diversity in Perunica (Schallreuter 2004).
TS 6c			Low diversity fauna due to end Ordovician mass extinction (Schallreuter 2004).

TS 5a-b	Trilobites	Vagrant and predominantly benthic, though some taxa considered to be planktonic; biogeographic realms and depth related communities may be recognised (Adrain <i>et al.</i> 2004; quantified biodiversity curves known for S. China and Australasia (both low latitude), Avalonia (Anglo-Welsh section) and Baltica (both mid latitude), and S. America (migrated from mid to high latitude in this interval) (Adrain <i>et al.</i> 2004); qualitative data on migrations and distribution data also available (e.g. Boucot <i>et al.</i> 2003; Fortey & Cocks 2003, 2005).	S. China: increasing generic diversity with peak diversity for Ordovician attained in TS 5b, notable differentiation between biofacies; Australasia: decrease to moderate generic diversity following TS 4c-5a extinction; Baltica: stable, moderate to high generic diversity, significant decrease to moderate species diversity (TS 4c-5a); Avalonia: slight increase in generic diversity and slight decrease in species diversity (part of gradual TS 5a-d trend, which may reflect deepening); S. America: increase to moderate species diversity TS 4c-5a, decrease to low species diversity TS 5a-b which might reflect the end of carbonate deposition related to either drowning or poleward migration (Adrain <i>et al.</i> 2004). Diversification of Whiterock fauna across low palaeolatitudes displacing incumbent Ibex fauna (Adrain <i>et al.</i> 2004).
TS 5c			S. China: sharp decline generic diversity; Australasia: increase in generic diversity in TS 5b-d radiation; Baltica: v. slight increase in generic diversity; Avalonia: slight increase in generic diversity and slight decrease in species diversity (part of gradual TS 5a-d trend, which may reflect deepening); S. America: continued decrease in species diversity (part of TS 5b-6c trend) poorly diverse endemic <i>Dalmanitina</i> fauna indicative of cool waters (Adrain <i>et al.</i> 2004). Cyclopyge fauna found in deep waters in mid and low palaeolatitudes, cool water community in the Mediterranean realm (Boucot <i>et al.</i> 2003); distinctive tropical fauna within low latitudes (Fortey & Cocks 2005).
TS 5d			S. China: stable moderately high diversity fauna; Australasia: increase in generic diversity in TS 5b-d radiation, high faunal turnover; Baltica: stable, moderate to high generic diversity fauna; Avalonia: slight increase in generic diversity and slight decrease in species diversity (part of gradual TS 5a-d trend, which may reflect deepening); S. America: poorly diverse endemic <i>Dalmanitina</i> fauna and indicative of cold waters (Adrain <i>et al.</i> 2004). Cyclopyge fauna found in deep waters in mid and low palaeolatitudes, cool water community in the Mediterranean realm (Boucot <i>et al.</i> 2003);

			distinctive tropical fauna within low latitudes (Fortey & Cocks 2005).
TS 6a-b			S. China: similar diversity fauna from TS 5c-6a, with rapid decline in generic diversity from TS 6a-c; Australasia: decreased generic diversity as part of TS 5d-6c decline; Baltica: slight increase in generic diversity in TS 6a followed by TS 6a-c decline, possibly reflecting the wide range of trilobite biofacies present in at this time; Avalonia: slight increase in generic diversity and sharp increase in species diversity; S. America: poorly diverse endemic <i>Dalmanitina</i> fauna indicative of cold waters (Adrain <i>et al.</i> 2004). Cyclopyge fauna found in deep waters in mid and low palaeolatitudes, disappearance of cool water community in the Mediterranean realm (Boucot <i>et al.</i> 2003); radiation of diverse low latitude fauna into mid and high latitudes including the Mediterranean realm and NW Africa (Fortey & Cocks 2005).
TS 6c			S. China: low diversity cool water <i>Dalmanitina</i> fauna associated with end Ordovician mass extinction; Australasia: low diversity fauna; Baltica: low diversity cool water <i>Dalmanitina</i> fauna associated with end Ordovician mass extinction; Avalonia: low diversity cool water <i>Dalmanitina</i> fauna associated with end Ordovician mass extinction; S. America: slight increase in species diversity associated with radiation of the <i>Dalmanitina</i> fauna (Adrain <i>et al.</i> 2004). Disappearance of deep water Cyclopyge and Olenid biotopes (perhaps linked to increased deep-water ventilation), with warm water faunas restricted to the very lowest palaeolatitudes (Fortey & Cooper 2003, 2005; Adrain <i>et al.</i> 2004). large scale extinction (including the Ibex fauna) with survival favouring Whiterock faunal elements that had their initial radiation in lowest latitudes, especially low-latitude particle feeders and cool-water predators/scavenger (Adrain <i>et al.</i> 2004).

TABLE 2.3b Diversity & distribution of planktonic fossils present in high, mid and low latitudes. Time slices as Table 2.3a.

Time slices	Fauna	Habitat and/or controls on distribution	Change in diversity and/or distribution
TS 5a-b	Chitinozoans	Widespread planktonic taxon preserved in a broad suite of lithofacies; noted provinciality with good records of well-preserved taxa available for North Gondwana (high latitude); Baltica (mid latitude) and Laurentia (low latitude) (Paris <i>et al.</i> 2004).	North Gondwana: Major decrease in species diversity TS 4c-5b (Paris <i>et al.</i> 2004); Baltica: peak species diversity for Ordovician with slight decrease from TS 5a-b (Paris <i>et al.</i> 2004); Laurentia: low-moderate diversity fauna with increase in species diversity from TS 5a-b (Paris <i>et al.</i> 2004).
TS 5c			North Gondwana: low species diversity and increase in faunal turnover (Paris <i>et al.</i> 2004); Baltica: very slightly lowered species diversity (Paris <i>et al.</i> 2004) with short extinction and re-radiation event recognised with this interval in high resolution records from Estonia (Kaljo <i>et al.</i> 1996); Laurentia: major increase in species diversity which may be linked to the Taconic Orogeny which was responsible for the deepening of the Appalachian foreland basin (Paris <i>et al.</i> 2004). Onset of global decline in species diversity TS 5c-6c.
TS 5d			North Gondwana: increase in faunal turnover accompanying an increase to moderate species diversity (Paris <i>et al.</i> 2004); Baltica: similar species diversity to TS 5c (Paris <i>et al.</i> 2004); Laurentia: decreased species diversity which may reflect waning influence of the Taconic orogeny on deep water deposition (Paris <i>et al.</i> 2004). Continued decline in global diversity (Paris <i>et al.</i> 2004).
TS 6a-b			North Gondwana: gradual progressive decrease in diversity TS 5d-TS 6b (Paris <i>et al.</i> 2004); Baltica: decrease in diversity TS 5d-TS 6a with minor recovery in TS 6b (Paris <i>et al.</i> 2004); Laurentia: decrease in diversity TS 5d-6a, with increase in diversity TS 6a-b (Paris <i>et al.</i> 2004). Continued decline in global diversity (Paris <i>et al.</i> 2004).
TS 6c			Global decrease in diversity related to end Ordovician Mass extinction (Paris <i>et al.</i> 2004).

TS 5a-b	Graptoloid graptolites)	Planktonic with species diversity maxima achieved in off shore assemblages (Cooper <i>et al.</i> 1991; Finney & Berry 1997; Chen <i>et al.</i> 2000, 2005a or b) and at low and mid latitudes as opposed to high latitudes (Skevington 1994; Cooper <i>et al.</i> 1991, 2004; Underwood 1997; Zalasiewicz 2001). Diversity changes and trends track oceanic environmental changes with origination tending to occur in highstands (Cooper <i>et al.</i> 2004) and extinction occurring in low stands and intervals of cooling (Underwood 1997; Cooper <i>et al.</i> 2004; Chen <i>et al.</i> 2005; Finney <i>et al.</i> 2007; Loydell 2007; Fig. 6.1). Strong taphonomic bias towards preservation in dysoxic or anoxic mudrocks (e.g. Chapman 1991; Palmer 1991; Underwood 1992)	Global generic diversity high for Ordovician (Underwood 1997; Fig. 6.1). Normalised diversity low at low latitudes, i.e. Australia, but high at mid latitudes, i.e. in Avalonia, with low in extinction rates and moderate to high origination rates in both settings (Cooper <i>et al.</i> 2001). Widespread globally distributed fauna (Goldman <i>et al.</i> 2005; Vandenbroucke <i>et al.</i> 2007)
TS 5c			Decline of globally distributed fauna dominance of normalograptid fauna (Cooper <i>et al.</i> 2004; Goldman <i>et al.</i> 2005; Fig. 6.1); major decrease in global generic diversity (Underwood 1997; Armstrong 2007).
TS 5d			Low diversity fauna (Underwood 1997; Armstrong 2007) especially in mid and high latitudes and peak extinction rate for Ordovician (Cooper <i>et al.</i> 2007); high extinction rate in mid-latitudes with low origination rate, low extinction rates in low latitudes with relatively high origination rates (Cooper <i>et al.</i> 2007).
TS 6a-b			Minor recovery in global generic diversity (Underwood 1997); normalised still low in mid latitudes but higher at low latitudes with origination and extinction rates relatively low in all settings (Cooper <i>et al.</i> 2004) Low diversity, endemic graptolite fauna on Gondwana (Legrand 2003).
TS 6c			Near extinction of the graptoloid clade with only a few species of normalograptids present in this interval (Underwood 1997; Chen <i>et al.</i> 2000; 2005ab; Cooper <i>et al.</i> 2004; Finney <i>et al.</i> 2007).

TABLE 2.4 Compilation of stable carbon and oxygen isotope data for Ordovician and Silurian quoted as means with standard deviations and number of datapoints (N).

Chronostratigraphy	Age (Ma)	$\delta^{13}\text{C}_{\text{mean}}$	$\delta^{18}\text{O}_{\text{mean}}$	$\Sigma (\delta^{13}\text{C})$	$\sigma (\delta^{18}\text{O})$	N
late Pridoli	416.50	-0.31	-5.78	0.36	0.45	13
mid Pridoli	417.60	-0.46	-6.14	0.33	0.38	3
early Pridoli	418.50	-0.36	-5.47	0.38	0.32	14
late Ludfordian	419.50	5.51	-4.32	1.10	0.48	5
early Ludfordian	420.80	0.17	-6.15	0.43	0.40	6
<i>scanicus</i> Zone	421.80	-0.05	-5.58	0.26	0.22	7
<i>nilssoni</i> Zone	422.70	1.36	-5.03	0.35	0.27	3
<i>ludensis</i> Zone	423.30	1.19	-5.16	0.72	0.64	26
<i>nassa</i> Zone	424.60	1.37	-4.14	0.77	0.83	22
<i>lundgreni</i> Zone	425.50	0.43	-4.58	1.22	0.55	12
late Sheinwoodian	426.50	-0.74	-4.61	0.21	0.25	10
<i>riccartonensis</i> Zone	427.20	4.01	-4.44	1.27	0.72	12
<i>murchisoni</i> Zone	427.60	2.91	-4.60	2.08	0.81	12
<i>centrifugus</i> Zone	428.00	3.13	-4.59	1.53	1.12	2
<i>crenulata</i> Zone	430.00	1.36	-5.69	0.18	0.57	12
<i>griestonensis</i> Zone	431.90	0.96	-5.25	0.76	0.64	9
<i>crispus</i> Zone	433.00	1.03	-4.93	0.87	0.57	7
<i>turriculatus</i> Zone	434.50	1.33	-4.58	0.24	0.23	3
<i>sedgwickii</i> Zone	436.40	1.44	-4.44	0.70	0.24	4
<i>convolutus</i> Zone	436.90	1.14	-5.30	0.38	0.14	8
<i>leptotheca</i> Zone	437.30	1.26	-4.96	0.21	0.23	3
<i>triangulatus</i> Zone	438.40	0.94	-4.48	0.35	0.53	6
<i>cyphus</i> Zone	439.90	0.46	-5.12	0.55	0.37	2
<i>avatus</i> Zone	441.30	0.93	-3.65	1.28	0.40	2
<i>acuminatus</i> Zone	442.80	1.05	-3.15	0.08	0.31	3
<i>persculptus</i> Zone	444.20	0.93	-3.72	0.57	0.94	32
HICE	444.70	5.83	-2.27	1.07	0.75	34
<i>extraordinarius</i> Zone	445.20	0.73	-3.36	0.41	0.42	16
<i>pacificus</i> Zone	446.60	1.08	-4.48	0.71	0.60	48
<i>complexus</i> Zone	448.20	0.28	-4.97	0.32	0.99	27
<i>companulatus</i> Zone	449.30	0.19	-5.15	0.29	0.38	20
<i>linearis</i> Zone	451.10	0.10	-4.78	1.31	1.19	9
<i>clingani</i> Zone	454.00	0.27	-5.50	1.36	1.38	5
GICE	455.00	2.58	-3.00	0.08	0.21	5
late <i>wilsoni</i> Zone	456.00	0.27	-5.48	0.55	0.58	13
mid <i>wilsoni</i> Zone	456.50	-0.05	-5.12	0.67	0.31	36
early <i>wilsoni</i> Zone	456.90	0.30	-5.43	0.95	0.60	26
late <i>peltifer</i> Zone	457.40	-0.65	-5.35	0.81	0.75	8
mid <i>peltifer</i> Zone	457.90	-0.32	-4.89	0.60	0.41	16
early <i>peltifer</i> Zone	459.15	-0.94	-6.15	0.46	0.74	12
<i>gracilis</i> Zone	459.70	-0.39	-5.94	0.23	0.76	7
<i>teretiusculus</i> Zone	462.80	-0.35	-6.38	0.25	0.13	4
<i>murchisoni</i> Zone	464.70	-0.68	-6.47	0.04	0.70	6
<i>bifidus</i> Zone	465.90	-2.06	-6.08	0.25	0.38	7

<i>hirundo</i> Zone	467.00	-0.80	-6.51	0.63	0.79	26
<i>gibberulus</i> Zone	470.00	-1.45	-7.17	0.59	0.87	24
<i>nitidus</i> Zone	472.50	-2.42	-8.08	0.53	1.10	7
<i>deflexus</i> Zone	474.70	-0.99	-8.79	0.20	0.35	7
<i>approximatus</i> Zone	477.30	-0.96	-9.88	0.29	0.62	5
Tremadoc	483.45	-0.44	-9.13	0.38	0.27	3

3. *Dawsonia* Nicholson: revealing the diversity of the fauna preserved in graptolitic mudrocks

Abstract: Though little is known of the graptoloid reproductive mechanism, graptolites with putatively sac-like appendages, supposedly ovarian vesicles, have been known from the Moffat Shales Group, Southern Uplands, Scotland, for over 150 years. Locally, these co-occur with isolated, two-dimensional, discoidal or ovato-triangular fossils. In the 1870s, Nicholson interpreted these isolated fossils as being graptoloid 'egg-sacs', detached from their parent and existing as free-swimming bodies. He assigned them to the genus "*Dawsonia*", though the name was preoccupied by a trilobite, and named four species: "*D.*" *campanulata*, "*D.*" *acuminata*, "*D.*" *rotunda* (*sic.*) and "*D.*" *tenuistriata*. A reassessment of Nicholson's type material from the Silurian of Moffatdale, Scotland, and the Ordovician Lévis Formation of Quebec, Canada, shows that *Dawsonia* Nicholson comprises: the inarticulate brachiopods *Acrosaccus?* *rotundus*, *Paterula?* *tenuistriata* and *Discotretra* cf. *levisensis*; the tail-piece of the crustacean *Caryocaris acuminata*; and, the problematic fossil "*D.*" *campanulata*. Though "*D.*" *campanulata* resembles sac-like graptolite appendages, morphometric analysis reveals the similarity to be superficial and the systematic position of this taxon remains uncertain. There is no definite evidence of either "*D.*" *campanulata* or sac-like graptoloid appendages having had a reproductive function.

3.1 Introduction

Originally considered to be graptolite reproductive organs, the genus *Dawsonia* Nicholson provides an important insight into the fauna preserved in graptolitic mudrocks. Our knowledge of reproductive structures and strategies in the animal fossil record is sparse. Though

reproductive organs are occasionally found, they usually require exceptional preservation for their true nature to be discerned (e.g. Siveter *et al.* 2003; Dunlop *et al.* 2004). Whilst a certain amount is known of the reproductive strategies and mechanisms of the pterobranch hemichordates (Gilchrist 1915; Stebbing 1970; Dilly 1973; Hutt 1991), the extant sister group of the graptolites (Kozłowski 1947, 1948; Towe & Urbanek 1972; Crowther 1978; Cameron 2005), little is known about reproduction in the graptolites themselves (e.g. Urbanek & Jaanusson 1974). Likewise, as little is known of the buoyancy mechanism employed by the graptoloids (Bates 1987), any putatively vesicular graptoloid tissues (e.g. Fig. 3.1d, f) tend to attract interest and debate (e.g. Underwood 1993; Rickards *et al.* 1994).

There are many gaps in our knowledge of the earliest developmental stages of the graptolites, especially surrounding the events prior to the dispersal of their prosiculae (cone-shaped larvae). Working on well-preserved material from the Tremadoc of Poland, Kozłowski (1948) showed clutches of eggs and embryos in the autothecae of benthonic graptolites; similar structures have also been found in *Reticulograptus tuberosus*, a bushy tuboid graptolite from Götland, Sweden (Bulman & Rickards 1966). Unlike the graptoloids, benthonic graptolites have two types of thecae. These differentiated thecae have been interpreted as sexual dimorphs, with the smaller bithecae housing the male zooid and the larger autothecae housing the female (Kozłowski 1948), though this has yet to be confirmed. Nevertheless, the loss of bithecae in the graptoloids may indicate that their reproductive strategy altered as they colonised the plankton (Hutt 1991), and neither eggs nor embryos have been found in graptoloid thecae. Some workers have suggested that the graptolite synrhabdosome may represent short-lived congregations of several colonies in sexual congress (e.g. Zalasiewicz 1984) or asexually developing supercolonies (Ruedemann 1947; Bulman 1970). However, the nature of synrhabdosomes remains enigmatic (cf. Rigby 1993; Underwood 1993; Gutiérrez-Marco & Lenz 1998).

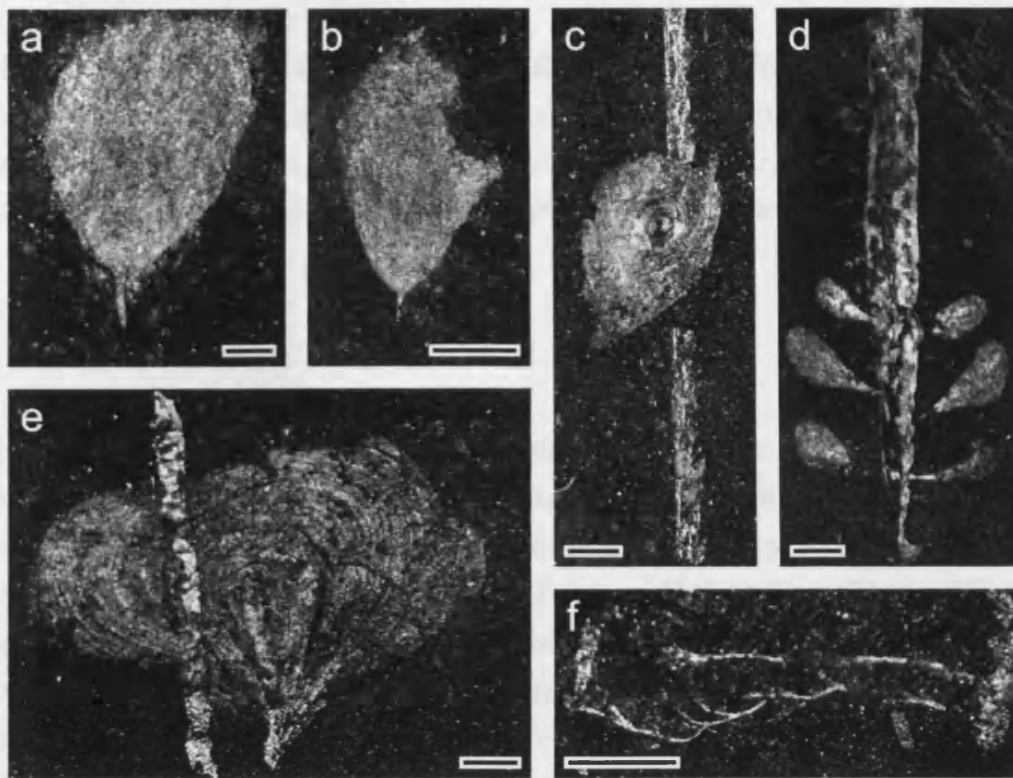


Fig. 3.1 Photomicrographs of supposed graptolite ovarian vesicles. (a-c) "*D.* *campanulata* Nicholson 1873 and (d-f) graptolites with appendages, Dobb's Linn, Birkhill Shale Formation. (a) lectotype, NHM P1976; (b) syntype, NHM P1976; (c) exhibiting a prominent "nipple" and juxtaposed to an indet. monograptid, though preserved on a different sedimentary lamina, NHM P1976; (d) *Dittograptus?* sp. (Elles 1940) with well-preserved scopulae ('graptogonophores'), SM A13731; (e) nemal vane of *?Pribylograptus incommodus* (Törnquist 1899) cf. Crowther (1978) overlain by indet. graptolite, see also Fig. 1.2h, NHM P1981; (f) detail of poorly-preserved scopula ('graptogonophore') of *Hallograptus bimucronatus* (Nicholson 1869), the scopula originates from the graptolite to the right, the concentric lines represent progressive growth increments constrained by the scopula's better margin, BU 1420. All specimens photographed under reflected light. Nicholson's specimens (a-c, e). Scale bar = 1 mm (a-c, e-f), 500 μ m (d).

In order to assess whether putatively vesicular graptoloid tissues played a role in reproduction, I have undertaken a thorough re-evaluation of sac-like graptolite appendages (Fig. 3.1d, f) and also of "*Dawsonia*" Nicholson 1873 (e.g. Figs 3.1, 3.2 & 3.3), which was originally interpreted as being an ovarian vesicle of a graptoloid detached from its parent colony. Though this genus has a long history of research, it has "caused

confusion ever since it was first described” (Williams, 1981). I initially establish the context in which the fossils were originally interpreted and how they have been subsequently reinterpreted, prior to re-evaluating them based on the original material and on new specimens.

3.2 History of research

Prior to Kozłowski’s seminal monograph of 1948, the zoological affinities of the graptolites attracted much debate. They were initially thought to be a moss (Von Bromell 1727), to be artefacts (Linnaeus 1768), or even, as Nimmo (1847) suggested, the tail spines of the Indian Ocean ray *Raja pastinaca*, though Nimmo had probably never seen a graptolite (Elles & Wood 1901-1918, p. xiii). Eventually, graptolites were recognised as colonies consisting of a series of cup-shaped orifices (thecae) and they were variously assigned to the Cnidaria and Bryozoa (see summaries in Elles & Wood 1901-1918; Kozłowski 1948; Crowther 1978). As the reproductive strategies employed in these groups differ considerably, no small part of the discussion of their systematic position focussed on the interpretation of rare, attached, putatively sac-like appendages (e.g. Nicholson 1872; Ulrich & Ruedemann 1931).

3.2.1 1850-1870: sac-like appendages and ‘graptogonophores’

Graptolites bearing sac-like appendages have been known since the 1850s, but due to “various [unspecified] accidental difficulties” (Logan *in* Hall 1865 and references therein) illustrations were not published until the next decade. Hall (1865) proposed that these appendages were reproductive bodies similar to hydrozoan gonothecae, and suggested that graptolites were closely related to the sertularians. It seems Hall’s work captured the imagination of the young H. Alleyne Nicholson: Hall’s monograph was likely used by Nicholson to aid the identification of the graptolites he collected in the Southern Uplands. Indeed, Nicholson (1866, 1872, 1873) regularly referred to Hall’s work on graptolite reproduction.



Fig. 3.2 Nicholson's illustrations of supposed graptolite ovarian vesicles, including (a-f) his "*Dawsonia*" type specimens (Nicholson 1873). (a) "*D.*" *acuminata*, (b) "*D.*" *rotunda*, (c-d) "*D.*" *tenuistriata*, (e-f) "*D.*" *campanulata*; (g-m) in Nicholson (1872); (n-o) Nicholson's handwritten specimen labels, NHM.

Whilst collecting the Silurian strata of the Southern Uplands in the summer of 1866, Nicholson discovered a variety of discoidal and ovato-triangular fossils associated with graptolites (e.g. Fig. 3.2). Though not found attached to graptolites themselves, these fossils resemble the supposed reproductive organs described by Hall (1865), and Nicholson (1866) argued that they represented graptolite ovarian vesicles which had detached from their parent colony, and called them 'graptogonophores'. He supported Hall's argument for a hydroid affinity for the graptolites, suggesting that the concentrically 'ribbed' discoidal specimens represented vertical compressions of a sertularian-like graptogonophore, and that the ovato-triangular specimens were preserved in profile. Nicholson supported his interpretation by illustrating several examples where the discoidal and ovato-triangular specimens were closely associated with graptoloids (e.g. Fig. 3.1c).

However, this work was controversial, drawing a vociferous reply from William Carruthers who argued that the associations of the supposed graptogonophores with graptolites were no more than fortuitous juxtapositions, and that the discoidal specimens most likely represented the brachiopod *Siphonotreta micula* (Carruthers 1867a). This precipitated a lengthy correspondence, with Nicholson (1867a, 1867b, 1867c, 1868b) arguing that graptolites were hydrozoans, largely on the basis of their reproductive strategy, whilst the more vehement Carruthers (1867b, 1867c, 1868a, 1868b) stated that considerations of zoological position should be based on 'normal' characters such as colony construction rather than on rare and ambiguous evidence. The latter felt that whilst graptolites were closely allied to the Hydrozoa, they also shared characters with the Polyzoa. As much by perseverance as by any tendency to provide new information, Nicholson's view that graptolites were extinct hydrozoans became more widely accepted. Nicholson's work subsequently focussed more on corals than graptolites (see Benton 1979); and, at this time, graptolite research itself also moved away from more theoretical discussions of their affinity with workers such as Lapworth focussing on the more practical concerns of taxonomy and biostratigraphy (e.g. Elles & Wood 1901-1918; Oldroyd 1990; Rushton 2001).

3.2.2 1870-1900: Graptolite reproduction and "*Dawsonia*" Nicholson

Nicholson's theory of graptolite reproduction supposed that once sufficiently mature, the 'graptogonophore' detached itself from its connection with the parent colony and became a free-swimming zooid (Nicholson 1868a). This assertion was supported in part by evidence for the co-occurrence of 'graptogonophores' and graptolites furnished with ramifying fibres (e.g. Fig. 3.1f) in the same strata (Nicholson 1872).

Nicholson (1873) noted that there were several distinct types of graptogonophore in the Ordovician Lévis Fm. at Point Lévis, Quebec. As it would be almost impossible to relate these back to the individual graptolite species they came from, he referred them to the form genus "*Dawsonia*", much in the manner that one names ichnotaxa independently

of the animal that constructed them. Nicholson (1873) named four species: "*D.*" *acuminata*, "*D.*" *rotunda*, "*D.*" *tenuistriata*, and "*D.*" *campanulata*. Gurley (1896), also working in Point Lévis, added two further species: "*D.*" *monodon* and "*D.*" *tridens*.

These species have disparate temporal and geographical ranges. "*D.*" *campanulata* is only known from Early Silurian strata of the British Isles (Nicholson 1873; Lapworth 1876, 1876-7; Marr & Nicholson 1888; Peach & Horne 1899; Williams 1981, 1996), though it occurs in both Laurentia (in Moffatdale, Scotland, and Coalpit Bay, Donaghadee, Northern Ireland) and Avalonia (the English Lake District), which were on either sides of the Early Palaeozoic Iapetus Ocean at this time. "*D.*" *rotunda* and "*D.*" *tenuistriata* are only found in the Ordovician Quebec Group at Point Lévis, Canada (Nicholson 1873), and Gurley's species have only been recorded in the Ordovician of North America at Point Lévis, Quebec, and the Deep Kill, near Melrose, New York (Ruedemann 1904, 1934; Vannier *et al.* 2003). However, "*D.*" *acuminata* appears to be more cosmopolitan, with Nicholson (1873) stating that it occurs at both Point Lévis, Canada, and in northern England. Nicholson (1873) noted that his concept of "*D.*" *acuminata* was similar to "*D.*" *campanulata* in both stratigraphic range and form, though he acknowledged that its outline was notably more triangular and its mucro (proximal termination) less sharply delineated.

Nicholson (1873) believed that his localities in the UK and Canada were contemporaneous and of similar age to graptolites bearing sac-like appendages (Hall 1865, Nicholson 1872), though graptolite biostratigraphy now reveals this to be untrue (cf. section 6 & refs in Fig. 3.5a). However, in the 1870s the age of the strata in the Southern Uplands sections was somewhat of an enigma (Oldroyd 1990; Rushton 2001), making correlation with North American sections problematic.

3.2.3 Twentieth century work on graptolite reproduction

The 20th century saw graptolite reproduction become a less prevalent area of research, and since a pterobranch affinity for graptolites has been clearly demonstrated (Kozłowski 1947, 1948; Towe & Urbanek 1972;

Crowther 1978), Nicholson's work has become largely overlooked. However, biserial graptoloids with sac-like appendages unquestionably attached to their rhabdosome continued to be described as reproductive structures in the early twentieth century (e.g. Elles 1940). Likewise, Ulrich and Ruedemann (1931) reported dendroid graptolites with swollen, oval appendages purportedly homologous with bryozoan oecia. However, these correspond to bithecae in terms of position and arrangement, and the specimens are too poorly preserved to discern their precise nature (Kozłowski 1948).

The discovery of eggs and embryos inside the autothecae of benthic graptolites (Kozłowski 1948; Bulman & Rickards 1966) led to a reinterpretation of sac-like appendages in graptolites. Kozłowski (1948) considered Hall's supposed 'egg sacs' to be chitinous envelopes associated with the zooids, though he did not speculate on their function, whilst Bulman (1964) figured several similar specimens in an early discussion of graptolite hydrodynamics. Similarly, more recent discussions of graptolite reproduction have overlooked these and other supposed reproductive organs (e.g. Crowther 1978; Hutt 1991; Underwood 1993). For example, the branching appendages described in Ruedemann (1936) were thought to represent epibionts (Kozłowski 1948). The swollen, oval appendages documented by Ulrich and Ruedemann (1931) might also be epibionts: Kozłowski (1965) showed that *Cephalocystis graptolithifilius*, a similar structure found on other graptolites, is in fact a cephalopod egg capsule comparable to those of the recent *Sepia officinalis* which encrusts the sea grass *Zostera*. Similarly, Underwood (1993) suggested that the putative cases of connection between graptogonophores and graptolites, as illustrated by Nicholson (1866), could plausibly represent parasitic outgrowths or epizoans colonising a graptolite 'benthic island' *sensu* Kaufmann (1978).

However, these and other examples of sac-like graptoloid appendages (e.g. Fig. 3.1d, f) are certainly distinct from the unambiguous parasites figured by Bates & Loydell (2000), but are superficially similar in form and preservation to "*D.*" *campanulata* and "*D.*" *acuminata*, however the latter is

phosphatic and therefore clearly differentiable. As such they require re-examination. Since Kozłowski's influential work 'graptogonophores' have generally been described as sac-like or vane-like appendages with little comment as to their function (e.g. Bulman 1964; Koren' & Rickards 1997).

3.2.4 A pterobranch-like model for graptolite reproduction?

Since scanning electron microscopy has been employed for studies of graptolite ultrastructure (e.g. Towe & Urbanek 1972; Crowther 1978, 1981), an affinity for graptolites with the pterobranch hemichordates has become widely accepted (e.g. Dilly 1993; Cameron 2005; Maletz *et al.* 2005). As such, recent discussions of reproduction in graptolites (e.g. Hutt 1991) have been premised on the belief that graptolites adopt pterobranch-like mechanisms (cf. Gilchrist 1915; Stebbing 1970). The pterobranchs *Rhabdopleura* and *Cephalodiscus* reproduce both sexually and asexually (Hutt 1991). Though most zooids in *R. compacta* are neuter or sexually immature, certain zooids may metamorphose and develop either an ovum or testis (Stebbing 1970). Whilst the sexes are separate in *Rhabdopleura*, certain species of *Cephalodiscus* colonies may be hermaphroditic, with certain zooids bearing both male and female reproductive organs (Horst 1939, Bulman 1970). Though its colonies are sessile and its zooids have limited movement, *Rhabdopleura* undergoes internal fertilisation, with its oviduct serving only as a conduit for sperm to reach the ova (Stebbing 1970). In both *Rhabdopleura* and *Cephalodiscus*, clutches of embryos remain in the creeping tube until they mature as ciliated, lecithotrophic larvae (Dilly 1973; Lester 1988a). The larva leaves the creeping tube as a free-swimming individual which secretes a collagenous, dome-shaped prosiculum (Dilly 1973; Dilly & Ryland 1985). Later, the larva metamorphoses under the prosiculum and emerges as a juvenile (Dilly & Ryland 1985; Lester 1988b) that settles on the substrate and later asexually buds to form a colony (Stebbing 1970; Dilly 1973).

Though there is little direct evidence of reproduction in the graptolite fossil record (cf. Hutt 1991), eggs and embryos have been reported in

certain specimens (Kozłowski 1948; Bulman & Rickards 1966). This would be consistent with graptolites producing a free-swimming lecithotrophic larva, that later secretes a prosicula (equivalent to the pterobranch prosiculum) in the plankton before maturing (cf. Williams & Clarke 1999) and budding to form a colony.

3.2.5 Historical interpretations of "*Dawsonia*" Nicholson

3.2.5.1 "*D.*" *monodon*, "*D.*" *tridens*, "*D.*" *acuminata*, and "*D.*" *campanulata*: crustaceans, molluscs or algae? These mucronate species have received more attention than the other species, which are dealt with below. "*D.*" *monodon* and "*D.*" *tridens* were originally described by Gurley (1896), but have long been considered to be tail-pieces of the crustacean *Caryocaris* (Ruedemann 1934; Rolfe in Theokritoff 1964). Rolfe (1969, p. 316) stated that "*Dawsonia*" is a junior synonym of *Caryocaris* Salter (1863), but did not re-examine Nicholson's material (Ian Rolfe, pers. comm.). Though "*D.*" *acuminata* has all but vanished from the literature, "*D.*" *campanulata* is often used.

Lapworth (1876-7) considered "*D.*" *campanulata* to be a member of the crustaceans in his catalogue of fossils from western Scotland, perhaps due to its similarity and common co-occurrence with the putative crustaceans *Aptychopsis* Barrande (1872), *Peltocaris* Salter (1863), and *Discinocaris* Woodward (1866) (Lapworth 1876, 1876-7; Marr & Nicholson 1888; Peach & Horne 1899). These putative crustaceans look similar to certain "*Dawsonia*" species: disarticulated valves of *Peltocaris* and *Aptychopsis* are similar to "*D.*" *campanulata* in outline, and *Discinocaris* has an ornament similar to that of "*D.*" *rotunda* and "*D.*" *tenuistriata*. However, none of the "*Dawsonia*" material examined in this study bears the characteristic dovetail symmetry that characterises complete specimens of these other taxa. Gürich (1928) also compared "*D.*" *campanulata* to *Peltocaris*, which he considered to be the covers of a hyolithid or chiton-like organism. However, this work offered no firm conclusions as to the affinities of "*Dawsonia*" and I have found no evidence of either hyolithids or chitons co-occurring in the same strata as it.

The affinities of *Aptychopsis*, *Peltocaris*, and *Discinocaris* remain uncertain. Rolfe (1969, p. 328) noted that “they have been compared and confused with graptolite ‘swim bladders’ and ‘gonangia’, eurypterid metastomata, hyolith opercula, polyplacophoran plates, bivalves, arthodire dermal plates, and branchiopod carapaces,” and he noted there was no evidence to support an affinity for either *Aptychopsis*, *Peltocaris*, or *Discinocaris* with the phyllocarids. Rolfe (1969, pp. 328-329) suggested that these taxa may perhaps represent the aptychi of soft-bodied cephalopods rather than being crustacean carapaces. However, he did not go as far as synonymising *Aptychopsis*, *Peltocaris*, and *Discinocaris* with the aptychus morpho-genus *Sidetes* Giebel *sensu* Moore & Sylvester-Bradley (1957).

There is no good reason to group “*D.*” *campanulata* with these supposed aptychi. Indeed, neither Gürich’s (1928) work nor a crustacean affinity gained serious consideration in the most recent re-examination of “*D.*” *campanulata*, which tentatively reinterpreted it as an alga (Williams 1981).

3.2.5.2 “*D.*” *rotunda* and “*D.*” *tenuistriata*: possible brachiopods?

Neither “*D.*” *rotunda* nor “*D.*” *tenuistriata* are mucronate: together they form a group of small, subcircular shelly-fossils. Though Nicholson (1873) stated that “*D.*” *rotunda* and “*D.*” *tenuistriata* appeared too variable in form and appearance to be inarticulate brachiopods, this assertion was questioned from the outset (Carruthers 1867a; Ruedemann 1904, 1934). More recently, Benton (1979) noted that some of the Nicholson’s type material may be small brachiopods.

3.2.5.3 Misdiagnoses.

Several incompatible forms have been erroneously assigned to “*Dawsonia*” Nicholson principally because little or no reference was made to the type specimens. As Benton (1979) noted, the trace fossil *Lockeia* U.P. James was misdiagnosed as “*Dawsonia*” by U.P. James’s son, J.F. James (1885, 1892). As “*Dawsonia*” is preserved as a body fossil, this name clearly cannot be applied to a trace fossil (Häntzschel 1965, 1975; Osgood 1970). However, the name “*Dawsonia*

cycla" is still used for another fossil from the Cincinnati area which consists of small, black, shiny discs that are found encrusting the surfaces of nautiloid conchs. Though Frey (1989) thought that these discs may represent the attachment sites of the dendroid graptolite *Mastigograptus*, they are now thought to represent the epibiont *Sphenothallus* (Neal & Hannibal 2000).

3.2.6 The current status of "*Dawsonia*" Nicholson

The name "*Dawsonia*" is still widely used by graptolite workers (e.g. Williams 1996), though now it is almost exclusively used as shorthand for "*D.*" *campanulata*, which is its type species (Miller 1889). No consensus as to its taxonomic status or systematic position has yet emerged. Though the genus "*Dawsonia*" was conceived to describe the egg sacs of a sertularian-like hydroid, this name has been applied to unrelated fossils from all of the major divisions of the bilateria. Its type species, "*D.*" *campanulata* was most recently interpreted as an alga (Williams 1981). *Dawsonia* Nicholson is junior homonym of the trilobite *Dawsonia* Hartt in Dawson (1868). With all the above in mind, Nicholson's genus is in need of taxonomic revision.

3.3 Material and methods used in this study

3.3.1 Nicholson's types and comparative material

Much of Nicholson's type and figured material is housed in the Natural History Museum [NHM], London, which purchased a collection of 1400 graptolites from Nicholson in 1883 (Benton 1979). The unfigured portion of Nicholson's collection remains in the Aberdeen University Geology Department, and is catalogued in Benton and Trewin (1978). Nicholson's material from the Lake District lies in the Harkness and Marr collections of the Sedgwick Museum, Cambridge [SM].

The type material of "*Dawsonia*" Nicholson, as recognised by Benton (1979) is in the G.J. Hinde collection of the NHM. It has been re-examined

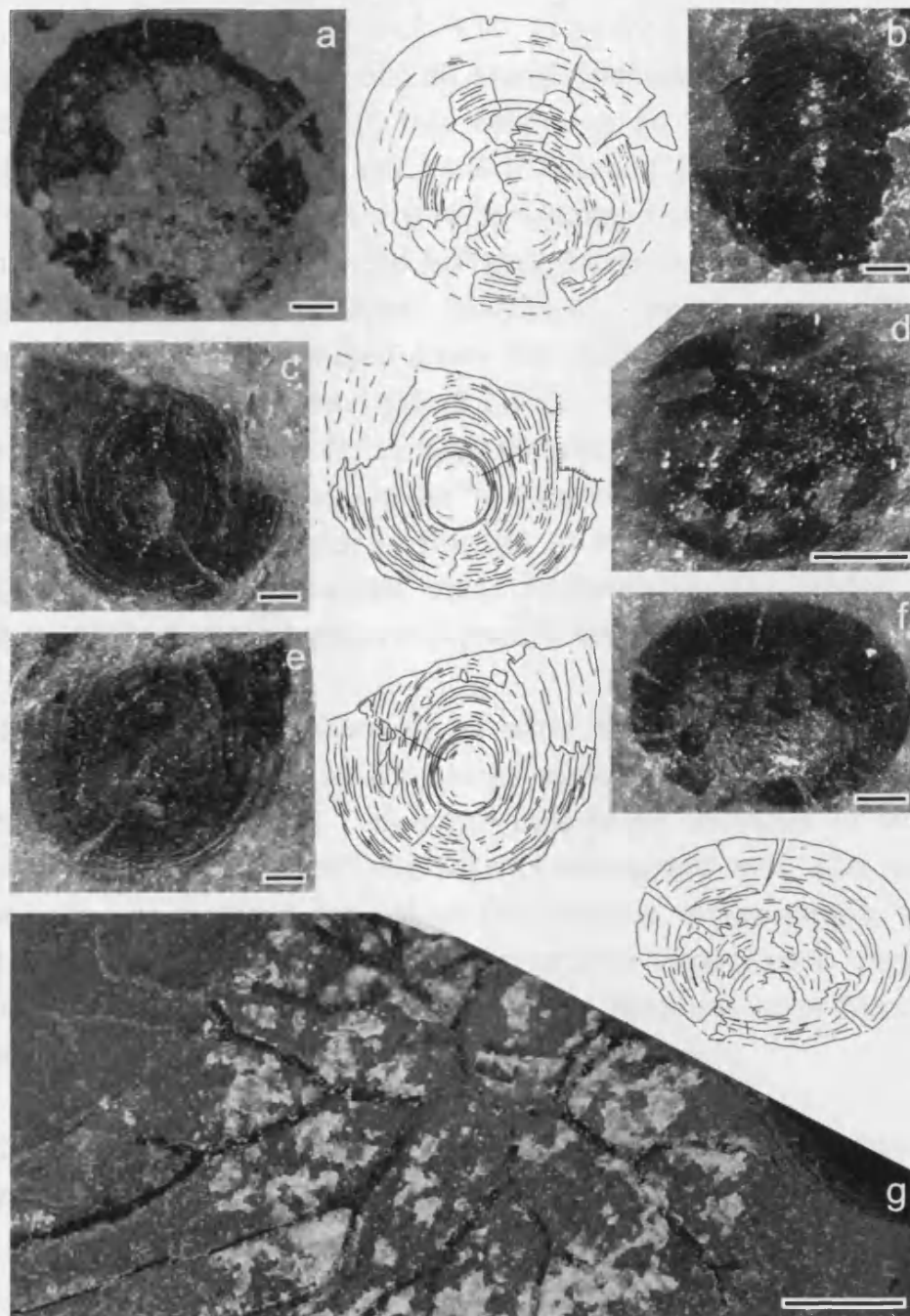


Fig. 3.3 Linguliform brachiopods (a-f) and a graptolite (g) from the Lévis Shale, Point Lévis, Quebec, Canada. (a-b, d) *Acrosaccus? rotunda* (Nicholson 1873): (a) pedicle valve, NHM P1985.3, (b) dorsal valve, NHM P1985.3, (d) lectotype, NHM P1982.1; (c, e) *Paterula? tenuistriata* (Nicholson 1873): (c) lectotype, NHM P1984.3, (e) counterpart NHM P1984.2; (f) *Discotreta* cf. *levisensis* (Walcott 1908), lectotype NHM P1984.2; (g) *Clonograptus* sp., NHM P1982. All specimens photographed under reflected light and are from Nicholson's material. All scale bars = 500 μ m.

and re-accessioned as part of this study. Nicholson did not identify any specimens from UK strata in this collection as "*D.*" *acuminata*, despite mentioning its occurrence in northern England (Nicholson 1873). Given that Nicholson's illustrations are often idealised woodcuts taking features from several specimens (Benton & Trewin 1978), it has been impossible to precisely determine his type specimens. However, as Nicholson's diagnoses can be recognised from his distinctive handwriting on the manuscript specimen labels (Fig. 3.2n-o), I have assigned lectotypes for each of his four species. "*D.*" *campanulata* remains the type species of the genus (secondary diagnosis, Miller 1889 *contra* Ruedemann 1904, 1934). Other comparative material is housed in the British Geological Survey [BGS] collections at Keyworth, near Nottingham, the Ulster Museum, Belfast [BEL] and in the Lapworth Museum, University of Birmingham [BU].

In order to compare "*Dawsonia*" with the sac-like appendages of graptolites, I undertook an extensive search of museum holdings and appropriate literature. "*D.*" *campanulata*-bearing localities in Moffatdale, southern Scotland, and the Lake District of England were also recollected to provide an unbiased sample of this species. I was unable to collect field specimens of graptolites bearing sac-like appendages, perhaps due to their relative rarity, and I rely entirely on museum collections for such graptolites.

In addition to the occurrences of "*Dawsonia*" noted in section 1.2 and above, Ruedemann (1904, p. 734) commented that "[*D.*" *campanulata*] is very common in the Trenton (Normanskill) graptolite shales of New York and Canada." However, I have not been able to identify this fossil amongst Ruedemann's original collections, although there are plenty of graptolites bearing 'graptogonophores' in his material. In addition, Ruedemann (1908) reported that in 1889, Ami named three new species of "*Dawsonia*" from graptolitic strata in the St Lawrence region of Canada. However, I have been unable to find any trace of Ami's "*Dawsonia*" species in either the literature or in museum collections. Likewise, I have been unable to find Gurley's type specimens of "*D.*" *monodon* and "*D.*"

tridens. Though they were once held in the collections of the New York State Museum, Albany, NY [NYSM] (Ruedemann 1934 & references therein), they are no longer in its possession. When Ruedemann (1904) illustrated "*D.*" *monodon* and "*D.*" *tridens* specimens from NYSM collections, he chose examples from the Quarry at the Deep Kill, near Melrose, New York, only copying Gurley's drawings of the Point Lévis material. This suggests that they were not in the NYSM at that time either. It may be that the specimens went missing at the very end of the 1800s when a long-term budget deficit led James Hall to sell many specimens to keep the Geological Survey and State Museum afloat (Ed Landing, pers. comm. 2004).

Though Ruedemann's (1904, 1934) material has been re-examined for comparative purposes, neither those specimens nor Nicholson's Point Lévis specimens clearly preserve the carapace. Given that *Caryocaris* taxonomy is primarily based on carapace morphology, I am unable to determine whether Ruedemann's specimens are truly synonymous with Gurley's species. As such, this chapter focuses on clarifying Nicholson's concept of the "*Dawsonia*" species, rather than entering the more nebulous realm of phyllopod systematics.

3.2.2 Methods used and terminology employed

All fossils have been studied under reflected light microscopy. Additionally, uncoated specimens were examined at 15KV in backscatter mode in Hitachi S-3600N and LEO 435VP SEMs, with phases identified using energy dispersive X-ray analyses (EDS) using Oxford Instruments INCA and ISIS software, respectively. The electron microscope techniques used closely follow those described in Martill *et al.* (1992) and Orr *et al.* (2002). Illustrated images have been digitally enhanced to increase the contrast between fossil and matrix.

Details of repositories and specimen numbers are listed with the appropriate figures and in the systematic section; details of the criteria used in the morphometric analysis are given in Fig. 3.5. As the brachiopod taxa were often incomplete, morphological measurements

were taken on well-preserved growth-lines as well as on outlines, though in each case these are clearly distinguished in the appropriate figure caption. All measurements were made on camera lucida drawings of x40 or x50 optical magnification, and recorded to an accuracy of greater than one percent.

Morphological terms used in systematic descriptions are as employed in Holmer & Popov (2000) for the brachiopod species, in Rachebouef *et al.* (2000) and references therein for the *Caryocaris* tail-pieces, and defined in Fig. 3.5 for "*D.*" *campanulata*. Because Nicholson's Point Lévis material consists entirely of disarticulated specimens, I have used morphological criteria to assess which forms could plausibly conjoin based on the present understanding of inarticulate brachiopods and *Caryocaris* in order to avoid unnecessary taxonomic inflation. Abbreviations used in the synonymy lists are those of Matthews (1973) and the qualifiers used in open nomenclature may be found in Bengtson (1988).

3.4 The nature of *Dawsonia* Nicholson

It is clear that "*Dawsonia*" is polyphyletic. The lectotype of "*D.*" *acuminata* is a furcal ramus from the tail-piece of the crustacean *Caryocaris acuminata* (Fig. 3.4). Other fossils within the fauna include telsons and carapace fragments which are considered conspecific given the present understanding of *Caryocaris* morphology (Fig. 3.4d). The lectotypes of "*D.*" *rotunda* and "*D.*" *tenuistriata* are linguliform brachiopods (Fig. 3.3c-d) and have been tentatively re-assigned to the genera *Acrosaccus* and *Paterula* respectively, and Nicholson's type collection also contains a form provisionally identified as *Discotreta* cf. *levisensis* (Fig. 3.3f). As no articulated specimens are present I cannot unambiguously determine which shells articulated in life. However, two of the four discrete shell morphotypes shown in Fig. 3.5c have indistinguishable outlines (with W/L ~1) and probably represent an unequivalved species. The other two shell morphotypes could not plausibly co-join (cf. Fig. 3.5c), consistent with

there being three species present in the collection. The systematic palaeontology of these taxa is dealt with in section 1.7.

The style of preservation of the above listed dawsoniids is different from the graptolites which co-occur in the Point Lévis fauna, suggesting that they were originally composed of non-graptolitic material. The graptolites are preserved as dull, black compressions, whereas the dawsoniids are generally in relief, having a horny texture and some having a bronze, pyritous sheen. EDS analyses of the Point Lévis dawsoniids specimens reveals that they are preserved as phosphate with some associated pyrite (Fig. 3.6f, g). This composition is consistent with these taxa being caryocarid arthropods and linguliform brachiopods rather than graptolites, which are carbonaceous. Therefore, these species of "*Dawsonia*" are reassigned to their appropriate clades and can be discounted from any consideration of graptolite reproduction.

Though Nicholson (1873) mentioned the occurrence of "*D.*" *acuminata* in English strata, I have been unable to identify it in UK collections. Morphometric analysis reveals that there is some overlap between "*D.*" *campanulata* and *C. acuminata* (Fig. 3.5b, d). However, even the most slender "*D.*" *campanulata* can be clearly distinguished from *C. acuminata* by the presence of a delineated mucro, its rounded latero-distal margin (Fig. 3.3), and its composition (Fig. 3.6a-d). It therefore seems most likely that Nicholson was either mistaken referring to slender "*D.*" *campanulata* morphotypes as "*D.*" *acuminata* in organic rather than phosphatic preservation, or he was perhaps confusing the tail-pieces of *Caryocaris wrighti* which occur in strata of the British Isles (Rushton & Williams 1996; Vannier *et al.* 2003) with *C. acuminata*. To avoid unnecessary confusion, I have included Nicholson's so-called "*D.*" *acuminata* from the British Isles within this amended definition of "*D.*" *campanulata*, with *C. acuminata* only referring to his Canadian material.

There is little similarity between "*D.*" *campanulata* and *Caryocaris* tail-pieces (cf. Figs 3.1 & 3.4), or indeed with the Point Lévis dawsoniids, the most notable differences being in its composition and outline. It is

preserved as an organic compression (Fig. 3.6a-d) unlike *Caryocaris*, which is preserved in phosphate (Fig. 3.6g). It is more symmetrical than either the carapace or furcal ramus of a *Caryocaris*, and notably more ovate than the *Caryocaris* telson. Its mucro is too centrally positioned to represent either an anterior horn or a postero-dorsal spine of the *Caryocaris* carapace, and it differs from the marginal spinules of the *Caryocaris* ramus in terms of size and position. Unlike a furcal ramus, the “body” of “*D.*” *campanulata* is ovato-triangular rather than ovato-parallelogrammic, and it lacks a serrated lateral margin. Though lacking a mucro, the grossly teardrop form of the *Caryocaris* telson is similar in shape to the “body” of “*D.*” *campanulata*. However, morphometric analysis (Fig. 3.5b) reveals no overlap between *Caryocaris* telsons (where $D/L < 0.2$) and “*D.*” *campanulata* (where $D/L \sim 0.2-0.6$).

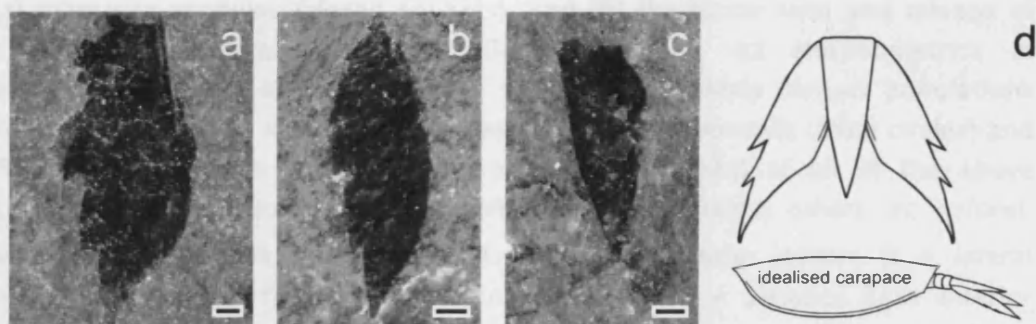


Fig. 3.4 *Caryocaris acuminata* (Nicholson 1873) from the Lévis Shale, Point Lévis, Quebec, Canada. (a) Furcal ramus, lectotype NHM P1985.3; (b) furcal ramus, NHM 1977, (c) telson, NHM P1984.3; (d) a reconstruction of the tail-piece and the whole animal (note schematic carapace). All specimens photographed under reflected light. Scale bars = 500 μm .

Though “*D.*” *campanulata* shares a similar preservation style to the sac-like appendages seen in graptolites (Fig. 3.6a-e), there is no evidence to support a homology. Whilst both are found as silvery organic films in the black shales of the Southern Uplands, “*Dawsonia*” cannot be recognised as a graptolite (Bulman 1970). Morphometric analysis reveals

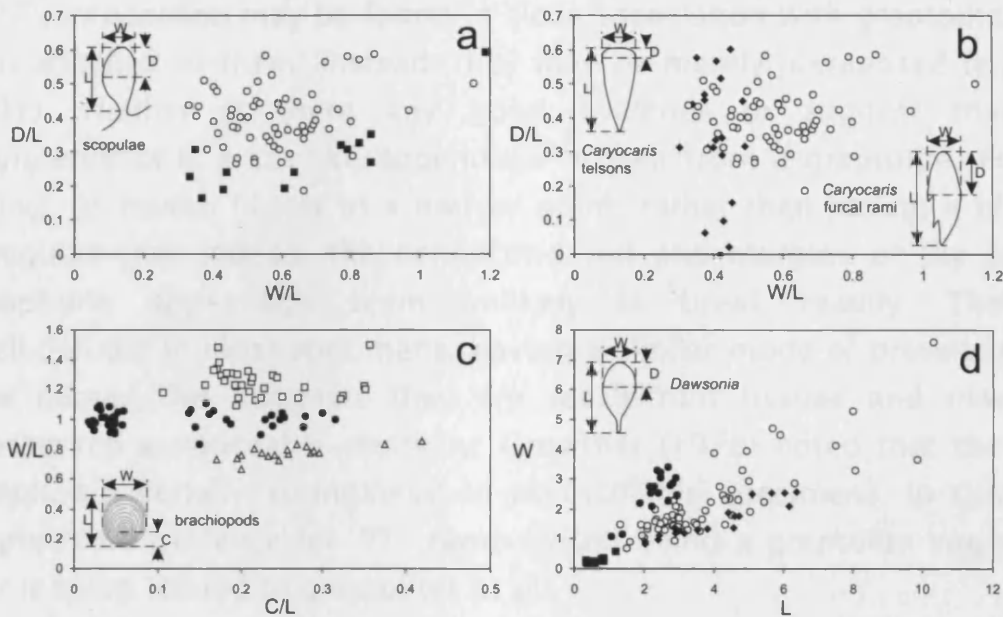


Fig. 3.5 Morphometric analyses. "*D.*" *campanulata* (open circles) compared with (a) graptolite scopulae (closed squares), and (b) the furcal rami and telsons of *Caryocaris acuminata* (combined, filled diamonds). (c) Morphometrics of brachiopod outlines and growth lines (combined) showing distinct populations corresponding to *Di.* cf. *levisensis* (open triangles), *A?* *rotunda* (filled circles) and *P?* *tenuistriata* (open squares). (d) Absolute sizes (mm) of all of the above specimens (brachiopod outlines shown as closed circles, others as before). Morphometric criteria as illustrated: L = anterior-posterior length; W = lateral width; D = distance from blunt margin to centroid; C = distance from anterior margin to growth centre of brachiopod. "*D.*" *campanulata* specimens are those listed under additional material in Section 6; brachiopod and *Caryocaris* specimens are Nicholson's specimens from the Lévis Shale Fm., Point Lévis, Quebec, with specimen numbers listed in Section 6. Graptolite scopulae measurements based on those specimens illustrated in Ruedemann (1908), Elles (1940), Bates & Kirk (1991), Štorch (1994) and Koren' & Rickards (1997), illustrations of "*D.*" *campanulata* were provided by Phil Wilby.

that the similarity between the two is superficial, with the graptolite appendages having a consistently more distal centroid (Fig. 3.5a). They are also more asymmetrical and more variable in their form than "*D.*" *campanulata*, and there is no discrete transition between their connecting rods and their lobate distal part, which is quite unlike the transition between the mucro and the lobate "body" in "*D.*" *campanulata*. Though

"D." campanulata may be found in close association with graptolites, it is not attached to them; instead, they may be merely juxtaposed (e.g. Fig. 3.1c). Neither is there any good evidence to suggest that *"D." campanulata* is a sac-like appendage broken from a graptolite. For one thing, its mucro tapers to a narrow point, rather than having a blunt or irregular end. Indeed, the connecting rod and margins of the sac-like graptolite appendage seem unlikely to break readily. They are well-defined in most specimens, having a similar mode of preservation to the nema. This suggests they are recalcitrant tissues and may have possessed a noticeable elasticity: Crowther (1978) noted that the nema displays a certain 'springiness' in acid-isolated specimens. In summary, there is no evidence for *"D." campanulata* being a graptolite egg-sac, or for it being related to graptolites at all.

A concentric, raised, nipple-like structure occurs in several specimens of *"D." campanulata* (e.g. Fig. 3.2f) and has previously been interpreted as evidence for it having originally had a hollow body (Williams 1981). Nicholson (1872, 1873) believed that this 'nipple' represented compression of a hollow three-dimensional egg-sac onto its more rigid mucro. However this does not appear to be the case, as many specimens reveal both a mucro and a 'nipple' (e.g. Fig. 3.1c), and some specimens show that *"Dawsonia"* may only partially overlap a 'nipple' (Fig. 3.6c). Instead, SEM investigation reveals the nipples to be composed of diagenetic pyrite adopting a rounded and concentric habit (cf. Allison 1988c; Underwood & Bottrell 1994). As such, the 'nipple' is best considered to be a product of compression of *"Dawsonia"* onto pyrite formed in early (?pre-compaction) diagenesis, rather than an intrinsic part of the fossil.

Detailed examination of the sac-like appendages of *Hallograptus bimucronatus* reveals that concentric lines are also present in them (Fig. 3.1f), cross-bracing better preserved margins. However, they are consistent with being the remnants of fusellar structures like those seen in the *Orthoretiolites hami* scopula (Bates & Kirk 1991). Such a mode of

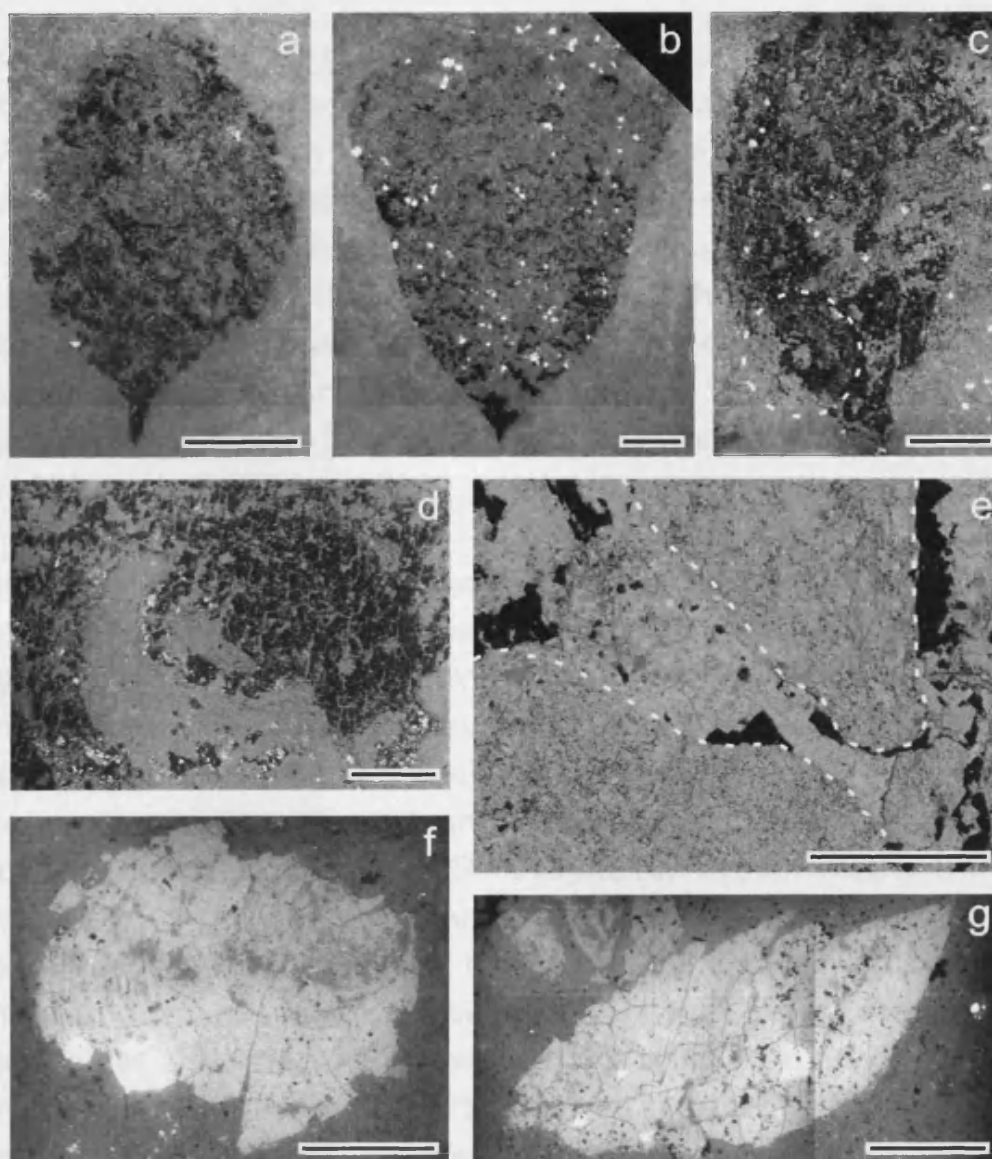


Fig. 3.6 Preservation of Nicholson's type material and a graptolite scopula. High contrast BS SEM images illustrating close-ups of (a-d) "*D.*" *campanulata*, (e) graptolite scopula, (f) brachiopod, and (g) *Caryocaris*. The low brightness of "*Dawsonia*" and the scopula indicate preservation as organic compressions; the high brightness of the brachiopod and *Caryocaris* reflects their primary phosphatic compositions; white areas are accessory diagenetic minerals and weathering products. (a) petal-shaped morph, BGS GSM 105817; (b) bell-shaped morph, BGS GSM 105816; (c) partially overlying and imprinting a diagenetic pyrite to produce a well-developed "nipple" (outlined), SM A20905a; (d) close-up of a "nipple" showing its concentric structure defined by diagenetic pyrites, SM A 20905a; *continued overleaf...*

fabrication would deny the possibility that these structures formed a housing from which an 'egg-sac' could easily detach as Nicholson (1868a, 1872) suggested. Nicholson believed that "*D.*" *campanulata* represented a graptolite egg-sac that became a free-swimming entity, supposing that it was hollow and filled with eggs whilst housed in a cup of ramifying fibres connected to the graptolite. He proposed that this 'ovarian vesicle' slid out once it was able to swim freely. However, if *Hallograptus* constructed its appendages in a manner comparable to the scopula of *O. hami*, it would represent a plate-like, rather than cup-like, structure (cf. Bates & Kirk 1991).

Indeed, it is doubtful whether sac-like graptolite appendages represent egg-sacs. The preponderance of these features in scalariform preservation suggests that they originated from the interthecal wall rather than connecting the thecae *per se*, so there is no direct evidence for their intimate connection with the zooid itself. Moreover, their regularity of form is inconsistent with what one would expect of an unambiguously vesicular structure such as the *Climacograptus wilsoni* vesicle (Williams 1994). Given that these structures are only known in the biserial graptolites, it seems unlikely that they are related to graptolite reproduction. Indeed, when such seemingly vesicular structures are found in graptolites they are often attributed to being floatation devices (e.g. Bulman 1963, 1970; Rickards 1975; Finney & Jacobsen 1985). In fact, the supposed float structure on the nemal of the Ordovician graptolite *Pseudclimacograptus angulatus* (Bulman) bears a remarkable similarity in shape "*D.*" *campanulata* (cf. Finney & Jacobsen 1985; Figs 3-4) although the latter occurs long after this graptolite had gone extinct. However, this similarity is almost certainly superficial. The 'float' has a distinctive ornament that runs parallel to its outline which is not seen in

Fig. 3.6 (continued from previous page) (e) holdfast and proximal body of scopula (outlined) attached to graptolite illustrated in Fig. 1.1d, SM A13731; (f) *A. rotunda*, syntype NHM P1985.2; g) furcal ramus of *C. acuminata*, NHM P1985. Specimens from the Birkhill Shale Fm. of Duffkinnel Burn (a-b), Coalpit Bay (c, d) and Dobb's Linn (e); and, Lévis Shale Fm., Point Lévis (f-g). Scale bar = 1 mm (a-c, f-g), 500 μ m (d-e).

"Dawsonia"; and it is hard to imagine how such a float would break off a nema to form the neatly tapering mucro seen in *"D." campanulata* or why these floats would cluster together in the manner so typical of *"D." campanulata* assemblages.

3.5 Discussion

Nicholson remains one of the great early graptolite workers, despite being wrong in his views of graptolite reproduction (Nicholson 1866, 1872, 1873, etc.). It was not until Clupáč (1970) discovered well-preserved caryocarids in limestone nodules from the Ordovician of Bohemia that the morphology of their tail-piece was fully understood; hence, it is understandable that Nicholson (1873) did not recognise *"D." acuminata* as such, despite recognising *Caryocaris* carapaces in the Point Lévis fauna. Nicholson's assertion that *"D." rotunda* and *"D." tenuistriata* were not brachiopods appears at odds with his (1867a) claim that "it is impossible that any palaeontologist, possessed of ordinary powers of observation, should fall into an error so gross [as to fail to recognise an inarticulate brachiopod]".

Noting the variability of form within *"D." tenuistriata*, for example, Nicholson (1873, p. 142) argued that describing the species as egg-sacs allowed for greater morphological plasticity, otherwise "we should have to believe there were four or five distinct species of brachiopods in these beds which is very unlikely" (the information in Benton (1979) confirms that Nicholson was not accustomed to such faunal diversity in UK sections). It appears that he conflated the beak of the brachiopods with the variably positioned "nipple" of *"D." campanulata* (e.g. Fig. 3.2), a false homology that underpinned his *"Dawsonia"* concept. So, in an age before taphonomy and palaeoenvironment were generally considered, when many species were only known from disarticulated fragments, Nicholson explained the vagaries of variable preservation and differing morphology in a strikingly diverse fauna by appealing to his theory of graptolite reproduction.

3.6 Conclusions

There is no evidence to support the notion that "*Dawsonia*" is related to graptolite reproduction. Likewise, there is no strong case for sac-like appendages on graptolites having a reproductive function, given the discovery of eggs and embryos in the thecae of benthonic graptolites, and our knowledge of reproduction in the pterobranchs (Kozłowski 1948; Bulman & Rickards 1966; Stebbing 1970; Dilly 1973; Hutt 1991). Neither sac-like appendages nor synrhabdosomes seem to have any role in graptolite reproduction, with both recently reassessed as relating to hydrodynamics and cooperative feeding strategies respectively (Page *et al.* 2004, 2006a).

All known species of "*Dawsonia*" have been reassigned to valid genera except "*D.*" *campanulata*, which is best considered a problematicum. "*D.*" *acuminata* Nicholson, "*D.*" *tridens* Gurley and "*D.*" *monodon* Gurley represent the tail-pieces of *Caryocaris acuminata* (Nicholson 1873). I suggest that *C. monodon* (Gurley) should not apply to specimens from Point Lévis (*contra* Ruedemann, 1934). "*D.*" *rotunda* Nicholson is tentatively reassigned to the brachiopod genus *Acrosaccus*, and "*D.*" *tenuistriata* Nicholson is accommodated by the brachiopods *Paterula? tenuistriata* and *Discotreta cf. levisensis* (Walcott 1908). The trace fossil misdiagnosed as *Dawsonia* Nicholson by J.F. James (1885, 1892) has long been known to represent the trace fossil *Lockeia* U. P. James (1879) (see Benton 1979), whilst "*Dawsonia cyclo*" most likely represents the epibiont *Sphaenothallus* (Frey 1989; Neal & Hannibal 2000).

"*D.*" *campanulata* remains a problematicum, and further information is needed before it can be assigned to any major group. Though *Dawsonia* Nicholson is an invalid generic name, it would be premature to formally re-describe it until further information pertaining to the affinity of "*D.*" *campanulata* is available. That nobody has provided a more definite idea of what "*D.*" *campanulata* may represent in the hundred years since

Nicholson's early death can be taken as a minor tribute to the man who clearly recognised its uniqueness.

3.7 Systematic palaeontology

Phylum *Arthropoda*, von Siebold & Stannius, 1845
Superclass *Crustacea* Pennant, 1777
Class *Malacostraca* Latrielle, 1806
Subclass *Phyllocarida* Packard, 1879
Order *Archaeostraca* Claus, 1888
Family *Caryocarididae* Racheboeuf, Vannier & Ortega, 2000
Genus *Caryocaris* Salter, 1863

- * 1863 *Caryocaris* n. gen. Salter, p. 139.
- non* 1868 *Dawsonia* Hartt *in* Dawson, p 655.
- p. 1873 *Dawsonia* Nicholson, pp. 139-140 *pars.*
1896 *Dawsonia* Nicholson; Gurley, p. 88.
1904 *Caryocaris* Salter; Ruedemann, pp. 738-742.
1969 *Caryocaris* Salter; Rolfe *in* Moore, p. 316.
2000 *Caryocaris* Salter; Racheboeuf, Vannier & Ortega, pp. 322-323.

Remarks. The synonymy above is in addition to the detailed list in Racheboeuf, Vannier & Ortega (2000). In the absence of a carapace, a tail-piece consisting of elongate, leaf-shaped furcal rami and a shorter, narrow triangular telson is sufficient to diagnose the genus (Racheboeuf, Vannier & Ortega, 2000, p. 328).

Caryocaris acuminata (Nicholson, 1873)
(Figs 3.4 & 3.6g)

- vp. 1873 *Dawsonia acuminata* n. gen. et n. sp. Nicholson, pp. 140-141, figs 3a-a' *pars.*

- v. 1873 *Caryocaris* sp. Nicholson, p. 143.
- . 1896 *Caryocaris oblongus* n. sp. Gurley, p. 87, pl. 4 fig. 2.
- p. 1896 *Caryocarus* [sic] *curvilatus* n. sp. Gurley, pp. 87-88 *pars*, ?pl. 4 fig. 3, ?pl. 5 fig. 3.
- . 1896 *Dawsonia monodon* n. sp. Gurley, p. 88, pl. 5 fig. 4.
- . 1896 *Dawsonia tridens* n. sp. Gurley, p. 88, pl. 5 fig. 5.
- non* 1904 *Caryocaris* cf. *curvilineatus* [sic] Gurley; Ruedemann, p. 738, pl. 17 fig. 17.
- non* 1904 *Caryocaris* cf. *oblongus* Gurley; Ruedemann, p. 738, pl. 17 figs 14-16.
- p. 1904 *Dawsonia tridens* Gurley; Ruedemann, p. 741 *pars*, ?pl. 17 fig. 18, *non* pl. 17 figs. 19-20 [= *C. monodon*].
- p. 1904 *Dawsonia monodon* Gurley; Ruedemann, pp. 741-742 *pars*, fig. 105, ?pl. 17 figs 21-23, *non* pl. 17 figs 24-26 [= *C. monodon*].
- non* 1934 *Caryocaris curvilata* Gurley; Ruedemann, p. 92, pl. 22 figs 1-9.
- p. 1934 *Caryocaris monodon* (Gurley); Ruedemann, p. 93-95 *pars*, *non* pl. 22 figs 10-14.

Type material. NHM P1985.3 lectotype (furcal ramus).

Additional material. Syntypes NHM P1977, P1982.1-3, P1984.1-2, P1985.3-5, P1988.3: 0 complete carapaces; 8 incomplete carapace fragments; 0 articulated tail-pieces; 11 well-preserved furcal rami; 7 telsons; 15 poorly-preserved or fragmentary furcal rami, telsons and indeterminate fragments.

Type locality. Lévis Shale, Point Lévis, Quebec, Canada. Lévis Formation, Ordovician (Arenig).

Description. Carapace outline indeterminate; linear corrugated ornament on fragments. Tail-piece with narrow triangulate telson lacking ridge or carina; furcal rami elongate, leaf-shaped, ca. 1.5 times longer than telson on average, with acuminate distal margin, bearing large, triangular, posteriorly-directed spines along their outer margin; distinctive narrow ridge and furrow adjacent to its proximal inner margin along its proximal third. Telson ranges from 1.8-2.9 mm in length and 0.9-1.5 mm in width. Furcal ramus ranges from 2.7-6.1 mm in length and 1.3-2.5 mm in width;

smaller specimens may have two marginal spines (e.g. Fig. 3.4b), larger specimens are stouter and more asymmetrical and have three marginal spines (e.g. 3.6g).

Remarks. Until the morphology of its carapace is better known, *C. acuminata* should remain a species separate from *C. monodon* and other caryocarids. *C. acuminata* refers exclusively to caryocarids from Point Lévis and *C. monodon* refers to caryocarids from the exposure at the Deep Kill at Melrose, as laid out in the synonymy above. Though the outline of the tail piece is similar in both localities, the morphology of the tail-piece alone is not well enough placed in the hierarchy of characters to determine synonymy at a species level (Racheboeuf, Vannier & Ortega 2000, p. 328). The variation in number of marginal spines may represent allometric growth (cf. Rushton & Williams 1996); however, small spines may not necessarily be apparent on poorly preserved specimens (see Fig. 1.4b).

As the type specimens of *C. oblongus* Gurley, "*D.*" *monodon* Gurley and "*D.*" *tridens* Gurley are presumed lost meaning so these junior synonymys are only known from Nicholson's material. Therefore, these species can be suppressed as junior synonymys. This is supported by comparison with Gurley's original descriptions and illustrations: "*D.*" *tridens* corresponds exactly with my observations on the furcal ramus of *C. acuminata*, whilst "*D.*" *monodon* most likely represents an articulated *Caryocaris* tail-piece preserved in lateral view. *C. oblongus* presumably represents the fragments of a carapace. Nicholson (1873) also noted *Caryocaris* carapace fragments in the Point Lévis fauna. Similarly, *Caryocarus* [sic] *curvilatus*, described as an aberrant graptolite in Gurley (1896), is most likely an articulated abdomen and tail-piece. Likewise, I wholeheartedly concur with Ruedemann (1904, 1934) that "*D.*" *monodon* and "*D.*" *tridens* represent parts of a crustacean rather than being unusual graptolites.

Though no articulated specimens are present in Nicholson's collection, it seems more parsimonious to describe the disarticulated parts as one species rather than several. Nicholson described "*D.*" *acuminata* prior to mentioning the specimens which he referred to

Caryocaris sp. As such, there seems little controversy in retaining the specific name *acuminata*, which refers to the pointed end of the furcal ramus.

Phylum Brachiopoda Duméril, 1806
Subphylum Linguliformea Williams *et al.*, 1996
Class Lingulata Gorjansky & Popov, 1985

Remarks. I place the three species of brachiopods from Nicholson's Point Lévis material within the Lingulata on the basis of their organophosphatic composition, rudimentary articulation and larval shells. As noted above, many authors have considered them to be brachiopods, though they have not been formally assigned to the phylum until now.

Order Lingulida Waagen, 1885
Superfamily Linguloidea Menke, 1828
Family Paterulidae Cooper, 1956
Genus *Paterula?* Barrande, 1879

non 1868 *Dawsonia* Hartt *in* Dawson, p. 655.

p. 1873 *Dawsonia* Nicholson, pp. 139-140 *pars*.

* 1879 *Paterula* n. gen. Barrande, Pl. 110.

2000 *Paterula* Barrande; Holmer & Popov, 2000, p 75.

Paterula? tenuistriata (Nicholson, 1873)
(Fig. 3.3c, e)

vp. 1873 *Dawsonia tenuistriata* Nicholson, pp. 141-142 *pars*, Figs 3 c-d'.

Type material. Lectotype: NHM P1984.3 (part), P1984.2 (counterpart).

Additional material. NHM P1984.1-3, P1985.3 (5 valves).

Type locality. Lévis Shale, Point Lévis, Quebec, Canada. Lévis Formation, Ordovician (Arenig).

Description. Shell with elongate oval outline, convex. Apex and limbus submarginal to subcentral. Anterior-posterior valve length 1.4->3.4 mm, valve breadth 1.2-3.7 mm, typical specimen breadth >2 mm; length-width ratio 1.2-1.5, typically 1.35; maximum breadth at anterior-posterior midpoint. Growth lines continuous and fine, equally prominent, regular 0.04-0.1 mm spacing throughout the valve.

Remarks. Though this genus is typically unequivalved, only a single valve is present in Nicholson's collections. As *Dawsonia* Nicholson is an invalid taxon there is no conflict of names. While there is some similarity between this form and the younger taxon *P. cf. portlocki* Geinitz (1852) as illustrated by Henningsmoen *in* Waern *et al.* (1948), the material described herein is too poorly preserved to properly compare the taxa. As such, Nicholson's collections need to be supplemented with additional material exhibiting the shell's internal view before this taxon can be precisely placed. Therefore, I have kept the taxon in open nomenclature.

Superfamily Discinoidea Gray, 1840

Family Discinidae Gray, 1840

Genus *Acrosaccus?* Willard, 1928

non 1868 *Dawsonia* Hartt *in* Dawson, p. 655.

p. 1873 *Dawsonia* Nicholson, p. 139-140 *pars.*

* 1928 *Acrosaccus* n. gen. Willard, p. 258.

2000 *Acrosaccus* Willard; Holmer & Popov, 2000, p. 86.

Acrosaccus? rotundus (Nicholson 1873)

(Fig. 3.3a-b, d)

v. 1873 *Dawsonia rotunda* Nicholson, pp. 141-142, figs 3c-3d'.

Type material. Lectotype NHM P1982.1.

Additional material. Syntypes: NHM P1984.2-3, P1985.3 (13 valves: 2 dorsal, 5 pedicle, 6 indet.)

Type locality. Lévis Shale, Point Lévis, Quebec, Canada. Lévis Formation, Ordovician (Arenig).

Description. Shell unequivalved with subcircular outline, equally biconvex. Beak slightly submarginal on one valve and submarginal to subcentral on the other. Anterior-posterior valve length 2.1-2.9 mm, valve breadth 2.1-3.0 mm; length-breadth ratio 0.95-1.1, typically slightly elongate. Growth lines continuous, some more prominent, regular 0.05-0.1 mm spacing, growth lines more clearly defined towards the anterior margin, particularly in valve with submarginal to subcentral beak.

Remarks. Though no articulated specimen is known, the two valves can be inferred as belonging to a single species as their outlines are indistinguishable, suggesting they once did meet. By comparison with the type species, *A. schuleri* Willard (1928), the valve with the more marginal beak is assumed to be the dorsal valve, and the valve with the more central beak being the pedicle valve.

As *Dawsonia* Nicholson is an invalid taxon there is no conflict of names. However, Nicholson's collections need to be supplemented with additional material displaying conjoined valves and internal views for the generic assignment to be confirmed. Until then the taxon should remain in open nomenclature.

I have corrected Nicholson's use of the name 'rotunda' to 'rotundus'.

Superfamily? *Acrotheloidea* Walcott & Schuchert *in* Walcott, 1908

Family? *Acrothelidae* Walcott & Schuchert *in* Walcott, 1908

Subfamily? *Conodiscinae* Rowell, 1965

Genus *Discotreta* Ulrich & Cooper (1936)

non 1858 *Dawsonia* Hartt *in* Dawson, p. 655.

p. 1873 *Dawsonia* Nicholson, p. 139-140 *pars*.

* 1936 *Discotreta* n. gen. Ulrich & Cooper, 1936, p. 619.

2000 ?*Discotreta* Ulrich & Cooper, 1936; Holmer & Popov, 2000, p. 94-95.

Remarks. There appears to be some doubt as to the affinity of the genus, with Rowell (1965) considering it *Incertae Familae* and Holmer & Popov (2000) expressing a degree of uncertainty in its systematic position. These specimens do not preserve sufficient characters to contribute to the debate. There is no doubt, however, in the status of the generic name, as the invalidity of the name *Dawsonia* Nicholson avoids conflict.

Discotreta cf. *levisensis* (Walcott, 1908)
(Fig. 3.3f)

- p. 1873 *Dawsonia tenuistriata* Nicholson; p. 141-142 *pars, non* Figs 3 c-d'.
- * 1908 *Acrothele levisensis* Walcott, 1908, p. 85, pl. 8 fig. 13.
1936 *Discotreta levisensis* (Walcott, 1908); Ulrich & Cooper, p. 619.
1938 *Discotreta levisensis* (Walcott, 1908); Ulrich & Cooper, pl. 6a.
1965 *Discotreta levisensis* (Walcott, 1908); Rowell, p. 281, fig 176.
2000 *Discotreta levisensis* (Walcott, 1908); Holmer & Popov, fig. 47.2a-d.

Type material. Lectotype GSC 8230, paratypes GSC 8230a, b; housed in the Geological Survey of Canada collections.

Material. NHM P1984.1-3, P1985.3-5 (9 valves).

Type locality. Lévis Shale, Ordovician (Arenig); Point Lévis, Quebec, Canada.

Diagnosis. As Ulrich & Cooper (1936).

Description. Shell unequivalved with transversely suboval outline, equally biconvex. Apex submarginal to subcentral and posteriorly positioned, seemingly more submarginal in one valve than the other. Anterior-posterior length 1.0-2.6 mm, valve breadths 1.2-3.4 mm, typical breadth around 3 mm; length-breadth ratio 0.65-0.9, typically 0.8;

maximum breadth at anterior posterior midpoint. Growth lines continuous, more clearly defined away from the apex, regular 0.06-0.11 mm spacing throughout the valve.

Remarks. The quality of preservation, especially the lack of internal features, precludes precise assignment. The valve with the most submarginal apex is most likely the ventral valve by comparison with the specimens of *Di. levisensis* illustrated in Holmer & Popov (2000, Fig. 47, 2a-d).

This species was originally accommodated in Nicholson's (1873) concept of "*D.*" *tenuistriata* which allowed for considerable variation in the position of the apex by comparison with the variably positioned 'nipples' (actually diagenetic pyrite) in "*D.*" *campanulata*. However, as Nicholson's description is of an elongate oval fossil, it seems best to remove this form from "*D.*" *tenuistriata* and compare it with *Di. levisensis*. As it is unknown whether Nicholson's Point Lévis material was collected from the precise locality and horizon of Walcott (1908), this material should not be assigned topotype status.

Phylum, Class, Order & Family uncertain

Genus "*Dawsonia*" Nicholson

- non* 1858 *Dawsonia* Hartt in Dawson, p. 655.
- p. 1873 *Dawsonia* Nicholson, pp. 139-140, *pars*.
- p. 1889 *Dawsonia* Nicholson; Miller, p. 184.
- non* 1904 *Caryocaris* Salter; Ruedemann pp. 738-742.
- non* 1969 *Caryocaris* Salter; Rolfe in Moore, p. 316.
- non* 1970 *Lockeia* James; Osgood, pp. 308-312.
- p. 1981 *Dawsonia* Nicholson; Williams, p. 55.
- non* 1989 "*Dawsonia*"; Frey, fig. 7.

Type species. "*Dawsonia*" *campanulata* Nicholson; secondary diagnosis, Miller (1889).

Diagnosis. Ovato-triangular carbonaceous fossil consisting of a flat, tapering lobate body and a sharply-delineated, narrow triangular mucro. Specimens range in size from 3-12 mm length and 1-4mm width, with the mucro itself being typically less than 0.5 mm in length, and seemingly isometric growth.

“Dawsonia” campanulata Nicholson
(Figs 3.1a-c, 3.6a-c)

- non* 1837 *Prionotus pristis* Hisinger, p. 114, pl. 35 fig. 5.
- non* 1843 *Graptolithus (Prionotus) Sedgewickii* [*sic*] Portlock, p. 318, pl. 19 fig. 1.
- p.* 1866 *Graptolites sedgewickii* (Portlock) pl. 17 fig. 3 *pars.*
- v.* 1867 *Diplograpsus pristis* (Hisinger); Nicholson, pp. 111-113, pl. 7 figs 21-21b.
- v.** 1873 *Dawsonia campanulata* Nicholson, pp. 142-143, fig. 3e-f.
- p.* 1873 *Dawsonia acuminata* Nicholson, pp. 142-143, *pars.*
- v.* 1877 *Dawsonia* sp.; Lapworth, p.7, pl. 7 figs 23a-d.
- .* 1981 *Dawsonia campanulata* Nicholson; Williams p. 55, pl. 6 figs 1-15, pl. 7 fig. 6.
- .* 1995 *Dawsonia* sp.; Williams, p. 196, pl. 36 fig. 16.

Type Material. Lectotype NHM P1976.

Additional Material. Topotypes in Nicholson’s collection NHM P1976; material measured in Fig. 1.5: BGS GSM 105814-9, GSE 10800-1, 3366, PHW 501-553, 18E 73,81,90,94-5,99,102-4,112-3,117 and SM A38754; additional material: SM A20905a-c, A20906; BEL K681; NHM 55641.1-2, 55647.

Type locality. Dob’s Linn, near Moffat, Scotland. Birkhill Shale Formation, Silurian: Llandovery: Rhuddanian.

Range & horizons. Rhuddanian to Aeronian (Llandovery, Silurian) of the British Isles. Birkhill Shale Formation (Moffat Shale Group) in Dob's Linn, Garpol Linn, Plewlands Burn and Duffkinnel Burn, Southern Uplands, Scotland, and in Coalpit Bay, Donaghadee, Northern Ireland; Skelgill Formation (Stockdale Group) in Spengill, nr Sedbergh, Howgill Fells, and Hol Beck, Skelgill, English Lake District.

Description. As genus.

Remarks. "*D.*" *campanulata* cannot be easily accommodated in any higher taxonomic group. It is clearly unrelated to graptolite scopulae, and bears little similarity to either phyllocarids or algae. Although recent works have tried to accommodate it in these groups (cf. Rolfe 1969 and Williams 1981, respectively), neither assignment is entirely convincing. Meanwhile, Underwood (1993, Fig. 4e) illustrated a carbonaceous fossil that looks conspicuously "*Dawsonia*" -like as a faecal pellet. In the most detailed recent study of "*Dawsonia*", Williams (1981) argued that it represented a spore-carrying alga. He stated that "*D.*" *campanulata* had an open, flared "posterior margin, giving the [hollow] body a 'crocus flower' type of appearance". However, it is an order of magnitude larger than such spore-carrying alga in the modern oceans (Tappan 1980) and there is no evidence to suggest it had significant three-dimensionality in life. The 'nipples' seen associated with "*D.*" *campanulata* superficially suggest a three dimensionality, but, as noted in section 3, they actually represent compression of the fossil on to diagenetic pyrite in the sediment. This pyrite notably differs in fabric from the pyrite infill of hollow cavities (cf. Allison 1988c; Underwood & Bottrell 1994). Moreover, "*D.*" *campanulata* lacks the morphological variation seen when unambiguously hollow tissues such as the *Climacograptus wilsoni* vesicle are found flattened in these shales (cf. Williams 1994). And, although the distal margin of "*D.*" *campanulata*'s lobate body may be fragmented (e.g. Fig. 3.1b), and, at times, less-well delineated than the proximal end and mucro (e.g. Fig. 3.6b), there are many examples showing a well-defined, rounded distal margin (e.g. Figs 3.1a, c & 3.6a, c), suggesting that this represents variability in preservation rather than a crocus-flower-like morphology.

With this in mind, "*Dawsonia*" is best considered to be a flat problematicum rather than a hollow alga.

4. Maturation of graptolites catalyses phyllosilicate formation in very-low grade metamorphism

Abstract: Graptolites are commonly preserved in mudrocks as carbonaceous fossils encased in authigenic phyllosilicate coronas. These have previously been held to have formed as “strain shadows” in tectonism. This chapter examines the controls on phyllosilicate formation on graptolites (and by inference other carbonaceous fossils) by making a detailed examination of graptolites preserved in four different geological settings: [1] well-constrained stratigraphic units that can be traced up and down metamorphic grade; [2] between localities showing a contrast in their degree of tectonic strain; [3] at palaeontologically diverse sites where graptolites and shelly fossils coexist; & [4] in localities displaying variable pyritisation. Authigenic phyllosilicates were observed on graptolites and other carbonaceous fossils in strata that have undergone very-low grade metamorphism regardless of apparent tectonic strain. Authigenic phyllosilicates were not observed on coexisting shelly fossils or pyrite euhedra, nor were they found in association with graptolites at lower grades. The general absence of authigenic phyllosilicates in association with inorganic rigid bodies in strained facies precludes a simple “strain shadow” model for their formation. Conversely, petrographic evidence suggests that phyllosilicates formed on denatured graptolite periderm as it underwent volume-loss in maturation. Thus, it seems that phyllosilicate formation occurs due to temperature-dependent mineral-organic interactions catalysed by volatile release in the gas window.

4.1 Introduction

Very-low grade metamorphism witnesses both the maturation of sedimentary organic matter as well as the authigenesis of a broad suite of

phyllosilicates; though this chapter principally deals with the formation of phyllosilicates at deep diagenetic grade, at temperatures and pressures equivalent to gas window conditions (Merriman & Frey 1999), I illustrate many specimens from anchizone rocks, and use very low-grade metamorphism *sensu* Árkai *et al.* (1999, Fig 5.1) (i.e. very low-grade metamorphism = deep diagenetic and anchizone grades). Both kerogen maturation and phyllosilicate formation in very low-grade metamorphism may significantly alter the porosity and permeability of sedimentary rocks, which may, in turn, impinge upon the migration and accumulation of hydrocarbons (cf. Freed & Peacor 1989; Hunt 1996) and potentially affect the underground disposal of radioactive waste (cf. Lalieux *et al.* 1996). Carbonaceous fossils are preserved as kerogens (e.g. Bustin *et al.* 1989; Stankiewicz *et al.* 2000; Gupta *et al.* 2006b, 2007b) and such fossils are commonly found in association with authigenic phyllosilicates in mudrocks that have experienced very-low grade metamorphism (e.g. Chapman 1991; Underwood 1992; Page *et al.* 2005, 2006b). Yet, despite the widespread occurrence of such fossils, our knowledge of phyllosilicate formation on carbonaceous fossils, and its relation to maturation or otherwise, remains uncertain¹.

This chapter serves to examine the controls on phyllosilicate formation on organic-walled fossils using graptolitic mudrocks. Though the formation of phyllosilicates in the early diagenesis of exceptionally preserved fossils has been invoked to explain the preservation of soft-bodied animals (e.g. Gabbott *et al.* 1998; Orr *et al.* 1998; Orr & Briggs 1999), the authigenic phyllosilicates that occur in association with graptolites have generally been held to have formed as strain shadows in tectonism (Crowther 1981; Jenkins 1987; Chapman 1991; Underwood 1992; Sherlock *et al.* 2003). This is no doubt due to alignment of such phyllosilicates with cleavage in some examples (e.g. Figs 4.1b & 4.2e-f) and absence from graptolites in shallow diagenetic grade facies (Figs 4.1c & 4.3a; Table 4.2). Synkinematic phyllosilicates found in association with graptolites has been exploited to calculate strain (e.g. Jenkins 1987) and

¹ "Everyone's saying something completely fucking different," M.J. Norry, personal communication, Nov. 2005

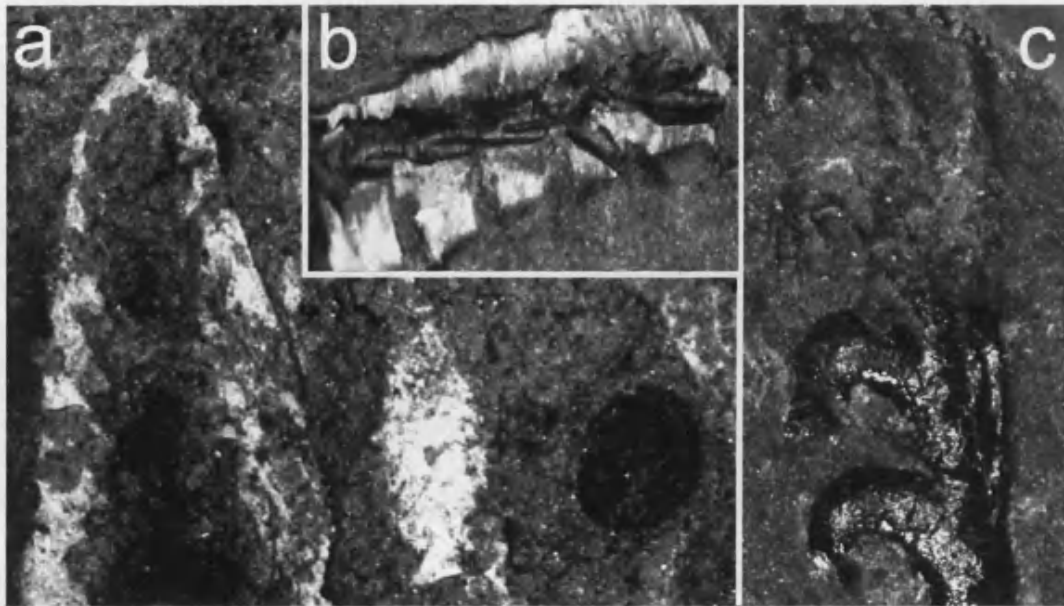


Fig. 4.1 Photomicrographs illustrating graptolite preservation. (a) Flattened graptolites preserved in a cleaved mudrock as carbonaceous compressions with chlorite coronas and a linguliform brachiopod with no associated phyllosilicates; LEIUG 77303: Aberiddi Bay, Wales, UK. (b) Graptolite preserved as pyrite steinkern encased synkinematic illite in a cleaved mudrock (photograph courtesy of Jan Zalasiewicz): Nant Paradwys, Wales, UK. (c) Graptolite from a shallow diagenetic grade facies preserved as pyrite steinkern moulded in sediment without any associated phyllosilicate growth; AAP 00149: Gorstwainweillall, Wales, UK.

date deformation (Sherlock *et al.* 2003). These and other works either tacitly or explicitly argued that the formation of phyllosilicates on graptolites was a direct consequence of tectonic strain (e.g. Underwood 1992). Contrastingly, this study shows that the development of strain is neither necessary nor sufficient to explain phyllosilicate formation on graptolites. Instead, petrographic evidence suggests that volatile release in maturation catalysed the formation of authigenic phyllosilicates on graptolites.

This result may prove significant for our understanding of changes of porosity and permeability of mudrocks in deep diagenesis, which may improve our understanding of previously cryptic processes within facies

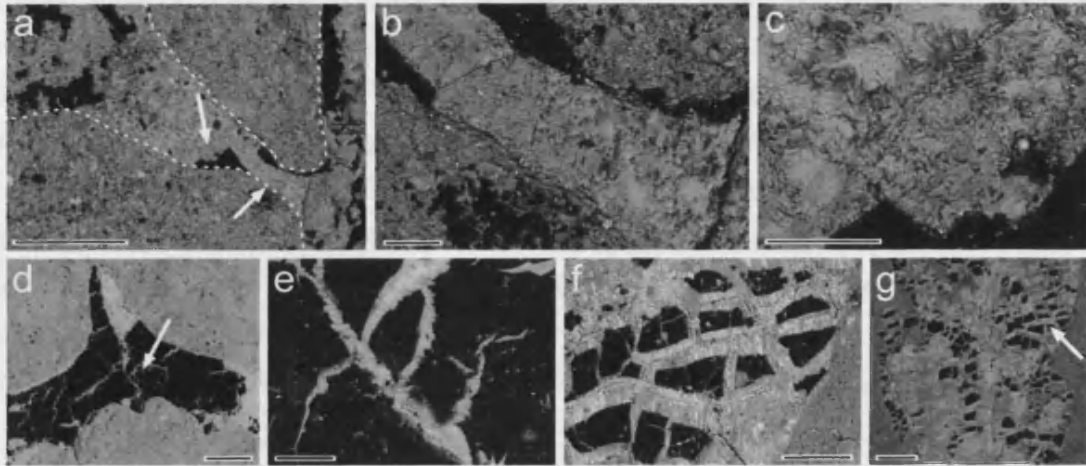


Fig. 4.2 Authigenic phyllosilicates associated with graptolites in hand specimen. High-contrast backscattered SEM images of graptolites preserved as compression fossils from high anchizone grade facies. The black phase is organic carbon and authigenic phyllosilicates are apparent due to their difference in backscatter contrast compared to the sedimentary matrix. (a-c) A scopula of a flattened graptolite which shows no evidence of having undergone strain (see also Fig 3.1), note the variability of phyllosilicate alignment between areas (b) and (c), which are indicated by arrows in (a). (d-e) Flattened graptolite showing tension gashes formed in strain, which are filled synkinematic phyllosilicates as shown in detail in area (e), which is indicated by arrow in (d). (f-g) Flattened graptolite preserved as chocolate-tablet boundinage in a high-strain facies, (f) detail of area indicated by arrow in [g] showing synkinematic phyllosilicates. (a-c) SM A13731 Dob's Linn, Scotland, UK; (d-e) NYSM 5795: Ordovician (Arenig), The Deep Kill, nr. Melrose, NY, USA; (f-g) MWL 5229: Dinas Island, Cardigan, Wales. Scale bars: 0.5 mm (a, e & h), 200 μ m (g) & 50 μ m (b-c, f).

during the accumulation of hydrocarbon reserves (cf. Freed & Peacor 1989; Hunt 1996).

4.2 Material and methods

To assess the processes controlling the formation of phyllosilicates on carbonaceous fossils, I examined over 1000 fossils in mudstones and siltstones from more than 30 localities in four different geological

settings: [1] between shallow diagenetic and very-low metamorphic grade facies within well-constrained stratigraphic units; [2] between strained and unstrained hemipelagic mudrocks; [3] at palaeontologically diverse sites where graptolites and shelly fossils coexist; [4] in localities displaying variable pyritization. These settings were chosen in order to achieve isotaphonomic conditions where one could examine the respective roles of metamorphic grade, tectonic strain, fossil composition, and fossil rigidity in the formation of phyllosilicates on carbonaceous fossils. Details of the specimens studied, their metamorphic grades and their repositories are given in Tables 4.3 & 4.4.

All material was studied using scanning electron microscopy on an Hitachi S-3600N microscope at the University of Leicester. The specimens were imaged in back-scatter mode at an accelerating voltage of 15KV, and phases identified by Energy Dispersive X-ray (EDX) microanalysis using Oxford INCA software. To allow accurate identification of carbonaceous matter, polished thin sections and hand specimens were examined uncoated under low-vacuum conditions. The polished thin sections have subsequently been carbon-coated and EDX identifications have been confirmed using electron microprobe analysis on a Jeol JXA 8600 Superprobe at the University of Leicester and comparison with unpublished X-ray diffraction (XRD) data of bulk rock samples from fossil bearing localities, which are held at the British Geological Survey (BGS). Unless otherwise stated, all metamorphic and stratigraphic information is taken from recent BGS mapping of the Early Palaeozoic Welsh and Lake District Basins, UK (Roberts *et al.* 1996; Davies *et al.* 1997; Evans *et al.* 1997; Millward *et al.* 2000; Schofield *et al.* 2004). White mica crystallinity Kubler index (KI) threshold values for phyllosilicate formation on graptolites were obtained by comparing the preservation of graptolites from localities with known KI values (Dick Merriman & Phil Wilby, personal communications, June 2006), and BGS archive XRD data were used to distinguish illite from muscovite.

Locality	Flattened graptolites	Pyritized graptolites	Diagenetic pyrite	Shelly fossils	Organic laminae
Abereiddi bay, St David's, Wales, UK	chl, ill	chl, ill	qz	O	?chl
Cerig Gwynion Quarry, Rhayader, Wales, UK	chl, ill	chl, ill	qz	-	-
Dinas Island, Cardigan, Wales, UK	chl, ill	chl	qz	-	chl, ill, ka
Llanrhaiadr, Powys, Wales, UK	chl, ill	-	qz	O	chl, ill
The Deep Kill, nr Melrose, NY, USA	chl, ill	-	-	qz	-
White Horse, Barkbethdale, Lake District, UK	chl, ill	-	-	O	-
Ystraddffin, nr. Unlle, Wales, UK	chl, ill	chl, ill, qz*	qz	-	-

* Later, synkinematic phase formed after phyllosilicates, see Section 4.3.4 and Figs 4.4g & j.

Table 4.1 Authigenic minerals associated with different bodies. Data from thin sections and hand specimens of very-low grade mudrocks as detailed in Table 4.3. ka = kaolinite, other abbreviations and symbols as Table 4.2 and Fig. 4.4.

Formation	'early' deep diagenesis (KI $\Delta^{\circ}2\theta$: 1.0-0.6)	'mid' deep diagenesis (KI $\Delta^{\circ}2\theta$: 0.6-0.55)	'late' deep diagenesis (KI $\Delta^{\circ}2\theta$: 0.55-0.42)	Anchizone (KI $\Delta^{\circ}2\theta$: 0.42-0.35)	Epizone (KI $\Delta^{\circ}2\theta$ < 0.25)
Blaen Myherin Mst.	-	-	-	X	-
Borth Mudstone	-	-	X	-	-
Builth Mudstone	-	-	X	X	X
Caerau Mudstone	-	-	X	X	-
Cwmere	-	-	X	X	X
Nantmel Mudstone	-	I	X	-	-
Tycwttta Mudstone	-	I	X	-	-
St Cynllo's Church	O	I	X	-	-

Table 4.2 Threshold KI values for phyllosilicate formation on graptolites. O = no authigenic minerals on graptolites; I = incipient formation of phyllosilicates on graptolites; X = abundant authigenic phyllosilicates on graptolites; - = no data. Diagenetic/metamorphic zones follow internationally accepted definitions based on KI values (Merriman & Frey, 1999), although I have arbitrarily divided the deep diagenetic zone. This table summarises material studied and KI values in Table 4.4

4.3 Results and their implications for phyllosilicate authigenesis

This study reveals a fundamental association between carbonaceous fossils that have experienced “gas window” conditions and authigenic phyllosilicate “coronas” (Table 4.1). In the above-listed settings [1]-[4] I made the following observations:

[1] Well-constrained stratigraphic units of varying grade. Authigenic phyllosilicates were only found in association with graptolites from strata with KI values ≤ 0.6 ; no authigenic phyllosilicates were found on graptolites from localities with KI values > 0.6 (Table 4.2; Figs 4.1 & 4.3). This threshold is equivalent to dry gas window conditions (Merriman & Frey 1999), which under normal geothermal gradients are achieved at c. 150°C and depths of 4-5 km. All observations reported hereafter refer to facies of equivalent or higher grade to this threshold.

[2] Between rocks with differing degrees of tectonic strain. Authigenic phyllosilicates were observed in association with graptolites preserved in cleaved, poorly-cleaved and uncleaved facies (e.g. Figs. 4.1 4.3, 4.4 & 4.5); they may also occur on graptolites which show no evidence of tectonic strain (Fig. 4.2a-c).

[3] At palaeontologically diverse sites. Where graptolites coexist with other fossils in the same bedding plane assemblage, authigenic phyllosilicates were found to be restricted to graptolites and other carbonaceous fossils and may be associated with the organic laminae of shelly fossils. No authigenic phyllosilicates were observed to be associated with shelly fossils themselves, but locally, in facies that have undergone significant strain, these fossils may be encased by quartz (Table 4.1, Fig. 4.3b-c) as noted below (Section 4.3.1d).

[4] At localities showing variable pyritisation. Authigenic phyllosilicates were found to be associated with graptolites, regardless of whether they are preserved as compression fossils or as pyrite steinkerns (Table 4.1; Fig. 4.4). However, authigenic phyllosilicates were not seen to encase

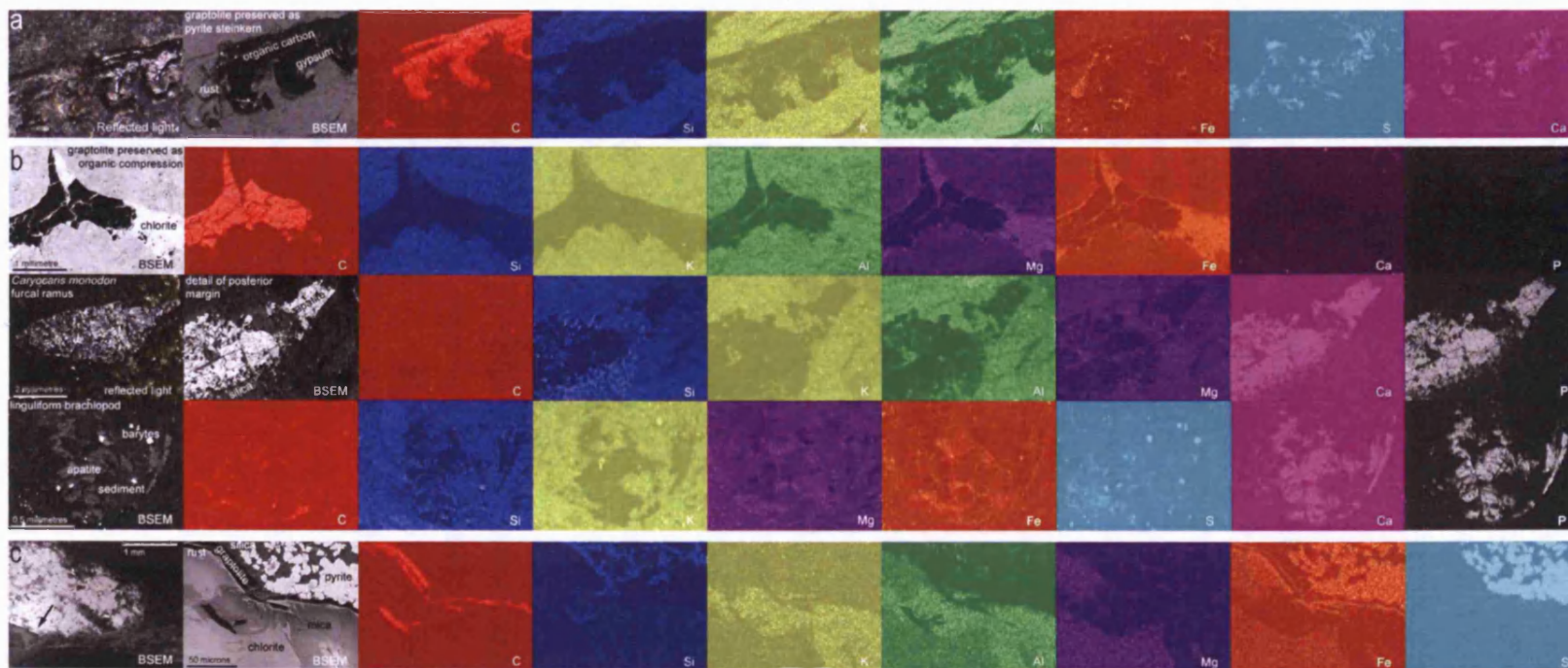


Fig. 4.3 Elemental maps of graptolites, shelly fossils and diagenetic pyrite. (a) Graptolite preserved in a shallow diagenetic grade facies with no associated authigenic phyllosilicates (see also Fig. 4.1c): Fe & S/Ca enrichments represent iron oxides and gypsum (presumably products of supergene weathering), other metals show no discernable difference from the matrix; Gorstwainweillall, Wales, UK; AAP 00149. (b) Graptolite (top, C/Mg/Fe enrichments) and shelly fossils (below, Ca/P enrichments) all preserved in a bedding plane assemblage in an anchizone grade facies, note that authigenic chlorite (Fe/Mg enrichment, K/Si depletion compared to the matrix) is only found associated with the graptolite, the *Caryocaris* furcal ramus (middle) is associated with authigenic quartz (Si enrichment); The Deep Kill, nr Melrose, NY, USA; NYSM 5795. (c) Thin section showing detail of graptolite (arrow, C enrichment) preserved compressed against an early diagenetic pyrite nodule (Fe/S enrichments) in an anchizone grade facies, note that authigenic phyllosilicates (illite: K, Al enrichment; and chlorite: Fe/Mg enrichment) are associated with the graptolite and not the nodule, though the nodule's 'stockwork' is infilled with quartz (Si enrichment, Al/K/Fe/Mg depletion; Cerig Gwynion Quarry, nr Rhyader, Wales, UK; AAP 00102. Scale bars as labelled.

early diagenetic pyrite nodules, euhedra and overpyrite of similar size in the absence of periderm (Table 4.1; Figs 4.3c, 4.4k-l & 4.5j-k). In tectonically-strained rocks, early diagenetic pyrite was locally seen to be associated with authigenic quartz, though pyrite was not found to be closely associated with authigenic phyllosilicates (Table 4.1) as noted below (Section 4.3.1 d).

4.3.1 Comparison with strain-shadow model

A strain-shadow model is neither necessary nor sufficient to explain the formation of phyllosilicates on graptolites in the gas window. None of the following observations are compatible with a strain-shadow model for phyllosilicate formation:

[A] Authigenic phyllosilicates were seen to be associated with graptolites that show no evidence of having undergone tectonic deformation (e.g. Fig. 4.2a-c). Even in weakly-cleaved facies, such authigenic phyllosilicates form irregular, botryoidal ‘coronas’ about graptolites. Even in weakly deformed rocks, these coronas vary in their habit and orientation and no coherent strain regime can be inferred from them (e.g. Figs 4.4a-c). In these cases, these phyllosilicates show no regular crystal habit (e.g. Figs 4.5a-d), unlike the unambiguously synkinematic phyllosilicates from high strain facies (Figs 4.4g-h). In fact, these botryoidal phyllosilicate coronas may be displaced by later synkinematic phyllosilicates (e.g. Figs 4.4g-h & 4.6a).

[B] Authigenic phyllosilicates were seen to be associated with graptolites regardless of their rigidity or rheology, with similar sized phyllosilicate ‘coronas’ occurring on both flattened and pyritised graptolites (e.g. Fig. 4.4). Meanwhile, early diagenetic pyrite bodies of equivalent size and rigidity to pyritised graptolites were not seen to be associated with authigenic phyllosilicates (e.g. Figs 4.3c & 4.4k-l; Table 4.1). Where pyritised graptolites are preserved with a coating of overpyrite extending from a distal aperture or the like, phyllosilicate coronas only encase the “exposed” portion of the carbonaceous fossil and not the overpyrite (e.g. Figs 4.4a-c & 4.5l).

[C] Authigenic phyllosilicates were seen to occur in voids inside rigid bodies, viz. pyritised graptolites (e.g. Figs 4.4c, 4.5i & 4.6). Internal cavities in undeformed rigid bodies cannot represent a strain-shadow.

[D] Within any one locality, authigenic phyllosilicates were seen to be associated with carbonaceous fossils, whereas, in rocks which have experienced notable tectonic deformation, quartz strain-shadows locally occurred around rigid mineral bodies such as early diagenetic pyrite or shelly fossils (Figs 4.3b, 4.4g, i-j & 4.5j-l; Table 4.1). For example, Fig. 4.3c shows a graptolite preserved adjacent to a pyrite nodule. The graptolite is associated with authigenic phyllosilicates, which do not encase the pyrite nodule; however, the nodule's 'stockwork', which would have originally been filled with detrital phyllosilicates, is now filled with authigenic quartz. Likewise, Fig. 4.5l shows a pyritised graptolite preserved in a strongly-cleaved mudrock with authigenic phyllosilicates associated with carbonaceous matter at the graptolite's thecal aperture, whilst an authigenic quartz strain-shadow is associated with euhedral overpyrite at the opposite end of the fossil. Although Passchier & Trouw (1996, Fig 6.18, p. 146) illustrate a quartz-calcite-chlorite strain fringe in association with a euhedral pyrite crystal in a "carbonaceous slate" (seemingly devoid of macrofossils), the chlorite is strongly associated with the carbonaceous matrix, rimming the quartz and calcite. Thus, even in this situation, authigenic phyllosilicates show a strong affinity for carbonaceous matter, whilst quartz rather than phyllosilicate strain-shadows may form on other rigid bodies.

A strain-shadow model may only be applicable to the subset of localities where graptolites are preserved in association with only unambiguously synkinematic phyllosilicates (e.g. Figs 4.1a, 4.2e-f, & 4.5g-h). And, indeed, the displacement of botryoidal phyllosilicate coronas by synkinematic phyllosilicates highlights that phyllosilicates began to form prior to the development of significant strain (NB from hereon in the term 'corona' is used exclusively for botryoidal phyllosilicate bodies which have no regular crystal habit). In strained facies, the absence of authigenic phyllosilicates on shelly fossils or pyrite euhedra demonstrates that strain alone can not bring about

their formation. So, while authigenic phyllosilicates may be found in association with graptolites in strained facies, and though graptolites preserved in association with synkinematic phyllosilicates have been exploited to provide strain information (e.g. Jenkins 1987), it is not strain but some other factor that governs the initial formation of phyllosilicates on graptolites.

4.3.2 Association of phyllosilicates with carbonaceous fossils

The above observations highlight the strong link between authigenic phyllosilicates and carbonaceous fossils (see also Table 4.1). Meanwhile, Chapter 5 shows that in bedding plane assemblages preserving several different carbonaceous fossils, a distinct set of authigenic phyllosilicates is associated with each different type of carbonaceous fossil. This latter observation indicates a strong link between fossil composition and phyllosilicate authigenesis. Previous workers have linked the formation of monazite in diagenesis and low-grade metamorphism to the presence of organic carbon undergoing maturation (Evans *et al.* 2002; Wilby *et al.* 2007), and Milodowski & Zalasiewicz (1991) showed that organic-rich layers governed the redistribution of rare earth elements during deep diagenesis. These studies demonstrated that carbonaceous matter should not be considered inert under such conditions, and show that carbonaceous fossils can represent key sites for mineral authigenesis in very-low grade metamorphism (e.g. Wilby *et al.* 2007). As such, the association of authigenic phyllosilicates and graptolites is best considered to result from mineral-organic interactions in deep diagenetic grade facies.

4.3.3 Relation between maturation & phyllosilicate formation

Phyllosilicate formation on graptolites occurred once graptolite periderm had undergone volume loss in maturation. Fig. 4.6 shows a graptolite three-dimensionally preserved as a pyrite steinkern encased in a phyllosilicate corona. Pyritisation occurred in early diagenesis before the graptolite had undergone significant compaction, preserving its original outline with high fidelity. The interthecal septum is detailed in Figs 4.6c-d,

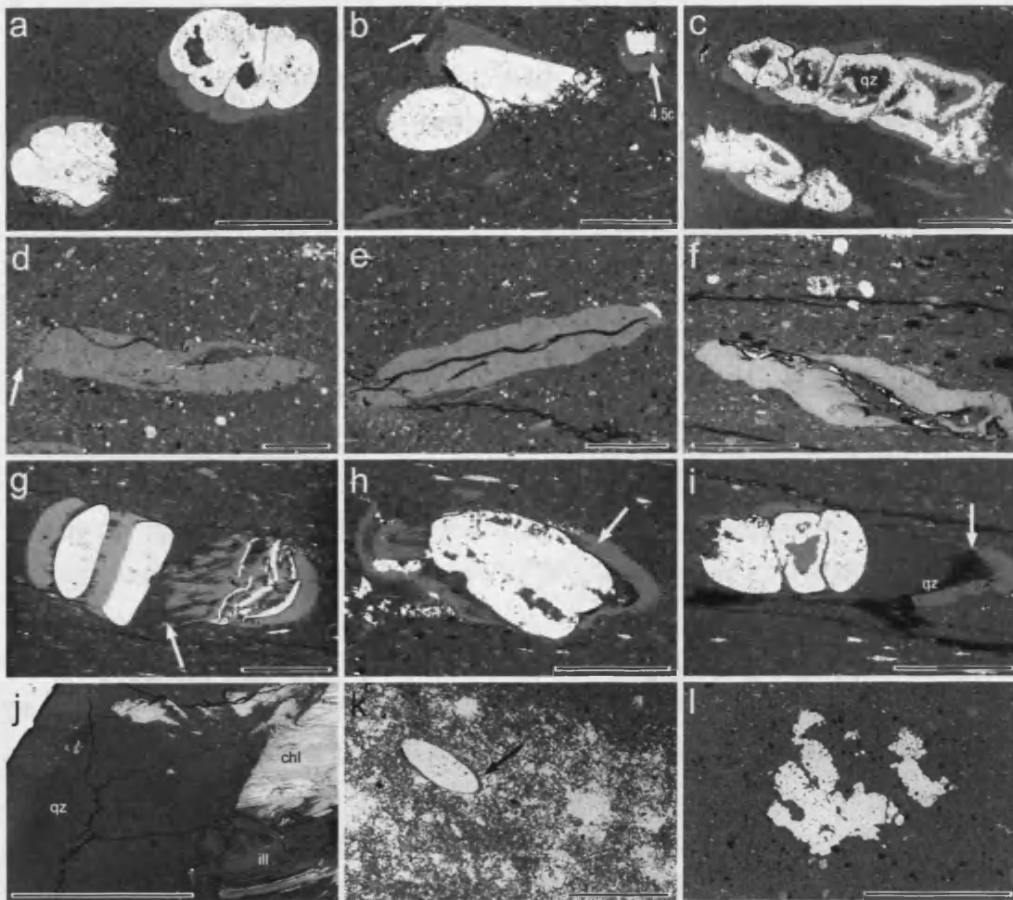


Fig. 4.4 Thin sections showing authigenic minerals in graptolitic mudrocks. High-contrast backscattered SEM images from low-strain anchizone (a-f. k-l) and high-strain epizone grade facies (g-j), specimens from Cerig Gwynion Quarry, nr Rhayader, and Ystraddfin, nr Unlle, Wales, UK respectively. Unless otherwise noted, the white phase is pyrite, light grey phase chlorite (chl), the mid grey phase illite (ill), the dark grey phase quartz (qz) the black phase is organic carbon. Note that authigenic phyllosilicates 'coronas' are found in association graptolite periderm and not pyrite. (a-c) pyritised and (d-f) flattened graptolites, showing variability of corona morphology, all in similar orientation with regard to bedding and strain: note that despite this rock's weak tectonic fabric, no coherent strain information can be garnered from the habit of these coronas; gradational rather than sharp contact between corona and sedimentary matrix shown by arrows in (a) and (d); inclusions in coronas: (b) pyrite (arrow), and (c) carbon (bottom right); (e) truncation of early diagenetic pyrite by corona. Graptolites (g-j) preserved with both phyllosilicate coronas and synkinematic phyllosilicates: (g) synkinematic phyllosilicates displaced by quartz; phyllosilicate coronas displaced by (h) synkinematic phyllosilicates and (g) synkinematic quartz; (j) detail of area indicated by arrow in (g). Association of phyllosilicates with pyritised graptolites but not pyrite bodies: (k) pyritised graptolite associated with phyllosilicate corona (arrow) in pyrite-rich layer; (l) warping of laminae around a pyrite nodule. Specimen numbers: (a) AAP 00104, (b) AAP 00102,

showing it precisely delineated by pyrite. The area in between the pyrite was originally entirely filled with the periderm of the interthecal septum (Fig. 4.6c), which typically has 10-20 μm thickness (see Crowther 1981). This periderm has subsequently undergone significant volume loss (cf. Figs 4.6c-d), and the area of the interthecal septum is now infilled with phyllosilicates together with denatured periderm (Fig. 4.6d). Note that the phyllosilicate infill here differs significantly from synkinematic phyllosilicates that occupy interthecal spaces created by strain (e.g. Figs 4.3g-h). As phyllosilicates can only form in the interthecal septum once space has been created, phyllosilicate formation on graptolites must have occurred after the periderm had undergone volume-loss by the expulsion of volatiles in maturation (cf. Belek & de Koranyi 1990; Gilkson *et al.* 1992).

The link between phyllosilicate formation and the maturation of periderm is supported by KI values indicating that phyllosilicate authigenesis begins in the gas window (Table 4.2; cf. Merriman & Frey 1999), which represents peak maturation conditions of graptolite periderm. Though graptolite periderm was originally composed of collagen (Towe & Urbanek 1972; Crowther 1981; Gupta *et al.* 2006b), pyrolysis studies show that it alters in diagenesis to a composition closely resembling that of Type II kerogen (Bustin *et al.* 1989; Gupta *et al.* 2006b). During gas window conditions, Type II kerogens undergo peak maturation (e.g. Baskin 1997; Seewald 2003) generating natural gases, carbon dioxide, nitrogen, hydrogen sulphide and carboxylic acids (Seewald 2003) and leaving an inert kerogenous residue, which occupies a reduced volume (cf. Belek & de Koranyi 1990; Gilkson *et al.* 1992; Uysal *et al.* 2004). This, combined with the petrographic evidence outlined above (esp. Fig. 4.6; Tables 4.1 & 4.2), clearly indicates that phyllosilicate formation on graptolites is intimately linked with periderm maturation.

Fig. 4.4 (*continued from previous page*) (c) AAP 00100.2, (d-e) AAP 00102, (f) AAP 00108.2, (g) AAP 00108.1, (h) AAP 00108.2, (i) AAP 00108.2, (j) AAP 00108.1, & (k-l) AAP 00100.2. Scale bars: 1 mm (a, c & g-i), 0.5 mm (k-l) & 200 μm (b, d-e & j).

4.3.4 Order of formation: illite, chlorite and quartz

There is good petrographic evidence to constrain the order of the formation of authigenic illite, chlorite and quartz. Illite is consistently more intimately associated with periderm than chlorite is (e.g. Figs 4.3c, 4.4g & 4.6d; Chapter 5). If phyllosilicate coronas grew outwards from the graptolite's edge (cf. Section 4.4), then this would indicate that illite formed prior to chlorite. Meanwhile, in some cases quartz precipitated after these phases. Fig. 4.4j shows quartz cross cutting synkinematic illite and chlorite, and Fig. 4.4c shows quartz as a late-stage void-fill that precipitated after chlorite. Fig. 4.5l shows a graptolite in a cleaved rock with synkinematic chlorite next to the periderm's edge and quartz occurring on overpyrite, suggesting that in some cases, quartz and phyllosilicates may be coeval. Thus, illite appears to have formed prior to chlorite, both of which began to form before quartz in at least some examples. This is entirely consistent with the normal order of the precipitation of these phases in a closed system (cf. Section 5.4): illite formation depletes the hydrothermal fluid of K & Al, before chlorite formation removes other cations such as Fe, Mg & Ca, leaving a silica-rich fluid from which quartz may precipitate (Boles & Franks 1979; Hower 1981; Lanson *et al.* 1996; Gabbott *et al.* 1998; Meunier 2005).

4.4 A simple model for phyllosilicate formation on graptolites

The above observations indicate that phyllosilicate formation occurred on graptolites due to temperature-dependent clay-organic interactions in the gas window. Authigenic phyllosilicates were not found on graptolites from facies with KI > 0.60 (Fig. 4.1c; Table 4.2), but occur on graptolites and other organic-walled microfossils from facies of higher grade (Fig 4.3; Tables 4.1 & 4.2; Chapter 5). Thus phyllosilicate coronas must begin to form under gas window conditions (cf. Merriman & Frey 1999). Where graptolites are preserved as pyrite steinkerns in facies which have passed through the gas window, phyllosilicate 'coronas' encase only the carbonaceous matter and not overpyrite (Figs 4.4a-c, l, & 4.5l); authigenic phyllosilicates are neither associated with diagenetic pyrite bodies nor shelly fossils when either

are preserved alongside graptolites (Fig 4.3; Table 4.1). Unlike pyrite and shelly fossils, graptolite periderm is far from refractory under these conditions, which see it undergoing volatile release in maturation (cf. Section 4.3.3). Fig 4.7 provides a schematic illustration of the transition of such assemblages through the gas window, with phyllosilicate coronas forming on graptolites during maturation, and silica 'strain fringes' forming on other rigid bodies in cleaved facies. These authigenic phyllosilicates are euhedra with a neomorphic habit, indicating that they could not have formed from a smectite precursor by diffusion in the lattice (cf. Inoue *et al.* 1990). What's more, they may occupy areas within fossil graptolites which were not occupied by phyllosilicates in early diagenesis. For example, authigenic phyllosilicates may occur both within the void of a previously empty thecal cavity (e.g. Fig. 4.4c) and can infill interthecal septa (e.g. Fig. 4.6; Section 4.3.3). The occurrence of authigenic phyllosilicates in such cavities indicated that they formed by diffusion in a fluid phase.

Whilst it is clear that the maturation of periderm catalysed the precipitation of phyllosilicates, the precise mechanism is less certain². For example, clay minerals may be adsorbed or precipitated on to organic substrates (e.g. Lagaly 1984; Odom 1984), or have their formation mediated by mineral-organic interactions (e.g. Konhauser & Urrutia 1999; Worden *et al.* 2006). Alternatively, clay minerals may precipitate directly into voids (e.g. Wilkinson & Hazeldine 2002), which may include those created by volume-loss in maturation (cf. Fig. 4.6), or they may form due to changes in the ambient hydrothermal fluid chemistry, which itself could result from the release of volatiles in maturation (e.g. Curtis 1985). Contrastingly, clay minerals also play a major role in catalysing the breakdown of kerogens during maturation (Goldstein 1983), and Stotzky (1980) has shown that such clay-organic interactions may occur in both directions, with organics adsorbing on to clays and clays adsorbing on to organics equally well. Meanwhile, Curtis (1985) documented that phyllosilicates may form by replacement of detrital clays due to chemical changes influenced by changes in the concentration of organic acids and carbon dioxide, both of which may be expelled

² Norry probably has something uncouth to say about this too.

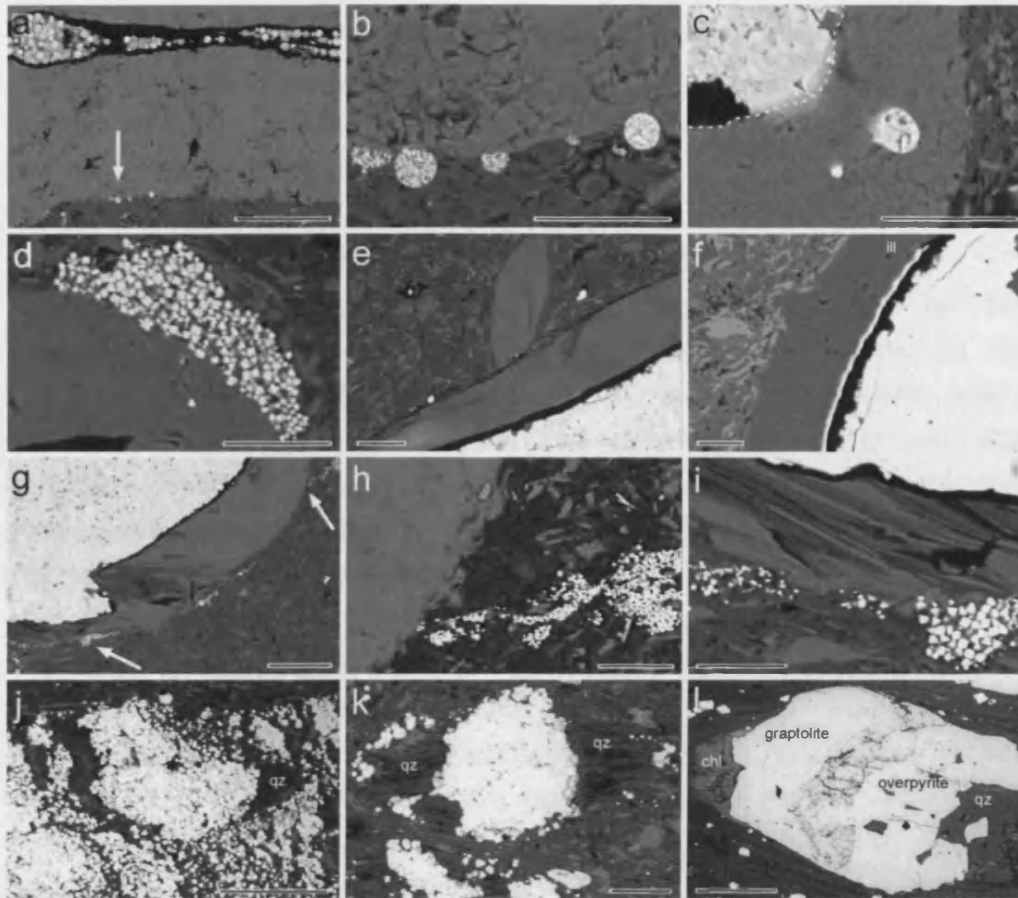


Fig. 4.5 Petrography of phyllosilicate 'coronas' and quartz strain shadows. High-contrast backscattered SEM images from low anchizone (a-i) and epizone grade facies (j-l), respectively from Cerig Gwynion Quarry, nr Rhayader (a-i), Ystraddfin, nr Unlle (j-k), & Dinas Island, Cardigan (l), all Wales, UK. Phases as Fig. 4.4. Note that authigenic phyllosilicates 'coronas' are found in association with graptolite periderm and not pyrite, which may be associated with quartz. Relation between pyrite, detrital phyllosilicates, chlorite-mica stacks and coronas: (a) truncation of pyrite framboids by corona (arrow) but not at the margin of the graptolite's periderm; (b) detail of area indicated in (a); (c) pyrite inclusions in corona rounded by resorption, detail of area indicated in Fig. 4.4b; (d) truncation of framboidal pyrite-body by corona, detail of Fig. 4.5e; (e) truncation of chlorite-mica stack by corona; (f) sharp contact between corona and sedimentary matrix (the white phase coating the external surface of the periderm is in this case iron oxide, which presumably formed in weathering, rather than diagenetic pyrite which forms the infill); (g) truncation of pyrite 'lamina' (arrows) shown in detail in (h) and (i), which are both slightly and differently rotated compared to (g). Quartz associated with pyrite in high-strain rocks: (j-k) synkinematic quartz associated with framboids; (l) quartz associated with overpyrite and chlorite associated with exposed periderm on pyritised graptolite. Specimen numbers: (a-b) AAP 00102, (c) AAP 00102, (d) AAP 00102, (e-i) AAP 00104, (j-k) AAP 00108.2 & (l) E74526. Scale bars: 1 mm (a, c & g-i), 0.5 mm (k-l) & 200 μ m (b, d-e & j).

In maturation (e.g. Seewald 2003). So, it seems that phyllosilicates either [a] precipitated directly on to an organic substrate and continued to grow away from it, or [b] formed by replacement of the pre-existing sedimentary phases.

4.4.1 Phyllosilicate formation vis-à-vis volume change

Phyllosilicate formation could have conceivably occurred by two opposing mechanisms, which are in principle analogous to the mechanisms [a] and [b] discussed above: namely, [a] growth into a swollen void, and [b] replacement of the sediment. I have termed these models 'hydrothermal jacking', and 'wholesale replacement' respectively, and they are illustrated in Fig. 4.8. These models may be tested based on observations such as the relative scarcity of pyrite in the coronas, as well as the truncation of pre-existing phases, such as chlorite-mica stacks (e.g. Fig. 4.5e), as well as conserving rock volume. Conservation of matter requires any model for formation of phyllosilicate coronas on graptolites to address how their growth relates to any change the rock volume. These models must also explain their botryoidal morphology and the compositional variation and the lack of regular crystal habit within them (coronas can thus be distinguished from synkinematic phyllosilicates associated with graptolites). The remainder of this section is given discussing the key observations which pertain to a better understanding of corona growth before to discussing the two opposing models for phyllosilicate formation in Sections 4.4.1 & 4.4.2.

Volume of the coronas and their shape and growth. Phyllosilicate coronas occupy a greater space than can be achieved by periderm shrinkage alone: unbandaged graptolite periderm is generally 10-20 μm thick (e.g. Fig 4.6; Crowther 1981), whilst these coronas generally occupy 100-200 μm (e.g. Figs 4.4 & 4.5). The perimeter of these coronas is consistently greater in length than their inner margin, adjacent to the graptolite itself (e.g. Figs 4.4a-c & e-g), their perimeter is also consistently more convex than the graptolite's outline, and its botryoidal shape may contain more inflection points than are in the graptolite's outline. This indicates that the phyllosilicates that define the corona's perimeter formed *in situ* rather than forming adjacent to

the graptolite and being displaced away from the graptolite, perhaps by the growth of later phyllosilicates in-between the corona's outer margin and the graptolite. Instead, it seems more likely that phyllosilicate growth initiated adjacent to the graptolite and progressed away from it. We know that these phyllosilicates formed by diffusion in a fluid phase (see above), and also that they formed at a time when the periderm was expelling volatiles in maturation. It therefore seems reasonable to consider the graptolite and the surrounding rock as the locus for fluid activity and phyllosilicate growth. The fact that illite is more intimately associated with periderm than chlorite (e.g. Fig 4.6) is consistent with phyllosilicate growth continuing away from the graptolite. In a closed system, the formation of illite is limited by the availability of K & Al, meaning that as more illite forms, these elements are consumed, with chlorite forming once as the fluid becomes depleted in K & Al (Hower *et al.* 1976; Boles & Franks 1979; Meunier 2005). Therefore phyllosilicate formation seems to have initiated next to the graptolite and progressed outwards.

Scarcity of pyrite & truncation of pre-existing phases. Compared with the surrounding matrix, there is a general absence of pyrite from the coronas (e.g. Figs 4.4b, d-e & 4.5a). This could be explained by either model (Fig 4.8) and is discussed below. Likewise, other pre-corona phases such as pyrite framboids and chlorite-mica stacks (e.g. Figs 4.5 b, d-e & g-i) appear to be truncated by the corona, which could be explained if these phases [a] grew against the graptolite's flat edge and were subsequently displaced by phyllosilicates that grow within the void created by the hydrothermal fluid, or [b] were replaced by the corona (cf. Fig. 4.8).

4.4.2 Hydrothermal jacking?

The 'hydrothermal jacking' model proposes that phyllosilicates formed within a swollen void around the graptolite, which was created by hydrothermal fluids prizing the rock apart in a manner analogous to the workings of a hydraulic jack. This would see phyllosilicate coronas being a special case of vein formation (cf. Gaboury & Daigneault 2000), which would require the hydrothermal fluid to have an internal pressure equivalent to lithostatic pressure. As well as

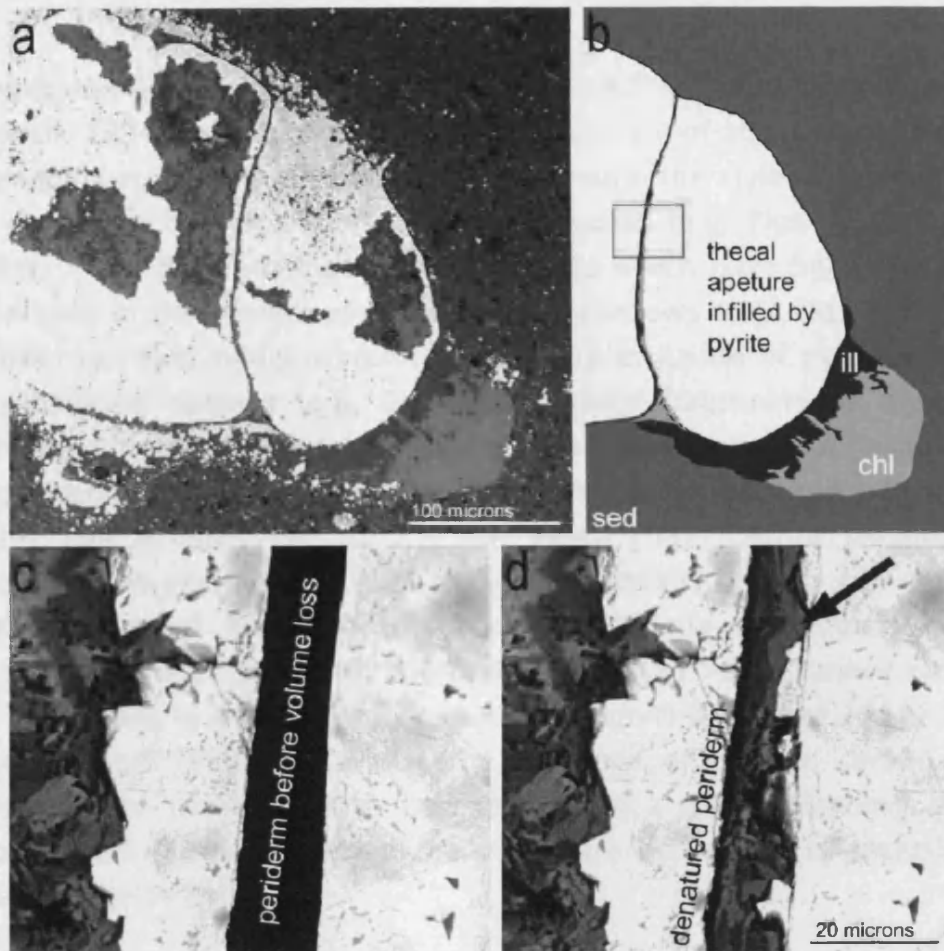


Fig 4.6 Phyllosilicate authigenesis facilitated by volume-loss in maturation. Back-scattered SEM images (a, d) and schematics (b-c), phases as Fig. 4.4. Detail of area delimited by red box in (b) is shown: (c) before maturation with schematic periderm filling the interthecal septum; and (d) after maturation, authigenic phyllosilicates infill the space created by periderm having undergone volume loss. AAP 00102.

explaining the general scarcity of pyrite from phyllosilicate coronas, this model overcomes the problems of conserving rock volume, with authigenic phyllosilicates being precipitated from an external source.

There are several difficulties with this model. Previous studies on the pyritisation of graptolites and other fossils have not identified truncated framboids grown against the fossil's margin (cf. Hudson 1982, Bjerreskov 1991; Underwood & Bottrell 1994). Instead, graptolite periderm is either coated by microcrystalline pyrite (e.g. Crowther 1981; Underwood & Bottrell 1994), or may have pyrite framboids

deeply impressed into it creating clear pock-marks (Underwood & Bottrell 1994), which makes this displacement-of-already-truncated-framboids scenario seem unlikely. Furthermore, the style of truncation of the pyrite bodies at the margin of coronas (e.g. Figs 4.5 b & d) differs markedly from that of pyrite bodies which have been forcibly displaced in the growth of quartz strain shadows (e.g. Figs 4.5 j-k). Neither can this model account for the rare inclusion of pyrite within phyllosilicate coronas (e.g. Fig. 4.5c). Whilst fragments of organic carbon within the coronas (e.g. Figs 4.1c, e & 4.5g) may have flaked off a graptolite and been suspended in the hydrothermal fluid relatively easily due to their low density (cf. Bates 1987) before becoming entombed by phyllosilicate growth, this scenario is unlikely to explain the presence of pyrite within the coronas. Pyrite is a significantly denser phase than periderm, and pyrite 'grains' of $>5\mu\text{m}$ cannot easily be suspended in an aqueous medium (cf. Wignall & Newton 1998; see also Hudson 1982). So, whilst the presence of organic carbon in phyllosilicate 'coronas' could be explained by a special pleading, this model does not adequately explain the rare occurrence of inclusion phases such as pyrite.

The lack of a regular crystal habit within the phyllosilicate coronas poses a further problem for this model. Implicit in the hydrothermal jacking model is the notion that these phyllosilicates grew to occupy either an emergent or existing void; however, they do not exhibit any obvious empty space-filling textures. In sandstones and siltstones fibrous illite and chlorite rosettes may occupy interstitial spaces, with crystals tending to point into the void (e.g. Boles & Franks 1979; Lanson *et al.* 1996; Wilkinson & Hazeldine 2002; Butterfield *et al.* 2007). This is not dissimilar to the habit of authigenic chlorite when it occupies previous empty thecal cavities (e.g. Fig. 4.4c; *contra*. Fig. 4.6, which shows a thecal cavity filled with ?recrystallised, uncompacted detrital phyllosilicates). Meanwhile, where phyllosilicates grew to occupy an emergent void, such as the space created when periderm in the interthecal septum underwent volume loss (e.g. Fig. 4.6), they display a distinctive crystal habit, with their long axes aligned parallel to its margins. Though it is possible that these phyllosilicates grew

into a pre-existing or emergent void, there seems to be little evidence from their texture to support it.

A further problem with the hydrothermal jacking model, though, comes from the strong affinity of phyllosilicates for carbonaceous fossils rather than inorganic bodies such as overpyrite (e.g. Fig 4.4a-c & 4.5l; Table 4.1). Though it is plausible that phyllosilicate formation may have initiated on denatured periderm as it underwent volume loss in maturation (Section 4.4), this model attributes its continued growth to the infill of a swollen void that expanded around the graptolite. Yet, there is no good reason why such a swollen void would only occupy the areas immediately adjacent to the graptolite's periderm and not continue to encapsulate neighbouring areas beyond the periderm itself. In fact, this view of phyllosilicate formation having been 'seeded' on the periderm before continuing to grow should allow phyllosilicate growth to extend laterally as well as outward. In which case, it would encase both overpyrite and periderm alike. This problem is exacerbated by the spatial partitioning of quartz and phyllosilicates about graptolites. Figures 4.3c & 4.5l show authigenic phyllosilicates encasing graptolite periderm and authigenic quartz encasing diagenetic pyrite on the opposite side of the graptolite. Both these phases precipitated from a fluid phase into an area originally occupied by the sedimentary matrix. In these examples, a fluid-filled area may have existed on either side of the graptolite and that phyllosilicate formation occurred on the graptolite's denatured periderm. Yet, this model can not explain why phyllosilicate growth did not continue to fill all areas adjacent to the graptolite rather than just those adjacent to the periderm. Given these objections, it seems that the hydrothermal jacking model can not sufficiently account of the formation of phyllosilicate coronas on graptolites.

4.4.3 Wholesale replacement of the sediment?

An alternative model sees phyllosilicate coronas forming by wholesale replacement of the sedimentary matrix that surrounded the graptolite (Fig. 4.8). This model accounts for most of the features displayed by the phyllosilicate coronas. Balthasar (2004) and Butterfield *et al.* (2007)

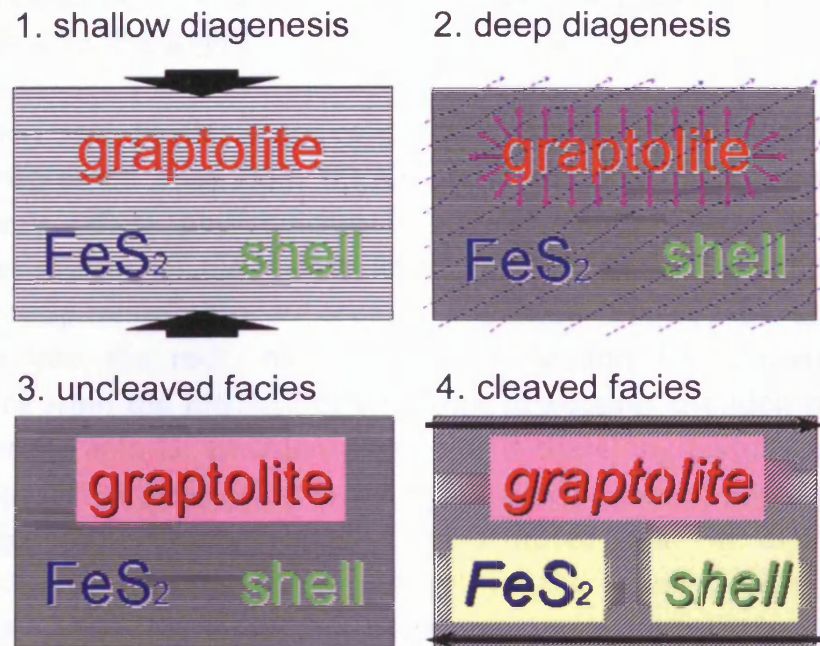


Fig. 4.7 The diagenetic history of graptolitic mudrocks. Pink arrows represent volatiles expelled in maturation, and blue arrows represent the hydrothermal fluid; pink boxes represent authigenic phyllosilicates and cream boxes represent authigenic quartz.

have shown that both chlorite and white mica can form late-stage replacements of pre-existing phases, and such phyllosilicates may show no regular crystal habit (e.g. Balthasar 2004). Meanwhile, Curtis (1985) documented that phyllosilicates may form by replacement of detrital clays through interactions with organic acids and carbon dioxide, both of which may be expelled in the maturation of kerogens (e.g. Seewald 2003). The general absence of pyrite from phyllosilicate coronas may be attributed to it undergoing dissolution. This may also explain the occasional presence of pyrite within coronas as it may not fully dissolve in all cases and the rounded shape of otherwise angular pyrite euhedra may itself indicate resorption (e.g. Fig. 4.5c). Wagner & Boyce (2006) have shown that pyrite may be unstable during very-low grade metamorphism due to oxidation or through increased pH, as well as changes in the activity of sulphur; and pyrite metamorphism may itself be linked to interactions between chlorite and sulphidic fluids (Phillips & Groves 1984). As such, the 'wholesale replacement' model may also explain the truncation of earlier diagenetic phases

such as framboids and chlorite-mica stacks by phyllosilicate coronas (cf. Figs 4.5b, d-e & g-i).

This view sees phyllosilicate coronas forming behind a reaction front that progressed away from the graptolite along a diffusion gradient. This may reflect phyllosilicate formation being induced by pH/Eh changes due to volatile release (cf. Curtis 1985; Seewald 2003) rather than precipitation onto an organic substrate followed by continued growth into the rock. As discussed in Section 4.4.1, there is no evidence from the phyllosilicate texture to support the idea that they precipitated into an emergent void. Nor is there any textural evidence to suggest that phyllosilicates are either precipitated or adsorbed onto an organic substrate. Lagaly (1984) noted that in such cases phyllosilicates tend to align parallel to the plane of the organic substrate. However, there is no difference in crystal habit between the phyllosilicates that are immediately adjacent to periderm and those that are within the middle of the corona (Fig 4.5 a, c & d). Thus, the homogenous texture throughout the corona seems best taken as evidence that these phyllosilicates all formed by the same process rather than by some form of 'seeding' followed by continued growth, consistent with the notion of growth by wholesale replacement.

This model also provides a more adequate explanation of the strong affinity of phyllosilicates for organic matter, and, particularly, their conspicuous absence from overpyrite. If phyllosilicate replacement of the sediment was a consequence of changes in pH/Eh due to volatile release (cf. Curtis 1985; Seewald 2003), then it would only have occurred in areas influenced by the diffusion of volatiles away from the periderm. So, in areas where there is no periderm exposed to the sediment, such as in areas of overpyrite, there is no source of volatiles, hence no authigenic phyllosilicates. This model also explains the absence of authigenic phyllosilicates from certain partially pyritised thecal cavities. Figs 4.4a & 4.6a show thecal cavities filled with uncompacted detrital phyllosilicates, whilst Fig 4.4c shows thecal cavities filled with authigenic phyllosilicates. Authigenic phyllosilicates appear to be absent from cavities which appear to be fully sealed by pyrite infill, whilst they are present in cavities which had a direct

connection to the periderm (and thus diffusing volatiles) by to either an incomplete pyritisation or fracture. Though there is a generally sharp division between the corona and matrix (e.g. Figs 4.4a & c), suggesting a remarkably complete reaction, Figs 4.4b & d show a more ragged transition from corona to matrix, with excess chlorite present in the surrounding sedimentary matrix. So, unlike the hydrothermal jacking model, the replacement model requires no special pleading to explain the high-fidelity association of authigenic phyllosilicates with periderm and not overpyrite.

Meanwhile, Chapter 5 demonstrates that, in bedding plane assemblages preserving several different organically preserved taxa, distinct assemblages of phyllosilicates are found in association with each type of carbonaceous fossil. The hydrothermal jacking model would propose that as each taxon underwent maturation, the locus of hydrothermal fluid activity would move from one taxon to another, resulting in the observed taxon-specific phyllosilicate distribution (Table 5.1). However, this seems somewhat incongruous. Where two different types of carbonaceous fossil are found in close association with one another (e.g. Figs 5.2b & d), this view posits that a 'pool' of hydrothermal fluid sat above one type of carbonaceous fossil but did not spread laterally onto the adjacent fossil. Given that the internal pressure of this fluid must have been greater than lithostatic pressure to create a void, it seems unlikely that the void would not spread laterally onto the adjacent fossil. Instead, this taxon-specific phyllosilicate distribution seems better explained by the sediment replacement model, with a different assemblage of phyllosilicates forming as each carbonaceous fossil underwent volatile release in maturation (Section 5.4).

The botryoidal shape of the coronas may also be better explained by wholesale replacement of the sedimentary matrix (cf. Curtis 1985). After all, similar botryoidal textures have been reported from other examples of late-stage replacement (e.g. Balthasar 2004); whilst the strikingly convex outline of these coronas (e.g. Figs 4.4a-f) may, for example, represent the area influenced by the diffusion of volatiles from the graptolite (much in the in the same way that the area of grass

eaten by a goat tethered to a tree creates a more convex outline than that of the tree to which was tied). In which case, the morphology of the coronas, should reflect the progress of volatiles along a concentration gradient away from the graptolite, with authigenic phyllosilicates replacing the sediment in the area influenced by their diffusion.

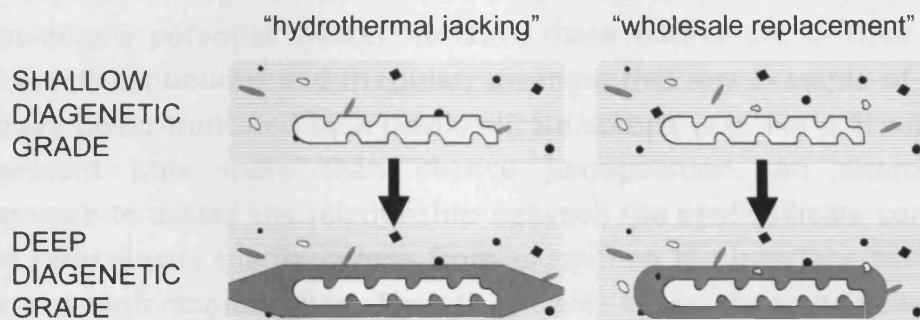


Fig. 4.8 Alternative models for growth of phyllosilicates on graptolites (schematic).

4.4.4 Distinguishing between the models

A critical test for distinguishing between these two models lies in the relationship between the phyllosilicate coronas and the sedimentary matrix. Fig. 4.8 illustrates the alternative models. Unlike the 'hydrothermal jacking' model, in the 'wholesale replacement' model phyllosilicate coronas truncate sedimentary laminae rather than deflecting them. Though this test should in theory be sufficient to confirm or deny either model, it is somewhat ambiguous in practice. In part this is because the hemipelagic laminations exhibited by these strata are too poorly defined to accurately determine whether individual lamina are truncated or deflected (e.g. Fig 4.4). This is exacerbated by the problem of determining whether the warping of these laminae is due to phyllosilicate growth or to differential compaction. It is clear that the pyritisation of graptolites occurred prior to significant compaction, explaining their three-dimensional preservation (e.g. Underwood 1992), and thus sediment around such early diagenetic pyrite would have undergone differential compaction, warping adjacent laminae (cf. Fig. 4.4l). As such, any warped laminae found around pyritised graptolites may be better explained by compaction rather than deflection. Meanwhile, the phyllosilicate

coronas associated with flattened graptolites are not of a sufficiently large size to discern whether the diffuse hemipelagic laminae are deflected or truncated (e.g. Figs 4.4d-f).

Because the laminae are too diffuse themselves to determine whether they are truncated or deflected by the coronas, an alternative approach is needed. Though pyrite bodies may follow sedimentary laminae providing a potential marker horizon, these bodies are in their very nature discontinuous and irregular, meaning that any example of such a body being truncated by a phyllosilicate corona (e.g. Fig 4.5h) might represent little more than chance juxtaposition. An alternative approach to assess the relationship between the phyllosilicate coronas and sedimentary matrix comes from examining the interface between them at high magnification. Though in some cases, the transition from matrix to corona is abrupt (e.g. Fig 4.5f), in others it is more diffuse (e.g. Fig. 4.5h). Whilst an abrupt transition would be consistent with either model of corona growth, a more diffuse transition seems more consistent with the wholesale replacement model, as the reaction may not have gone to completion, leaving some relict sedimentary structure visible at the edge of the phyllosilicate corona (e.g. Fig. 4.5h).

Compared to the 'hydrothermal jacking' model, the 'wholesale replacement' model seems to require less special pleading. However, it is clear that further data are needed to confirm this model. At present my data is limited to specimens where large phyllosilicate coronas are fully formed, and these seemingly cannibalised any evidence of their earliest growth. By seeking evidence of the earliest growth of such phyllosilicates, it should be possible to test this model. One opportunity for determining this may come from examining further material, that show incipient phyllosilicate growth on graptolites such as those identified in Table 4.2.

4.5 Discussion

By directly linking phyllosilicate formation to the maturation of kerogens, this study provides a novel mechanism of clay mineral

authigenesis. As noted above, euhedral phyllosilicates can not form from detrital phyllosilicates by diffusion in the lattice (Section 4.4), whilst the proposed 'wholesale replacement' model differs significantly from other examples of phyllosilicate growth by diffusion in a fluid phase which generally require a precipitation into a pre-existing void (e.g. Boles & Franks 1979; Lanson *et al.* 1996; Wilkinson & Hazeldine 2002; Uysal *et al.* 2003). Corona growth is best viewed as a special case of the reactions documented by Curtis (1985) where one clay mineral may replace another due to Eh/pH changes influenced by volatile release in the kerogen maturation (cf. Seewald 2003). Similarly, the resorption of early diagenetic pyrite and its replacement by phyllosilicates may be a consequence of Eh/pH changes which could also be influenced by volatile release (cf. Curtis 1985; Wagner & Boyce 2006), especially as pyrite metamorphism has been linked to chlorite formation (Phillips & Groves 1984). This mode of phyllosilicate formation may also account for the occurrence of phyllosilicates on other organic-walled fossils in mudrocks. For example, phyllosilicates have been reported to occur on plant fossils, and organically-preserved arthropods, nautiloids and brachiopods from a variety of different strata of very-low metamorphic grade (e.g. Chapter 5; Underwood 1992; Butterfield *et al.* 2007). If this mechanism of phyllosilicate authigenesis catalysed by volatile release in maturation is more widely applicable, then it has significant implications for understanding how the porosity and permeability of mudrocks may change under conditions associated with hydrocarbon generation and migration (cf. Freed & Peacor 1989; Hunt 1996).

4.5.1 Comparison with other studies

This work shows that a strain shadow model is neither necessary nor sufficient to explain the formation of phyllosilicates on graptolites. Though synkinematic phyllosilicates may occur on graptolites in tectonically-strained facies (e.g. Figs 4.4g-h), their absence from other rigid bodies in close association (Table 4.1) shows that tectonic strain alone is insufficient to bring about phyllosilicate formation. Instead these synkinematic phyllosilicates may represent either recrystallisation of pre-existing phyllosilicates (e.g. Orr *et al.* 1998), or perhaps a continuation of the phyllosilicate corona once strain had

developed (cf. Fig 4.4h) with the local stress field serving to influence the migration of volatiles and the diffusion of fluids within the rock. This view contrasts strongly with all other previous works concerning phyllosilicate formation on graptolites which emphasised their relation with strain (e.g. Jenkins 1987; Chapman 1991; Underwood 1992). Though ^{40}Ar - ^{39}Ar analyses of white mica in strain fringes on Silurian graptolites have been used to precisely date low-temperature deformation (Sherlock *et al.* 2003), producing an age consistent with independent evidence, this work exploited unambiguously synkinematic phyllosilicates. A similar approach might be attempted using a phyllosilicate corona to date the transition through the gas window, and, with this in mind, it is important to emphasise that unless there is direct evidence of synkinematic growth, authigenic phyllosilicates found on carbonaceous fossils should not be used to provide information concerning strain.

This study provides new information concerning the link between kerogen maturation and phyllosilicate formation. Though Uysal *et al.* (2004) linked the alteration of diffuse organic matter and the subsequent precipitation of illite to a regional hydrothermal event, they provided relatively little information concerning the mechanism of phyllosilicate growth. They argued that volume loss in maturation may have increased the rock's porosity (e.g. Belek & de Koranyi 1990; Gilkson *et al.* 1992), with illite precipitation occurring within pore spaces around denatured organics before continuing into the surrounding rock. These observations seem entirely compatible with those made in this study. However, as noted in Sections 4.4.2-4, the phyllosilicates occurring immediately adjacent to denatured periderm have a different habit from those that precipitated into an emergent void, whilst the continued growth of phyllosilicates into the surrounding rock requires replacement driven by Eh/pH changes. So, though phyllosilicates may precipitate directly into any voids that are created at in maturation (e.g. Fig 4.6d), it seems more likely that the dominant process of phyllosilicate growth on graptolites is wholesale replacement of the surrounding rock driven by the release of volatiles in maturation (cf. Curtis 1985; Seewald 2003).

4.5.2 Implications for morphological study

The preservation of graptolites beneath a phyllosilicate film often enhances their visibility under reflected light (cf. Towe 1996), and many taxonomic works have been made on species preserved in this manner (e.g. Rickards 1970; Hutt 1974; Jenkins 1987; Williams 1982; Zalasiewicz & Tunnicliff 1994; Zalasiewicz & Williams 1999). For example, the type specimen of *Huttagraptus? praematurus* (Toghill) is preserved as a chlorite film, with numerous other specimens showing preservation of fine detail in phyllosilicate films (Zalasiewicz *et al.* 2003); whilst the preservation of graptolites entirely as a phyllosilicate film has been documented elsewhere (Jenkins 1987) presumably as a consequence of periderm flaking away or becoming oxidised in weathering (cf. Underwood 1992). Though graptolites have been used as strain indicators in tectonised rocks (e.g. Jenkins 1987; Cooper 1990), and many authors have indicated and accounted for such distortion of tectonised graptolites (e.g. Rickards 1970; Jenkins 1987), this study has shown that relatively large phyllosilicate coronas can form on graptolites that show little or no evidence of tectonic distortion (e.g. Figs 4.2a-c). Such phyllosilicate coronas may ape the graptolite's outline with a remarkable fidelity (e.g. Fig 4.4a), and the detail of fine structures may be apparent in this mode of preservation (e.g. Zalasiewicz *et al.* 2003), it is clear that such authigenic phyllosilicates define an area larger than the fossil itself (e.g. Fig 4.4). Given that these coronas can grow at least 200 μm thick, any measurements of a fossil's outline taken from the phyllosilicate film rather than preserved periderm may represent an overestimate. With this in mind, it seems that extra care is needed when working with material in this mode of preservation, ensuring that one is measuring the carbonaceous fossil rather than the phyllosilicate film, especially as periderm may not always survive rock splitting, especially if part and counterpart are not available.

Though periderm may undergo significant volume loss in very-low grade metamorphism (e.g. Fig. 4.6), any size change resulting from this is negligible compared to the size of the graptolite itself. However, this volume loss may go some way to explaining the general loss of

microstructural/fusellar preservation in graptolites in very-low grade metamorphic mudrocks (e.g. Underwood 1992). Both flattened and pyritised graptolites may preserve fusellar structure in low-grade mudrocks (Crowther 1981; Zalasiewicz *et al.* 2007), but at higher metamorphic grades (such as in graptolites from the Cerig Gwynion Quarry) fusellar structure only seems to be apparent in pyritised graptolites and not in flattened graptolites (cf. Blackett *et al.* in review, Fig. 5). Likewise, Crowther (1981, p. 20, pl. 16, Figs 5-6) noted that micron-scale detail of the periderm's endocortex was preserved in a pyritised graptolite from the tectonised mudrocks of the Rheidol Gorge, where it was equally well-preserved in both the pyrite mould and the denatured periderm. Where fusellae structure is preserved in graptolites from Cerig Gwynion Quarry, it is either preserved in both their denatured periderm and the pyrite mould or not at all. These observations might be explained by periderm volume-loss in maturation (cf. Fig 4.6): if the original fusellar structure was cast by pyrite prior to compaction, it could be re-cast by the periderm when it underwent volume loss, viz. the residual kerogen acted as a 'shrink-wrap' preserving a structure already fossilised in pyrite. Hence in metamorphic mudrocks, pyritised graptolites may preserve fusellar structure, but flattened graptolites, lacking a pyrite mould to serve as a template for re-casting their fusellar structure, have had it destroyed in maturation.

With the combination of distortion in diagenetic flattening (e.g. Sudbury 1958; Briggs & Williams 1981), followed by the loss of fusellar structure and encasement by phyllosilicates in maturation serving to complicate the morphological preservation of flattened graptolites in metamorphic mudrocks, it seems that caution should be applied in interpreting their morphology. As other authors have noted, fully pyritised graptolites may provide a more reliable indication of their outline than flattened graptolites (e.g. Sudbury 1957; Briggs & Williams 1981; Blackett *et al.* in review), and this observation seems especially pertinent where graptolites are preserved in association with phyllosilicates.

4.6 Conclusions

Phyllosilicate formation on graptolites occurred in the gas window, catalysed by volatile expulsion as their periderm underwent maturation. This process may apply to other authigenic phyllosilicates that are found in association with carbonaceous fossils in very-low grade mudrocks. Phyllosilicate authigenesis occurred by diffusion in a fluid phase, and such phyllosilicates appear to have precipitated into emergent and pre-existing voids as well as replacing the surrounding rock to form a phyllosilicate corona that encased the fossil. This mode of phyllosilicate formation differs significantly from previous models of phyllosilicate authigenesis on carbonaceous fossils, and it may have some implications for understanding how porosity and permeability change during the very-low metamorphism of mudrocks.

TABLE 4.3 Specimens included Table 4.1

Locality	Hand specimens	Thin sections
White Horse	SM A17837-17840	-
The Deep Kill	NYSM 5791-5798	-
Dinas Island	MWL 5229-5330	E74526a-d
Llanrhaidr	RE 905	-
Cerig Gwynion Quarry	-	AAP 00100-00104
Ystraddfin	-	AAP 00105-00108
Abereiddi Bay	LEIUG 77298-77305, AAP 00160-00161	-

TABLE 4.4 KI values and specimen numbers for Table 4.2

Formation	specimens	KI	Formation	Specimens	KI
Blaen Myherin Mdst Fm.	JZ 3590-3600	0.35	Caerau Mst. Fm.	DJ 9433-9465	0.25
Blaen Myherin Mdst Fm.	JZ 6204-6219	0.34	Caerau Mst. Fm.	DJ 8931-8936	0.24
Borth Mudstones Fm.	JZ 9325-9387	0.45	Cwmere Fm.	JZ 904-924	0.48
Borth Mudstones Fm.	JZ 8209-8211	0.46	Cwmere Fm.	MWL 2962-2963	0.45
Borth Mudstones Fm.	JZ 6998-7002	0.50	Cwmere Fm.	JZ 2454- 2501	0.31
Borth Mudstones Fm.	JZ 7805	0.45	Cwmere Fm.	JZ 4993- 4994	0.29
Borth Mudstones Fm.	JZ 8198-8208	0.45	Cwmere Fm.	JZ 8598- 8602	0.20
Builth Mudstones Fm.	JZ 3357-3373	0.45	Nantmel Mst. Fm.	JZ 3555- 3557	0.59
Builth Mudstones Fm.	SPT 3368-3383	0.39	Nantmel Mst. Fm.	JZ 2387- 2453	0.56
Caerau Mst. Fm.	DJ 8169-8193	0.46	St Cynllo's Church Fm.	JZ 1086- 1108	0.63
Caerau Mst. Fm.	JZ 1251-1426	0.35	St Cynllo's Church Fm.	JZ 5295- 5372	0.63
Caerau Mst. Fm.	JZ 1431-1489	0.35	St Cynllo's Church Fm.	JZ 5450- 5453	0.57
Caerau Mst. Fm.	SPT 1793-1835	0.30	Tycwtta Mst. Fm.	JZ 3351	0.60
Caerau Mst. Fm.	DJ 8670-8706	0.30	Tycwtta Mst. Fm.	JZ 3352	0.58
Caerau Mst. Fm.	JZ 2196- 2221	0.30	Tycwtta Mst. Fm.	JZ 5821- 5845	0.55

Abbreviations: LEIUG: Geology Department, University of Leicester, UK; NYSM, New York State Museum, Albany, NY, USA; SM: Sedgwick Museum, Cambridge, UK; all other abbreviations refer to specimens housed at the British Geological Survey, Keyworth.

5. A reassessment of the taphonomy of the Burgess Shale by comparison with graptolitic mudrocks

Abstract: Despite the Burgess Shale's palaeobiological importance, there is little consensus regarding its taphonomy. Burgess Shale fossils are preserved as organic compressions coated in films of cleavage-aligned phyllosilicates; similar phyllosilicate films occur on other organic compression fossils, such as graptolites. Phyllosilicates are known to form on graptolites in very-low grade metamorphism due to mineral- organic interactions during maturation. However, the Burgess Shale phyllosilicate films have been previously considered to represent permineralisation in earliest diagenesis as they exhibit an anatomy-specific composition. Yet, in bedding plane assemblages where graptolites are preserved with other organic compression fossils, phyllosilicate films show a remarkable taxon-specificity: distinct phyllosilicate assemblages are associated with each different type of carbonaceous fossil, due to differences in their maturation pathways. As such, I argue that the anatomy-specific phyllosilicate distribution in Burgess Shale fossils reflects differences in the late diagenesis of labile and recalcitrant anatomy. This calls existing models of Burgess Shale-type preservation into doubt, with phyllosilicate films forming too late to account for decay retardation or exceptional preservation in the Burgess Shale.

5.1 Introduction

Exceptional preservation of soft-bodied animals in Burgess Shale-type deposits underpins our understanding of early animal evolution (e.g. Butterfield 1995; Conway Morris 2006). However, there is much debate regarding their preservation (cf. Butterfield 1996; Orr *et al.* 1998; Petrovich 2001; Gaines *et al.* 2005; Page *et al.* 2006b; Butterfield *et al.* 2007) and until the taphonomy of such deposits is better resolved, it remains unclear whether such fossils accurately represent early metazoan diversity. Burgess Shale-type (BST) preservation is

considered to be a largely Cambrian phenomenon, suggesting that it represents a non-actualistic process (e.g. Butterfield 1995; Orr *et al.* 2003). Bearing this in mind, opinion remains divided as to whether the “Cambrian explosion” genuinely represents the diversification of the bilaterians (e.g. Budd & Jensen 2000; Conway Morris 2006) or merely the opening of a taphonomic window (e.g. Butterfield 1995), thence the first appearance of bilaterians in the fossil record (cf. Cooper & Fortey 1998; Adouette *et al.* 1999).

Butterfield (1990) stated that BST preservation is characterised by the organic preservation of recalcitrant, extracellular tissues, rather than labile, cellular tissues such as muscles or visceral organs: a corollary being that this taphonomic mode only preserves cuticular organisms (e.g. Butterfield 2006). This concept was introduced to distinguish localities with *preservation* similar to that of the Burgess Shale from localities that merely contain a similar fauna (Butterfield 1990). The most recent redefinition of BST preservation refers to the “exceptional” preservation of both carbonaceous macrofossils and microfossils in siliciclastic facies (Butterfield 1995, 2003). However, palynological preparations of sediments from the Burgess Shale yield relatively poorly-preserved microfossils (Gostlin 2006). Meanwhile, some authors argue that the Burgess Shale displays organic preservation of labile anatomy and acuticular organisms, notably acorn worms (Boulter 2003; Conway Morris 2006) and soft-bodied molluscs (Caron *et al.* 2006). The preservation of such taxa calls for the concept of BST preservation to be critically re-examined (this may also establish whether this taphonomic mode was restricted to the Cambrian, cf. Butterfield 1995).

Though BST preservation refers only to the selective preservation of cuticular anatomy (e.g. Butterfield 1990, 1996, 2003, 2005), soft-bodied organisms from the Burgess Shale display three distinct preservational styles, more than one of which may be found within any one fossil (e.g. Fig. 5.1a-d): carbonaceous compressions (i.e. BST preservation), three-dimensional phosphatized soft tissues (Butterfield

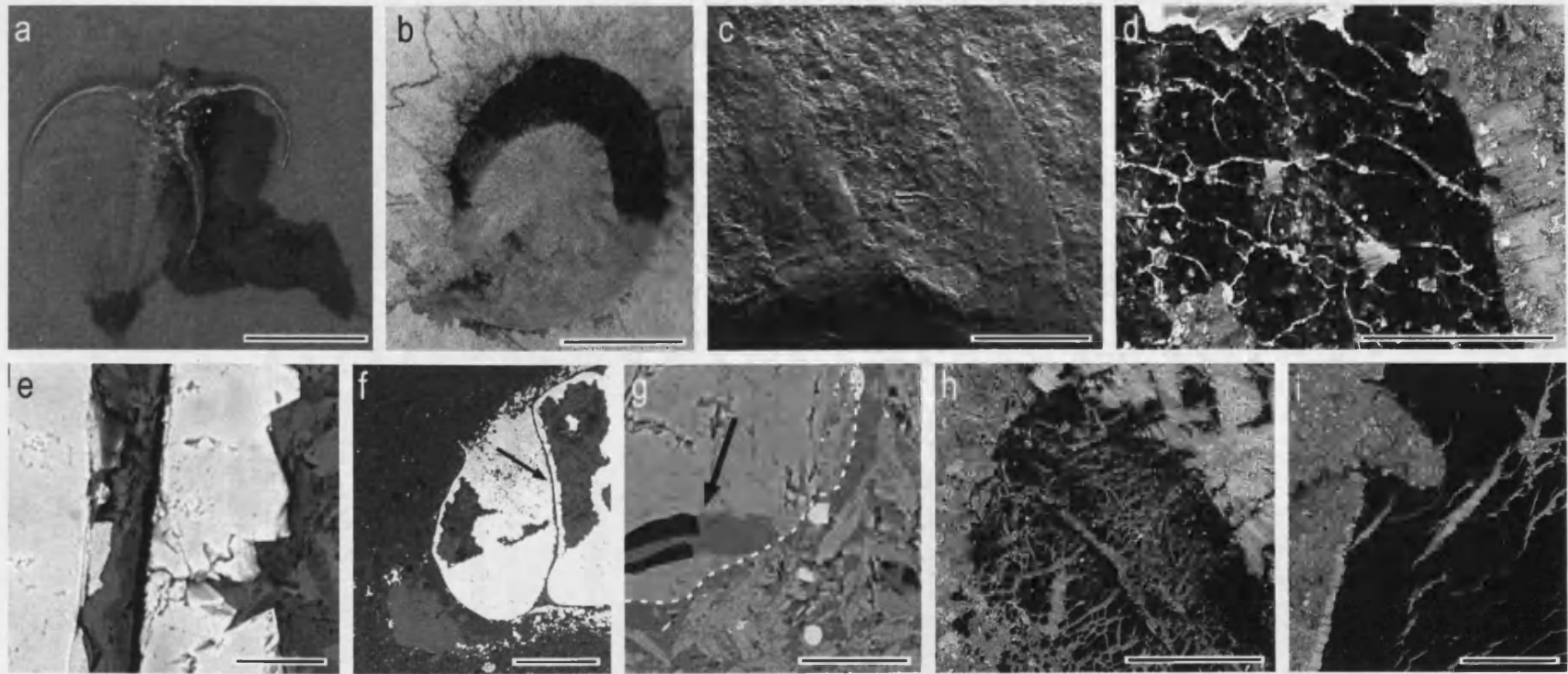


Fig 5.1 Fossil preservation in (a-d) the Burgess Shale and (e-i) graptolitic mudrocks [photomicrographs of specimens submerged in water (a-b), environmental secondary electron micrograph showing topographic contrast (c) and backscattered scanning electron micrographs showing compositional contrast (d-i): the black phase is organic carbon and the grey phases are phyllosilicates, the lightest gray phases are either pyrite (e-g) or secondary gypsum (d)]. Variations in organic preservation in: (a) *Marrella splendens* with 'shiny' cuticular exoskeleton and the dark stain, ROM 75-22; (b) *Eldonia* sp. with 'shiny' gut and duller outline, SM A1715; (c) pleurae of trilobite *Oryctocephalus reynoldsi* cross-cut by cleavage, BS trilobites may be preserved by cleavage-aligned phyllosilicates and no discernable calcite (Butterfield *et al.* 2007) ROM 75-11; (d) *Canadaspis* sp. carapace with tension gashes filled with cleavage-aligned phyllosilicates, ROM WT89-2. *Continued overleaf...*

2002), and phyllosilicate films (e.g. Orr *et al.* 1998). These phyllosilicate films may display an anatomically-specific elemental distribution, which Orr *et al.* (1998) interpreted as forming in early diagenesis due to contrasts in the decay of different tissues. They claimed “authigenic [phyllosilicate] mineralization was fundamental to preserving these fossils,” (Orr *et al.* 1998, p. 1173). Significantly, Orr *et al.* (1998) argued that the presence of phyllosilicates within internal cavities inside these compression fossils indicated that they formed in earliest diagenesis as decay-induced collapse would have occluded voids, preventing later infill. Though these phyllosilicates are now aligned to cleavage (Fig. 5.1c, d), Orr *et al.* (1998) argued that this represented recrystallisation of early diagenetic clays during metamorphism. However, phyllosilicate films are not present in all deposits with BST preservation (e.g. Gaines *et al.* 2005) and recent work has shown that high-fidelity phyllosilicate templates can form on carbonaceous fossils in their late diagenetic history (e.g. Chapter 4; Page *et al.* 2005, 2006b). Meanwhile, Butterfield *et al.* (2007) observed phyllosilicate replacement of trilobite shells and late-stage mineral veinlets in the Burgess Shale, showing that at least some phyllosilicates formed in the deposit’s later taphonomic history. Though Butterfield *et al.* (2007, p. 542) state “we see no evidence or necessity for early diagenetic aluminosilicification,” they provide no evidence of how late-stage phyllosilicate authigenesis may account for either [1] the anatomically-specific phyllosilicate distribution observed in Burgess

Fig. 5.1 (*Continued from overleaf*) Thin sections showing late-diagenetic phyllosilicates occupying voids in organic compression fossils: (e) detail of (f) interthecal septum (arrow) of a graptolite preserved as pyrite steinkern: this space is now occupied with phyllosilicates (e) but was originally occupied by periderm, which has subsequently undergone volume-loss in maturation and now ‘shrink wraps’ the septum’s right-hand margin, AAP 00102; (g) phyllosilicates within (arrow) and around (dashed line) a flattened graptolite, AAP 00102. Cleavage-aligned syndeformational phyllosilicates associated with: (h) arthropod “soft parts” and carapace (top right), note the difference in their preservational style, MWL 5229; (i) diplograptid with tension gashes, GSM 105819. Repositories: ROM = Royal Ontario Museum; SM = Sedgwick Museum; other prefixes = British Geological Survey. Scale bars: 10 mm (a); 5mm (b); 0.5 mm (c); 200 μ m (h, f); 100 μ m (d); 50 μ m (i); 25 μ m (g); 10 μ m (e).

Shale fossils (Orr *et al.* 1998; Zhang & Briggs 2007), or [2] the occurrence of authigenic phyllosilicates within the internal cavities of compression fossils (cf. Orr *et al.* 1998).

This chapter serves to assess whether authigenic phyllosilicate formation in early diagenesis was responsible for the exceptional preservation of soft-bodied animals (e.g. Orr *et al.* 1998), or whether their fossilisation can be accounted for by the selective preservation of recalcitrant, cuticular anatomy alone as put forward by the BST preservation view of Burgess Shale taphonomy (Butterfield 1990, 1995, 2003). The earliest diagenetic history of the Burgess Shale is difficult to assess given its alteration in epizone grade metamorphism and lack of low-grade equivalents (Powell 2003). Nevertheless, the factors governing exceptional preservation in the Burgess Shale may in principle be inferred by comparing its taphonomic history with that of other mudrocks preserving organic compression fossils, enabling one to discriminate which processes are normal geological phenomena and which processes are unique to the exceptionally preserved fossils of the Burgess Shale. Here I demonstrate that differences in the maturation of different kerogens can 'catalyse' the formation of phyllosilicates with distinct compositions in late diagenesis (cf. Chapter 4; Page *et al.* 2005, 2006b). This preservation is entirely normal in graptolitic mudrocks where the preservation of recalcitrant extracellular carbon as organic compressions is common (Chapman 1991; Underwood 1992), though not associated with the exceptional preservation of soft-bodied animals (Palmer 1991). As such, early diagenetic phyllosilicate mineralization does not seem to account for the decay retardation and organic preservation of Burgess Shale fossils (cf. Orr *et al.* 1998).

5.2 Material and methods

This study compares phyllosilicate films on Burgess Shale fossils with similar films occurring on various taxa preserved in graptolitic mudrocks. Graptolitic mudrocks are a widespread facies in which organic preservation of recalcitrant organic matter as kerogens is

entirely normal (e.g. Underwood 1992). I examined authigenic phyllosilicates in bedding assemblages in which graptolites, brachiopods, arthropods and problematica are preserved as organic compression fossils, which were deposited in deep-water mudrocks from the Welsh Basin and Southern Uplands in the UK (Table 5.1). These strata underwent very-low grade regional metamorphism in the Acadian Orogeny and during accretionary burial respectively (Roberts *et al.* 1996; Merriman & Roberts 2001). The taxa investigated each had distinct *in vivo* organic carbon compositions, namely: [1] collagenous graptolite periderm (Figs 5.2a, c-d); [2] chitinous brachiopod organic laminae (Fig. 5.2c), and arthropod carapaces (Figs 5.2a-b); and [3] labile arthropod “soft parts” (Figs 5.1h, 5.2b); and [4] the organic-walled problematicum *Dawsonia* Nicholson (Fig. 5.2d) which is of indeterminate original organic composition (see Chapter 3). Phyllosilicates formed on carbonaceous fossils in very-low grade metamorphism and are not found on similar fossils at shallow diagenetic grade (e.g. Chapter 4; Underwood 1992; Page *et al.* 2005). I compared different taxa preserved as compression fossils on single sedimentary laminae, meaning that every fossil in each assemblage has experienced identical pressure and temperature conditions during its taphonomic history.

I compared the texture, distribution, mineralogy and elemental composition of the phyllosilicates on the exceptionally-preserved fossils of the Burgess Shale with those in the multi-faunal assemblages from graptolitic mudrocks using a variable pressure scanning electron microscope (Hitachi S-3600N) with an Oxford Instruments X-ray (EDX) detector. The uncoated specimens were imaged in back-scatter mode at 15kv, and elemental mapping was undertaken with high counts. To account for topographic effects, mapped specimens were rotated 180° and remapped to check that differences in elemental distribution are genuine rather than a consequence of shadowing (cf. Martill *et al.* 1992). Phases were also identified by quantitative (EDX) microanalysis and identifications were confirmed by XRF and XRD analysis of fossils and the rock (see Fig. 5.3).

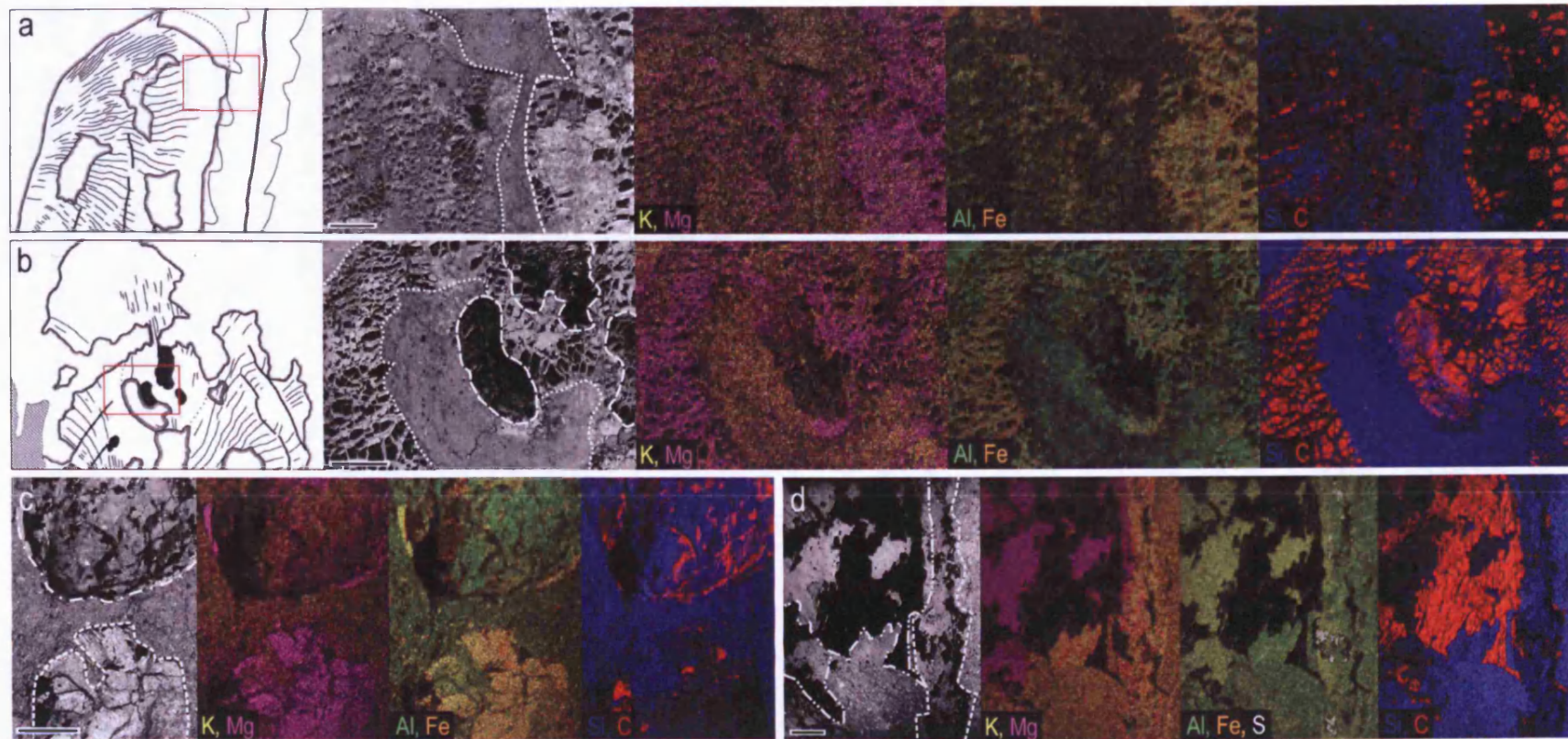


Fig. 5.2 Kerogen-specific elemental distribution: backscattered scanning electron micrographs and elemental abundance maps for assemblages of (a-b) graptolites (dashed line) & bivalved arthropods preserving (a-b) carapaces (dotted line) and (b) "soft parts" (long dashes), MWL 5229; (c) graptolites (dashed line) & organically-preserved brachiopods (dots & dashes), RE 907; and (d) graptolites (dashed line) & two "*Dawsonia*" specimens (top left, double dots & dashes), GSM 105819. All maps show area of BSEM image [=red box in illustrations (a) & (b)], Elements labelled in the appropriate colour on each map. Scale bars = 0.5 mm.

5.3 Results

There are distinct differences in the compositions of the phyllosilicate films associated with the kerogens preserving each different taxon/anatomical type (Table 5.1; Figs 5.2 & 5.3). These authigenic phyllosilicates can be distinguished from the sedimentary matrix by their relative elemental abundances (Figs 5.1 & 5.2) and by their texture, which bears a remarkable similarity to phyllosilicate films associated with Burgess Shale fossils (cf. Figs 5.1d, h-i). I will deal with each graptolitic mudrock assemblage in turn:

Graptolites & bivalved arthropods: the phyllosilicates associated with graptolites are enriched in Mg and Fe, and depleted in Si relative to those associated with arthropod carapaces (Fig. 5.2a). Compared to the rock, phyllosilicates associated with carapaces are enriched in Fe, Mg and Al, and relatively depleted in K (Fig. 5.2a, b); compared to those associated with carapaces, phyllosilicates associated with arthropod soft-parts are relatively enriched in Al, Si and K, and rimmed by an enrichment in Fe and Mg (Fig. 5.2b). The differences between the phyllosilicate assemblages associated with graptolites, carapaces and 'soft-parts' are supported by quantitative EDX microanalyses of synkinematic phyllosilicates in interstices between the 'rafts' of organic carbon (Fig. 5.3c).

Graptolites & brachiopods: phyllosilicates associated with graptolites are enriched in Fe and Mg relative to both the brachiopods and the sediment, and depleted in K, Si and Al (Fig. 5.2c). Phyllosilicates associated with brachiopods are slightly enriched in K, Al and Si relative to the rock, and the brachiopods are rimmed by an anomaly of enhanced Fe and Mg. Quantitative EDX microanalyses of authigenic phyllosilicates (recognised by their textural difference from the rock) confirm that different phyllosilicate assemblages are associated with graptolites and brachiopods.

Graptolites & "*Dawsonia*": relative to those associated with "*Dawsonia*", the phyllosilicates associated with graptolites are enriched in K and Si and depleted in Fe and Mg; the phyllosilicates associated with both

Specimen	Locality	Metamorphic grade	Chitinous anatomy	Collagenous anatomy	Other anatomy
Graptolites & brachiopods (Fig. 5.2c)	Llanrhaiadar, central Wales. Caradoc, Ordovician.	Low anchizone	Organic laminae	Periderm	-
			Illite-dominated clay assemblage	Chlorite-dominated clay assemblage	-
Graptolites & " <i>Dawsonia</i> " (Fig. 5.2d)	Dob's Linn, S. Scotland. Llandovery, Silurian.	High anchizone	-	Periderm	" <i>Dawsonia</i> "
			-	Illite & chlorite clay assemblage	Principally chlorite
Graptolites & arthropods (Fig. 5.2a-b)	Dinas Island, SW Wales. Caradoc, Ordovician.	High anchizone	Carapaces	Periderm	"soft parts"
			Illite-dominated clay assemblage	Chlorite-dominated clay assemblage	Kaolinite & illite clay assemblage
<i>Marrella splendens</i>	Burgess Shale, Canada. Middle Cambrian.	Epizone	ag, an, cs, ts	-	cc, ss, st
			Si-rich micas	-	K, Al-rich micas
<i>Alalcomeneaus cambricus</i>	Burgess Shale, Canada. Middle Cambrian.	Epizone	cs, ts	-	dt, eyes
			Si-rich micas	-	K, Al-rich micas
<i>Opabinia regalis</i>	Burgess Shale, Canada. Middle Cambrian.	Epizone	cs, es, ga, ts	-	ss, dt, eyes
			Si-rich micas	-	K, Al-rich micas

Table 5.1 Late diagenetic phyllosilicates formed on different kerogens. Phyllosilicate identifications for specimens mapped in Fig. 5.2 based on EDX/XRD data (Fig. 5.3), while, for Burgess Shale taxa, I rely on the elemental maps and mineral identifications in Orr *et al.* (1998) for *M. splendens* & *A. cambricus*, and Zhang & Briggs (2007) for *O. regalis*. Metamorphic grade determinations for British specimens are based on unpublished white mica crystallinity data held in the BGS data archive (Dick Merriman & Rob Barnes, personal communications June 2006 & 2007 respectively); Powell (2003) determined a greenschist (= epizone) grade for the Burgess Shale based on the peak metamorphic mineral assemblage. Abbreviations: ag = axial gut; an = antennae, cc = cephalic canals; cs = cephalon or cephalic shield/spines; dt = digestive tract; es = eye stalks; ga = great appendage; ss = biserially-repeated structures in the abdomen, which may represent organs or muscles in *Marrella* (Orr *et al.*, 1998), and may represent extensions of the gut in *Opabinia* (Butterfield, 2002; Zhang & Briggs, 2007); st = stomach; ts = tergites.

fossils are enriched in Mg and depleted in Si relative to the rock (Fig. 5.2d). Quantitative EDX microanalyses of authigenic phyllosilicates (recognised by their textural difference from the rock) confirm that different phyllosilicate assemblages are associated with graptolites and “*Dawsonia*”.

The phyllosilicate assemblage associated with any one kerogen type (*viz.* graptolite periderm, “*Dawsonia*”, brachiopod organic laminae, arthropod carapace, and “soft parts”) is, in this study, consistent throughout each assemblage and between each locality. That is, originally chitinous fossils are predominately associated with illite, originally collagenous graptolites are predominately associated with chlorite though less so than the problematicum “*Dawsonia*”, and the arthropod soft-parts are associated with kaolinite, which is not found in association with either originally-chitinous or collagenous fossils (Table 5.1; Fig. 5.3).

5.4 Model to account for kerogen-specific phyllosilicates

The kerogen-specific phyllosilicate distribution in graptolite mudrocks reflects the maturation of different kerogens. Each graptolitic mudrock-hosted assemblage contains fossils with distinct *in vivo* compositions (Table 5.2; Section 5.2); such fossils can retain largely unaltered molecular preservation of their original chemistry over long timescales (e.g. Stankiewicz *et al.* 1998a; Ansara *et al.* 2007; Schweitzer *et al.* 2007). Pyrolysis experiments have shown that different diagenetic pathways are experienced between organic fossils as a consequence of their original composition (e.g. Briggs 1999; Gupta *et al.* 2007a). For example, graptolites and arthropods respectively resemble Type I/Type II and Type II kerogens (Bustin *et al.* 1989; Stankiewicz *et al.* 1997, 1998b, 2000; Gupta *et al.* 2006a, 2007b). The timing and nature of maturation varies between kerogens (e.g. Hunt 1996), with the relative proportion and composition of the volatiles they release being a product of their original composition and the ambient conditions, and changing as maturation progresses (e.g. Hunt 1996; Seewald 2003). The maturation of organic carbon has been

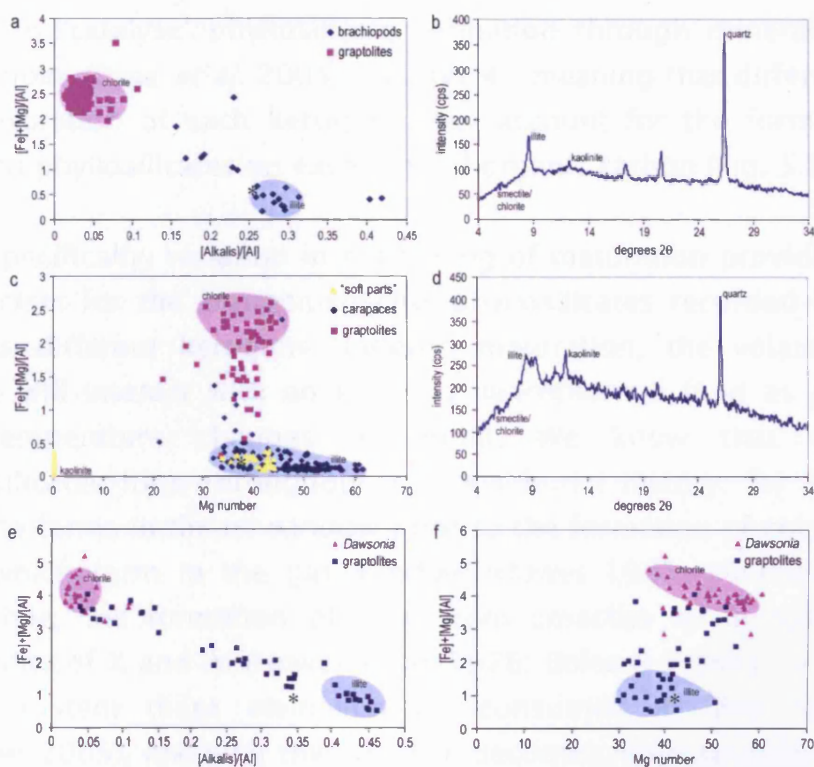


Fig. 5.3 Kerogen-specific phyllosilicate assemblages. Elemental molecular ratio plots (a, c, e-f) for authigenic phyllosilicates associated with carbonaceous fossils and XRD traces for bulk rock samples (b, d) for specimens preserving bedding plane assemblages of (a-b) organically-preserved brachiopods and graptolites mapped in Fig. 5.2c, RE 907, (c-d) arthropods with soft parts and graptolites mapped in Figs 5.2a-b, MWL 5229, and (e-f) "*Dawsonia*" and graptolites, GSM 105819. All phases are identified on each graph, and in each graph (a, c, e-f) graptolites = squares; chitinous fossils = diamonds; fossils of indeterminate original composition = triangles; bulk rock = asterisks. Points plotting on the mixing line in between the shaded clouds representing each phase possibly indicate overlaps between two crystals in analyses. These graphs show that (a-b) brachiopods are associated with a phyllosilicate assemblage dominated by illite with lesser chlorite and graptolites are associated with a phyllosilicate assemblage of almost pure chlorite; (c-d) arthropod soft-parts are preserved in association with a mixed assemblage of kaolinite and illite, while arthropod carapaces are associated with a phyllosilicate assemblage dominated by illite with lesser chlorite, and graptolites are associated with a phyllosilicate assemblage dominated by chlorite with lesser illite and (e-f) "*Dawsonia*" are associated with a phyllosilicate assemblage of chlorites and graptolites are associated with a phyllosilicate assemblage of illite and chlorite. Bulk rock compositions (a, c, e-f) determined from XRF analyses. Uncoated material was examined in partial vacuum (20Pa) to avoid charging effects, elemental abundance data were obtained using energy dispersive x-ray analyses compared to a cobalt standard; several different fossils of each taxon/anatomical type were analysed in each assemblage.

shown to 'catalyse' phyllosilicate formation through mineral-organic interactions (Page *et al.* 2005; Chapter 4), meaning that differences in the maturation of each kerogens may account for the formation of different phyllosilicates on each type of organic carbon (Fig. 5.2).

More specifically, variation in the timing of maturation provides a key mechanism for the kerogen-specific phyllosilicates recorded in Table 5.1. As different kerogens undergo maturation, the volatiles they release will interact with an evolving hydrothermal fluid as pressure and temperature changes in burial. We know that different phyllosilicates form throughout a rock's burial history: for example, kaolinite forms in the oil window prior to the formation of chlorite and illite, which form in the gas window (Hower 1981; Meunier 2005). Meanwhile, the formation of illite from smectite is limited by the availability of K and Al (Hower *et al.* 1976; Boles & Franks 1979). In a closed system these elements are consumed in illite formation (Meunier 2005), meaning that chlorite becomes more abundant as the reaction progresses. Thus, as each kerogen underwent peak maturation, a different assemblage of phyllosilicates formed: kaolinite formed on arthropod "soft parts", then illite formed on chitinous fossils, and finally chlorite formed on collagenous fossils as well as "*Dawsonia*".

5.5 Comparison with the Burgess Shale and BST preservation

This model for phyllosilicate formation is entirely compatible with the distribution of phyllosilicates on Burgess Shale fossils (see Table 5.1). I propose that these phyllosilicates formed in maturation and later recrystallised as micas (cf. Meunier 2005). Based on the presence of phyllosilicates in internal cavities of Burgess Shale fossils, Orr *et al.* (1998) argued that phyllosilicate authigenesis occurred before the fossils had undergone collapse due to decay (i.e. in earliest diagenesis). However, there is good petrographic evidence that carbonaceous fossils can undergo significant volume loss due to volatile release in maturation (Fig 5.1e; Chapter 4; Uysal *et al.* 2004). Thus, void space may be created in carbonaceous fossils long after

compaction and their initial organic preservation, and such voids may be infilled by phyllosilicates (Figs 5.1 e-g).

This model also accounts for the anatomically-specific phyllosilicate distribution in Burgess Shale arthropods (Orr *et al.* 1998; Zhang & Briggs 2007). In these fossils, recalcitrant anatomy is preserved in association with Si-rich, K, Al-depleted mica whereas labile anatomy is preserved in association with K, Al-rich mica (Table 5.1), clearly showing that these anatomical types have undergone different diagenetic pathways. The *in vivo* histology of these anatomical types is notably dissimilar: 'recalcitrant anatomy' represents cuticle, which would have originally been composed of cuticulin and chitin (e.g. Butterfield 1990), whereas 'labile anatomy' includes eyes, putative visceral organs or ?musculature and parts of the digestive tract (Table 5.1). As highlighted above, differing types of organic matter can be preserved as different kerogens (e.g. Hunt 1996; Gupta *et al.* 2007a), and comparison with graptolitic mudrocks shows that, during maturation, different phyllosilicates form on each type of kerogen (Table 5.1; Section 5.4). This provides a mechanism for anatomically-specific phyllosilicates to form in the late diagenetic history of Burgess Shale fossils (cf. Orr *et al.* 1998).

5.5.1 Implications for BST preservation

That both labile and recalcitrant anatomy underwent distinct taphonomic pathways, poses a significant problem for the concept of BST preservation. Butterfield (2003, p. 167) defined BST preservation as "the 'exceptional' preservation of non-mineralizing organisms as carbonaceous compressions in marine shales," and argued that this taphonomic mode only preserves recalcitrant extracellular secretions such as cuticle, chaetae, jaws and organic-walled microfossils rather than labile, cellular anatomy (see also Butterfield 1990; 1995; 2006). Though labile anatomy, such as parts of the digestive tract and eyes, may have been associated with a thin cuticular membrane *in vivo*, its original histology was markedly dissimilar to that of recalcitrant anatomy (Richards 1952; Phillipson 1961; Ossorio & Bacon 1994); moreover, the differing diagenetic pathways experienced by labile and recalcitrant anatomy highlights that the organic preservation of labile

anatomy is distinguishable from that of cuticle *per se*. And while there is a taphonomic bias towards the preservation of such recalcitrant organic matter in the Burgess Shale (e.g. Butterfield 1990), which may account for the preponderance of arthropods and priapulid worms in its fauna (e.g. Conway Morris 1986), the selective preservation of recalcitrant, cuticular anatomy seems insufficient to account for the exceptional preservation seen in Burgess Shale fossils. There is widespread organic preservation of recalcitrant extracellular secretions such as arthropod cuticle, graptolite periderm, scolecodonts and acritarchs, especially in dysoxic and anoxic shales (cf. Butterfield 1990; Underwood 1992), but this represents normal rather than exceptional preservation (cf. Briggs 2003). For example, insects and beetles commonly occur as well-preserved organic fossils in Quaternary strata (e.g. Brodersen & Bennike 2003) and this undoubtedly represents the preservation of cuticle. However, such fossils are not associated with the exceptional preservation that characterises the Burgess Shale itself, highlighting the fact that the key taphonomic pathways in the Burgess Shale are not only those associated with the preservation of cuticle.

BST preservation should instead be reassessed based on what makes the Burgess Shale exceptional. Recent work on the Burgess Shale fauna has identified several notably acuticular clades preserved as organic compressions (e.g. Briggs *et al.* 1994; Caron & Jackson, 2006), including acorn worms (see also Boulter, 2003), cnidarians (e.g. *Mackenzia*), ctenophores (e.g. *Ctenorhabdus*). BST preservation has the potential to capture anatomical parts with a range of decay resistance including labile anatomy. For example, Burgess Shale arthropods preserve labile anatomy, such as their digestive tract, as well as their carapaces and tergites. Similarly, the enigmatic fossil *Eldonia* (Fig. 5.1b) displays two distinct types of organic preservation: Butterfield (1996) considered its highly reflective gut to represent recalcitrant, cuticular matter, yet this taxon's well-defined outline is relatively dull, suggesting it may have had a different original composition. Meanwhile, the *Marrella* dark stain and the enigmatic fossil *Amwiskia* preserve 'diffuse' organic matter rather than cuticular anatomy (Butterfield 1990; Orr *et al.* 1998). The *Marrella* dark stain (Fig. 5.1a) is a poorly-delineated compression that has been

interpreted as fluids leaked from the decaying organism (e.g. Orr *et al.* 1998). However, the phyllosilicates associated with it are reasonably similar to those associated with recalcitrant anatomy (Orr *et al.* 1998), indicating that it may represent an extracellular secretion. One intriguing possibility is that it may represent organic preservation of the cell-walls of a bacterial biofilm that formed about a more labile organic structure which has since decayed (cf. McNamara *et al.* 2006). Thus, labile anatomy may be preserved without preserving labile tissues themselves. As such, there is compelling evidence for the preservation of labile and non-cuticular structures in the Burgess Shale.

Labile, acuticular anatomy, such as musculature and visceral organs, have been preserved as organic compressions elsewhere in the geological record, occurring in both siliciclastic (e.g. Beyermann & Hasenmaier 1973; Aldridge & Purnell 2005), and calcareous facies (e.g. Ruben *et al.* 1999; Grogan & Lund 2002). Likewise, bones (Schweizer *et al.* 2005; McNamara *et al.* 2006) and amber (Henwood 1992) may also contain organic preservation of labile, cellular tissues. However, all the above occurrences are rare in the fossil record, and taxonomically restricted in any one fauna. Conversely, the taphonomy of the Burgess Shale is characterised by the abundant organic preservation of labile anatomy in a relatively diverse fauna. With this in mind, my re-examination of BST preservation may contribute to a better understanding of its fauna, aiding the diagnosis of distinct anatomy within fossils (cf. Zhang & Briggs 2007), and suggesting that truly soft-bodied fossils may occur in such deposits. For example, there is no good taphonomic reason why the enigmatic fossil *Pikaia* should not be a cephalochordate (e.g. Conway Morris & Whittington 1979; cf. Butterfield 1990), neither should Caron *et al.*'s (2006) suggestion that *Odontogriphus* is a soft-bodied mollusc be discounted on preservational grounds alone (cf. Butterfield 2006).

The organic preservation of labile anatomy requires decay suppression within weeks of death (Briggs 2003) and cannot easily be accommodated in any existing model of Burgess Shale preservation. I show that authigenic clays formed too late to stabilise labile tissues and bring about their exceptional preservation (cf. Orr *et al.* 1998).

Other models for organic preservation in the Burgess Shale are based on the preservation of recalcitrant anatomy alone, and may not explain the preservation of labile anatomy as kerogens (e.g. Butterfield 1995; Petrovich 2001). Meanwhile, it is uncertain whether taphonomic models based on so-called BST deposits (e.g. Gaines *et al.* 2005) are applicable to Burgess Shale itself, given this reassessment of BST preservation: Butterfield (1995) listed a series of localities that he considered to display BST preservation yet his definition of BST preservation would include any locality where graptolites or any other organic compression fossils occur, and it is unclear whether the taphonomic mode of any of these so called BST localities is actually the same as that of the Burgess Shale. As such, the Burgess Shale itself should be re-examined to establish what factors in earliest diagenesis could have been responsible for decay suppression and the organic preservation of labile anatomy (cf. Caron & Jackson 2006).

5.5 Conclusions

Burgess Shale-type preservation is best considered as representing the abundant preservation of both recalcitrant and labile anatomy in taxonomically diverse organic compression fossils within marine shales. Though anatomically-specific phyllosilicates may occur on the fossils of the Burgess Shale, these formed too late in diagenesis to be responsible for organic preservation. This work also shows that carbonaceous fossils can behave as chemically distinct entities over geologically long time scales, rather than undergoing conversion to homogenous, stable kerogens in earliest diagenesis. Meanwhile, the preservation of recalcitrant organic matter such as cuticle in black shales is a geologically normal phenomenon, and if animals capable of secreting cuticle had evolved in the Ediacaran, they should occur in black shales of that age.

6. In which the work is concluded

This thesis views graptolitic mudrocks in an Earth system context, providing some new insights into ancient climate, very low-grade metamorphism and the preservation of organic carbon. Chapters 2 & 3 deal with the palaeoclimatic and palaeoecological aspects of graptolitic mudrocks, examining the oceanographic conditions associated with their deposition and the fauna that is preserved within them. Chapters 4 & 5 employ multifaunal assemblages (such as those discussed in Chapter 3) to establish the taphonomic history of graptolitic mudrocks, focussing mainly on their very low-grade metamorphism, before using this to reassess Burgess Shale-type preservation.

Chapter 2 shows that the Early Palaeozoic contained a 40 million year interval of extensive glaciations during the Early Palaeozoic Icehouse (EPI). Previous workers had emphasised that this interval was dominated by greenhouse conditions and a warm climate (Gibbs *et al.* 2000; Montañez 2002; Church & Coe 2003), interrupted only by one short-lived glacial event in the Hirnantian (e.g. Brenchley *et al.* 1994, 2003; Sutcliffe *et al.* 2001). The Hirnantian glaciation has been generally considered responsible for the end-Ordovician mass extinction, based in part on the view that the transition from stable greenhouse to icehouse and back was extremely rapid (e.g. Brenchley *et al.* 1994; Chen *et al.* 2005). Though the Hirnantian glaciation does indeed correspond to a major faunal turnover (Sheehan 2001; Brenchley *et al.* 2003; Chen *et al.* 2005), the recognition of a further six glacial events in the EPI (Table 2.1) raises questions about the primacy of glaciation in causing the end-Ordovician mass extinction, suggesting that other factors may have also been significant in a longer crisis.

During the EPI, the widespread, seemingly global deposition of graptolite mudrocks corresponds to each episode of glacial amelioration (Fig. 2.3). Deglacial warming was most likely triggered by increased atmospheric CO₂ (e.g. Shackleton 2000; Zachos *et al.* 2001;

Kump 2002; Siegenthaler *et al.* 2005; Royer 2006), with burial of organic carbon in deglacial anoxic mudrocks then acting as a negative feedback mechanism, drawing down atmospheric CO₂, and possibly preventing runaway warming (Fig. 2.6). Thus, the deposition of graptolite mudrocks was fundamentally related to climate modulation, although the pattern observed here differs markedly from that predicted by the 'P/S events' model of Early Palaeozoic climate (cf. Aldridge *et al.* 1993; Jeppsson *et al.* 1995). However, both that model and my data agree that graptolitic mudrocks and marine anoxia were related to increased stratification of the water column during warmer intervals.

This view of graptolitic mudrocks contrasts markedly with many established views of the graptoloid palaeoecology. Finney & Berry (1997, p. 919) proposed that "the depositional setting of typical graptolitic shale was the area of the sea floor under continental-margin upwelling zones where graptolites flourished and within the oxygen-minimum zone where their rhabdosomes were preserved" (Fig. 1.1b). However, Section 2.3.1 establishes that, though upwelling may account for short-lived, localised deposition of anoxic mudrocks, it is a far from adequate explanation for the widespread, synchronous deposition of widespread graptolitic mudrocks. In fact, the premise that graptoloids flourished in areas of high primary production (Finney & Berry 1997) seems somewhat uncertain given the relative scarcity of graptoloids in the organic-rich Silurian "hot shales" on northern Gondwanan margin. These have a characteristically high organic content, which has been interpreted as the result of high primary productivity (cf. Lüning *et al.* 2000) but lack a diverse graptoloid fauna (e.g. Underwood *et al.* 1997; Lüning *et al.* 2000; Armstrong *et al.* 2005). Instead, the deposition of graptolitic mudrocks is best considered to relate to changes in marine redox conditions which relate to ocean stratification and deep-water circulation (e.g. Fig 2.6; Section 2.7) rather than them representing the graptolite biotope *per se*.

Comparison of graptoloid diversity records (e.g. Underwood 1998) with redox stratigraphy during the EPI (Fig. 5.1) suggests that there

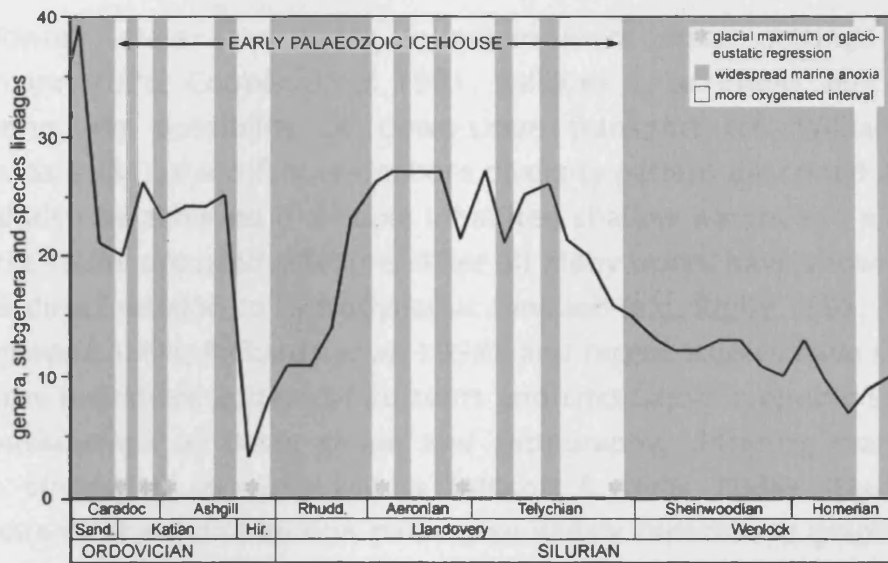


Fig 5.1 Comparison of graptolite diversity (after Underwood 1997) with anoxic intervals from the Caradoc–Wenlock (see Ch 2).

was, to a first approximation, no strong link between graptolite diversity and widespread intervals of marine anoxia (see also Leggett *et al.* 1981). For example, graptolite diversity was relatively low in the earliest Rhuddannian and early Sheinwoodian, but relatively high in the early Caradoc, all of which were intervals characterised by widespread anoxia; however, graptolite diversity is relatively high throughout the mid Aeronian, in deep-water settings the sea floors were predominantly well-oxygenated with only brief “windows” of localised anoxia (Chapter 2; Loydell 1998; Zalasiewicz 2001). This apparent decoupling of marine redox conditions and graptoloid diversity suggests there is little evidence to support the notion that graptolites generally inhabited oxygen-poor waters (cf. Fig. 1.1a).

Though some models of graptolite depth zonation propose that certain graptolites thrived in oxygen-poor mid-waters of several kilometres depth (e.g. Berry *et al.* 1987; Cooper *et al.* 1991; Chen *et al.* 2005; Finney *et al.* 2007), there is no definite evidence in support of depth zonation in graptolites. Many studies report that some taxa are preserved in both proximal and distal settings whilst others only occur in more distal settings as part of a more diverse graptoloid fauna; this has generally been interpreted to mean that ubiquitous taxa lived in

shallower waters than those found in more distal settings (e.g. Erdtmann 1976; Cooper *et al.* 1991; Williams *et al.* 2004). But, even ignoring the possibility of down-slope transport (cf. Williams & Rickards 1984), the offshore-onshore diversity pattern described above could also be achieved if all taxa inhabited shallow waters and a more diverse fauna occurred offshore. After all many works have shown that bears direct relation to hydrodynamic function (e.g. Rigby 1991, 1992; Underwood 1993; Rickards *et al.* 1998), and recent studies have shown that the nearshore pattern of currents and circulation in epeiric seas is a consequence of basin shape and topography, differing markedly from circulation in open waters (Allison & Wells 2006). Thus the onshore-offshore distribution pattern so widely reported in graptolites (e.g. Cooper *et al.* 1991; Finney & Berry 1997; Williams *et al.* 2004; Chen *et al.* 2005) might just represent a variation between forms adapted to dwell in nearshore as opposed to offshore hydrodynamic regimes with others able to occupy either environment.

Viewing graptolites as predominantly epiplanktonic provides a better explanation of widely reported observation that their diversity is greatest at lower latitudes and warmer temperatures (e.g. Skevington 1970; Rickards 1975; Cooper *et al.* 1991, 2004; Underwood 1997; Zalasiewicz 2001). Their extant relatives the pterobranch hemichordates are not found in waters below 12°C (Barnes *et al.* 2003) and thrive in tropical environments (Rigby & Dilly 1993), being of reduced size in cooler waters (Rigby & Sudbury 1995). No such size change is seen between the supposed shallow and deep-water graptolites, nor is it easy to reconcile why a predominantly deep-water habitat would produce the pronounced meridional diversity gradient reported in Cooper *et al.* (1991). The physics of thermohaline circulation require the deep marine environment to be of a much more homogenous nature than shallow waters, which show greater variability in their circulation and temperature structure (Broecker 1982; van Andel 1994). As such it seems more likely that the changes in graptolite faunal composition and diversity between latitudes relate to meridional changes in surface waters as is seen in the modern zooplankton, which achieve their peak diversity in the mixed layer (Van Andel 1994; Armstrong & Brasier 2005) and are of lower diversity and

more cosmopolitan in deeper waters. Thus, like pterobranchs, the greater abundance of graptolites in tropical environments may represent their preference for warm tropical waters rather than cold deep waters.

This view of graptolites as predominantly mixed layer dwellers is certainly consistent with the preservation of graptolites in facies displaying hummocky cross stratification (Floyd & Williams 2001) which reflects their preservation in rocks that were deposited under oxic conditions above the storm wave base (e.g. Ito *et al.* 2001). Instead, that the majority of the graptolite fossil record occurs in anoxic or dysoxic mudrocks (Chapman 1991; Underwood 1992) may be more an artefact of their taphonomy than their palaeoecology, especially as anoxia is a general prerequisite for the preservation of organic-walled fossils (Allison 1988a, b; Butterfield 1990; Orr *et al.* 2003). This then sees graptoloids as a mixed layer zooplankton whose diversity and abundance was roughly independent of the deep water anoxic environment in which they were abundantly preserved (Fig. 1.1c).

As well as contributing to the workings of the Early Palaeozoic carbon cycle, the preservation of organic matter in graptolitic mudrocks contributed to a major interval of oil source rock deposition (Berner 2003), including the “hot shales” mentioned above (e.g. Lüning *et al.* 2000). However, the generation of economic hydrocarbon reserves is also dependent on the maturation of such organic matter as well as the subsequent migration and accumulation of the volatiles released at this time (Hunt 1996; Seewald 2003). Chapter 4 demonstrates that phyllosilicate formation on organic-walled fossils was catalysed by their maturation, which may have some significance for understanding how porosity and permeability changes may affect hydrocarbon migration (cf. Freed & Peacor 1989; Hunt 1996). It also shows that rather than acting as inert bodies during very-low grade metamorphism, organic-walled fossils can act as key sites for mineral authigenesis long after their decay avoidance and fossilisation in early diagenesis.

This model of how late-stage phyllosilicate formation may occur on organic-walled fossils has been used to reassess the taphonomy of the Burgess Shale (Chapter 5), showing that the formation of phyllosilicate films on these fossils cannot account for their decay avoidance and exceptional preservation (cf. Orr *et al.* 1998). Instead, these phyllosilicate films formed relatively late in the fossil's taphonomic history, with different minerals forming on different anatomical types due to differences in their organic preservation. These observations are key to understanding the exceptional preservation of these soft-bodied animals. Rather than concentrating on the preservation of cuticular anatomy (e.g. Butterfield 1990, 1997, 2003), which is a relatively normal phenomenon (Section 5.5), any taphonomic model for Burgess Shale-type preservation must explain the organic preservation of both labile and recalcitrant anatomy. This may in principle be achieved by making detailed observations on Burgess Shale fossils to establish what factors in their earliest diagenesis may have been responsible for such preservation. For example, the *Marrella* dark stain is a diffuse organic compression that is generally held to represent the preservation of decaying fluids that leaked from the animal's carcass (Orr *et al.* 1998). If these leaked from the animal at the sediment-water interface or in an uncompacted sediment, they would have likely dispersed (Whittington 1980), and if decay had continued after compaction, it would not be found preserved as a compression spread across a lamina as a Rorschach-like blob (Fig. 5.1a). With this in mind, rapid compaction of the quickly accumulated post-slide sediment (cf. Allison & Brett 1995; Gabbot *et al.* 2007) may have inhibited degradation by reducing porosity (Rothman & Forney 2007), and limiting microbial activity through dehydration, a process commonly used to preserve labile tissues in the food industry (Thorne 1986; Lawrie 1996), as well as facilitating decay-inhibiting clay-organic interactions that may have been involved in the preservation of recalcitrant anatomy (Butterfield 1990, 1997; Petrovich 2001).

The Early Palaeozoic represents a non-actualistic interval in Earth history, during which the biosphere and carbon cycle were markedly different from those that existed before and since (Section 2.1); as such, it needs to be considered in their own terms. Nonetheless, it had

a history of events which occurred in a causal order according to physical laws and this in principle may be inferred from its geological record. By the creation of a series of well-constrained stratigraphic and taphonomic histories through comparison and correlation between different facies and settings, this thesis has made reasonable inferences to further our knowledge of the workings of both this non-actualistic Earth system, as well as of the late-stage diagenetic processes that cannot easily be observed *in situ* or in the lab. It has expanded the paradigm in which graptolitic mudrocks may be viewed, using detailed observations based on well-documented regional studies to address whole Earth questions. And, in furthering our understanding of organic preservation, it has in turn furthered our knowledge of the fossil record and global environment in the time that saw the origin and diversification of a complex animal fauna and the early development of a significant terrestrial ecosystem.

List of references

- Abed, A.M., Makhlof, I.M., Amireh, B.S. & Khalil, B. 1993. Upper Ordovician glacial deposits in southern Jordan. *Episodes*, **16**, 316–328.
- Adrain, J.M., Edgecombe, G.D., Fortey, R.A., Hammer, Ø., Laurie, J.R., McCormick, T., Owen, A.W., Waisfeld, B.G., Webby, B.D., Westrop, S.R. & Zhou Z.-y. 2004. Trilobites. *In*: Webby, B.D., Paris, F., Droser, M.L., & Percival, I.G. (eds) *The Great Ordovician Biodiversification Event*. Columbia University Press, New York, New York, 231–254.
- Adoutte, A., Balavoine, G., Lartillot, N., & de Rosa, R., 1999. Animal evolution: the end of the intermediate taxa? *Trends in Genetics*, **15**, 104–108.
- Ainsaar, L., Meidla, T. & Martma, T. 1999. Evidence for a widespread carbon isotopic event associated with late Middle Ordovician sedimentological and faunal changes in Estonia. *Geological Magazine*, **136**, 49–62.
- Aldridge, R.J., Jeppsson, L. & Dorning, K. J. 1993. Early Silurian oceanic episodes and events. *Journal of the Geological Society, London*, **150**, 501–513.
- Aldridge, R.J. & Purnell, M. A., 2005. A new *Jamoytius*-like vertebrate from the Late Ordovician of South Africa and the interpretation of characters in the 'naked agnathans'. *PaleoBios*, **25** (supplement to 2), 12.
- Alexander, M. 1965. Biodegradation: problems of molecular recalcitrance and microbial fallibility. *Advances in Applied Microbiology*, **7**, 35–80.
- Alexander, M. 1973. Nonbiodegradable and other recalcitrant molecules. *Biotechnology and Bioengineering*, **15**, 611–647.
- Allison, P.A. 1988a. *Konservat-Lagerstätten*: cause and classification. *Palaeobiology*, **14**, 331–344.
- Allison, P.A. 1988b. The role of anoxia in the decay and mineralisation of proteinaceous macro-fossils. *Palaeobiology*, **14**, 139–154.
- Allison, P.A. 1988c. Taphonomy of the Eocene London Clay biota. *Palaeontology*, **31**, 1079–1100.
- Allison, P.A. & Brett, C.E. 1995. *In situ* benthos and paleo-oxygenation in the Middle Cambrian Burgess Shale, British Columbia, Canada. *Geology*, **23**, 1079–1082.

- Allison, P.A. & Briggs, D.E.G. 1991. *Taphonomy: releasing the data locked in the fossil record*. Plenum Press.
- Allison, P.A. & Wells, M.R. 2006. Circulation in large ancient epicontinental seas: What was different and why?, *Palaios*, 21, 513–515.
- Ansara, J.M., Schweitzer, M.H., Freimark, L.M., Phillips, M. & Cantley, L.C., 2007. Protein sequences from Mastodon and *Tyrannosaurus rex* revealed by mass spectrometry. *Science*, 316, 280–285.
- Aoudeh, S.M. & Al-Hajri, S.A. 1995. Regional distribution and chronostratigraphy of the Qusaiba Member of the Qalibah Formation in the Nafud Basin, northwestern Saudi Arabia. *In: Al-Husseini, M.I. (ed.), Geo '94, The Middle East Petroleum Geosciences, vol. 1*. Gulf PetroLink, Bahrain, 143–154.
- Apollonov, M.K. 2000. Geodynamic evolution of Kazakhstan in the Early Palaeozoic (from classic plate tectonic positions). *In: Bespaev, H.A. (ed.), Geodynamics and minerageny of Kazakhstan*. VAC Publishing House, Almaty, 46–63. [In Russian].
- Árkai, P. Sassi, F.P. & Desmons, J. 1999. Very low- to low-grade metamorphic rocks. *Recommendations by the IUGS Subcommittee on the Systematics of Metamorphic Rocks*. http://www.bgs.ac.uk/SCMR/docs/papers/paper_5.pdf.
- Armstrong, H.A. 2007. On the cause of the Ordovician glaciation. *In: Williams, M., Haywood, A.M., Gregory, F.J., & Schmidt, D. N. (eds) Deep-Time perspectives on Climate Change: Marrying the signal from Computer Models and Biological Proxies*. The Micropalaeontological Society, Special Publications. The Geological Society, London, 101–121.
- Armstrong, H.A. & Brasier, M.D. 2005. *Microfossils* (2nd ed). Blackwell, Oxford, 296 pp.
- Armstrong, H.A. & Coe, A.L., 1997. Deep sea sediments record the geophysiology of the end Ordovician glaciation. *Journal of the Geological Society, London*, 154, 929–934.
- Armstrong, H. A., Turner, B. R., Makhlof, I. M., Weedon, G. P., Williams, M., Al Smadi, A. & Abu Salah, A. 2005. Origin, sequence stratigraphy and depositional environment of an Upper Ordovician (Hirnantian) deglacial black shale, Jordan. *Palaeogeography, Palaeoclimatology, Palaeoecology*, 220, 273–289.
- Armstrong, H. A., Turner, B. R., Makhlof, I. M., Weedon, G. P., Williams, M., Al Smadi, A. & Abu Salah, A. 2006. Reply to “Origin, sequence stratigraphy and depositional environment of an upper Ordovician (Hirnantian) deglacial black shale, Jordan”. *Palaeogeography, Palaeoclimatology, Palaeoecology*, 230, 356–360.

- Armstrong, T.R., Tracy, R.J. & Hames, W.E. 1992. Contrasting styles of Taconian, Eastern Acadian and Western Acadian metamorphism, central and western New England. *Journal of Metamorphic Geology*, **10**, 415–426.
- Arrhenius, S. 1896. On the influence of carbonic acid in the air upon the temperature on the ground. *Philosophical Magazine and Journal of Science*, **41**, 237–275.
- Astini, R.A. 1999. The Late Ordovician glaciation in the Proto–Andean margin of Gondwana revisited: geodynamic implications. *Acta Universitatis Carolinae, Geologica*, **43**, 171–173.
- Aufderheide, A.C. 2003. *The scientific study of mummies*. Cambridge University Press, Cambridge, 625 pp.
- Azmy, K., Veizer, J., Bassett, M. G., & Copper, P., 1998. Oxygen and carbon isotopic composition of Silurian brachiopods: Implications for coeval seawater and glaciations. *Geological Society of America Bulletin*, **110**, 1499–1512.
- Baas, M., Briggs, D.E.G., Van Heemst, J.D.H., Kear, A.J. & De Leeuw, J.W. 1995. Selective preservation of chitin during the decay of shrimp. *Geochimica et Cosmochimica Acta*, **59**, 945–951.
- Baker, S. J. 1981. The graptolite biostratigraphy of a Llandovery outlier near Llanystumdwy, Gwynedd, North Wales. *Geological Magazine*, **118**, 355–365.
- Balthasar, U. 2004. Shell structure, ontogeny and affinities of the Lower Cambrian bivalved problematic fossil *Mickwitzia muralensis* Walcott, 1913. *Lethaia*, **37**, 381–400.
- Barker, S., Higgins, J.A. & Elderfield, H. 2003. The future of the carbon cycle: review, calcification response, ballast and feedback on atmospheric CO₂. *Philosophical Transactions of the Royal Society of London*, **A361**, 1977–1999.
- Barnes, C.R. & Bolton, T.E. 1998 The Ordovician–Silurian boundary on Manitoulin Island, Ontario, Canada. *Bulletin of the British Museum, Natural History, Geology*, **43**, 247–253.
- Barnes, R.S.K., Calow, P.P., Olive, P.J.W., Golding, D.W. & Spicer, J.I. 2003. *The invertebrates*. Blackwell, Oxford, 496 pp.
- Baskin, D.K. 1997. Atomic H/C ratio of kerogen as an estimate of thermal maturity and organic matter conversion. *AAPG Bulletin*, **81**, 1437–1450
- Bates, D.E. 1987. The density of graptoloid skeletal tissue, and its implication for the volume and density of the soft tissue. *Lethaia*, **20**, 149–156.

- Bates, D.E., & Loydell, D.K. 2000. Parasitism on graptolites. *Palaeontology*, **43**, 1143–1151.
- Baženov, M.L., Collins A.Q., Degtârev, K.E, Levašova, N.M., Mikolaičuk, A.V., Pavlov, V.E. & Van der Voo, R. 2003. Paleozoic northward drift of the North Tien Shan (Central Asia) as revealed by Ordovician and Carboniferous paleomagnetism. *Tectonophysics*, **366**,113–141.
- Belek, V. & de Koranyi, A. 1990. Diagnostics of structural alteration in coal: porosity, changes with pyrolysis temperature. *Fuels*, **69**, 1502–1506.
- Bengtson, P. 1988. Open nomenclature. *Palaeontology*, **31**, 223–227.
- Benton, M.J. & Trewin, N.H. 1978. Catalogue of the type and figured material in the Palaeontology Collection, University of Aberdeen, with notes on the H.A. Nicholson collection. *Publications of the Department of Geology and Mineralogy, University of Aberdeen*, **2**, 28 pp.
- Benton, M.J. 1979. H.A. Nicholson (1844–1899), invertebrate palaeontologist: bibliography and catalogue of his type and figured material. *Royal Scottish Museum information series, Geology*, **7**, 96 pp..
- Berner, R.A. 1991. A model for atmospheric CO₂ over Phanerozoic time. *American Journal of Science*, **291**, 339–376.
- Berner, R.A. 1994. GEOCARB II: A revised model of atmospheric CO₂ over Phanerozoic time. *American Journal of Science*, **294**, 56–91.
- Berner, R.A. 1998. The carbon cycle and CO₂ over Phanerozoic time: the role of land plants. *Philosophical Transactions of the Royal Society, series B*, **353**, 75–82.
- Berner, R.A. 2001. Modelling atmospheric O₂ over Phanerozoic time. *Geochimica et Cosmochimica Acta*, **65**, 685–694.
- Berner, R.A. 2003. The long-term carbon cycle, fossil fuels and atmospheric composition. *Nature*, **426**, 323–326.
- Berner, R.A. 2006. GEOCARBSULF: A combined model for Phanerozoic atmospheric O₂ and CO₂ over Phanerozoic time. *Geochimica et Cosmochimica Acta*, **70**, 5653–5664.
- Berner, R.A. & Canfield, D.E. 1989. A new model for atmospheric oxygen over Phanerozoic time. *American Journal of Science*, **289**, 333–361.
- Berner, R.A. & Kothavala, Z. 2001. Geocarb III: A revised model of atmospheric CO₂ over Phanerozoic time. *American Journal of Science*, **301**, 182–204.

- Berner, R.A. & Raiswell, R. 1983. Burial of organic carbon and pyrite sulfur in sediments over Phanerozoic time: a new theory. *Geochimica et Cosmochimica Acta*, **47**, 855–862.
- Berner, R.A., Lasaga, A.C. & Garrels, R.M. 1983. The carbonate–silicate geochemical cycle and its effect on atmospheric Carbon Dioxide over the past 100 million years. *American Journal of Science*, **283**, 641–683.
- Berry, W.B.N., Wilde, P. & Quinby–Hunt, M.S. 1987. The oceanic non–sulfidic oxygen minimum zone; a habitat for graptolites? *Bulletin of the Geological Society of Denmark (Meddelelser fra Dansk Geologisk Forening)*, **35**, 103–114.
- Beuf, S., Biju–Duval, B., de Charpal, O., Rognon, P., Gariel, O. & Bennacef, A. 1971. *Les grès du Paléozoïque inférieur au Sahara (Sédimentation et discontinuités, evolution structurale d'un craton)*. Publication de l'Institut Français Pétrole, **18**, 464 pp.
- Beyermann, K., & Hasenmaier, D., 1973. Identifizierung 180 Millionen Jahre alten, wahrscheinlich unverändert erhaltenen melanins. *Fresenius' Journal of Analytical Chemistry*, **266**, 202–205.
- Bickert, T., Pätzold, J., Samtleben, C. & Munnecke, A. 1997. Paleoenvironmental changes in the Silurian indicated by stable isotopes in brachiopod shells from Gotland, Sweden. *Geochimica et Cosmochimica Acta*, **61**, 2717–2730.
- Bigarella, J.J., 1970. Continental drift and palaeocurrent analysis. *Second Gondwana symposium, Proceedings and Papers*. Council for Scientific and Industrial Research, Pretoria, South Africa, 73–97.
- Biju–Duval, B., Deynoux, M. & Rognon, P. 1974. Essai d'interprétation de “fractures en gradins” observées dans les formations glaciaires Précambriennes et Ordoviciennes du Sahara. *Revue de Géographie Physique et de Géologie Dynamique*, **26**, 503–512.
- Biju–Dival, B., Deynoux, M. & Rognon, P. 1981. Late Ordovician tillites of the Central Sahara. In: Hambrey, M.J., & Harland, W.B. (eds). *Earth's pre–Pleistocene glacial record*. Cambridge University Press, Cambridge, 99–107.
- Bjerreskov, M. 1975. Llandoveryan and Wenlockian graptolites from Bornholm. *Fossils and Strata*, **8**, 1–94.
- Bjerreskov, M. 1991. Pyrite in Silurian graptolites from Bornholm, Denmark. *Lethaia*, **24**, 351–361.

- Blackett, E.J., Page, A.A., Zalasiewicz, J.A., Williams, M., Rickards, R.B. & Davies, J.R. 2008. A refined graptolite biostratigraphy for the late Ordovician–early Silurian of central Wales. *Lethaia*, **41**, in press.
- Boles, J.R., & Franks, S.G. 1979. Clay diagenesis in Wilcox Sandstones of southwest Texas: implications of smectite diagenesis on sandstone cementation. *Journal of Sedimentary Petrology*, **49**, 55–70.
- Botting, J.P. 2001. The relationship between pyroclastic volcanism and Ordovician diversification. *In*: Crame, J.A. & Owen, A.W. (eds). *Palaeobiogeography and biodiversity change*. Geological Society Special Publication, **194**, 99–113.
- Bottjer, D.J., Droser, M.L., Sheehan, P.M. & McGhee Jr., G.R. 2001. The ecological architecture of major events in the Phanerozoic history of marine invertebrate life. *In*: Allmon, W.D. & Bottjer, D.J. (eds). *Evolutionary palaeoecology*. Columbia University Press, New York, 35–61.
- Boucot, A.J. Rong, J.–Y., Chen, X. & Scotese, C.R. 2003. Pre–Hirnantian Ashgill climatically warm event in the Mediterranean region. *Lethaia*, **36**, 119–132.
- Boulter, E., 2003. A new enteropneust–like hemichordate from the Middle Cambrian Burgess Shale. *Palaeontological Association Newsletter*, **54**, 120.
- Brenchley, P.J. 1988. Environmental changes close to the Ordovician–Silurian boundary. *Bulletin of the British Museum of Natural History (Geology)*, **43**, 377–385.
- Brenchley, P.J. & Štorch, P. 1989. Environmental changes in the Hirnantian (upper Ordovician) of the Prague Basin, Czechoslovakia. *Geological Journal*, **24**, 165–181.
- Brenchley, P.J., Marshall, J.D., Carden, G.A.F., Robertson, D.B.R., Long, D.G.F., Meidla, T., Hints, L. & Anderson, T.F. 1994. Bathymetric and isotopic evidence for a short-lived Late Ordovician glaciation in a greenhouse period. *Geology*, **22**, 295–298.
- Brenchley, P.J., Carden, G.A., Hints, L., Kaljo, D., Marshall, J.D., Martma, T., Meidla, T. & Nölvak, J. 2003. High–resolution isotope stratigraphy of Late Ordovician sequences: constraints on the timing of bio–events and environmental changes associated with mass extinction and glaciation. *Geological Society of America, Bulletin*, **115**, 89–104.
- Briggs, D.E.G., 1999. Molecular taphonomy of animal and plant cuticles: selective preservation and diagenesis. *Philosophical Transactions of the Royal Society of London*, **B354**, 7–16.
- Briggs, D.E.G., 2003. The role of decay and mineralization in the preservation of soft-bodied fossils. *Annual Review of Earth and Planetary Sciences*, **31**, 275–

- 301 Briggs D.E.G., & Kear A.J. 1993. Decay and preservation of polychaetes: taphonomic thresholds in soft-bodied organisms. *Paleobiology*, **19**, 107–135.
- Briggs, D.E.B. & Williams, S.H. 1981. The restoration of fossil graptolites. *Lethaia*, **14**, 157–164.
- Briggs, D.E.G., Erwin, D.H., & Collier, F.J., 1994. *The Fossils of the Burgess Shale*. Smithsonian Institution Press, Washington & London, 238 pp.
- Briggs, D.E.G., Kear, A.J., Baas, M., De Leeuw, J.W. & Rigby, S. 1995. Decay and composition of the hemichordate Rhabdopleura: implications for the taphonomy of graptolites. *Lethaia*, **28**, 15–23.
- Brodersen, K.P., & Bennike, O., 2003. Interglacial Chironomidae (Diptera) from Thule, Northwest Greenland: matching modern analogues to fossil assemblages. *Boreas*, **32**, 560–565.
- Broecker, W.S. 1982. Glacial to interglacial changes in ocean chemistry. *Progress in Oceanography*, **11**, 151–197.
- Bruckschen, P., Oesmann, S. & Veizer, J. 1999. Isotope stratigraphy of the European Carboniferous: proxy signals for ocean chemistry, climate and tectonics. *Chemical Geology*, **161**, 127–163.
- Bruton, D.L., Erdtmann, B.-D. & Koch, L. 1982. The Nærnes section, Oslo Region, Norway: a candidate for the Cambrian–Ordovician boundary stratotype at the base of the Tremadoc Series. *In*: Bassett, M.G. & Dean, W.T. (eds) *The Cambrian – Ordovician boundary: sections, fossil distributions, and correlations*. National Museum of Wales, Geological Series, **3**, 61–69.
- Brunton, F.R., Smith, L., Dixon, O.A., Copper, P., Nestor, H. & Kershaw, S. 1998. Silurian reef episodes, changing seascapes, and paleobiogeography. *In*: Landing, E. & Johnson, M. E. (eds). *Silurian cycles, linkages of dynamic stratigraphy with atmospheric, oceanic, and tectonic changes*. New York State Museum Bulletin, **491**, 265–282.
- Budd, G.E. & Jensen, S. 2000. A critical reappraisal of the fossil record of the bilaterian phyla. *Biological Reviews*, **75**, 253–295.
- Büggish, W. & Astini, R. 1993. The Late Ordovician ice age: new evidence from the Argentine Precordillera. *In*: Findlay, R.H., Unrug, R., Banks, M.R. & Veevers, J.J. (eds). *Gondwana Eight – Assembly, Evolution and Dispersal*. Balkema, Rotterdam, 439–447.
- Bulman, O.M.B. 1964. Lower Palaeozoic plankton. *Quarterly Journal of the Geological Society of London*, **120**, 455–476.

- Bulman, O.M.B. 1970. Graptolithina, with sections on Enteropneusta and Pterobranchia. In Teichert, C. (ed.) *Treatise on Invertebrate Palaeontology, Part V*. Boulder, Colorado & Lawrence, Kansas: Geological Society of America & University of Kansas Press, 101 pp.
- Bulman, O.M.B. & Rickards, R.B. 1966. A revision of Wiman's dendroid and tuboid graptolites. *Bulletin of the Geological Institution of the University of Uppsala*, **43**, 1–73.
- Bustin, R.M., Link, C., & Goodarzi, F, 1989. Optical properties and chemistry of graptolite periderm following laboratory simulated maturation. *Organic Geochemistry*, **14**, 355–364.
- Butterfield, N.J. 1990. Organic preservation of non-mineralizing organisms and the taphonomy of the Burgess Shale. *Paleobiology*, **16**, 272–286.
- Butterfield, N.J. 1995. Secular distribution of Burgess–Shale–type preservation. *Lethaia*, **28**, 1–13.
- Butterfield, N.J., 1996. Fossil preservation in the Burgess Shale: reply. *Lethaia*, **29**, 109–112.
- Butterfield, N.J. 1997. Plankton ecology and the Proterozoic–Phanerozoic transition. *Paleobiology*, **23**, 247–262.
- Butterfield, N.J. 2001. Cambrian food webs. In: Briggs, D.E.G. & Crowther, P.R. (eds). *Palaeobiology II*. Blackwell Science. Oxford, 40–43.
- Butterfield, N.J., 2002. *Leandroilia* guts and the interpretation of three-dimensional structures in Burgess Shale–type fossils. *Paleobiology*, **28**, 155–171.
- Butterfield, N.J. 2003. Exceptional fossil preservation and the Cambrian explosion. *Integrative and Comparative Biology*, **43**, 166–177.
- Butterfield, N.J. 2006. Hooking some stem–group "worms:" fossil lophotrochozoans in the Burgess Shale. *BioEssays*, **28**, 1161–1166.
- Butterfield, N.J., Balthasar, U., & Wilson, L., 2007. Fossil diagenesis in the Burgess Shale. *Palaeontology*, **50**, 537–543.
- Calner, M., & Eriksson, M.E. 2006. Silurian research at the crossroads. *GFF*, **128**, 73–74.
- Calner, M., Jeppsson, L., & Munnecke, A. 2004. The Silurian of Gotland – Part I: Review of the stratigraphic framework, event stratigraphy, and stable carbon and oxygen isotope development. *Erlanger geologische Abhandlungen, Sonderband*, **5**,

113–131.

- Came, R.E., Eiler, J.M., Veizer, J., Azmy, K., Brand, U. & Weidman, C.R. 2007. Coupling of surface temperatures and atmospheric CO₂ concentrations during the Palaeozoic era. *Nature*, **449**, 198–201.
- Cameron, C.B. 2005. A phylogeny of the hemichordates based on morphological characters. *Canadian Journal of Zoology*, **83**, 196–215.
- Caputo, M. V. 1998. Ordovician–Silurian glaciations and global sea–level changes. *In*: Landing, E. & Johnson, M. E. (eds). *Silurian cycles, linkages of dynamic stratigraphy with atmospheric, oceanic, and tectonic changes*. New York State Museum Bulletin, **491**, 15–25.
- Caputo, M.V. & Crowell, J.C. 1985. Migration of glacial centers across Gondwana during Paleozoic Era. *Geological Society of America, Bulletin*, **96**, 1020–1036.
- Caputo, M.V. & Lima, E.C. 1984. Estratigrafia, idade e correlação do Grupo Serra Grande – Bacia do Parnaíba. *Congresso Brasileiro de Geologia*, **33**, 740–753.
- Caron, J.B., & Jackson, D.A. 2006. Taphonomy of the Greater Phyllopod Bed Community, Burgess Shale. *Palaios*, **21**, 451–465.
- Caron, J.B., Scheltema, A.H., Schander, C. & Rudkin, D. 2006. A soft–bodied mollusc with radula from the Middle Cambrian Burgess Shale. *Nature*, **442**, 159–163.
- Carozzi, A.V., Pamplona, H.R.P., Castro, J.C., Contreiras, C.J.A. 1973. Ambientes deposicionais e evolução tecto–sedimentar da seção elástica paleozóica da Bacia do Médio Amazonas. *Congresso Brasileiro de Geologia*, **27**, 279–314.
- Carpenter, S.J., & Lohmann, K.C., 1995. $\delta^{18}\text{O}$ and $\delta^{13}\text{C}$ values of modern brachiopods. *Geochimica et Cosmochimica Acta*, **59**, 3749–3764.
- Carruthers, W. 1867a. Note on the systematic position of the Graptolites and on their supposed ovarian vesicles. *Geological Magazine*, **4**, 70–72.
- Carruthers, W. 1867b. Graptolites. *Geological Magazine*, **4**, 187.
- Carruthers, W. 1867c. Graptolites. *Geological Magazine*, **4**, 336.
- Carruthers, W. 1868a. A revision of the British Graptolites, with descriptions of the new species, and notes on their affinities. *Geological Magazine*, **5**, 64–74 & 125–133.
- Carruthers, W. 1868b. Classification of Graptolites. *Geological Magazine*, **5**, 199–200.

- Catling, D.C. & Claire, M. 2005. How Earth's atmosphere evolved to an oxic state: A status report. *Earth and Planetary Science Letters*, **237**, 1–20.
- Caton, L.S. 1954. The economic influence of the developments in shipbuilding techniques, 1450 to 1485. *Storia al Giorno d'Oggi*, **1**, 69–96. [in Italian]
- Cave, R. 1979. Sedimentary environments of the basinal Llandovery of mid-Wales. *In*: Harris, A.L., Holland, C.H. & Leake, B.E. (eds). *The Caledonides of the British Isles – reviewed*. Special Publication of the Geological Society, London, **8**, 517–26.
- Cave, R., & Dixon, R.J. 1993. The Ordovician and Silurian of the Welshpool area. *In*: Woodcock, N.H. & Bassett, M.G. (eds) *Geological excursions in Powys, central Wales*. Geological Series – National Museum of Wales, **14**, 51–84
- Chamberlin, T.C. 1899. An attempt to frame a working hypothesis of the cause of glacial periods on an atmospheric basis. *Journal of Geology*, **7**, 545–584.
- Chapman, A.J. 1991. How are they preserved? *In*: Palmer, D., & Rickards, R.B. (eds). *Graptolites: writing in the rocks*. The Boydell Press, Woodbridge, Surrey, 6–11.
- Cherns, L. & Wheeley, J.R. 2007. A pre-Hirnantian (Late Ordovician) interval of global cooling – the Boda Event re-assessed. *Palaeogeography, Palaeoclimatology, Palaeoecology*, **251**, 449–460.
- Chen, X., Rong J., C. E. Mitchell, D. A. T. Harper, Fan Junxuan, Zhan Renbin, Zhang Yuandong, Li Rongyu & Wang Yi. 2000. Late Ordovician to earliest Silurian graptolite and brachiopod biozonation from the Yangtze region, South China, with a global correlation. *Geological Magazine*, **137**, 623–650.
- Chen, X., Melchin, M.J., Sheets, H.D., Mitchell, C.E., & Fan J.-x. 2005. Patterns and Processes of latest Ordovician graptolite extinction and recovery based on data from South China. *Journal of Paleontology*, **79**, 842–861.
- Cherns, L. & Wright, V.P. 2000. Missing molluscs as evidence of large-scale, early skeletal aragonite dissolution in a Silurian sea. *Geology*, **28**, 791–794.
- Church, K.D. & Coe, A.L. 2003. Processes controlling relative sea-level change and sediment supply. *In*: Coe, A.L. (ed.). *The Sedimentary Record of Sea-Level Change*. Cambridge University Press, Cambridge, 99–117.
- Clarkson, E.N.K. 1998. *Invertebrate palaeontology and evolution* (3rd ed). Blackwell, Oxford, 452.
- Clupáč, I. 1970. Phyllocarid crustaceans of the Bohemian Ordovician. *Sborník Geologických věd, řada P*, **12**, 41–75.

- Cocks, L.R.M. & Torsvik, T.H. 2002. Earth geography from 500 to 400 million years ago: A faunal and palaeomagnetic review. *Journal of the Geological Society of London*, **159**, 631–644.
- Cocks, L.R.M., Woodcock, N.H., Rickards, R.B., Temple, J.T. & Lane, P.D. 1984. The Llandovery Series of the type area. *Bulletin of the British Museum (Natural History): Geology*, **38**, 131–182.
- Cohen, A.S., Coe, A.L., Harding, S.M. & Schwark, L. 2004. Osmium isotope evidence for the regulation of atmospheric CO₂ by continental weathering. *Geology*, **32**, 157–160.
- Collins & Gernaey 2001. Proteins. *In*: Briggs, D.E.G. & Crowther, P.R. (eds). *Palaeobiology II*. Blackwell Science, Oxford, 245–247.
- Conway Morris, S. & Whittington, H.B. 1979. The animals of the Burgess Shale. *Scientific American*, **241**, 122–133.
- Conway Morris, S. 1977. Fossil priapulid worms. *Special Papers in Palaeontology*, **20**, 95 pp.
- Conway Morris, S. 1986. The community structure of the Middle Cambrian phyllopod bed (Burgess Shale). *Palaeontology*, **29** 423–467
- Conway Morris, S. 2006. Darwin's dilemma: the realities of the Cambrian 'explosion'. *Philosophical Transactions of the Royal Society of London*, **B361**, 1069–1083.
- Cooper, A., & Fortey, R.A. 1998. Evolutionary explosions and the phylogenetic fuse. *Trends in Ecology and Evolution*, **13**, 151–156.
- Cooper, R.A. 1990. Interpretation of tectonically deformed fossils. *New Zealand Journal of Geology & Geophysics*, **33**, 321–332.
- Cooper, R.A., & Sadler, P.M. 2004. The Ordovician Period. *In*: Gradstein, F.M., Ogg, J.G. & Smith, A.G. (eds) *A Geologic Time Scale 2004*. Cambridge University Press, Cambridge, 165–187.
- Cooper, R.A., Fortey, R.A. & Lindholm, K. 1991. Latitudinal and depth zonation of early Ordovician graptolites. *Lethaia*, **24**, 199–218.
- Cooper, R.A., Maletz, J., Taylor, L., & Zalasiewicz, J. 2004. Graptolites: Patterns of Diversity across Paleolatitudes. *In*: Webby, B.D., Paris, F., Droser, M.L., & Percival, I.G. (eds) *The Great Ordovician Biodiversification Event*. Columbia University Press, New York, 281–293.

- Cope, J.C.W. 2002. Diversification and biogeography of bivalves during the Ordovician Period. *In: Crame, J.A. & Owen, A.W. (eds). Palaeobiography and Biodiversity Change: A comparison of the Ordovician and Mesozoic–Cenozoic radiations.* Geological Society, London, Special Publications, 194, 33–52.
- Cope, J.C.W. 2004. Rostroconch and Bivalve Molluscs. *In: Webby, B.D., Paris, F., Droser, M.L., & Percival, I.G. (eds) The Great Ordovician Biodiversification Event.* Columbia University Press, New York, 196–208.
- Copper, P. 1994. Ancient reef ecosystem expansion and collapse. *Coral Reefs*, 13, 3–11.
- Cramer, B.D. & Saltzman, M.R. 2005. Sequestration of ^{12}C in the deep ocean during the early Wenlock (Silurian) positive carbon isotope excursion. *Palaeogeography, Palaeoclimatology, Palaeoecology*, 219, 333–349
- Cramer, B.D., & Saltzman, M.R. 2007. Fluctuations in epeiric sea carbonate production during Silurian positive carbon isotope excursions: A review of proposed paleoceanographic models: *Palaeogeography, Palaeoclimatology, Palaeoecology*, in press.
- Crowell, J.C., Suárez-Soruco, R. & Rocha-Campos, A.C. 1981. The Silurian Cancañiri (Zapla) Formation of Bolivia, Argentina and Peru. *In: Hambrey, M.J., & Harland, W.B. (eds). Earth's pre-Pleistocene glacial record.* Cambridge University Press, Cambridge, 902–907.
- Crowley, T.J. & Berner, R.A. 2001. CO_2 and climate change. *Science*, 292, 870–872.
- Crowther, P.R. 1978. *Graptolite fine structure and its bearing on mode of life and zoological affinities.* Unpublished PhD thesis, University of Cambridge, 455 pp.
- Crowther, P.R. 1981. The fine structure of graptolite periderm. *Special Papers in Palaeontology*, 26, 119 pp.
- Curry, K.J., Bennett, R.H., Mayer, L.M., Curry, A., Abril, M., Biesiot, P.M. & Hulbert, M.H. 2007. Direct visualization of clay microfabric signatures driving organic matter preservation in fine-grained sediment. *Geochimica et Cosmochimica Acta*, 71, 1709–1720.
- Curtis, C.D. 1985. Clay mineral precipitation and transformation during burial diagenesis. *Philosophical Transactions of the Royal Society of London*, A315, 91–105.
- Darwin, C. 1859. *On the origin of species by means of natural selection.* Penguin Classics, London, 469 pp.

- Davies, J.R. & Waters, R. A. 1995. The Caban Conglomerate and Ystrad Meurig Grits Formation – nested channels and lobe switching on a mud dominated latest Ashgill to Llandovery lobe–apron, Welsh Basin, UK. *In*: Pickering, K.T., Hiscott, R.N., Kenyon, N.H., Ricci Lucchi, F. & Smith, R.D.A. (eds). *Atlas of deep water environments: architectural style in turbidite systems*. Chapman & Hall, London, 182–93.
- Davies, J.R., Fletcher, C.J.N., Waters, R.A. Wilson, D. Woodhall, D.G. & Zalasiewicz, J.A. 1997. *Geology of the country around Llanilar and Rhayader*. Memoir of the British Geological Survey, Sheets 178 and 179 (England and Wales). HMSO.
- Davies, J.R, Waters, R.A., Wilby, P.R., Williams, M. & Wilson, D. 2003. *Geology of Cardigan and Dinas Island district – a brief explanation of the geological map. Sheet explanation of the British Geological survey*. 1:50000 sheet 193 (including part of sheet 210) Cardigan & Dinas Island (England & Wales). British Geological Survey, Keyworth, Nottingham.
- Dawson, J.W. 1868. *Acadian Geology*. Macmillan, London 188 pp.
- Destombes, J., Holland, H., & Willefert, S. 1985. Lower Palaeozoic rocks of Morocco. *In*: Holland, C.H. (ed.). *Lower Palaeozoic of north–western and west–central Africa*. Lower Palaeozoic Rocks of the World, 4. John Wiley & Sons, 91–337.
- Deynoux, M. & Trompette, R. 1981. Late Ordovician tillites of the Taodeni Basin, West Africa. *In*: Hambrey, M.J., & Harland, W.B. (eds). *Earth's pre–Pleistocene glacial record*. Cambridge University Press, Cambridge, 89–96.
- Deynoux, M., Sougy, J., & Trompette, R. 1985. Lower Palaeozoic rocks of west Africa and the western part of central Africa. *In*: Holland, C.H. (ed.). *Lower Palaeozoic of north–western and west–central Africa*. Lower Palaeozoic Rocks of the World. 4, John Wiley & Sons, London, 337–497.
- Diaz–Martinez, E. 2007. The Sacta Limestone Member (early Wenlock): cool–water, temperate carbonate deposition at the distal foreland of Gondwana's active margin, Bolivia. *Palaeogeography, Palaeoclimatology, Palaeoecology*, in press.
- Diaz–Martinez, E., & Grahn, Y. 2007. Early Silurian glaciation along the western margin of Gondwana (Peru, Bolivia, and northern Argentina): Palaeogeographic and geodynamic setting. *Palaeogeography, Palaeoclimatology, Palaeoecology*, in press
- Dilly, P.N. 1973. The larva of *Rhabdopleura compacta* (Hemichordata). *Marine Biology*, 18, 69–86.
- Dilly, P.N. 1993. *Cephalodiscus graptolitoides* sp. nov. a probable extant graptolite. *Journal of Zoology*, 229, 69–78.

- Dilly, P.N. & Ryland, J.S. 1985. An intertidal *Rhabdopleura* (Hemichordata, Pterobranchia) from Fiji. *Journal of Zoology*, **205**, 611–623.
- Doré, F. 1981. The late Ordovician tillite in Normandy (Armorican Massif) *In*: Hambrey, M.J., & Harland, W.B. (eds). *Earth's pre-Pleistocene glacial record*. Cambridge University Press, Cambridge, 582–584.
- Doré, F. & Le Gall, J. 1973. Presence et position stratigraphique de la tillite Ordovicienne dans le Maine (E. du Massif Armoricain). *Bulletin de la Societe Geologique de France*, **15**, 32–33.
- Droser, M.L. & Finnegan, S. 2003. The Ordovician radiation: a follow-up to the Cambrian explosion? *Integrative and Comparative Biology*, **43**, 178–184.
- Dunlop, J.A., Anderson, L.I., Kerp, H. & Hass, H. 2004 for 2003. A harvestman (Arachnida: Opiliones) from the Early Devonian Rhynie cherts, Aberdeenshire, Scotland. *Transactions of the Royal Society of Edinburgh: Earth Sciences*, **94**, 341–354.
- Eastler, T.E. 1969. Silurian geology of the Change Islands and eastern Notre Dame Bay, Newfoundland. *Memoir of the American Association of Petroleum Geologists*, **12**, 425–432.
- Efremov, E. A., 1940. Taphonomy: a new branch of paleontology. *Pan-American Geologist*, **74**, 81–93.
- Elderfield, H. 2002. Climate change: Carbonate mysteries. *Science*, **296**, 1618–1621.
- Elles, G.L. 1940. Graptogonophores. *Geological Magazine*, **77**, 283–288.
- Elles, G.L. & Wood, E.M.R. 1901–1918. *A monograph of British Graptolites*. Palaeontographical Society, London, 539 pp.
- Erdtmann, B.D. 1976. Ecostratigraphy of Ordovician graptoloids. *In* Bassett, M.G. (ed.). *The Ordovician System*. Cardiff, University of Wales Press and National Museum of Wales. Cardiff, 621–643.
- Erdtmann, B.-D. 1982. Palaeobiogeography and environments of planktic dictyonemid graptolites during the earliest Ordovician. *In*: Bassett, M.G. & Dean, W.T. (eds) *The Cambrian – Ordovician boundary: sections, fossil distributions, and correlations*. National Museum of Wales, Geological Series, **3**, 9–27.
- Evans, J.A., Zalasiewicz, J.A., Fletcher, I., Rasmussen, B. & Pearce, N.G. 2002. Dating diagenetic monazite in mudrocks: constraining the oil window? *Journal of the Geological Society, London*, **159**, 619–622.

- Evans, D.A.D. 2003. A fundamental Precambrian–Phanerozoic shift in earth's glacial style? *Tectonophysics*, **375**, 353–385.
- Eyles, N. 1993. Earth's glacial record and its tectonic setting. *Earth Science Reviews*, **35**, 1–248.
- Finney, S.C. & Jacobson, S.R., 1985. Flotation devices in planktic graptolites. *Lethaia*, **18**, 349–359.
- Finney, S.C. & Berry, W.B.N. 1997. New perspectives on graptolite distributions and their use as indicators of platform margin dynamics. *Geology*, **25**, 919–922.
- Finney, S.C., Berry, W.B.N. & Cooper, J.D. 2007. The influence of denitrifying seawater on graptolite extinction and diversification during the Hirnantian (latest Ordovician) mass extinction event. *Lethaia*, **40**, 281–291.
- Floyd, J.D. & Williams, M. 2003 for 2002. A revised correlation of Silurian rocks in the Girvan district, SW Scotland. *Transactions of the Royal Society of Edinburgh, Earth Sciences*, **25**, 383–392.
- Foree, E.G., & McCarty, P.L. 1970. Anaerobic decomposition of algae. *Environmental Science and Technology*, **4**, 842–849.
- Fortey, R.A. & Cocks, L.R.M. 2003. Palaeontological evidence bearing on global Ordovician–Silurian continental reconstructions. *Earth Science Reviews*, **61**, 245–307.
- Fortey, R.A. & Cocks, L.R.M. 2005. Late Ordovician global warming – The Boda Event. *Geology*, **33**, 405–408.
- Fortey, R.A. & Skevington, D. 1980. Correlation of Cambrian–Ordovician boundary between Europe and North America: new data from western Newfoundland. *Canadian Journal of Earth Sciences*, **17**, 382–388.
- Fortey, R.A., Landing, E. & Skevington, D. 1982. Cambrian–Ordovician boundary sections in the Cow Head Group, western Newfoundland. In: Bassett, M.G. & Dean, W.T. (eds) *The Cambrian – Ordovician boundary: sections, fossil distributions, and correlations*. National Museum of Wales, Geological Series, **3**, 9–27.
- Fortey, R.A., Harper, D.A.T., Ingham, J.K., Owen, A.W. & Rushton, A.W.A. 1995. A revision of Ordovician series and stages from the historical type area. *Geological Magazine*, **132**, 15–30.
- Fortey, R.A., Harper, D.A.T., Ingham, J.K., Owen, A.W., Parkes, M.A., Rushton, A.W.A. & Woodcock, N.H. 2000. A revised correlation of Ordovician rocks in the British Isles. *Geological Society of London Special Report*, **24**, 1–83.

- Frakes, L.A., Francis, J.E., Syktus, J.I., 1992. *Climate Modes of the Phanerozoic*. Cambridge University Press, Cambridge, 286 pp.
- Freed, R.L. & Peacor, D.R. 1989. Geopressured shale and sealing effect of smectite to illite transition. *AAPG Bulletin*, **73**, 1223–1232.
- Frey, R.C. 1989. Palaeoecology of a well-preserved nautiloid assemblage from a Late Ordovician shale unit, western Ohio. *Journal of Paleontology*, **63**, 604–620.
- Frey, R.C. Beresi, M.S., Evans, D.E., King, A.H. & Percival, I.G. 2004. Nautiloid Cephalopods, Molluscs. *In: Webby, B.D., Paris, F., Droser, M.L., & Percival, I.G. (eds) The Great Ordovician Biodiversification Event*. Columbia University Press, New York, 209–214.
- Fryda, J. & Rohr, D.M. 2004. Gastropods. *In: Webby, B.D., Paris, F., Droser, M.L., & Percival, I.G. (eds) The Great Ordovician Biodiversification Event*. Columbia University Press, New York, 184–195.
- Gabbott S.E., 1998, Taphonomy of the Upper Ordovician Soom Shale lagerstatte, South Africa: an example of soft tissue preservation in clay minerals. *Palaeontology*, **41**, 631–667.
- Gabbott, S.E., Zalasiewicz, J.A. & Collins, D.H. 2007. Sedimentation of the Burgess Shale (Mid-Cambrian, British Columbia). *Journal of the Geological Society, London*, in press.
- Gaboury, D. & Daigneault, R. 2000. Flat vein formation in a transitional crustal setting by self-induced fluid pressure equilibrium – an example from the Geant Dormant gold mine, Canada. *Ore Geology Reviews*, **17**, 155–178.
- Gaines, R.R. Kennedy, M.J., & Droser, M.L., 2005. A new hypothesis for Burgess Shale-type preservation in the Middle Cambrian Wheeler Shale, House Range, Utah, *Palaeogeography, Palaeoclimatology, Palaeoecology*, **220**, 193–205.
- Gallego-Torres, D., Martínez-Ruiz, F., Paytan, A., Jiménez-Espejo, F.J., & Ortega-Huertas, M. 2007. Pliocene–Holocene evolution of depositional conditions in the eastern Mediterranean: Role of anoxia vs. productivity at time of sapropel deposition. *Palaeogeography, Palaeoclimatology, Palaeoecology*, **246**, 424–439.
- Gatinskiy, Y.G., Klochko, V.P., Rozman, K.S. & Trofimov, D.M. 1966. Novyye dannyye po stratigrafii paleozoyskikh otlozheniy yuzhnoy Sakhary. *Akadwmii Nauk SSSR, Doklady*, **170**, 1154–1157.
- Geinitz, H. B. 1852. Die Versteinerungen der Grauwackenformation in Sachsen und der angrenzenden Ländern. Abt. 1. Die Graptolithen. Leipzig.

- Gensel, P.G. & Edwards, D. 2001. *Plants invade the land: evolutionary and environmental perspectives*. Columbia University Press, New York.
- Ghienne, J.-F. 2003. Late Ordovician sedimentary environments, glacial cycles, and post-glacial transgression in the Taoudeni Basin, West Africa. *Palaeogeography, Palaeoclimatology, Palaeoecology*, **189**, 117–145.
- Ghienne, J.-F., Boumendjal, K., Paris, F., Videt, B., Racheboeuf, P. & Ait Salem, H. 2007. The Cambrian–Ordovician succession in the Ougarta Range (western Algeria, North Africa) and interference of the Late Ordovician glaciation on the development of the Lower Palaeozoic transgression on northern Gondwana. *Bulletin of Geosciences*, **82**, 183–214.
- Gibbs, M., Barron, E.J. & Kump, L.R. 1997. An atmospheric pCO₂ threshold for glaciation in the Late Ordovician. *Geology*, **25**, 447–450.
- Gibbs, M.T., Bice, K.L., Barron, E.J. & Kump, L.R. 2000. Glaciation in the early Paleozoic "greenhouse"; the roles of paleogeography and atmospheric CO₂. *In*: Huber, B.T., MacLeod, K.G. & Wing, S.L., (eds) *Warm Climates in Earth History*. Cambridge University Press, Cambridge, 386–422.
- Gilchrist, J.D.F. 1915. Observations on the Cape *Cephaloscus* (*C. gilchristae* Ridewood) and some of its early stages. *Annals and Magazine of Natural History, series 8*, **16**, 233–243
- Gilksn, M., Taylor, D. & Morris, D. 1992. Lower Palaeozoic and Precambrian petroleum source rocks and the coalification path of alginite. *Organic Geochemistry*, **18**, 881–897.
- Goldman, D., Leslie, S.A., Nölvak, J. & Young, S. 2005. The Black Knob Ridge section, southeastern Oklahoma, USA: a possible Global Stratotype–Section and Point (GSSP) for the base of the Middle Stage of the Upper Ordovician Series. <http://www.stratigraphy.org/BKR.pdf>
- Goldstein, T.P. 1983. Geocatalytic reactions in the formation and maturation of petroleum. *AAPG Bulletin*, **67**, 152–159.
- Gostlin K. 2006. Sedimentology and palynology of the Burgess Shale. Unpublished PhD thesis, University of Toronto, 245 pp.
- Grahn, Y. & Caputo, M.V. 1992. Early Silurian glaciations in Brazil. *Palaeogeography, Palaeoclimatology, Palaeoecology*, **99**, 9–15.
- Grahn, Y. & Paris, F. 1992. Age and correlation of the Trombetas Group, Amazonas Basin, Brazil. *Revue de Micropaleontologie*, **35**, 197–209.

- Grogan, E.D. & R. Lund, R., 2002. The geological and biological environment of the Bear Gulch Limestone (Mississippian of Montana) and a model for its paleoreconstruction. *Geobios*, **24**, 295–315.
- Gupta, N.S., Briggs, D.E.G., Michels, R., Evershed, R.P. & Pancost, R. D. 2006a. Organic preservation of fossil arthropods: an experimental study. *Proceedings of the Royal Society of London*, **B273**, 2777–2783.
- Gupta, N.S., Briggs, D.E.G. & Pancost, R. D. 2006b. Molecular taphonomy of fossil graptolites. *Journal of the Geological Society of London*, **163**, 897–900.
- Gupta, N.S., Briggs, D.E.G., Collinson, M.E., Evershed, R.P., Michels, R., & Pancost, R.D., 2007a. Molecular preservation of plant and insect cuticles from the Oligocene Enspel Formation, Germany: evidence against derivation of aliphatic polymer from sediment. *Organic Geochemistry*, **38**, 404–418.
- Gupta, N.S., Tetlie, O.E., Briggs, D.E.G. & Pancost, R.D. 2007b. Fossilization of Eurypterids: A product of molecular transformation. *Palaios*, **22**, 439–447.
- Gürich, G. 1928. Über *Dawsonia* Nicholson, *Peltocaris* Salter und über die Graptolithen-Studien von E. Manck. *Zentrablatt für Mineralogie, Geologie und Paläontologie*, **29B**, 531–537.
- Gurley, R.R. 1896. North American graptolites: new species and vertical ranges. *Journal of Geology*, **4**, 63–102.
- Gutiérrez-Marco, J.C. & Lenz, A.C. 1998. Graptolite synrhabdosomes: biological or taphonomic entities? *Paleobiology*, **24**, 37–48.
- Gutiérrez-Marco, J.C. & Štorch, P. 1998. Graptolite biostratigraphy of the Lower Silurian (Llandovery) shelf deposits of the Western Iberian Cordillera, Spain. *Geological Magazine*, **135**, 71–92.
- Hall, J. 1865. Graptolites of the Quebec Group. *Geological Survey of Canada, Canadian Organic Remains, Decade 2*. 151 pp.
- Hamoumi, N. 1999. Upper Ordovician glaciation spreading and its sedimentary record in Moroccan North Gondwana margin. In: Kraft, P. & Fjaka, O. (eds) *Quo vadis Ordovician?* Acta Universitatis Carolinae, Geologica, **43**, 111–114.
- Häntzschel, W. 1965. Vestigia invertebratum et problematica. In Westphal, F. (ed.) *Fossilium Catalogus (I: Animalia)*, **108**, 140 pp.
- Häntzschel, W. 1975. Trace fossils and problematica. In C. Teichert (ed.) *Treatise on Invertebrate Paleontology, Part W, Miscellanea*. Geological Society of America & University of Kansas Press, 269 pp.

- Harper, D.A.T., Cocks, L.R.M., Popov, L.E., Sheehan, P.M., Bassett, M.G., Copper, P., Holmer, L.E., Jisuo J. & Rong J.-y. 2004. Brachiopods. *In: Webby, B.D., Paris, F., Droser, M.L., & Percival, I.G. (eds) The Great Ordovician Biodiversification Event.* Columbia University Press, New York, 157–178.
- Harper, D.A.T. 2006. The Ordovician biodiversification: Setting an agenda for marine life. *Palaeontology, Palaeoclimatology, Palaeoecology*, **232**, 148–166.
- Hatch, J.R., Jacobson, S.R., Witzke, B.J., Risatti, J.B., Anders, D.E., Watney, W.L., Newell, K.D., & Vuletich, A.K., 1987. Possible late Middle Ordovician organic carbon isotope excursion: evidence from Ordovician oils and hydrocarbon source rocks, mid-continent and east-central United States. *AAPG, Bulletin*, **71**, 1342–1354.
- Havlíček, V. & Massa, D. 1973. Brachiopodes de l'Ordovicien Supérieur de Libye occidentale: implications stratigraphiques regionales. *Geobios*, **6**, 267–290.
- Hayes, J.M., Strauss, H. & Kaufman, A.J. 1999. The abundance of ¹³C in marine organic matter and isotopic fractionation in the global biogeochemical cycle of carbon during the past 800 Ma. *Chemical Geology*, **161**, 103–125.
- Hays, P.D., & Grossman, E.L. 1991. Oxygen isotopes in meteoric calcite cements as indicators of continental paleoclimate. *Geology*, **19**, 441–444.
- Haywood, A.M., Dekens, P., Ravelo, A.C., & Williams, M. 2005. Warmer tropics during the mid-Pliocene? Evidence from alkenone paleothermometry and a fully coupled ocean-atmosphere GCM. *Geochemistry, Geophysics, Geosystems*, **6**, Q03010.
- Henningsmoen, G. 1969. Short account of Cambrian and Tremadocian of Acado-Baltic province. *In: Kay, M. (ed.) North Atlantic geology and continental drift. Memoir of the American Association of Petroleum Geologists*, **12**, 110–115.
- Henwood, A., 1992. Exceptional preservation of dipteran flight muscle and the taphonomy of insects in amber. *Palaios*, **7**, 203–212.
- Herrmann, A.D., Patzkowsky, M.E. & Pollard, D. 2003. Obliquity forcing with 8–12 times preindustrial levels of atmospheric pCO₂ atmospheric CO₂ during the Late Ordovician glaciation. *Geology*, **31**, 485– 488.
- Herrmann, A.D., Patzkowsky, M.E. & Pollard, D. 2004a. The impact of paleogeography, pCO₂, poleward ocean heat transport and sea level change on global cooling during the Late Ordovician. *Palaeogeography, Palaeoclimatology, Palaeoecology*, **206**, 59– 74.
- Herrmann, A.D., Haupt, B.J., Patzkowsky, M.E., Seidov, D. & Slingerland, R.L. 2004b. Response of Late Ordovician paleoceanography to changes in sea level, continental

- drift, and atmospheric pCO₂: potential causes for long-term cooling and glaciation. *Palaeogeography, Palaeoclimatology, Palaeoecology*, **210**, 385–401.
- Holland, H.D. 1978. *The chemistry of the atmosphere and the ocean*. Wiley Interscience, New York, 352 pp.
- Holmer, L.E. & Popov, L.E. 2000. Lingulata, Actrotretida & Siphonotretida. *In*: Kaesler, R.L. (ed.) *Treatise on Invertebrate Paleontology. Part H, Brachiopoda*. Geological Society of America & University of Kansas Press, p 32–146.
- Horst, C.J. van der. 1939. Hemichordata. *In*: Bronns, H.G. (ed) *Klassen und Ordnungen des Tier-Reichs wissenschaftlich dargestellt in Wort und Bild*. Akademische Verlagsgesellschaft, Leipzig, 737 pp.
- Hovius, N. 1998. Controls on sediment supply by large rivers. *In*: Shanley K.W. & McCabe P.J. (eds). Relative role of eustasy, climate, and tectonism in continental rocks. SEPM Special Publication, **59**, 3–16.
- Hower, J., 1981. X-ray diffraction identification of mixed-layer clay minerals. *In*: Longstaffe, F.J. (ed.). *Clays and the Resource Geologist*. Short Course Handbook, Mineralogical Association of Canada, 39–80.
- Hower, J., Eslinger, E.V., Hower, M.E., & Perry, E.A. 1976. Mechanism of burial and metamorphism of argillaceous sediments. *Geological Society of America, Bulletin*, **87**, 725–737.
- Hudson, J.D. 1982. Pyrite in ammonite-bearing shales from the Jurassic of England and Germany. *Sedimentology*, **29**, 639–667.
- Hunt, J.M., 1996. *Petroleum Geochemistry and Geology*. W.H. Freeman, San Francisco. 617 p.
- Hutchinson, R.D. 1952. The stratigraphy and trilobite faunas of the Cambrian sedimentary rocks of Cape Breton Island, Nova Scotia. *Geological Survey of Canada, Memoir*, **263**.
- Hutt, J. E. 1974. The Llandovery graptolites of the English Lake District. Part 1. *Monograph of the Palaeontographical Society*, **128**, 1–56.
- Hutt, J.A. 1991. What was their sex life like? *In* Palmer, D. & Rickards, R.B. (eds) *Graptolites: writing in the rocks*. Boydell Press, Woodbridge, Surrey, 50–53.
- Inoue, A., Watanabe, T., Kohyama, N. & Brusewitz, A.M. 1990. Characterization of Illitization of Smectite in Bentonite Beds at Kinnekulle, Sweden. *Clays and Clay Minerals*, **38**, 241–249.

- Irigoien, X., Huisman, J. & Harris, R.P. 2004. Global biodiversity patterns of marine phytoplankton and zooplankton. *Nature*, **429**, 863–867.
- Ito, M. Ishigaki, A., Nishikawa, T. & Saito, T. 2001. Temporal variation in the wavelength of hummocky cross-stratification: Implications for storm intensity through Mesozoic and Cenozoic. *Geology*, **29**, 87–89.
- James, J.F. 1885. The fucoids of the Cincinnati Group, Part 2. *Journal of the Cincinnati Society of Natural History*, **7**, 161–162.
- James, J.F. 1892. Manual of the paleontology of the Cincinnati Group, Part 2. *Journal of the Cincinnati Society of Natural History*, **14**, 45–72.
- James, N.P., Bone, Y., & Kyser, T.K., 1997, Brachiopod $\delta^{18}\text{O}$ values do reflect ambient oceanography: Lacepede Shelf, southern Australia. *Geology*, **25**, 551–554.
- James, U.P. 1879. Descriptions of new species of fossils and remarks on some others from the Lower and Upper Silurian rocks of Ohio. *The Paleontologist*, **3**, 17–24.
- Jenkins, C.J. 1987. The Ordovician graptoloid *Didymograptus murchisoni* in South Wales and its use in three-dimensional absolute strain analysis. *Transactions of the Royal Society of Edinburgh: Earth Sciences*, **78**, 105–114.
- Jenness, S.E. 1963. Terra Nova and Bonavista map-areas, Newfoundland. *Geological Survey of Canada, Memoir*, **327**, 184 pp.
- Jeppsson, L. 1990. An oceanic model for lithological and faunal changes tested on the Silurian record. *Journal of the Geological Society, London*, **147**, 663–74.
- Jeppsson, L. 1997. The anatomy of the Mid-Early Silurian Ireviken Event and a scenario for P–S events. In: Brett, C.E., Baird, G.C. (eds.), *Paleontological Events: Stratigraphic, Ecological, and Evolutionary Implications*. Columbia University Press, New York, 451–492.
- Jeppsson, L., Aldridge, R. J. & Dorning, K. J. 1995. Wenlock (Silurian) oceanic episodes and events. *Journal of the Geological Society, London*, **152**, 487–98.
- Johnson, M. E. 1996. Stable cratonic sequences and a standard for Silurian eustasy. In: Witzke, B.J., Ludvigson, G.A. & Day, J. (eds). *Paleozoic sequence stratigraphy: views from the North American craton*. Geological Society of America Special Paper, **306**, 203–11
- Johnson, M.E. 2006. Relationship of Silurian sea-level fluctuations to oceanic episodes and events. *GFF*, **128**, 115–122.

- Johnson, M.E., Kaljo, D.L. & Rong, J.-Y. 1991. Silurian eustasy. *In*: Bassett, M.G., Lane, P.D. & Edwards, D. (eds). *The Murchison symposium*. Special Papers in Palaeontology, **44**, 145–63.
- Kaljo, D. & Martma, T. 2006. Application of carbon isotope stratigraphy to dating the Baltic Silurian rocks, *GFF*, **128**, 123–129.
- Kaljo, D., Kiipli, T. & Martma, T. 1997. Carbon isotope event markers through the Wenlock–Pridoli sequence in Ohesaare (Estonia) and Priekule (Latvia). *Palaeogeography, Palaeoclimatology, Palaeoecology*, **132**, 211–224.
- Kaljo, D., Kiipli, T. & Martma, T. 1998. Correlation of carbon isotope events and environmental cyclicity in the East Baltic Silurian. *In*: Landing, E. & Johnson, M.E. (eds.). *Silurian Cycles: Linkages of Dynamic Stratigraphy with Atmospheric, Oceanic and Tectonic Changes*. New York State Museum Bulletin, **491**, 297–312.
- Kaljo, D., Hints, L., Hints, O., Martma, T., Nõlvak, J., 1999. Carbon isotope excursions and coeval biotic–environmental changes in the late Caradoc and Ashgill of Estonia. *In*: Kraft, P. & Fjaka, O. (eds). *Quo vadis Ordovician?* Acta Univesitatis Carolinae, Geologica, **43**, 507–510.
- Kaljo, D., Hints, L., Martma, T. & Nõlvak, J. 2001. Carbon isotope stratigraphy in the latest Ordovician of Estonia. *Chemical Geology*, **175**, 49–59.
- Kaljo, D., Martma, T., Mannik, P. & Viira, V. 2003. Implications of Gondwana glaciations in the Baltic Late Ordovician and Silurian and a carbon isotopic test of environmental cyclicity. *Bulletin de la Societe Geologique de France*, **174**, 59–66
- Kaljo, D., Boucot, A.J., Corfield, R.M., Herisse, A.L., Koren', T.N., Kriz, J., Männik, P., Märss, T., Nestor, V., Shaver, R.H., Siveter, D.J. & Viirda, V. 1996. Silurian Bio-Events. *In*: Walliser, O. H. (ed.) *Global events and events stratigraphy*. Springer-Verlag, Berlin Heidelberg, 173–224.
- Kaljo, D., Hints, L., Martma, T., Nõlvak, J. & Oraspõld, A. 2004. Late Ordovician carbon isotope trend in Estonia, its significance in stratigraphy and environmental analysis. *Palaeogeography, Palaeoclimatology, Palaeoecology*, **210**, 165–185.
- Kaljo, D., Martma, T. & Saadre, T. 2007. Post–Hunnebergian Ordovician carbon isotope trend in Baltoscandia, its environmental implications and some similarities with that of Nevada. *Palaeogeography, Palaeoclimatology, Palaeoecology*, in press.
- Kaufmann, E.G. 1978. Benthic environments and palaeoecology of the Posidonienschiefer (Toarcian). *Neues Jahrbuch für Geology und Paläontologie, Abhandlungen*, **157**, 18–36.

- Kegel, W. 1953. Contribuição para o estudo do Devoniano da Bacia do Parnaíba. *Boletim da Divisão de Geologia e Mineralogia, Rio de Janeiro*, 141, 1–48.
- Kennedy, M.J. 1981. The early Palaeozoic Stoneville Formation, northern Newfoundland. In: Hambrey, M.J., & Harland, W.B. (eds). *Earth's pre-Pleistocene glacial record*. Cambridge University Press, Cambridge, 713–716.
- King, L. M. 1994. Subsidence analysis of eastern Avalonian sequences; implications for Iapetus closure. *Journal of the Geological Society, London*, 151, 647–657.
- Konhäuser, K.O. & Urrutia, M.M. 1999. Bacterial clay authigenesis: a common biogeochemical process. *Chemical Geology*, 161, 399–413.
- Koren', T. & Rickards, R.B. 1997. Taxonomy and evolution of Llandovery biserial graptoloids from the southern Urals, western Kazakhstan. *Special Papers in Palaeontology*, 54, 103 pp.
- Koren', T.L., Popov, L.E., Degtjarev, K.E., Kovalevsky, O.P. & Modzalevskaya, T.L. 2003. Kazakhstan in the Silurian. In: Landing, E. & Johnson, M. E. (eds). *Silurian lands and seas: Palaeogeography outside of Laurentia*. New York State Museum, Bulletin, 493, 323–344.
- Kozłowski, R. 1947. Les affinités des graptolithes. *Biological Reviews of the Cambridge Philosophical Society*, 22, 93–108.
- Kozłowski, R. 1948. Les graptolithes et quelques nouveaux groupes d'animaux du tremadoc de la Pologne. *Acta Palaeontologica Polonica*, 3, 1–235.
- Kozłowski, R. 1965. Oeufs fossiles des Cephalopodes? *Acta Palaeontologica Polonica*, 10, 3–9.
- Krug, A.Z. & Patzkowsky, M.E. 2007. Geographic variation in turnover and recovery from the Late Ordovician mass extinction. *Paleobiology*, 33, 435–454.
- Kump, L.R. 2002. Reducing uncertainty about carbon dioxide as a climate driver. *Nature*, 419, 188–190.
- Kump, L.R., Arthur, M.A., 1999. Interpreting carbon-isotope excursions: carbonates and organic matter. *Chemical Geology*, 161, 181–198.
- Kump, L.R., Arthur, M.A., Patzkowsky, M.E., Gibbs, M.T., Pinkus, D.S. & Sheehan, P.M. 1999. A weathering hypothesis for glaciation at high atmospheric pCO₂. *Palaeogeography, Palaeoclimatology, Palaeoecology*, 152, 173–187.

- Lagaly, G., 1984. Clay-organic interactions. *Philosophical Transactions of the Royal Society of London*, **A311**, 315-332.
- Lalieux, P., Thury, M. & Horseman, S. 1996. Radioactive waste disposal in argillaceous media. *NEA Newsletter*, **Spring**, 34-36.
- Landing, E., Taylor, M.E. & Erdtmann, B.-D. 1978. Correlation of the Cambrian-Ordovician boundary between the Acado-Baltic and North American faunal provinces. *Geology*, **6**, 75-78.
- Lanson, B., Beaufort, D., Berger, G., Baradat, J., & Lacharpagne, J.C. 1996. Illization of diagenetic kaolinite-to-dickite conversion series: late stage diagenesis of the Lower Permian Rotliegend sandstone reservoir. *Journal of Sedimentary Research*, **66**, 501-518.
- Lapworth, C. 1876. Fossils of the Moffat Series. In Armstrong, J., Young, J. & Robertson, D. (eds) *Catalogue of Western Scottish Fossils*. Blackie & Son, Glasgow, 164 pp.
- Lapworth, C. 1876-77. On the Graptolites of County Down. *Proceedings of the Belfast Naturalists' Field Club - Appendix*, **4**, 125-144.
- Lastowka, A.M., Brown, E.M., & Maffia, G.J. 2005. A comparison of chemical, physical and enzymatic cross-linking of bovine type I collagen fibrils. *Journal of American Leather Chemists' Association*, **100**, 196-202.
- Lawrie, R.A. 1996. *Lawrie's Meat Science*. 6th ed. Woodhead Publishing, Cambridge, 336 pp.
- Le Heron, D.P., Sutcliffe, O.E., Whittington, R.J., Craig, J., 2005. The origins of glacially related soft-sediment deformation structures in Upper Ordovician glaciogenic rocks: implication for ice sheet dynamics. *Palaeogeography, Palaeoclimatology, Palaeoecology*, **218**, 75-103.
- Lee, C. & Chen, X. 1962. Cambrian and Ordovician graptolites from Sandu, S Guizhou (Kueichou). *Acta Palaeontologica Sinica*, **10**, 12-35.
- Leggett JK. 1980. British Lower Paleozoic black shales and their palaeo-oceanographic significance. *Journal of the Geological Society, London*, **137**, 139-156.
- Leggett, J.K. 1987. The Southern Uplands as an accretionary prism; the importance of analogues in reconstructing palaeogeography. *Journal of the Geological Society, London*, **144**, 737-752

- Leggett, J.K., McKerrow, W.S., Morris, J.H., Oliver, G.J.H. & Phillips, W.E.A. 1979. The north-western margin of the Iapetus Ocean. *In*: Harris, A.L., Holland, C.H. & Leake, B.E. (eds). *The Caledonides of the British Isles; reviewed*. Special Publication of the Geological Society, London, **8**, 499–512.
- Leggett, J.K., McKerrow, W.S., Cocks, L.R.M., & Rickards, R.B. 1981. Periodicity in the early Palaeozoic marine realm. *Journal of the Geological Society*, **138**, 167–176.
- Legrand, P. 1969. Description de *Westonia chudeaui* sp. nov. Brachiopode inarticulé de l'Adrar mauritanien (Sahara occidental). *Bulletin de la Société Géologique de France*, **11**, 251–256.
- Legrand, P. 1970. Les couches à *Diplograptus* du Tassili de Tarit (Ahmet, Sahara algérien). *Bulletin de la Société d'Histoire Naturelle de Afrique du Nord*, **60**, 3–58.
- Legrand, P. 1974. – Essai sur la paléogéographie de l'Ordovicien du Sahara algérien. *Notes et Mémoires de Compagnie Française des Pétroles*, **11**, 121–138.
- Legrand, P. 1985. Lower Palaeozoic rocks of Algeria. *In*: Holland, C.H. (ed.). Lower Palaeozoic of north-western and west-central Africa. Lower Palaeozoic Rocks of the World, **4**. John Wiley & Sons, London, 5–89.
- Legrand, P. 2003. Paléogéographie du Sahara algérien à l'Ordovicien terminal et au Silurien inférieur. *Bulletin de la Société Géologique de France*, **174**, 19–32.
- Legrand, P., Poueyto, A. & Rouaix, S. 1959. De quelques faunes des Grès inférieurs sur la bordure septentrionale du Hoggar (Sahara). *Bulletin de la Société Géologique de France*, **7(1)**, 796–802.
- Lester, S.M. 1988a. Fine structure of the heart vesicle and pericardium in the pterobranch *Rhabdopleura* (Hemichordata). *American Zoologist*, **22**, 938.
- Lester, S.M. 1988b. Settlement and metamorphosis of *Rhabdopleura normani* (Hemichordata: Pterobranchia). *Acta Zoologica*, **69**, 111–120.
- Linnaeus, C. 1768. *Systema Naturae* (12th edition), **3**, 236 pp.
- Locklair, R.E. & Lermann, A. 2005. A model of Phanerozoic cycles of carbon and calcium in the global ocean: Evaluation and constraints on ocean chemistry and input fluxes. *Chemical Geology*, **217**, 113–126.
- LoDuca, S.T. & Brett, C.E. 1997. The *Medusaegraptus* Epibole and Lower Ludlovian Konservat-Lagerstätten of Eastern North America. *In*: Brett, C.E. & Baird, G.C. (eds). *Paleontological Events: Stratigraphic, Ecological, and Evolutionary Implications*. Columbia University Press, New York, 369–406.

- Lovelock, J.E. 1972. Gaia as seen through the atmosphere. *Atmospheric Environment*, **6**, 579–580.
- Lovelock, J.E. & Margulis, L. 1974. Atmospheric homeostasis by and for the biosphere– The Gaia hypothesis. *Tellus*, **26**, 2–10.
- Lowenstam, H. A., 1961, Mineralogy, $^{18}\text{O}/^{13}\text{C}$ ratios, and strontium and magnesium contents of recent and fossil brachiopods and their bearing on the history of oceans. *Journal of Geology*, **69**, 241–260.
- Loydell, D.K. 1994. Early Telychian changes in graptoloid diversity and sea level. *Geological Journal*, **29**, 355–68.
- Loydell, D.K. 1998. Early Silurian sea-level changes. *Geological Magazine*, **135**, 447–471.
- Loydell, D.K. 2007. Early Silurian positive $\delta^{13}\text{C}$ excursions and their relationship to glaciations, sea-level changes and extinction events. *Geological Journal*, **42**, 531–546.
- Loydell, D.K., & Nestor, V. 2005. Integrated graptolite and chitinozoan biostratigraphy of the upper Telychian (Llandovery, Silurian) of the Ventspils D–3 core, Latvia. *Geological Magazine*, **142**, 369–376.
- Loydell, D. K., Kaljo, D. & Männik, P. 1998a. Integrated biostratigraphy of the lower Silurian of the Ohesaare core, Saaremaa, Estonia. *Geological Magazine*, **135**, 769–783.
- Loydell, D.K., Zalasiewicz, J.A. & Cave, R. 1998b. Predation on graptoloids: new evidence from the Silurian of Wales. *Palaeontology*, **41**, 423–427.
- Loydell, D. K., Männik, P. & Nestor, V. 2003. Integrated biostratigraphy of the lower Silurian of the Aizpute–41 core, Latvia. *Geological Magazine*, **140**, 205–229.
- Ludvigson, G.A., Witzke, B.J., Gonzalez, L.A., Carpenter, S.J., Schneider, C.L., & Hasiuk, F.H. 2004. Late Ordovician (Turinian–Chatfieldian) carbon isotope excursions and their paleoceanographic significance. *Palaeogeography, Palaeoclimatology, Palaeoecology*, **210**, 187–214.
- Lüning, S., Craig, J., Loydell, D.K., Storch, P. & Fitches, B. 2000. Lower Silurian “hot shales” in North Africa and Arabia: regional distribution and depositional model. *Earth Science Reviews*, **49**, 21–200
- Lüning, S., Shahin, Y.M., Loydell, D.K., Al-Rabi, H.T., Masri, A., Tarawneh, B., Kolonic, S., 2005. Anatomy of a world-class source rock: distribution and depositional

- model of Silurian organic-rich shales in Jordan and implications for hydrocarbon potential. *AAPG Bulletin*, **89**, 1397–1427.
- Lüning, S., Loydell, D. K., Štorch, P., Shahin, Y., & Craig, J. 2006. Origin, sequence stratigraphy and depositional environment of an upper Ordovician (Hirnantian) deglacial black shale, Jordan – Discussion. *Palaeogeography, Palaeoclimatology, Palaeoecology*, **230**, 352–355.
- Maack, R. 1957. Über Vereisungsperioden und Vereisungsspuren in Brasilien. *Geologische Rundschau*, **45**, 547–595.
- Mabillard, J.E., & Aldridge, R.J. 1985. Microfossil distribution across the base of the Wenlock Series in the type area. *Palaeontology*, **28**, 89–100.
- Maletz, J., Steiner, M. & Fatka, O. 2005. Middle Cambrian pterobranchs and the question: What is a graptolite? *Lethaia*, **38**, 1–14.
- Männil, R. & Meidla, T. 1994. The Ordovician System of the East European Platform (Estonia, Latvia, Lithuania, Belorussia, parts of Russia, Ukraine and Moldova). *In*: Webby, B.D, Ross, R.J. & Zhen, Y.Y. *The Ordovician System of the East European Platform and Tuva (southeastern Russia)*. IUGS Publication, **28**, 1–52.
- Marr, J.E. & Nicholson, H.A. 1888. The Stockdale Shales. *Quarterly Journal of the Geological Society of London*, **44**, 654–732.
- Marr, J.E., 1925. Conditions of deposition of the Stockdale Shales of the Lake District. *Quarterly Journal of the Geological Society of London*, **81**, 113–131.
- Marshall, J.D. & Middleton, P. D. 1990. Changes in marine isotopic composition and the Late Ordovician glaciation. *Journal of the Geological Society, London*, **147**, 1–4.
- Marshall, J.D., Brenchley, P.J., Mason, P., Wolff, G.A., Astini, R.A., Hints, L., Meidla, T., 1997. Global carbon isotopic events associated with mass extinction and glaciation in the late Ordovician. *Palaeogeography, Palaeoclimatology, Palaeoecology*, **132**, 195–210.
- Martill, D.M., Wilby, P.R. & Williams, N. 1992. Elemental mapping: a technique for investigating delicate phosphatized fossil soft tissues. *Palaeontology*, **35**, 869–874.
- Martin, R. E. 1995. Cyclic and secular variation in microfossil biomineralization – clues to the biogeochemical evolution of Phanerozoic oceans. *Global and Planetary Change*, **11**, 1–23.
- Matthews, S.C. 1973. Notes on open nomenclature and on synonymy lists. *Palaeontology*, **16**, 233–237.

- Massa, D., Havlíček, V. & Bonnefous, J. 1977. Stratigraphic and faunal data on the Ordovician of the Rhadames Basin (Libya and Tunisia). *Bulletin des Centres des Recherches Exploration – Production Elf Aquitaine*, 1, 3–27.
- McCann, A.M. & Kennedy, M.J. 1974. A probable glacio-marine deposit of Late Ordovician–Early Silurian age from the north central Newfoundland Appalachian Belt. *Geological Magazine*, 111, 549–564
- McClure, H.A. 1978. Early Palaeozoic glaciation in Arabia. *Palaeogeography, Palaeoclimatology, Palaeoecology*, 25, 315–26.
- McDougall, M. & Martin, M. 2000. Facies models and sequence stratigraphy of the Upper Ordovician outcrops of the Murzuq Basin, SW Libya. *In*: Solas, M.A & Worsley, D. (eds) *Geological exploration in Murzuq Basin*. Elsevier, Amsterdam, 223–236.
- McKerrow, W.S., Mac Niocail, C., & Dewey, J.F. 2000. The Caledonian Orogeny redefined. *Journal of the Geological Society, London*, 157, 1149–1154.
- McNamara, M.E., Orr, P.J., Kearns, S.L., Alcalá, L., Anadón, P., & Peñalver–Mollá, E., 2006. High-fidelity organic preservation of bone marrow in ca. 10 Ma amphibians. *Geology*, 34, 641–644.
- Melchin, M.J. 1989. Llandovery graptolite biostratigraphy and paleobiogeography, Cape Phillips Formation, Canadian Arctic Islands. *Canadian Journal of Earth Sciences*, 26, 1726–1746.
- Melchin, M.J. & Holmden, C. 2006. Carbon isotope chemostratigraphy in Arctic Canada: Sea-level forcing of carbonate platform weathering and implications for Hirnantian global correlation. *Palaeogeography, Palaeoclimatology, Palaeoecology*, 234, 186–200.
- Melchin, M.J., Cooper, R.A. & Sadler, P.M. 2004. The Silurian Period. *In*: Gradstein, F.M., Ogg, J.G. & Smith, A.G. (eds). *A Geologic Time Scale 2004*. Cambridge University Press, Cambridge, 165–187.
- Merino, D., 1991. Primer registro de conodontos siluricos en Bolivia. *Revisita Tecnica de YPF*, 12, 271–274.
- Merriman, R.J. & Frey, M. 1999. Patterns of very low-grade metamorphism in metapelitic rocks *In*: Frey, M & Robinson, D. (eds) *Low-Grade Metamorphism*. Blackwell Science, Oxford, 61–107.
- Merriman, R.J., & Roberts, B. 2001 for 2000. Low-grade metamorphism in the Scottish Southern Uplands terrane: deciphering the patterns of accretionary burial, shearing and cryptic aureoles. *Transactions of the Royal Society of Edinburgh, Earth Sciences*, 91, 521–537.

- Meunier, A., 2005, *Clays*. Springer-Verlag, Berlin & Heidelberg, 472 pp.
- Meybeck, M. 1982. Carbon, nitrogen, and phosphorus transport by world rivers. *American Journal of Science*, **282**, 401–450.
- Middleton, P.D., Marshall, J.D., Brenchley, P.J., 1991. Evidence for isotopic changes associated with Late Ordovician glaciation, from brachiopods and marine cements of central Sweden. *In*: Barnes, C.R. & Williams, S.H. (eds.) *Advances in Ordovician Geology*. Geological Survey of Canada Papers, **90**, 313–323.
- Miller, A.I. 2004. The Ordovician radiation: toward a new global synthesis. *In*: Webby, B.D., Paris, F., Droser, M.L., & Percival, I.G. (eds) *The Great Ordovician Biodiversification Event*. Columbia University Press, New York, 380–388.
- Miller, A.I. & Connolly, S.R. 2001. Substrate affinities of higher taxa and the Ordovician Radiation. *Paleobiology*, **27**, 768–778
- Miller, A.I. & Mao, S.G. 1995. Association of orogenic activity with the Ordovician radiation of marine life. *Geology*, **23**, 305–308.
- Miller, M.A. & Melvin, J. 2005. Significant new biostratigraphic horizons in the Qusaiba member of the Silurian Qalibah formation of central Saudi Arabia, and their sedimentologic expression in a sequence stratigraphic context. *GeoArabia*, **10**, 49–92.
- Miller, S.A. 1889. *North American Geology and Paleontology*. Western Methodist Book Concern, Cincinnati, 664 pp.
- Millward, D., Johnson, E. W. Beddoe-Stephens, B. & Young, B. 1999. *The Geology of the Ambleside District*. Memoir of the British Geological Survey. Sheet 38 (England & Wales). HMSO, London.
- Milodowski, A.E. & Zalasiewicz, J.A. 1991. Redistribution of rare earth elements during diagenesis of turbidite/hemipelagite mudrock sequences of Llandovery age from central Wales. *Geological Society Special Publication*, **57**, 101–124.
- Montañez, I.P. 2002. Biological skeletal carbonate records changes in major-ion chemistry of paleo-oceans. *PNAS*, **99**, 15852–15854.
- Monterey, G. & Levitus, S. 1997. Seasonal variability of mixed layer depth for the world ocean. *In*: NOAA Atlas NESDIS 14. *National Oceanic and Atmospheric Administration*, U.S. Government Printing Office, Washington D.C.
- Moore, R.C. & Sylvester-Bradley, P.C. 1957. Taxonomy and nomenclature of aptychi. *In*: Moore, R. C. (ed.) *Treatise on Invertebrate Palaeontology, Part L*. Geological Society of America & University of Kansas Press, 465–471.

- Mu, E.-z. 1988 The Ordovician–Silurian boundary in China. *Bulletin of the British Museum (Natural History)*, **43**, 117–131.
- Mullins, G. L. & Aldridge, R. J. 2004. Chitinozoan biostratigraphy of the basal Wenlock Series (Silurian) global stratotype section and point. *Palaeontology*, **47**, 745–773.
- Munnecke, A., Samtleben, C. & Bickert, T. 2003. The Ireviken event in the Lower Silurian of Gotland, Sweden – relation to similar Palaeozoic and Proterozoic events. *Palaeogeography, Palaeoclimatology, Palaeoecology*, **195**, 99–124.
- Neal, M.L. & Hannibal, J.T. 2000. Paleoecologic and taxonomic implications of *Sphenothallus* and *Sphenothallus*-like specimens from Ohio and areas adjacent to Ohio. *Journal of Paleontology*, **74**, 369–380.
- Nestor, H. & Stock, C.W. 2001. Recovery of the stromatoporoid fauna from the end-Ordovician mass extinction. *Bulletin of the Tohoku University Museum*, **1**, 329–337.
- Nicholson, H.A. 1866. On some fossils from the graptolitic shales of Dumfriesshire. *Geological Magazine*, **3**, 107–113.
- Nicholson, H.A. 1867a. Graptolites of the Moffat Shales. *Geological Magazine*, **4**, 135–136.
- Nicholson, H.A. 1867b. Graptolites. *Geological Magazine*, **4**, 238–239.
- Nicholson, H.A. 1867c. On a new genus of Graptolites, with notes on reproductive bodies. *Geological Magazine*, **4**, 256–263.
- Nicholson, H.A. 1868a. On the nature and zoological position of the Graptolitidae. *Annals and Magazine of Natural History, decade 4*, **1**, 55–61.
- Nicholson, H.A. 1868b. I. – The Graptolites of the Skiddaw Series, etc. II. – On the classification of Graptolites. *Geological Magazine*, **5**, 150–152.
- Nicholson, H.A. 1872. *A Monograph of the British Graptolitidae*. Blackwood & Sons, Edinburgh & London, 133 pp.
- Nicholson, H.A. 1873. On some fossils from the Quebec group of Point Lévis, Quebec. *Annals and Magazine of Natural History, decade 4*, **11**, 133–143.
- Nielsen, A.T. 2003a. Ordovician sea level changes: a Baltoscandinavian perspective. *In: Webby, B.D., Paris, F., Droser, M. & Percival, I.G. (eds). The Great Ordovician Biodiversification Event*. Columbia University Press, New York, 84–93.

- Nielsen, A.T. 2003b. Late Ordovician sea level changes: evidence of Caradoc glaciations? *Geophysical Research Abstracts, European Geosciences Union*, **5**, 11119.
- Nimmo, J. 1847. Fossil Graptolithus. *Calcutta Journal of Natural History*, **7**, 358–359.
- Nölvak, J., Hints, O., & Männik, P. 2006. Ordovician timescale in Estonia: recent developments. *Proceedings of the Estonian Academy of Sciences, Geology*, **55**, 95–108.
- Obut, A.T. & Sobolevskaja, R.F. 1962. Problemi neftegazonosti Sovjetskoj Arktiki: Paleontologija i biostratigrafija: Graptoliti rannego Ordovika na Taimyre. *Trudy Nauchno-Issledovatel'skogo Instituta Geologii Arktiki*, **127**, 65–85.
- Odom, I.E. 1984. Smectite clay-minerals: properties and uses. *Philosophical Transactions of the Royal Society of London*, **A311**, 391–409.
- Oldroyd, D.R. 1990. *The Highland controversy: Constructing Geological Knowledge through Fieldwork in Nineteenth-Century Britain*. Science and Its Conceptual Foundations series. Chicago University Press, Chicago.
- Orr, P.J. 2001a. Bathymetric Indicators. *In*: Briggs, D.E.G. & Crowther, P.R. (eds). *Palaeobiology II*. Blackwell Science, Oxford, 479–482.
- Orr, P.J. 2001b. Colonization of the deep-marine environment during the early Phanerozoic: the ichnofaunal record. *Geological Journal*, **36**, 265–278.
- Orr, P.J. & Briggs, D.E.G. 1999. Exceptionally preserved conchostracans and other crustaceans from the Upper Carboniferous of Ireland. *Special Papers in Palaeontology*, **62**, 1–68.
- Orr, P.J., Briggs, D.E.G. & Kearns, S.L. 1998. Cambrian Burgess Shale animals replicated in clay minerals. *Science*, **281**, 1173–1175.
- Orr, P.J., Kearns, S.L. & Briggs, D.E.G. 2002. Backscattered electron imaging of fossils exceptionally-preserved as organic compressions. *Palaios*, **17**, 110–117.
- Orr, P.J., Benton, M.J. & Briggs, D.E.G. 2003. Post-Cambrian closure of the deep water slope-basin taphonomic window. *Geology*, **31**, 769–772.
- Osgood, R.G. 1970. Trace fossils of the Cincinnati area. *Palaeontographica Americana*, **6**, 281–444.
- Osorio, D. & Bacon, J.P. 1994. A good eye for arthropod evolution. *Bioessays*, **16**, 419–424.

- Page, A.A., Wilby, P.R., Williams, M. & Zalasiewicz, J.A. 2004. Graptogonophores, scopulae & Dawsonia: putative reproductive organs reconsidered. *Palaeontological Association Newsletter*, **57**, 128.
- Page, A.A., Backus, R.J., Rickards, R.B. & Zalasiewicz, J.A. 2006a. The graptolite synrhabdosome: evidence of cooperation between automobile colonies. *Palaeontological Association Newsletter*, **63** (supplement), 32.
- Page, A.A., Wilby, P.R., & Zalasiewicz, J.A., 2005. Clay-organic interactions in graptolitic mudrocks. *Palaeontological Association Newsletter*, **60**, 55.
- Page, A.A., Gabbott, S.E., Wilby, P.R., & Zalasiewicz, J.A., 2006b. Phyllosilicate-organic interactions in low-grade metamorphism of mudrocks: implications for Burgess Shale type preservation. *In: Qun, Y., Yongdong, W., & Weldon, E.A., (eds), Ancient life and modern approaches*. University of Science and Technology of China Press, Beijing, 171.
- Page, A.A., Zalasiewicz, J.A., Williams, M., & Popov, L.E., 2007. Were transgressive black shales a negative feedback modulating glacioeustasy in the Early Palaeozoic Icehouse? *In: Williams, M., Haywood, A.M., Gregory, F.J., & Schmidt, D. N. (eds) Deep-Time perspectives on Climate Change: Marrying the signal from Computer Models and Biological Proxies*. The Micropalaeontological Society, Special Publications. The Geological Society, London. In press.
- Palmer, D. 1991. What other organisms did they live with? *In: Palmer, D., & Rickards, R.B. (eds). Graptolites: writing in the rocks*. The Boydell Press, 41-50.
- Pancost, R.D., Freeman, K.H., Patzkowsky, M.E., Wavrek, D., & Collister, J.W., 1998. Molecular indicators of redox and marine photoautotroph composition in the late Middle Ordovician of Iowa, USA. *Organic Geochemistry*, **29**, 1649-1662.
- Pancost, R.D., Freeman, K.H., & Patzkowsky, M.E., 1999. Organic matter source variation and the expression of a late Middle Ordovician carbon isotope excursion. *Geology*, **27**, 1015-1018.
- Paris, F., Achab, A., Asselin, E., Chen X.-h., Grahn, Y., Nölvak, J., Obut, O., Samuelsson, J., Sennikov, N., Vecoli, M., Verniers, J., Wang X.-f. & Winchester-Seeto, T. 2004. Chitinozoans. *In: Webby, B.D., Paris, F., Droser, M.L., & Percival, I.G. (eds) The Great Ordovician Biodiversification Event*. Columbia University Press, New York, 294-311.
- Parrish, J.T., 1982. Upwelling and petroleum source beds, with reference to Palaeozoic. *AAPG Bulletin*, **66**, 750- 774.
- Passchier, C.W. & Trouw, R.A.J. 1995. *Microtectonics*. Springer-Verlag, Berlin, 283 pp.

- Patzkowsky, M.E., Slupik, L.M., Arthur, M.A., Pancost, R.D. & Freeman, K.H. 1997. Late Middle Ordovician environmental change and extinction: harbinger of the Late Ordovician or continuation of Cambrian patterns? *Geology*, **25**, 911–914.
- Peach, B.N. & Horne, J. 1899. The Silurian Rocks of Britain. Vol. I: Scotland. *Memoirs of the Geological Survey of the United Kingdom*. HMSO, Edinburgh, 749 pp.
- Peralta, S.H. & Carter, C.H. 1999. Don Braulio Formation (late Ashgillian–early Llandoveryan, San Juan Precordillera, Argentina): stratigraphic remarks and paleoenvironmental significance. *Acta Universitatis Carolinae, Geologica*, **43**, 225–228.
- Petrovich, R., 2001. Mechanisms of fossilization of the soft-bodied and lightly armored faunas of the Burgess Shale and of some other classical localities. *American Journal of Science*, **301**, 683–726.
- Phillipot, A. & Robardet, M. 1971. Nouvelles donnees sur les formations siluriennes de Domfront (Orne). *Bulletin de la Societe Geologique et Mineralogique de Bretagne, Serie C*, **3**, 41–47.
- Phillips, G.N. & Groves, D.I. 1984. Fluid access and fluid–wall rock interaction in the genesis of the Archean gold–quartz vein deposit at Hunt Mine, Kambalda, Western Australia. In: Forster, R.P. (ed). *Gold '82*. Geological Society of Zimbabwe, Special Publication, **1**, 59–416.
- Phillipson, J. 1961. Histological Changes in the Gut of *Mitopus tnorio* (Phalangiida) during Protein Digestion. *Quarterly Journal of Microscopical Science*, **102**, 217–226.
- Pickerill, R.K., Pajari, G.E. & Currie, K.L. 1979. Evidence of Caradocian glaciation in the Davidsville Group of north–eastern Newfoundland. *Current research, Part C, Papers of the Canadian Geological Survey*, **79**, 67–72.
- Piper, D.J.W. 1972. Sediments of the Middle Cambrian Burgess Shale. *Lethaia*, **5**, 169–175.
- Piper, D.Z. & Perkins, R.B. 2004. A modern vs. Permian black shale – the hydrography, primary productivity, and water–column chemistry of deposition. *Chemical Geology*, **206**, 177–197.
- Porębska, E., & Sawłowicz, Z. 1997 Palaeoceanographic linkage of geochemical and graptolite events across the Silurian–Devonian boundary in Bardzkie Mountains (Southwest Poland). *Palaeogeography, Palaeoclimatology, Palaeoecology*, **132**, 343–354.

- Portlock, J.E. 1843. Report on the geology of the county of Londonderry, and parts of Tyrone and Fermanagh. Andrew Milliken, Dublin, & Longman, Brown, Green and Longmans, London, 784 pp.
- Poulsen, C. 1922. Om Dictyograptus-skiferen paa Bornholm. *Danmarks Geologiske Undersøgelse*, **4**, 1–28.
- Powell, W., 2003, Greenschist-facies metamorphism of the Burgess Shale and its implications for models of fossil formation and preservation. *Canadian Journal of Earth Sciences*, **40**, 13–25.
- Powell, W.G., Johnston, P.A, & Collom, C.J. 2003 Geochemical evidence for oxygenated bottom waters during deposition of fossiliferous strata of the Burgess Shale Formation. *Palaeontology, Palaeoclimatology, Palaeoecology*, **201**, 249–268.
- Pratt, W.T., Woodhall, D.G., Howells, M.F. 1995. *Geology of the country around Cadair Idris*. Memoir for 1:50,000 Geological Sheet 149 (England and Wales). London, HMSO.
- Qing, H. & Veizer, J. 1994. Oxygen and carbon isotope composition of Ordovician brachiopods: implications for coeval seawater. *Geochimica Cosmochimica Acta*, **58**, 1501–1509.
- Racheboeuf, P., Vannier, J. & Ortega, G. 2000. Ordovician phyllocarids (Arthropoda; Crustacea) from Argentina. *Paläontologisches Zeitschrift*, **74**, 317–333.
- Rahmstorf, S. 2002. Ocean circulation and climate during the past 120,000 years, *Nature*, **419**, 207–214.
- Raymo, M.E. 1991, Geochemical evidence supporting TC Chamberlin's theory of glaciation. *Geology*, **19**, 344–347.
- Richards, A.G. 1952. Studies on Arthropod Cuticle. VIII. The Antennal Cuticle of Honeybees, with Particular Reference to the Sense Plates. *Biological Bulletin*, **103**, 201–225.
- Rickards, R.B. 1970. The Llandovery (Silurian) graptolites of the Howgill Fells, Northern England. *Palaeontographical Society Monographs*, **123**, 108 pp.
- Rickards, R.B. 1975 Palaeoecology of the Graptolithina, an extinct class of the phylum Hemichordata. *Biological Reviews*, **50**, 397–436.
- Rickards, R.B. 1999. A Century of Graptolite Research in Cambridge. *The Geological Curator*, **7**, 71–76.
- Rickards, R.B., & Woodcock, N.H. 2005. Stratigraphical revision of the Windermere

- Supergroup (Late Ordovician–Silurian) in the southern Howgill Fells, NW England. *Proceedings of the Yorkshire Geological Society*, **55**, 263–285.
- Rickards, R. B., Hamed, M. A. & Wright, A. J. 1994. A new Arenig (Ordovician) graptolite fauna from the Kerman District, east-central Iran. *Geological Magazine*, **131**, 35–42.
- Rickards, R.B., Rigby, S., Rickards, J. & Swales, C. 1998. The hydrodynamics of graptolites assessed by laser Doppler anemometry. *Palaeontology*, **41**, 737–752.
- Ridgwell, A. 2005. A Mid Mesozoic Revolution in the regulation of ocean chemistry. *Marine Geology*, **217**, 339–357.
- Rigby, S. 1991. Feeding strategies of graptolites. *Palaeontology*, **34**, 797–815.
- Rigby, S. 1992. Graptoloid feeding efficiency, rotation and astogeny. *Lethaia*, **25**, 51–68.
- Rigby S. 1993. Population analysis and orientation studies of graptoloids from the Middle Ordovician Utica Shale, Quebec. *Palaeontology*, **36**, 267–282.
- Rigby, S. & Dilly P.N. 1993. Growth rates of pterobranchs and the lifespan of graptolites. *Paleobiology*, **19**, 459–475.
- Rigby, S. & Sudbury, M. 1995. Graptolite ontogeny and the size of the graptolite zooid. *Geological Magazine*, **132**, 427–433.
- Robardet, M., Henry, J.L., Nion, J., Paris, F. & Pillet, J. 1972. La Formation du Pont-de-Caer (Caradocien) dans les synclinaux de Domfront et de Sees (Normandie). *Societe Geologique du Nord, Annales*, **92**, 117–137.
- Roberts, B., Merriman, R.J., Hirons, S.R., Fletcher, C.J.N., & Wilson, D., 1996. Synchronous very low-grade metamorphism, contraction and inversion in the central part of the Welsh Lower Palaeozoic Basin. *Journal of the Geological Society, London*, **153**, 277–285.
- Rocha-Campos, A.C. 1981. Early Palaeozoic lappo Formation of Paraná, Brazil. In: Hambrey, M.J., & Harland, W.B. (eds). *Earth's pre-Pleistocene glacial record*. Cambridge University Press, Cambridge, 908–909.
- Rohling, E.J. 1994. Review and new aspects concerning the formation of Mediterranean sapropels, *Marine Geology*, **122**, 1–28.
- Rohling, E.J. & Gieskes, W.W.C. 1989. Late Quaternary changes in Mediterranean Intermediate Water density and formation rate. *Paleoceanography*, **4**, 531–545.

- Rolfe, W.D.I. 1969. Phyllocarida. *In: Teichert, C. (ed.) Treatise on Invertebrate Paleontology. Part R, Arthropoda 4.* Geological Society of America & University of Kansas Press, 296–330.
- Rong, J.-Y., Boucot, A.J., Su Y.-Z. & Strusz, D.L. 1995. Biogeographical analysis of Late Silurian brachiopod faunas, chiefly from Asia and Australia. *Senckenberg Lethaea*, **28**, 39–60.
- Ronov, A.B., Khain, V.E., Balukhovskiy, A.N. & Seslavinsky, K.B. 1980. Quantitative analysis of Phanerozoic sedimentation. *Sedimentary Geology*, **25**, 311–325.
- Ross, C.A. & Ross, J.R.P. 1995. North American Ordovician depositional *sequences and correlations*. *In: Cooper, J.D., Finney, S.C. (eds), Ordovician Odyssey.* SEPM, Pacific Section, Fullerton California, 309–313.
- Ross, C.A. & Ross, J.R.P. 1996. Silurian sea-level fluctuations. *In: Witzke, B.J., Ludvigson, G.A. & Day, J. (eds) Paleozoic sequence stratigraphy: views from the North American craton.* Geological Society of America, Special Paper, **306**, 187–92.
- Ross, J.R.P. 1985. Biogeography of Ordovician ectoproct (bryozoan) faunas. *In: Nielsen, C. & Larwood, G.P. (eds). Bryozoa: Ordovician to recent.* Olsen & Olsen, Denmark, 265–271.
- Rothman, D.H. & Forney, D. C. 2007. Physical model for the decay and preservation of marine organic carbon. *Science*, **316**, 1325–1328.
- Rothman D. H., Hayes J. M. & Summons R. E. 2003. Dynamics of the Neoproterozoic carbon cycle. *PNAS*, **100**, 8124–8129.
- Rowell, A.J. 1965. Inarticulata. *In: Moore, R.C. (ed.) Treatise on Invertebrate Paleontology. Part H, Brachiopoda.* Geological Society of America & University of Kansas Press, 260–296.
- Royer, D.L. 2006. CO₂-forced climate thresholds during the Phanerozoic. *Geochimica et Cosmochimica Acta*, **70**, 566–5675.
- Royer, D.L., Berner, R.A., Montañez, I.P., Tabor, N.J., & Beerling, D.J. 2004. CO₂ as a primary driver of Phanerozoic climate. *GSA Today*, **14**, 4–10.
- Ruben, J.A., Dal Sasso, C., Geist, N.R., Hillenius, W.J, Jones, T.D. & Signore, M., 1999. Pulmonary function and metabolic physiology of theropod dinosaurs. *Science*, **283**, 514–516.
- Rudwick, M.J.S. 1985. The great Devonian controversy: *The shaping of scientific knowledge among gentlemanly specialists.* Science and its conceptual foundations series. Chicago University Press, Chicago, 483 pp.

- Ruedemann, R. 1904. Graptolites of New York. Part I. *New York State Museum, Memoir*, 7, 807 pp.
- Ruedemann, R. 1908. Graptolites of New York. Part II. *New York State Museum, Memoir*, 11, 583 pp.
- Ruedemann, R. 1934. Paleozoic plankton of North America. *Geological Society of America, Memoir*, 2.
- Ruedemann, R. 1936. Ordovician graptolites from Quebec and Tennessee. *Journal of Paleontology*, 10, 385–387.
- Ruedemann, R. 1947. Graptolites of North America. *Geological Society of America, Memoir*, 19, 651 pp.
- Rushton, A.W.A. 1982. The biostratigraphy and correlation of the Merioneth–Tremadoc Series boundary in North Wales. In: Bassett, M.G. & Dean, W.T. (eds) *The Cambrian – Ordovician boundary: sections, fossil distributions, and correlations*. National Museum of Wales, Geological Series, 3, 9–27.
- Rushton, A.W.A. 2001 for 2000. The use of graptolites in the stratigraphy of the Southern Uplands: Peach's legacy. *Transactions of the Royal Society of Edinburgh, Earth Sciences*, 91, 341–347.
- Rushton, A.W.A. & Williams, M. 1996. The tail-piece of the crustacean *Caryocaris wrighti* from the Arenig rocks of England and Ireland. *Irish Journal of Earth Sciences*, 15, 107–111.
- Rushton, A., Sudbury, M., Hughes, R., Zalasiewicz, J.A. & Chen, X. 1991. Who were the famous graptolite workers? In: Palmer, D., & Rickards, R.B. (eds). *Graptolites: writing in the rocks*. The Boydell Press, Woodbridge, Surrey, 141–149.
- Rust, I.C. 1981. Early Palaeozoic Pakhuis Tillite, South Africa. In: Hambrey, M.J., & Harland, W.B. (eds). *Earth's pre-Pleistocene glacial record*. Cambridge University Press, 113–117.
- Sakko, A.L. 1998. The influence of the Benguela upwelling system on Namibia's marine biodiversity. *Biodiversity and Conservation*, 7, 419–433.
- Salter, J.W. 1863. Note on Skiddaw Slate Fossils. *Quarterly Journal of the Geological Society, London*, 19, 135–140.
- Saltzman, M.R. 2005. Phosphorus, nitrogen, and the redox evolution of the Paleozoic oceans. *Geology*, 33, 573–576.
- Saltzman, M.R., & Young, S.A. 2005. A long-lived glaciation in the Late Ordovician?

- Isotopic and sequence stratigraphic evidence from western Laurentia. *Geology*, **33**, 109–112.
- Samtleben, C., Munnecke, A., Bickert, T., & Pätzold, J., 2001. Shell succession, assemblage and species dependent effects on the C/O–isotopic composition of brachiopods: examples from the Silurian of Gotland. *Chemical Geology*, **175**, 61–107.
- Samtleben, C., Munnecke, A., Bickert, T., Pätzold, J., 1996. The Silurian of Gotland (Sweden): Facies interpretation based on stable isotopes in brachiopod shells. *Geologische Rundschau*, **85**, 278–292.
- Schallreuter, R. 2004. Ostracodes. In: Webby, B.D., Paris, F., Droser, M.L., & Percival, I.G. (eds) *The Great Ordovician Biodiversification Event*. Columbia University Press, New York, 260–265.
- Schenck, P.E. 1972. Possible Late Ordovician glaciation of Nova Scotia. *Canadian Journal of Earth Science*, **9**, 95–107.
- Schenck, P.E. & Lane, T.E. 1981. Early Paleozoic tillite of Nova Scotia, Canada. In: Hambrey, M.J., & Harland, W.B. (eds). *Earth's pre-Pleistocene glacial record*. Cambridge University Press, Cambridge, 707–710.
- Schofield, D.I., Davies, J.R., Waters, R.A., Wilby, P.R., Williams, M. & Wilson, D. 2004. *Geology of the Builth Wells district – a brief explanation of the geological map*. Sheet explanation of the British Geological Survey. 1:50000 sheet 196 Builth Wells (England and Wales). British Geological Survey, Keyworth, Nottingham.
- Schweitzer, M.H., Wittmeyer, J.L., & Horner, J.R., 2005. Soft-tissue vessels and cellular preservation in *Tyrannosaurus rex*. *Science*, **307**, 1952–1955.
- Schweitzer, M.H., Suo, Z., Avci, R., Asara, J.M., Allen, M.A., Arce, F.T., & Horner, J.R., 2007. Analyses of soft tissue from *Tyrannosaurus rex* suggest the presence of protein. *Science*, **316**, 277–280.
- Scotese, C.R., & McKerrow, W.S. 1991. Ordovician plate tectonic reconstructions. Canadian Geological Survey Paper, **90–9**, 271–282.
- Scriver, A.E., Vance, D. & Rohling, E.J. 2004. New neodymium isotope data quantify Nile involvement in Mediterranean anoxic episodes. *Geology*, **32**, 565–568.
- Secord, J.A. 1986 *Controversy in Victorian geology: the Cambrian–Silurian dispute*. Princeton University Press, Princeton, 363 pp.
- Seewald, J.F. 2003. Organic–inorganic interactions in petroleum–producing sedimentary basins. *Nature*, **426**, 327–333.

- Sepkoski, J.J. 1981. A factor analytic description of the Phanerozoic marine fossil record. *Palaeobiology*, **17**, 58–77.
- Shackleton, N.J. 2000. The 100,000-year ice-age cycle identified and found to lag temperature, carbon dioxide, and orbital eccentricity. *Science*, **289**, 1897–1902.
- Shaviv, N. J. 2002. Cosmic ray diffusion from the galactic spiral arms, iron meteorites, and a possible climatic connection. *Physical Review Letters*, **89**, art. no. 051102.
- Shaviv, N. J. & Veizer, J. 2003. Celestial driver of Phanerozoic climate? *GSA Today*, **13**, --10.
- Sheehan, P. M. 2001. The Late Ordovician mass extinction. *Annual Review of Earth and Planetary Sciences*, **29**, 331–364.
- Sherlock, S.C., Kelley, S.P., Zalasiewicz, J.A., Schofield, D.I., Evans, J.A., Merriman, R.J., & Kemp, S. 2003. Precise dating of low-temperature deformation: strain-fringe analysis by $^{40}\text{Ar}/^{39}\text{Ar}$ laserprobe. *Geology*, **31**, 219–222.
- Shields, G.A., Carden, G.A.F., Veizer, J., Meidla, T., Rong, J.-Y. & Li, R.-Y. 2003. Sr, C and O isotope geochemistry of Ordovician brachiopods: a major isotopic event around the Middle–Late Ordovician transition. *Geochimica et Cosmochimica Acta*, **67**, 2005–2025.
- Shipman, P. 1981. *Life history of a fossil: An introduction to taphonomy and paleoecology*. Harvard University Press, Cambridge, Mass, 222 pp.
- Shuster, D.L., Ehlers, T.A., Rusmoren, M.E. & Farley, K. A. 2005. Rapid glacial erosion at 1.8 Ma revealed by $^4\text{He}/^3\text{He}$ Thermochronometry *Science*, **310**, 1668–1670.
- Siegenthaler, U., Stocker, T., Monnin, E., Lüthi, D., Schwander, J., Stauffer, B., Raynaud, D., Barnola, J.-M., Fischer, H., Masson-Delmotte, V. & Jouzel, J. 2005. Stable carbon cycle-climate relationship during the late Pleistocene. *Science*, **310**, 1313–1317.
- Siveter, D. J. 2000. The Ludlow series. *In*: Aldridge, R.J., Siveter, D.J., Siveter, D.J., Lane, P.D., Palmer, D. & Woodcock, N.H. (eds). *British Silurian stratigraphy*. Joint Nature Conservation Committee, Peterborough, 327–425.
- Siveter, D.J., Sutton, M., Briggs, D.E.G. & Siveter, D.J. 2003. An ostracode crustacean with soft parts from the Lower Silurian. *Science*, **302**, 1747–1751.
- Skevington, D. 1974. Controls influencing the composition and distribution of Ordovician graptolite provinces. *In*: Rickards, R.B., Jackson, D.E. & Hughes, C.P.

- (eds). *Graptolite studies in honour of O.M.B. Bulman*. Special Papers in Palaeontology, 13, 59–73.
- Smith, A.B. & McGowan, A.J. 2007. The shape of the Phanerozoic marine diversity curve: how much can be predicted from the sedimentary record of Europe? *Palaeontology*, 50, 765–774.
- Smith, A.G. & Pickering, K.T. 2003. Oceanic gateways as a critical factor to initiate icehouse Earth. *Journal of the Geological Society*, 160, 337–340.
- Solomon, D.H. & Rosser, J.D. 1965. Reactions catalyzed by minerals. Part I. Polymerization of styrene. *Journal of Applied Polymer Science*, 9, 1261–1271.
- Solomon, D.H. & Swift, J.D. 1967. Reactions catalyzed by minerals. Part II. Chain termination in free-radical polymerizations. *Journal of Applied Polymer Science*, 11, 2567–2575.
- Solomon, D.H. & Loft, B.C. 1968. Reactions catalyzed by minerals. Part III. The mechanism of spontaneous interlamellar polymerizations in phyllosilicates. *Journal of Applied Polymer Science*, 12, 1253–1262.
- Soper, N.J. & Woodcock, N.H. 2003. The lost Lower Old Red Sandstone of England and Wales: a record of post-lapetan flexure or Early Devonian transtension? *Geological Magazine*, 140, 627–647.
- Sprinkle, J. & Guensburg, T.E. Asterozoan, Echinozoan, Blastozoan, Crinozoan and Homalozoan Echinoderms. In: Webby, B.D., Paris, F., Droser, M.L., & Percival, I.G. (eds) *The Great Ordovician Biodiversification Event*. Columbia University Press, New York, 266–280.
- Staley, M. 2004. Darwinian selection leads to Gaia. *Journal of Theoretical Biology*, 218, 35–46.
- Stankiewicz, B.A., Briggs, D.E.G., & Evershed, R.P. 1997. Chemical composition of Palaeozoic fossil invertebrate cuticles as revealed by pyrolysis-gas chromatography/mass spectrometry. *Energy & Fuels*, 11, 515–521.
- Stankiewicz, B.A., Briggs, D.E.G., Evershed, R.P., Miller, R.F. & Bierstedt, A., 1998a. The fate of chitin in Quaternary and Tertiary strata. In: Stankiewicz, B.A. & Van Bergen, P.F. (eds.). *Nitrogen containing molecules in the biosphere and geosphere*. American Chemical Society Symposium Series, 707, 211–225.
- Stankiewicz, B.A., Scott, A.C., Collinson, M.E., Finch, P., Möslle, B., Briggs, D.E.G., & Evershed, R.P., 1998b. Molecular taphonomy of arthropod and plant cuticles from the Carboniferous of North America: Implications for the origin of kerogen. *Journal of the Geological Society, London*, 155, 453–462.

- Stankiewicz, A.R., Briggs, D.E.G., Michels, R., Collinson, M.E., Flannery, M.B. & Evershed, R.P., 2000. Alternative origin of aliphatic polymer in kerogen. *Geology*, **28**, 559–562.
- Stebbing, A.R.D. 1970. Aspects of the reproduction and life cycle of *Rhabdopleura compacta* (Hemichordata). *Marine Biology*, **5**, 205–211.
- Stewart, K., Kassakian, S., Krynytzky, M., DiJulio, D. & Murray, J.W. 2007. Oxidic, suboxic, and anoxic conditions in the Black Sea. *In: Yanko-Hombach, V., Gilbert, A.S., Panin, N. & Dolukhanov, P.M. (eds). The Black Sea Flood Question: Changes in Coastline, Climate, and Human Settlement, Part 1*. Springer, Netherlands, 1–21.
- Štorch, P. & Mergl, M. 1989. Králodvor/Kosov boundary and the late Ordovician environmental changes in the Prague Basin (Barrandian area, Bohemia). *Sborník Geologických Věd, Geologie*, **44**, 117–153.
- Štorch, P. 1986. Ordovician–Silurian boundary in the Prague Basin (Barrandian area, Bohemia). *Sborník geologických věd, Geologie*, **41**, 69–103.
- Štorch, P. 1994. Graptolite biostratigraphy of the Lower Silurian (Llandovery and Wenlock) of Bohemia. *Geological Journal*, **29**, 137–65.
- Stotzky, G. 1980. Surface interactions between clay minerals & microbes, viruses and soluble organics, and their probable importance to the ecology of microbes in soil. *In: Berkeley, R.C.W., Lynch, J.M., Melling, J., Rutter, P.R & Vincent, B. (eds). Microbial adhesion to surfaces*. Ellis Horwood Ltd, Chichester, 231–248.
- Stotzky, G., Schiffenbauer, M., Lipson, S.M. & Yu, B.H. 1981. Surface interactions between viruses, clay minerals, and microbial cells: mechanisms and implications. *In: Goodard, M. & Butler, M (eds), Viruses and wastewater treatment*. Pergamon Press, Oxford, 199–204.
- Strachan, R.A. 2000. Mid-Ordovician to Silurian sedimentation and tectonics on the northern active margin of Iapetus. *In: Woodcock, N.H. & Strachan, R.A. (eds) Geological history of Britain and Ireland*. Blackwell, Oxford, 107–123.
- Suárez-Soruco, R. 1995. Comentarios sobre la edad de la Formación Cancañiri. *Revista Técnica de Yacimientos Petrolíferos Fiscales Bolivianos*, **16**, 51–54.
- Sudbury, M. 1958. Triangulate monograptids from the *Monograptus gregarius* Zone of the Rheidol Gorge. *Philosophical Transactions of the Royal Society*, **B241**, 481–554.
- Sutcliffe, O.E., Dowdeswell, J.A., Whittington, R.J., Theron, J.N. & Craig, J. 2000. Calibrating the Late Ordovician glaciation and mass extinction by the eccentricity of Earth's orbit. *Geology*, **28**, 967–970.

- Sutcliffe, O.E., Harper, D.A.T., Salem, A.A., Whittington, R.J. & Craig, J. 2001. The development of an atypical *Hirnantia* brachiopod Fauna and the onset of glaciation in the late Ordovician of Gondwana. *Transactions of the Royal Society of Edinburgh, Earth Sciences*, **92**, 1–14.
- Sutton, M.D. Briggs, D.E.G., Siveter, D.J., Siveter, D.J. & Gladwell, D.J. 2005. A starfish with three-dimensionally preserved soft-parts from the Silurian of England. *Proceedings of the Royal Society of London*, **B272**, 1001–1006.
- Tappan, H. 1980. *The paleobiology of plant protists*. W.H. Freeman & Co, San Francisco, 1028 pp.
- Taylor, P.D. & Ernst, A. 2004. Bryozoans *in*: Webby, B.D., Paris, F., Droser, M.L., & Percival, I.G. (eds) *The Great Ordovician Biodiversification Event*. Columbia University Press, New York, 147–156.
- Theng, B.K.G. 1979. *Formation and Properties of Clay-Polymer Complexes*. Elsevier, Amsterdam, 362 pp.
- Theokritoff, G. 1964. Taconic stratigraphy in northern Washington County, New York. *Bulletin of the Geological Society of America*, **75**, 171–190.
- Thong-Dzuy, T., Boucot, A.J., Rong J.-Y. & Fanf, Z.-J. 2001. Late Silurian marine shelly fauna of Central and Northern Vietnam. *Geobios*, **34**, 315–338.
- Thorne, S. 1986. *The History of Food Preservation*. Parthenon, London, 292 pp.
- Tissot, B.P. & Welte, D.H. 1984. Petroleum formation and occurrence. Springer-Verlag.
- Tobin, K.J., Bergström S.M., & De La Garza, P. 2005. A mid-Caradocian (453 Ma) drawdown in atmospheric pCO₂ atmospheric CO₂ without ice sheet development? *Palaeogeography, Palaeoclimatology, Palaeoecology*, **226**, 187–204
- Toghill, P. 1968. The graptolite assemblages and zones of the Birkhill Shales (Lower Silurian) at Dobb's Linn. *Palaeontology*, **11**, 654–678.
- Törnquist, S.L. 1899. Researches into the Monograptidae of the Scanian Rastrites Beds. *Acta Universitatis Lundensis*, **35**, 1–25.
- Torsvik, T.H. 1998. Palaeozoic palaeogeography: A North Atlantic viewpoint. *GFF*, **120**, 109–118.
- Towe, K.M., 1996. Fossil preservation in the Burgess Shale. *Lethaia*, **29**, 107–108.

- Towe, K. M. & Urbanek, A. 1972. Collagen-like structures in Ordovician graptolite periderm. *Nature*, **237**, 443–445.
- Tucker, M.E. & Reid, P.C. 1973. The sedimentology and context of late Ordovician glacial marine sediments from Sierra Leone, West Africa. *Palaeogeography, Palaeoclimatology, Palaeoecology*, **13**, 289–307.
- Ulrich, E.O. & Cooper, G.A. 1936. New genera and species of Ozarkian and Canadian Brachiopoda, *Journal of Palaeontology*, **10**, 616–631.
- Ulrich, E.O. & Cooper, G.A. 1938. Ozarkian and Canadian Brachiopoda. *Geological Society of America, special paper*, **13**, 323 pp.
- Ulrich, E.O. & Ruedemann, R. 1931. Are the graptolites bryozoans? *Bulletin of the Geological Society of America*, **42**, 589–604.
- Underwood, C.J. 1992. Graptolite Preservation and Deformation. *Palaios*, **7**, 178–186.
- Underwood, C.J. 1993. The position of graptolites in Lower Palaeozoic planktic ecosystems. *Lethaia*, **26**, 189–202.
- Underwood, C.J. 1998. Population structure of graptolite assemblages. *Lethaia*, **31**, 33–41.
- Underwood, C.J., Crowley, S.F., Marshall, J.D. & Brenchley, P.J. 1997. High resolution carbon isotope stratigraphy of the basal Silurian stratotype (Dob's Linn, Scotland) and its global correlation. *Journal of the Geological Society, London*, **154**, 709–718.
- Underwood, C.J. & Bottrell, S.H. 1994. Diagenetic controls on the pyritization of graptolites. *Geological Magazine*, **131**, 315–327.
- Underwood, C. J., Deynoux, M. & Ghienne, J.-F. 1998. High Palaeolatitude (Hodh, Mauritania) recovery of graptolite fauna after the Hirnantian (end Ordovician) extinction event. *Palaeogeography, Palaeoclimatology, Palaeoecology*, **142**, 91–105.
- Urbanek, A. & Jaanusson, V. 1974. Genetic polymorphism as evidence of outbreeding in graptoloids. In: Rickards, R.B., Jackson, D.E. & Hughes, C.P. (eds) Graptolite studies in honour of O.M.B. Bulman. *Special Papers in Palaeontology*, **13**, 15–18.
- Uysal, I.T., Glikson, M., Golding, S.D. & Southgate, P.N. 2004 Hydrothermal control on organic matter alteration and illite precipitation, Mt Isa Basin, Australia. *Geofluids*, **4**, 131–142.

- van Andel, T.N. 1994. *New views on an old planet*. Cambridge University Press, Cambridge, 440 pp.
- Vandenbroucke, T., Armstrong, H.A., Williams, M. & Zalasiewicz, J.A. 2007. Ground truthing Ordovician climate models using spatial analyses of chitinozoans and graptolites. *Palaeontological Association Annual Meeting, Abstracts & Programme*, 51, 91.
- Vannier, J., Racheboeuf, P., Brussa, E., Williams, M., Rushton, A.W.A., Servais, T. & Siveter, D.J. 2003. New cosmopolitan arthropod zooplankters in the Ordovician seas. *Palaeogeography, Palaeoclimatology, Palaeoecology*, 195, 173–191.
- Veizer, J., Bruckschen, P., Pawellek, F., Podlaha, O., Jasper, T., Korte, C., Strauss, H., Azmy, K., & Ala, D., 1997, Oxygen isotope evolution of Phanerozoic seawater. *Palaeogeography, Palaeoclimatology, Palaeoecology*, 132, 159–172.
- Veizer, J., Godderis, Y. & François, L.M. 2000. Evidence for decoupling of atmospheric CO₂ and global climate during the Phanerozoic eon. *Nature*, 408, 698–701.
- Velbel, M.A. 1993. Temperature dependence of silicate weathering in nature: How strong a negative feedback on long-term accumulation of atmospheric CO₂ and global greenhouse warming? *Geology*, 21, 1059–1062.
- Veizer, J., Ala, D., Azmy, K., Bruckschen, P., Buhl, D., Bruhn, F., Carden, G.A.F., Diener, A., Ebner, S., Godderis, Y., Jasper, T., Korte, C., Pawellek, F., Podlaha, O.G. & Strauss, H. 1999. ⁸⁷Sr/⁸⁶Sr, δ¹³C and δ¹⁸O evolution of Phanerozoic seawater. *Chemical Geology*, 161, 59–88.
- Vermeij, G.J. 1987. *Evolution and escalation: an ecological history of Life*. Princeton University Press, Princeton, N.J., 527 pp.
- Vermeij, G.J. 1995. Economics, volcanoes, and Phanerozoic revolutions. *Paleobiology*, 3, 245–258.
- Verniers, J., & Vandenbroucke, T.R.A. 2006. Chitinozoan biostratigraphy in the Dob's Linn Ordovician–Silurian GSSP, Southern Uplands, Scotland. *GFF*, 128, 195–202.
- von Bromell, M. 1727. Lithographiae Suecanae. *Acta literae Sueciae Upsaliae*, 1.
- Wadleigh, M.A. & Veizer, J. 1992. ¹⁸O/¹⁶O and ¹³C/¹²C in lower Paleozoic brachiopods: implications for the isotopic composition of sea water. *Geochimica Cosmochimica Acta*, 56, 431–443.
- Waern, B., Thorslund, P. & Henningsmoen, G. 1948. Deep boring through Ordovician and Silurian strata at Kinnekulle, Vestergotland. *Bulletin of the Geological Institutions of the University of Uppsala, New Series*, 32, 337–473.

- Wagner, T. & Boyce, A.J. 2006. Pyrite metamorphism in the Devonian Hunsrück Slate of Germany: Insights from laser microprobe sulfur isotope analysis and thermodynamic modeling. *American Journal of Science*, **306**, 525–552.
- Walcott, C.D. 1908. Cambrian Brachiopoda: descriptions of new genera and species. *Smithsonian Miscellaneous Collections*, **53**, 53–165.
- Walker, L.J., Wilkinson, B.H. & Ivany, L.C. 2002. Continental drift and Phanerozoic carbonate accumulation in shallow-shelf and deep-marine settings. *Journal of Geology*, **110**, 75–87.
- Watson, A.J. & Lovelock, J.E. 1983. Biological homeostasis of the global environment: the parable of Daisyworld. *Tellus*, **35B**, 284–289.
- Webb, G.E. 1997. Middle Ordovician *Tetradium* microatolls and a possible bathymetric gradient in tetradiid morphology. *Boletín de la Real Sociedad Española de Historia Natural*, **92**, 177–186
- Webby, B.D., 1992. Global biogeography of Ordovician corals and stromatoporoids. *In: Webby, B.D. & Laurie, J.R. (eds). Global Perspectives on Ordovician Geology*, Balkema, Rotterdam, 261–276.
- Webby, B.D. 2002. Patterns of Ordovician reef development. *In: Kiessling, W., Flügel, E. & Golonka, J. (eds). Phanerozoic Reef Patterns*, SEPM, Tulsa, 129–179.
- Webby, B.D. 2004. Stromatoporoids *in: Webby, B.D., Paris, F., Droser, M.L., & Percival, I.G. (eds) The Great Ordovician Biodiversification Event*. Columbia University Press, New York, 112–118.
- Webby, B.D., Percival, G.D., Edcombe, G.D., Cooper, R.A., Vandenberg, A.H.M., Pickett, J. W., Pojeta, J., Playford, G., Winchester-Setto, T., Young, G.C., Zhen, Y.-Y., Nicoll, R.S., Ross, J.R.P. & Schallreuter, R. 2000. Ordovician palaeobiogeography of Australasia. *Memoir of Association of Australasian Palaeontologists*, **23**, 63–126.
- Webby, B.D., Paris, F., Droser, M.L., & Percival, I.G. (eds) 2004a. *The Great Ordovician Biodiversification Event*. Columbia University Press, New York, 484 pp.
- Webby, B.D., Elias, R.J., Young, G.A., Neuman, B.E.E. & Kaljo, D. 2004b. Corals. *In: Webby, B.D., Paris, F., Droser, M.L., & Percival, I.G. (eds) The Great Ordovician Biodiversification Event*. Columbia University Press, New York, 124–146
- Whitaker, J.H.M. 1962. The geology of the area around Leintwardine, Herefordshire. *Quarterly Journal of the Geological Society*, **118**, 319–347.
- White, D.E., Barron, H.F., Barnes, R.P. & Lintern, B.C. 1991 Biostratigraphy of late Llandovery (Telychian) and Wenlock turbiditic sequences in the SW Southern

- Uplands, Scotland. *Transactions of the Royal Society of Edinburgh, Earth Sciences*, **82**, 297–322.
- Whittington, H.B. 1980. The significance of the fauna of the Burgess Shale, Middle Cambrian, British Columbia. *Proceedings of the Geologists' Association*, **91**, 127–148.
- Wignall, P.B. 1991. Model for transgressive black shales? *Geology*, **19**, 167–170.
- Wignall, P.B. 1994. *Black Shales*. Clarendon Press, Oxford, 127 pp.
- Wignall, P.B. & Maynard, J.R. 1993. The sequence stratigraphy of transgressive black shales. *In*: Katz, B.J. & Pratt, L. (eds). *Source rocks within a sequence stratigraphic framework*. American Association of Petroleum Geologists Studies in Geology, **37**, 35–47.
- Wignall, P.B. & Newton, R. 1998. Pyrite framboid diameter as a measure of oxygen deficiency in ancient mudrocks. *American Journal of Science*, **298**, 537–552.
- Wilby, P.R., Page, A.A., Zalasiewicz, J.A., Milodowski, A.E., Williams, M. & Evans, J.A. 2007. Syntectonic monazite in low-grade mudrocks: a potential geochronometer for cleavage formation? *Journal of the Geological Society, London*, **164**, 53–56.
- Wilkinson, A. & Haszeldine, R.S. 2002. Fibrous illite in oilfield sandstones – a nucleation kinetic theory of growth. *Terra Nova*, **14**, 56–60.
- Williams, M., Davies, J.R., Waters, R.A., Rushton, A.W.A. & Wilby, P.R. 2003. Stratigraphical and palaeoecological importance of Caradoc (Upper Ordovician) graptolites from the Cardigan area, southwest Wales. *Geological Magazine*, **140**, 549–571.
- Williams, M., Rushton, A.W.A., Wood, B., Floyd, J.D., Smith, R. & Wheatley, C. 2004. A revised graptolite biostratigraphy for the lower Caradoc (Upper Ordovician) of southern Scotland. *Scottish Journal of Geology*, **40**, 97–114.
- Williams, S.H. 1981. *Upper Ordovician and lowest Silurian graptolite biostratigraphy in southern Scotland*. Unpublished PhD thesis, University of Glasgow.
- Williams, S.H. 1982. The Late Ordovician fauna of the *anceps* bands at Dob's Linn, southern Scotland. *Geologica et Palaeontologica*, **16**, 29–56.
- Williams, S.H. 1994. Revision and definition of the *C. wilsoni* graptolite Zone (middle Ordovician) of southern Scotland. *Transactions of the Royal Society of Edinburgh: Earth Sciences*, **85**, 143–147.

- Williams, S.H. 1996. Graptolites. *In*: Harper, D.A.T. & Owen, A.W (eds) Fossils of the Upper Ordovician. *Palaeontological Association Field Guide to Fossils*, 7, 174–201.
- Williams, S.H. & Rickards, R.B. 1984. Palaeoecology of graptolitic black shales. *In*: Aspects of the Ordovician system. *Palaeontological Contributions from the University of Oslo*. Universitetsforlaget. 159–166.
- Williams, S.H. & Clarke, L.C 1999. Structure and secretion of the graptolite prosicula, and its application for biostratigraphical and evolutionary studies. *Palaeontology*, 42, 1003–1015.
- Woodcock, N. H. 1990. Sequence stratigraphy of the Palaeozoic Welsh Basin. *Journal of the Geological Society, London*, 147, 537–547
- Woodcock, N.H. 2000. Late Ordovician to Silurian evolution of Eastern Avalonia during convergence with Laurentia. *In*: Woodcock, N. H. & Strachan, R. A. (eds) *Geological history of Britain and Ireland*. Blackwell, Oxford, 168–186.
- Woodcock, N. H., Butler, A. J. , Davies, J. R. & Waters, R. A. 1996. Sequence stratigraphical analysis of late Ordovician and early Silurian depositional systems in the Welsh Basin: a critical assessment. *In*: Hesselbo, S.P. & Parkinson, D.N. (eds). *Sequence stratigraphy in British Geology*. Special Publication of the Geological Society, London, 103, 197–208.
- Worden, R.H., Needham, S.J. & Cuadros, J 2006. The worm gut: a natural clay factory and possible cause of diagenetic grain coats in sandstones. *Journal of Geochemical Exploration*, 89, 428–431.
- Yapp, C.J. & Poths, H. 1992. Ancient atmospheric CO₂ pressures inferred from natural goethites. *Nature*, 355, 342–344.
- Yolkin, E.A., Sennikov, N.V., Bakharev, N.K., Ixokh, N.G. & Yazikov, A.Yu. 1997. Periodicity of deposition in the Silurian and relationships of global geological events in the middle Paleozoic of the southwestern margin of the Siberian continent. *Geologiya i Geofizika* 38, 596–607.
- Young, G.M., 1981. Early Palaeozoic tillites of the northern Arabian Peninsula. *In*: Hambrey, M.J. & Harland, W.B. (ed.). *Earth's Pre-Pleistocene Glacial Record*. Cambridge University Press, 338– 340.
- Young, S.A., Saltzman, M.R., & Bergstrom, S.A., 2005, Upper Ordovician (Mohawkian) carbon isotope stratigraphy in Eastern and Central North America: regional expression of a perturbation of the global carbon cycle, *Palaeogeography, Palaeoceanography, Palaeoclimatology*, 222, 53–76.

- Zachos, J., Pagani, M., Sloan, L., Thomas, E. & Billups, K. 2001. Trends, rhythms, and aberrations in global climate 65 Ma to present. *Science*, **292**, 686–693.
- Zalasiewicz, J. A. 1984. Dichograptid synrhabdosomes from the Arenig of Britain. *Palaeontology*, **27**, 425–429.
- Zalasiewicz, J.A. 2001. Graptolites as constraints on models of sedimentation across Iapetus: a review. *Proceedings of the Geologists Association*, **112**, 237–251.
- Zalasiewicz, J. A. & Williams, M., 1999. Graptolite biozonation of the Wenlock Series (Silurian) of the Builth Wells district, central Wales. *Geological Magazine*, **136**, 263–283.
- Zalasiewicz, J.A. & Tunnicliff, S.P. 1994. Uppermost Ordovician to Lower Silurian graptolite biostratigraphy of the Wye valley, central Wales. *Palaeontology*, **37**, 695–720.
- Zalasiewicz, J.A., Rushton, A.W.A. & Owen A.W. 1995. Late Caradoc graptolitic faunal gradients across the Iapetus Ocean. *Geological Magazine*, **132**, 611–617.
- Zalasiewicz, J., Williams M. & Akhurst M. 2003. An unlikely evolutionary lineage: the Rhuddanian (Silurian, Llandovery) graptolites *Huttagraptus? praematurus* and *Coronograptus cyphus* re-examined. *Scottish Journal of Geology*, **39**, 89–96.
- Zalasiewicz, J.A., Rushton, A.W.A. & Vandenbroucke, T.R.A., Verniers, J. Stone, P. & Floyd, J.D. 2005. *Submission of Hartfell Score for the base of the middle stage of the Upper Ordovician Series*. www.ordovician.cn
- Zalasiewicz, J., Williams, M., Miller, M., Page, A., & Blakett, E. 2007. Early Silurian (Llandovery) graptolites from central Saudi Arabia: first documented record of Telychian faunas from the Arabian Peninsula. *GeoArabia*. In press.
- Zhang, X.-L., & Briggs, D.E.G., 2007. The nature and significance of the appendages of *Opabinia* from the Middle Cambrian Burgess Shale. *Lethaia*, **40**, 161–173.
- Zhang, S., Barnes, C.R. & Jowett, D.M.S. 2006. The paradox of the global standard Late Ordovician–Early Silurian sea level curve: Evidence from conodont community analysis from both Canadian Arctic and Appalachian margins. *Palaeogeography, Palaeoclimatology, Palaeoecology*, **236**, 246–271.
- Zhao, X., Coe, R.S., Gilder, S.A. & Frost, G.M. 1996. Palaeomagnetic constraints on the palaeogeography of China: implications for Gondwanaland. *Australian Journal of Earth Sciences*, **43**, 643–672.

Zhuravlev, A. 2001. biotic diversity and structure during the Neoproterozoic–Ordovician transition. *In*: Zhuravlev, A. & Riding, R. (eds). *The ecology of the Cambrian radiation*. Columbia University Press. New York, 173–199.